WSRC-STI-2006-00151
Revision 0

Keywords: Saltcake
Tank Farm
Characterization

Retention: Permanent

Analysis of Tank 28F Saltcake Core Samples FTF-456 – 467

C. J. Martino
D. J. McCabe
T. B. Edwards
R. L. Nichols

Publication date: February 28, 2007

SAVANNAH RIVER NATIONAL LABORATORY
WASHINGTON SAVANNAH RIVER COMPANY
Savannah River Site, Aiken, SC 29808

SRNL
SAVANNAH RIVER NATIONAL LABORATORY

This document was prepared in conjunction with work accomplished under Contract No. DE-AC09-96SR18500 with the U. S. Department of Energy

Disclaimer

This report was prepared as an account of work sponsored by an agency of the United States Government. Neither the United States Government nor any agency thereof, nor any of their employees, nor any of their contractors, subcontractors or their employees, makes any warranty, express or implied, or assumes any legal liability or responsibility for the accuracy, completeness, or any third party's use or the results of such use of any information, apparatus, product, or process disclosed, or represents that its use would not infringe privately owned rights. Reference herein to any specific commercial product, process, or service by trade name, trademark, manufacturer, or otherwise, does not necessarily constitute or imply its endorsement, recommendation, or favoring by the United States Government or any agency thereof or its contractors or subcontractors. The views and opinions of authors expressed herein do not necessarily state or reflect those of the United States Government or any agency thereof.

Summary

Twelve LM-75 core samplers from Tank 28F sampling were received by SRNL for saltcake characterization. Of these, nine samplers contained mixtures of free liquid and saltcake, two contained only liquid, and one was empty. The saltcake contents generally appeared wet.

A summary of the major tasks performed in this work are as follows:

- Individual saltcake segments were extruded from the samplers and separated into saltcake and free liquid portions.
- Free liquids were analyzed to estimate the amount of traced drill-string fluid contained in the samples.
- The saltcake from each individual segment was homogenized, followed by analysis in duplicate. The analysis used more cost-effective and bounding radiochemical analyses rather than using the full Saltstone WAC suite.
- A composite was created using an approximately equal percentage of each segment's saltcake contents. Supernatant liquid formed upon creation of the composite was decanted prior to use of the composite, but the composite was not drained.
- A dissolution test was performed on the sample by contacting the composite with water at a 4:1 mass ratio of water to salt. The resulting soluble and insoluble fractions were analyzed. Analysis focused on a large subset of the Saltstone WAC constituents.

The following are key observations from this work:

- The dissolved fraction of the undrained composite adjusted to a basis of a 6 M sodium solution, averaged 9.94E+07pCi/mL (0.38 Ci/gal) Cs-137 and 2.38E+04 pCi/mL of Tc-99. These results do not reflect three key aspects of sampling and sample handling: the large amount of free liquid received in the samplers was separated before sample homogenization, the supernatant liquid formed upon creation of the composite was separated prior to dissolution testing, and the analysis of free liquid indicates partial dilution and dissolution of the sample by drill string fluid. Adjustments to account for these effects would lead to higher estimated concentrations of the soluble radionuclides than those measured in the dissolution test solutions.
- Comparing pairs of analytes within all of the individual sample segments indicated that there was a large group of analytes that exhibited inter-correlation (Cs-137, Tc-99, Cs-removed Beta, Sb-126, Sn-126, Mass 133, Mass 135, Mass 137, Cr, P, NO_2^-, OH^-, NO_3^-, and moisture content).
- Residual insoluble material remaining after the dissolution testing was primarily sodium nitrate and aluminum hydroxide. The aluminum hydroxide phases identified were the $Al(OH)_3$ polymorphs bayerite and gibbsite.

Authors:

C. J. Martino, SRNL Advanced Characterization & Process Research Date

---

D. J. McCabe, SRNL Advanced Characterization & Process Research Date

---

T. B. Edwards, SRNL Statistical Consulting Section Date

R. L. Nichols, SRNL Environmental Restoration Technology Section Date

Design Check:

K. Adu-Wusu, SRNL Advanced Characterization & Process Research Date
(per Manual E7, Procedure 2.60)

Approvals/Review:

P. J. Hill, Manager, LW PIT, Data Acquisition, Evaluation, & Management Date

---

D. J. Martin, Manager, Tank Farm Process Engineering Date

W. R. Wilmarth, Manager, SRNL Advanced Characterization & Process Research Date

---

A. M. Murray, Manager, SRNL Actinide & Chemical Technology Section Date

Table of Contents

List of Figures

List of Tables

List of Acronyms

AA	Atomic Absorption
bdl	Below Detectable Level
BL	Bag Liquid
CI	Confidence Interval
DI	Deionized
DOE	Department of Energy
DoF	Degrees of Freedom
DSF	Drill String Fluid
FL	Free Liquid
FLC	Analysis suite for a Free Liquid Composite
FLS	Analysis suite for a Free Liquid Segment
IC	Ion Chromatography
ICP-ES	Inductively Coupled Plasma – Emission Spectroscopy
ICP-MS	Inductively Coupled Plasma – Mass Spectroscopy
IL	Interstitial Liquid
MS	Mean Squares
n	number of repeated measurements
PuTTA	Plutonium separation by thenoyltrifluoracetone
SC	Analysis suite for the Saltcake Composite
SCI	Analysis suite for the Saltcake Composite Insoluble solids
SEM	Scanning Electron Microscopy
SS	Analysis suite for a Saltcake Segment
SSI	Analysis suite for a Saltcake Segment Insoluble solids
SRNL	Savannah River National Laboratory
SRS	Savannah River Site
TIC	Total Inorganic Carbon
TOC	Total Organic Carbon
WAC	Waste Acceptance Criteria
XEDS	X-ray Energy Dispersive Spectroscopy
XRD	X-Ray Diffraction

1 Introduction

The Department of Energy (DOE) recognizes the need for the characterization of High-Level Waste (HLW) saltcake in the Savannah River Site (SRS) F- and H-area tank farms to support upcoming salt processing activities. As part of the enhanced characterization efforts, Tank 28F was sampled and the samples were analyzed at the Savannah River National Laboratory (SRNL).[1,2]

This report documents the characterization and dissolution testing activities on a set of Tank 28F saltcake core samples. The Task Technical and Quality Assurance Plan describes the planned activities performed in the course of this project.[3] Due to the nature of the samples upon receipt, free liquid (FL) analysis was added to the plan and sample draining was eliminated. Batch-wise dissolution of the saltcake composite was replaced by single-batch water dissolution. The focus of the characterization was shifted from a complete set of Saltstone waste acceptance criteria (WAC) analytes to a subset that focuses on the highly radioactive radionuclides.

The following are the main objectives of this work:

- Provide information useful in projecting the composition of dissolved salt by quantifying important components (such as actinides, ^{137}Cs, and ^{90}Sr). This characterization will assist in process selection for the treatment of salt solution and will provide data for the validation of dissolution modeling.

- Facilitate the estimation of the heel composition resulting from dissolution of the bulk saltcake.

- Gather information useful towards performing characterization in a manner that is more cost and time effective.

- Provide tank characterization information as a function of tank height.

2 Sample Contents

2.1 Measurements upon Sample Receipt and Free-Liquid Separation

Twelve samplers used for sampling Tank 28F saltcake were received by SRNL on February 14, 2006 and were placed in the Shielded Cells on February 15, 2006. Table 1 describes the contents of the Tank 28F samples. The samplers are Hanford-style universal samplers used with the LM-75 sampling drill rig. The samplers are approximately 1-1/8 inch inner diameter, and 19 inches long, with an internal volume of approximately 310 mL each. As evidenced by Figure 1, the samples contained an appreciable quantity of free liquids. Free liquid is not directly applicable to the goals of the saltcake characterization program.

We define "Free Liquid" (FL) for the saltcake samples as liquid that is within the sample chamber at the time of collection. There is no generic correlation between FL and any actual material in the saltcake tank. The users of FL characterization data must evaluate its potential origin on a case-by-case basis. We postulate that FL has the following sources: in-tank supernatant liquid (primarily for the top-most sample), a pocket of liquid from within the saltcake, saltcake interstitial liquid that has drained into the drill string during sampling, saltcake interstitial liquid that separated from the saltcake during transport, drill-string displacement fluid traced with sodium bromide (NaBr), a brine made from saltcake dissolved by drill-string displacement fluid (whether formed in-tank or during sample transport), or mixtures of any combinations of these materials.

We also define "Bag Liquid" (BL) as liquids or slurries that are collected from the sleeving material during sample processing (as opposed to FL which is collected from the sample chamber). This material usually originates from the back end of the sampler, between the back of the piston and the weep holes in the sample tube. Thus, the greatest quantity of BL is usually encountered in situations when the piston is not fully retracted. An alternative source of bag liquid is from inside of the sample chamber for instances where the ball valve was not completely closed. For those situations, the bag liquid would have been the free liquid as stated in the previous paragraph.

Table 1: Description of Tank 28F LM-75 Samples

Sample Name	Segment Number	Tank Location (inches from tank bottom)	Saltcake (g)	Free Liquid (g)	Bag Liquid (g)
FTF-456	28-1	298 to 279	38.81	263.18	0
FTF-457	28-2	279 to 260	210.87	29.68	0
FTF-458	28-3	260 to 241	0	95.39	26.79
FTF-459	28-4	241to 222	36.41	125.44	59.31
FTF-460	28-5	222 to 203	71.33	168.98	0
FTF-461	28-6	203 to 184	221.86	232.72	0
FTF-462	28-7	184 to 165	81.26	279.65	0
FTF-463	28-8	165 to 146	25.69	19.03	107.14
FTF-464	28-9	146 to 127	41.90	101.06	0
FTF-465	28-10	127 to 108	131.26	278.88	0
FTF-466	28-11	108 to 89	0	230.83	0
FTF-467	28-12	89 to 70	0	0	0
Total		298 to 70	859	1825	180

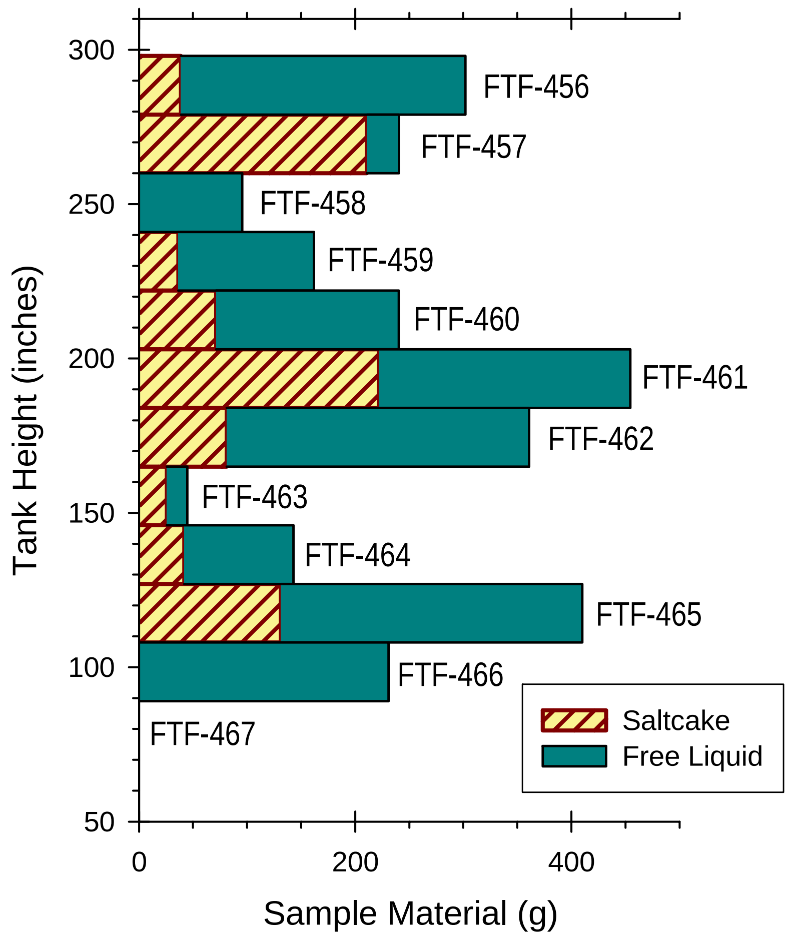

Figure 1: Contents of Tank 28F Samples

2.2 Salt Appearance and Observations during Extrusion

Figure 2 and Figure 3 contain a selection of images captured from the video tape of Tank 28F sample extrusion. As seen in Figure 2, FTF-456 (the upper-most material sampled) contained a much darker and larger grained salt than did the other two largest saltcake samples received. As seen in Figure 3, some materials in these samples were less saltcake-like and more similar to slurries of fine insoluble solids. Figure 4 contains photographs taken through the cell windows of the saltcake extruded from the samples into 16 oz. plastic-coated glass jars. Note that the jars in Figure 4 do not contain the complete quantity of the sample contents in most cases, as FL that was removed from the sampler before pushing the piston during the extrusion process was stored separately (see Figure 5). In general, all of the saltcake samples appeared moist or wet. Appendix A.1 contains a more complete account of the Tank 28F sample extrusion observations.

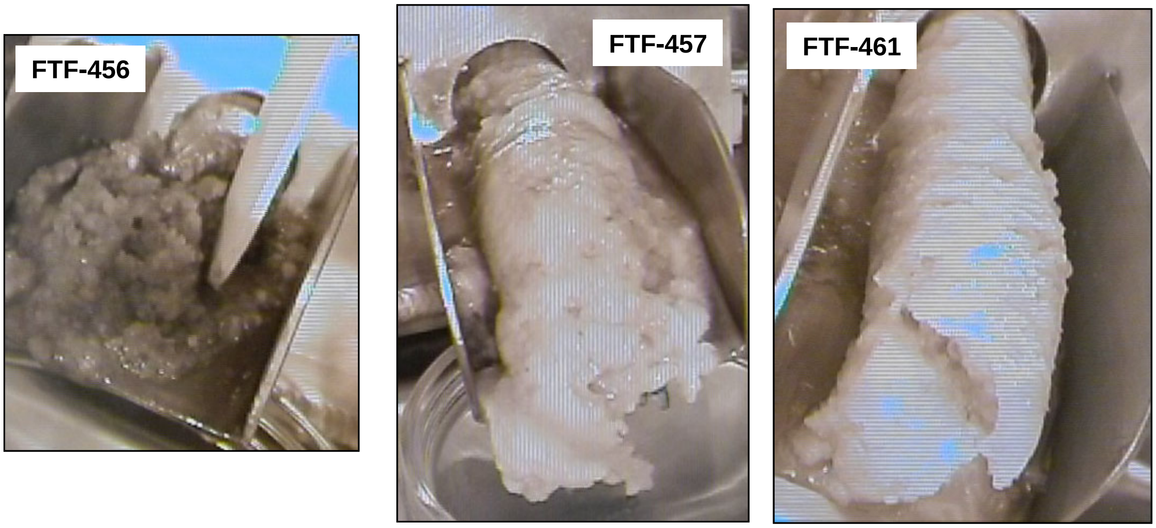

Figure 2: Moist Salt Extruded from Several Tank 28F Samples (FTF-456, 457 & 461)

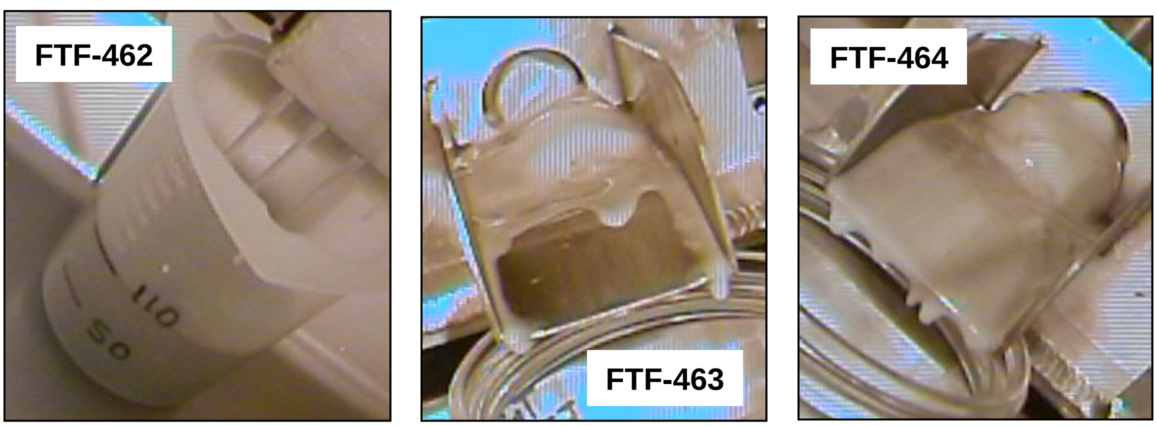

Figure 3: Fine Material in Free Liquid (FTF-462) and Saltcake (FTF-463 & 464)

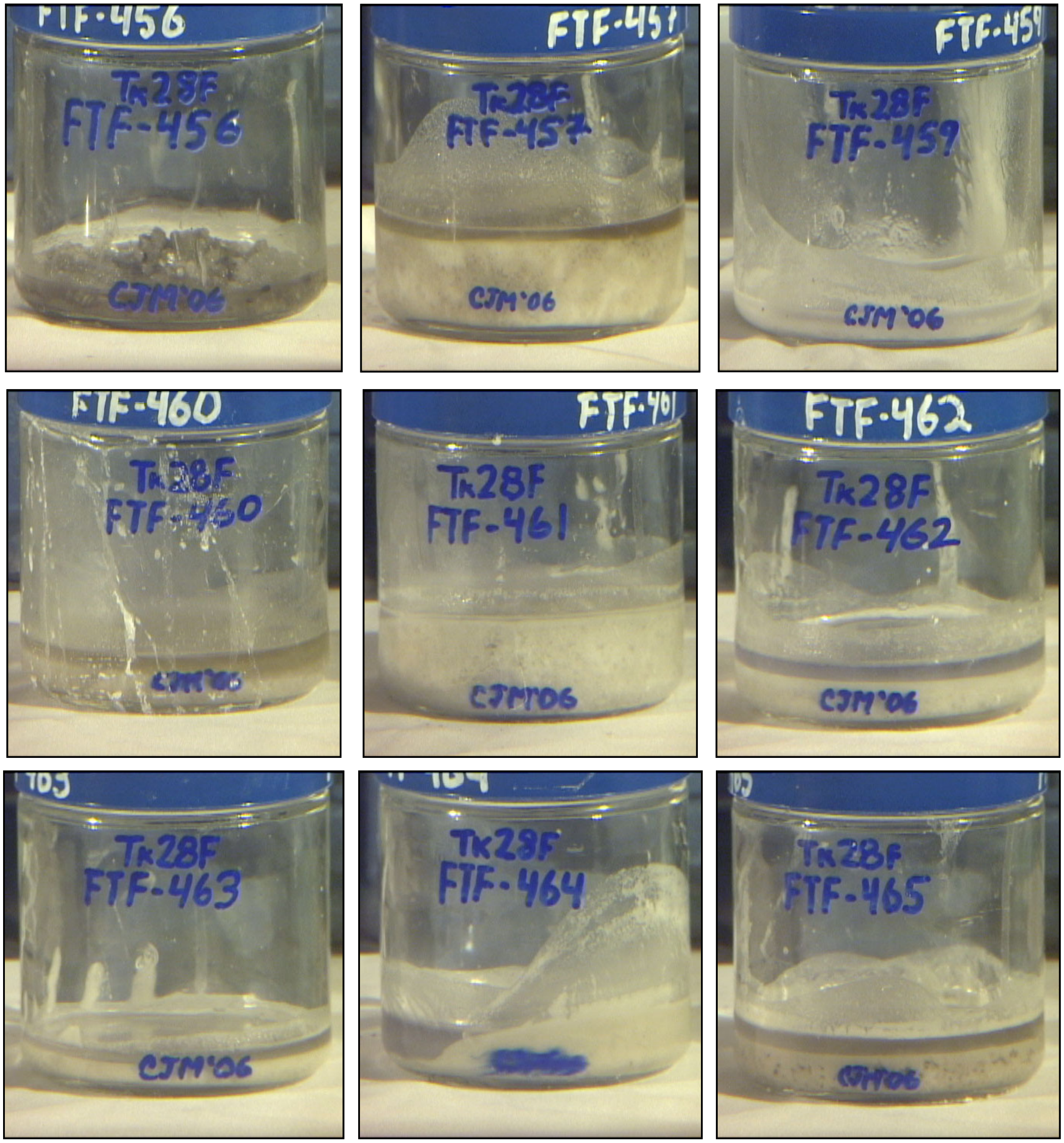

Figure 4: Extruded Salt from Tank 28F Samples (prior to complete solid/liquid separation) Shown in 16 oz. Glass Jars

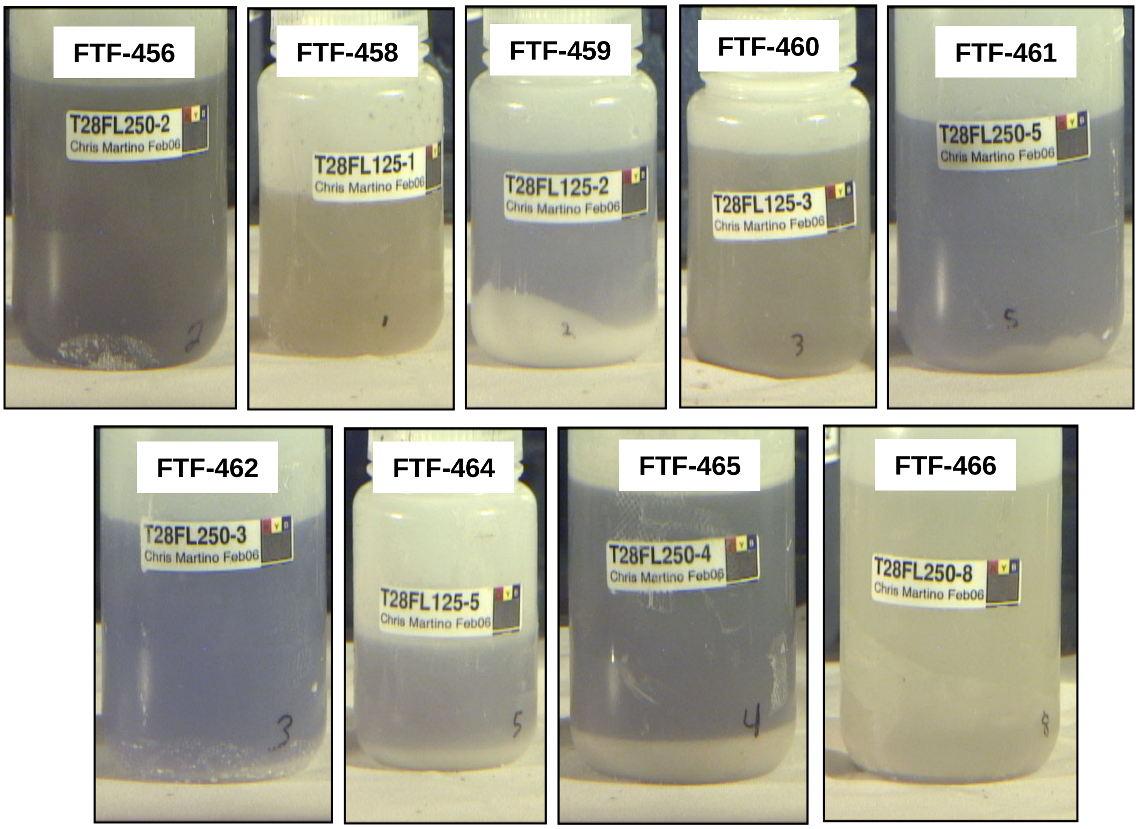

Figure 5: Free Liquid from Tank 28F Samples (prior to removal of entrained solids)

3 Experimental

Samples were extruded or emptied in the shielded cells and prepared for analysis. The analysis tasks consisted of two phases. The first phase was a characterization of the FL and saltcake contained in each sample segment. The second phase was an analysis of the water-soluble and water-insoluble portions of a composite of the saltcake segments. The first phase characterization involved anion, elemental, and primarily gross radionuclide analyses. The second phase characterization involved a more extensive set of radionuclides, focusing primarily on those isotopes in the Saltstone Waste Acceptance Criteria (WAC) that are categorized as “highly radioactive radionuclides.”

Prior to the analytical tasks, a more rigorous FL-saltcake separation was performed. Liquids were decanted from saltcake samples and combined with the FL samples. Solids that settled out in FL bottles were removed and transferred to saltcake segments. The photos in Figure 4 were taken before this repackaging of samples for more complete FL-saltcake separation.

Table 2 contains a matrix of analytes and analytical methods that each material involved in this program was tested for. We define the materials as: FLS, the free liquid from each sample; FLC, the free liquid from the salt composite or other liquid representative of interstitial liquid; SS, individual homogenized saltcake segments; SSI, the water-insoluble materials of each saltcake segment (which was not applicable in this task); SC, the dissolved salt solutions from the saltcake composite; and SCI, the residual insoluble solids from the dissolution of the saltcake composite.

The sample FL was measured with the in-cell gamma counter for determination of Cs-137 content. Aliquots of FL were diluted approximately 10-fold for submittal to analysis for anions by ion chromatography (Suite FLS).

Sub-samples of the homogenized saltcake segments were dissolved in atmospheric-pressure aqua regia at 115 °C and diluted 40-fold for analysis by much of Suite SS. Additional sub-samples of these materials were dissolved and diluted 40-fold with de-ionized water for the subset of Suite SS analyses for which aqua regia dissolution is not appropriate. Sample preparations were performed in duplicate. A composite was formed from approximately equal volume percentages of the saltcake samples. A dissolution test was performed on saltcake composite material by the method discussed in the Section 6.2. Dissolved salt solution was diluted 5-fold with either 2 M nitric acid or de-ionized water and submitted for Suite SC analyses. The residual insoluble solids were analyzed by Suite SCI after dissolution with pressurized aqua regia (where appropriate). Suite SSI was not performed on Tank 28F material.

Percent water was determined by drying small (1 to 2 g) portions of material to a constant weight at 115 °C. Densities of liquids were determined gravimetrically using 2 mL aliquots. The densities of the original saltcake solids were not measured. From previous samples, saltcake densities are typically 1.9 to 2.2 g/mL.[4] These samples are expected to be on the low end of that range due to their wet nature.

Table 2: Analytical Suites Used in Tank 28F Testing and Characterization

Material/Suite:	FLS	FLC	SS	SSI	SC	SCI	Analyte
Sample prep		*	*	*	*	*	
Gamma scan		*	*		*	*	Cs-134, Cs-137 (Ba-137m)
Beta scan					*		Cs-137
Cs-removed gamma		*	*		*	*	Individual Al-26, Co-60, Nb-94, Ru-106, Sb-125, Sn-126, Ce-144, Eu-154, Eu-155, Am-241, Am-243, Cm-245
Cs-removed beta		*	*		*	*	Upper bound of sum of beta emitters: H-3, Ni-63, Se-79, Sr-90, Tc-99, Pm-147, Sm-151, Pu-241
ICP-MS		*	*	*	*	*	Cobalt, Cs-135, Tc-99, Th-232, U-233, U-234, U-235, U-236, U-238, Np-237, Pu-242, (possibly Pu-239, Pu-240)
Cs-removed Gross alpha					*	*	Upper bound of sum of alpha emitters: Th-232, U-232, U-233, U-234, U-235, U-236, U-238, Np-237, Pu-238, Cm-242, Pu-242, Cm-244, Pu-239, Pu-240, Total alpha
ICP-ES (incl. K)		*	*	*	*	*	Al, Ba, Cd, Cr, Pb, Ag, B, Ca, Ce, Cu, Fe, K, Li, Mg, Mn, Mo, Ni, Si, Na, Sr, Ti, Zn, Zr
AA (K, As, Se, Hg)					*		K, As, Se, Hg
TIC/TOC		*	*		*		Carbonate, organic carbon
Total base/Free OH		*	*		*		Hydroxide
IC anions	*	*	*		*		Br, Cl, F, NO_3, NO_2, oxalate, PO_4, SO_4
Pu-238, Pu-239/240		*	*		*	*	Pu-238, Pu-239/240
Pu-241		*			*	*	Pu-241
C-14					*		C-14
Se-79		*			*		Se-79
Sr-90		*			*		Sr-90
I-129		*			*		I-129
Am/Cm		*			*		Am-241, 242m, 243; Cm-242, 244, 245
SEM						*	Microscopic morphology
XRD						*	Crystal identification
Density	*	*			*		density
Moisture Content		*	*		*		wt% water in material

FLS: Individual FL segments
FLC: FL composite (represents IL)
SS: Individual saltcake segments, FL from FTF-456 (supernate), other FL if necessary to identify saltcake components
SSI: Insoluble components of individual saltcake segments (if applicable)
SC: Water soluble components of saltcake composite
SCI: Insoluble components of saltcake composite

4 Free Liquid Analysis (Suite FLS)

Table 3 and Table 4 contain the results of IC measurement for anions, in-cell gamma measurement for Cs-137 and density measurements for the Free Liquid (FL) contained in Tank 28F samples. Where more than one analysis was performed, values are presented as averages and the percent relative standard deviations (%RSD) of two determinations. Values preceded by “<” were present at below detectable levels.

Due to the addition of NaBr as a tracer, the bromide content of the drill string fluid (DSF) added during sampling was nominally 1 wt%. The “wt% DSF” values, as reported in Table 3, are estimates of the percentage of the FL in each salt sample that can be attributed to the added DSF, as opposed to tank supernate, interstitial liquid, or salt solids. The “wt% DSF” values are estimated using two independent bases. The first method uses the the Br^- content of the added DSF as a basis. The percent DSF was calculated by dividing the Br^- result for the FL sample by the Br^- result for a sample of the DSF supplied to the F Tank Farm. The second method uses the in-cell gamma counter results for Cs-137 as a basis. For the second method to be accurate, the supernatant and interstitial liquids in the tank must have a consistent Cs-137 concentration top to bottom. The good linearity of the data (Figure 6) signifies the qualitative agreement of these two approaches and validates this assumption. The linear fit, however, does not cross the x-axis at the initial concentration of bromide (0.125 M). Similarly, the bromide and nitrite show good correlation, indicating that the nitrite in the supernate is being diluted by DSF (Figure 7).

Table 3: Free Liquid Analysis from Tank 28F Saltcake Core Samples, Part 1 of 2

FL Sample	Br^- (wt%)		NO_3^- (M)		NO_2^- (M)		^{137}Cs (Ci/gal)	density (g/mL)		wt% DSF	
	Average	%RSD	Average	%RSD	Average	%RSD		Average	%RSD	Br^- basis	^{137}Cs basis
FTF-456	2.28E-01	11.1%	2.11E+00	0.4%	1.21E+00	0.7%	3.1E+00	1.418	1.0%	23%	40%
FTF-457	2.55E-01	4.1%	2.07E+00	3.9%	1.01E+00	6.4%	2.7E+00	1.480	0.5%	26%	50%
FTF-458	4.82E-01	0.2%	2.09E+00	0.2%	6.36E-01	0.5%	1.8E+00	1.338	0.8%	50%	63%
FTF-459	1.71E-01	7.6%	1.71E+00	0.9%	1.50E+00	1.3%	4.1E+00	1.461	0.5%	18%	23%
FTF-460	2.99E-01	8.5%	2.63E+00	2.7%	9.91E-01	5.3%	2.8E+00	1.391	1.6%	31%	45%
FTF-461	1.48E-01	2.4%	1.63E+00	0.6%	1.60E+00	0.2%	4.5E+00	1.450	0.9%	15%	15%
FTF-462	2.01E-02	1.1%	1.42E+00	0.4%	1.89E+00	0.9%	5.4E+00	1.488	0.6%	2%	0%
FTF-463	4.81E-02	6.0%	1.55E+00	0.4%	1.86E+00	0.5%	5.2E+00	1.428	3.2%	5%	0%
FTF-464	1.01E-01	1.1%	1.47E+00	0.8%	1.87E+00	0.8%	5.3E+00	1.459	0.8%	10%	0%
FTF-465	1.83E-01	20.2%	1.54E+00	2.3%	1.48E+00	1.3%	4.4E+00	1.452	0.5%	19%	17%
FTF-466	7.65E-01	2.2%	2.36E-01	2.6%	2.85E-01	2.7%	8.7E-01	1.110	0.4%	79%	78%
DSF	9.72E-01	3.0%	*<9.68E-03*	--	*<1.30E-02*	--	--	1.015	0.0%	100%	--

Table 4: Free Liquid Analysis from Tank 28F Saltcake Core Samples, Part 2 of 2

FL Sample	SO_4^{2-} (M)		PO_4^{3-} (M)		Cl^- (M)		F^- (M)		$C_2O_4^{2-}$ (M)		CHO_2^- (M)	
	Average	%RSD	Average	%RSD	Average	%RSD	Average	%RSD	Average	%RSD	Average	%RSD
FTF-456	2.30E-02	1.1%	*<6.18E-03*	--	7.04E-03	1.7%	*<6.18E-03*	--	*<6.67E-03*	--	5.02E-03	27.5%
FTF-457	2.31E-02	2.5%	*<6.15E-03*	--	6.34E-03	1.9%	*<6.15E-03*	--	*<6.63E-03*	--	5.06E-03	3.7%
FTF-458	7.05E-02	0.5%	*<6.23E-03*	--	5.00E-03	0.1%	*<6.23E-03*	--	*<6.72E-03*	--	*<4.07E-03*	--
FTF-459	1.41E-02	0.2%	*<6.16E-03*	--	4.04E-03	2.8%	*<6.16E-03*	--	*<6.64E-03*	--	4.68E-03	3.9%
FTF-460	8.38E-02	2.7%	*<6.21E-03*	--	6.32E-03	0.1%	*<6.21E-03*	--	*<6.70E-03*	--	3.60E-03	2.7%
FTF-461	1.55E-02	0.9%	*<6.17E-03*	--	3.72E-03	15.9%	*<6.16E-03*	--	*<6.65E-03*	--	4.94E-03	7.3%
FTF-462	5.49E-03	3.9%	*<6.14E-03*	--	5.18E-03	11.2%	*<6.14E-03*	--	*<6.63E-03*	--	5.05E-03	7.3%
FTF-463	5.47E-03	2.8%	*<6.18E-03*	--	4.22E-03	3.2%	*<6.18E-03*	--	*<6.67E-03*	--	4.24E-03	6.1%
FTF-464	7.50E-03	1.0%	*<6.16E-03*	--	5.04E-03	2.2%	*<6.16E-03*	--	*<6.65E-03*	--	4.68E-03	0.1%
FTF-465	2.28E-02	1.0%	*<6.17E-03*	--	3.88E-03	8.9%	*<6.16E-03*	--	*<6.65E-03*	--	4.16E-03	4.3%
FTF-466	1.55E-02	0.6%	*<6.31E-03*	--	*<3.38E-03*	--	*<6.31E-03*	--	*<6.81E-03*	--	*<4.13E-03*	--
DSF	*<3.12E-03*	--	*<6.32E-03*	--	*<3.38E-03*	--	*<6.32E-03*	--	*<6.82E-03*	--	*<4.13E-03*	--

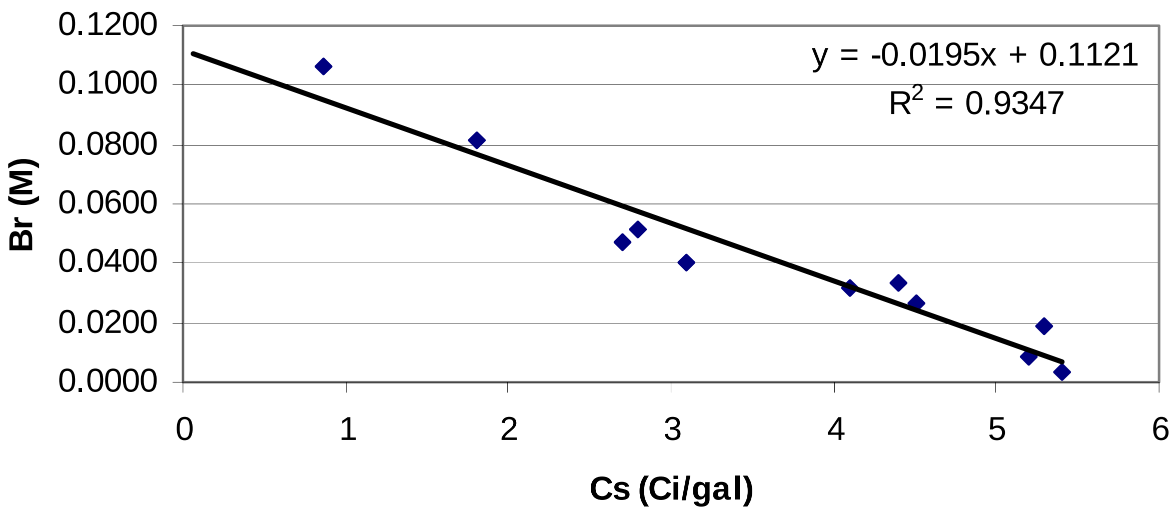

Figure 6: Bromide (Molarity) versus Cs-137 (Ci/gallon) in Free Liquid

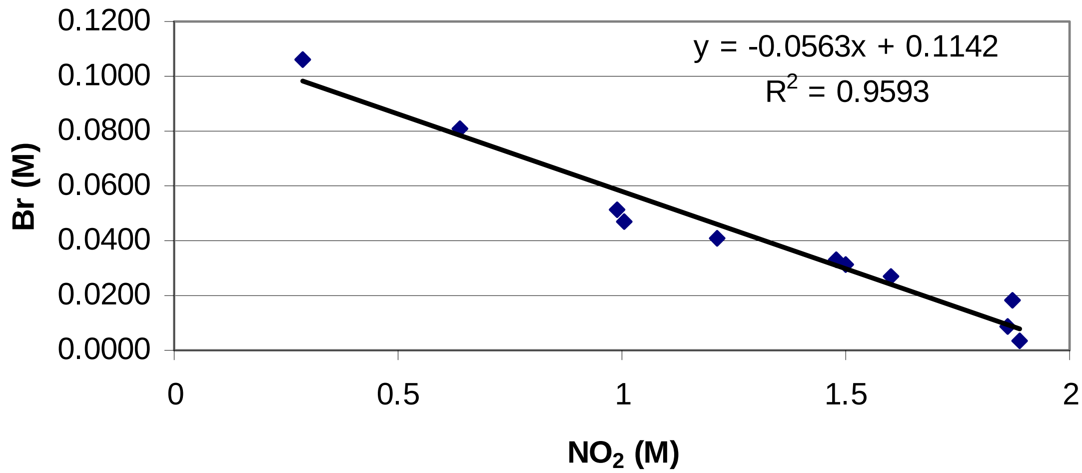

Figure 7: Bromide (Molarity) versus Nitrite (Molarity) in Free Liquid

5 Saltcake Segment Analysis

5.1 Saltcake Segment Results (Suite SS)

The first of the two primary ways in which we fulfill the characterization objectives for saltcake core samples is through analysis of the saltcake portion from each individual segment. This analysis is performed on salt that has not been drained or dried, and thus is reported on a wet saltcake basis. Free Liquids had been removed from the segments to the greatest extent possible prior to analysis. The segment results are for bulk undrained saltcake and thus contain soluble and insoluble components and material in both solid and liquid phases of the as-received saltcake. Some of the soluble components would have been removed during free liquid separation because they had dissolved in the DSF. Likewise, the insoluble species would be more concentrated in the saltcake segments.

Table 5 contains the moisture content results for the Tank 28F samples. Based on the number of determinations made and the standard deviation of those determinations, the upper and lower 95% confidence intervals (CI) on the sample average moisture contents are also presented. The saltcake composite had a moisture content 95% CI that ranged from 14.1 to 16.7 wt%. With the exception of the top two segments, the moisture content of the saltcake segments were all above 20 wt%, which is on the high end of what has previously been seen for saltcake. The presence of free liquid in the saltcake samples, whether the origin is from the tank or from the added drilling fluids, likely served to influence these moisture content measurements. The high measurements of saltcake moisture are supported by the visual observations noted for this sample set.

Table 5: Moisture Content of Saltcake Segments, Saltcake Composite, and Free Liquid (wt%).

Sample	Average	Standard Deviation	n	Lower 95% CI	Upper 95% CI
FTF-456 Saltcake	17.3%	4.8%	3	5.4%	29.2%
FTF-457 Saltcake	13.6%	1.8%	2	-2.3%	29.4%
FTF-459 Saltcake	39.5%	6.7%	3	22.9%	56.1%
FTF-460 Saltcake	21.9%	0.4%	3	21.0%	22.9%
FTF-461 Saltcake	32.2%	6.4%	3	16.2%	48.1%
FTF-462 Saltcake	24.1%	3.6%	3	15.2%	32.9%
FTF-463 Saltcake	30.7%	0.9%	3	28.4%	33.1%
FTF-464 Saltcake	37.9%	3.6%	3	28.9%	46.8%
FTF-465 Saltcake	24.8%	3.4%	3	16.3%	33.4%
Saltcake Composite	15.4%	1.2%	6	14.1%	16.7%
FTF-462 Free Liquid	51.8%	0.1%	3	51.4%	52.1%
15 wt% NaCl Standard	85.0%	0.3%	6	84.7%	85.2%

Table 6 and Table 7 contain the radiochemical, anion, and metals analyses for duplicate preparations of each homogenized undrained Tank 28F saltcake segment. Upon receipt of radiochemical analyses, there was evidence of solution contamination with Pu-238 from processing within the shielded cells. The Pu-238 to Pu-239/240 ratio was unexpectedly variable for duplicate preparations of individual segments and the process blanks contained levels of Pu-238 commensurate with the actual samples. Thus, the Pu-238 results for this portion of the saltcake characterization have an erratically high bias and are not considered in the statistical analyses. Three other results were judged to be outliers and were not used in the subsequent analysis. These discounted results are sodium for Prep 1 of FTF-461 and nitrate for Prep 2 of FTF-456 and FTF-457. These three results are not consistent with the overall set of results and are not physically realistic.

Table 8 provides a summary of Table 6 and Table 7 by taking either the average or the best result from the two preparations, whichever is more appropriate based on the following characteristics. For the majority of the analytes, Table 8 contains the average result from the two determinations from that segment. In some cases, however, the set of results contains below detectable level (bdl) values that are greater than other detectable values. For those cases, the detectable value is presented in Table 8 as the best value. For some cases as explained above, the best value is used when one of the duplicate results has been discounted. Again, values or averages preceded by “<” are below detectable levels and can be taken to be less than the detection limit provided. Values preceded by “<=” are averages of detectable values and detection limits, and can be considered to be less-than-or-equal-to the value provided.

Table 6: Analysis of Bulk Undrained Saltcake in Tank 28F Core Sample Segments, Part 1 of 2

			Saltcake Segments									
Analyte	Units	Method	FTF-456		FTF-457		FTF-459		FTF-460		FTF-461	
			Prep 1	Prep 2	Prep 1	Prep 2	Prep 1	Prep 2	Prep 1	Prep 2	Prep 1	Prep 2
Cs-137	pCi/g	γ	1.46E+08	1.41E+08	1.45E+08	1.37E+08	5.95E+08	5.50E+08	1.44E+08	1.53E+08	3.12E+08	2.73E+08
Pu-238 *	pCi/g	PuTTA	4.42E+03	3.63E+03	2.90E+03	2.64E+03	2.37E+03	4.41E+03	1.36E+04	2.58E+03	8.65E+03	1.26E+03
Pu-239/240	pCi/g	PuTTA	9.28E+03	3.13E+03	3.79E+03	4.86E+03	6.31E+03	4.11E+03	1.02E+04	1.07E+04	5.23E+03	5.18E+03
Co-60	pCi/g	Cs-rem γ	2.23E+02	<2.75E+02	<1.64E+02	<2.07E+02	<2.06E+02	<1.91E+02	<2.00E+02	<2.47E+02	<1.86E+02	<1.95E+02
Sb-126	pCi/g	Cs-rem γ	1.98E+03	1.68E+03	4.29E+02	4.21E+02	2.45E+03	3.94E+03	2.01E+03	2.09E+03	1.35E+03	1.63E+03
Sn-126	pCi/g	Cs-rem γ	3.05E+03	2.32E+03	4.64E+02	<3.79E+02	3.24E+03	3.50E+03	3.00E+03	2.98E+03	2.07E+03	2.52E+03
Eu-154	pCi/g	Cs-rem γ	4.14E+02	<3.82E+02	<2.45E+02	<3.11E+02	<3.02E+02	<3.23E+02	<3.20E+02	<3.64E+02	<2.18E+02	<2.96E+02
Am-241	pCi/g	Cs-rem γ	1.39E+03	<1.63E+03	1.30E+03	<8.78E+02	<9.37E+02	1.49E+03	2.23E+03	<1.35E+03	<1.08E+03	1.29E+03
Cs-rem beta	pCi/g	Cs-rem β	3.14E+05	2.79E+05	9.14E+04	8.15E+04	3.67E+05	4.95E+05	2.81E+05	2.75E+05	2.40E+05	2.59E+05
Tc-99	pCi/g	ICP-MS	<1.08E+05	7.95E+04	<1.12E+05	5.52E+04	1.39E+05	1.33E+05	<1.36E+05	4.50E+04	<1.14E+05	6.87E+04
F^-	wt %	IC	<8.85E-02	2.19E-02	<9.09E-02	1.40E-02	<9.52E-02	9.62E-03	7.91E-02	7.63E-02	5.13E-02	4.27E-02
CHO_2^-	wt %	IC	<4.42E-01	<1.75E-02	<4.55E-01	<1.87E-02	<4.76E-01	2.40E-02	<4.65E-01	<4.24E-01	2.14E-02	2.37E-02
Cl^-	wt %	IC	<8.85E-02	1.75E-02	<9.09E-02	<1.87E-02	<9.52E-02	2.88E-02	<9.30E-02	<8.47E-02	1.71E-02	2.37E-02
NO_2^-	wt %	IC	1.35E+00	9.87E-01	9.45E-01	9.63E-01	3.90E+00	3.77E+00	2.53E+00	2.56E+00	2.83E+00	3.18E+00
Br^-	wt %	IC	<4.42E-01	3.51E-02	<4.55E-01	<3.27E-02	<4.76E-01	6.73E-02	1.72E-01	1.69E-01	2.99E-02	3.32E-02
NO_3^-	wt %	IC	4.32E+01	8.33E+01 *	5.36E+01	9.11E+01 *	8.71E+00	1.05E+01	1.76E+01	2.08E+01	2.39E+01	2.03E+01
PO_4^{3-}	wt %	IC	<4.42E-01	<4.39E-01	<4.55E-01	<4.67E-01	<4.76E-01	<4.81E-01	<4.65E-01	<4.24E-01	<4.27E-01	<4.74E-01
SO_4^{2-}	wt %	IC	3.63E-01	3.82E-01	4.18E-01	4.86E-01	5.10E-01	4.04E-01	6.14E+00	5.51E+00	4.83E+00	3.61E+00
$C_2O_4^{2-}$	wt %	IC	5.75E-02	9.65E-02	3.18E-02	3.27E-02	<4.76E-01	3.37E-02	1.91E-01	1.78E-01	8.12E-02	7.58E-02
CO_3^{2-}	wt %	TIC	2.43E+00	4.43E+00	7.75E-01	8.93E-01	7.98E-01	7.79E-01	2.81E+00	2.42E+00	2.46E+00	2.18E+00
OH^-	wt %	Titration	1.35E+00	1.57E+00	1.08E+00	1.35E+00	5.91E+00	6.70E+00	3.80E+00	3.46E+00	4.50E+00	5.64E+00
AlO_2^-	wt %	Titration	1.57E+00	1.55E+00	6.17E+00	6.89E+00	1.43E+01	1.42E+01	4.39E+00	4.25E+00	6.56E+00	6.43E+00
AlO_2^-	wt %	ICP-ES	5.92E-01	6.34E-01	5.75E+00	5.48E+00	1.18E+01	1.39E+01	1.34E+00	1.53E+00	8.72E+00	4.50E+00
Ag	wt %	ICP-ES	<4.94E-04	6.74E-04	<5.15E-04	6.51E-04	<5.93E-04	5.82E-04	<6.23E-04	7.42E-04	6.22E-04	6.41E-04
Al	wt %	ICP-ES	2.71E-01	2.90E-01	2.63E+00	2.51E+00	5.38E+00	6.38E+00	6.11E-01	6.99E-01	3.99E+00	2.06E+00
Ba	wt %	ICP-ES	<7.97E-04	<9.79E-04	<8.30E-04	<9.13E-04	<9.56E-04	<8.37E-04	<1.00E-03	<9.84E-04	<8.47E-04	<8.19E-04
Ca	wt %	ICP-ES	<1.42E-03	<1.75E-03	<1.48E-03	<1.63E-03	<1.71E-03	<1.49E-03	<1.79E-03	<1.76E-03	<1.51E-03	<1.46E-03
Ce	wt %	ICP-ES	<1.54E-02	2.02E-02	<1.60E-02	2.14E-02	<1.85E-02	1.93E-02	<1.94E-02	2.33E-02	<1.64E-02	1.90E-02
Cr	wt %	ICP-ES	<6.59E-03	<8.10E-03	<6.86E-03	<7.55E-03	1.07E-02	1.39E-02	<8.30E-03	<8.14E-03	1.29E-02	7.80E-03
Cu	wt %	ICP-ES	<2.57E-04	<3.16E-04	<2.68E-04	<2.95E-04	<3.09E-04	<2.70E-04	<3.24E-04	<3.18E-04	<2.74E-04	<2.65E-04
Fe	wt %	ICP-ES	3.92E-02	2.35E-02	1.35E-02	5.45E-03	7.57E-03	7.90E-03	1.67E-02	3.67E-03	6.36E-03	3.55E-03
Gd	wt %	ICP-ES	<4.95E-04	7.04E-04	<5.15E-04	6.97E-04	<5.93E-04	6.28E-04	<6.23E-04	7.33E-04	<5.26E-04	7.34E-04
K	wt %	ICP-ES	<2.70E-01	<3.32E-01	<2.81E-01	<3.09E-01	<3.24E-01	<2.83E-01	<3.40E-01	<3.33E-01	3.78E-01	<2.78E-01
Li	wt %	ICP-ES	3.06E-02	5.44E-02	3.79E-02	5.56E-02	4.52E-02	5.80E-02	4.92E-02	6.57E-02	7.28E-02	6.82E-02
Mn	wt %	ICP-ES	2.05E-03	1.02E-03	2.69E-04	<1.07E-04	2.33E-04	<9.82E-05	1.80E-04	<1.16E-04	2.22E-04	<9.62E-05
Na	wt %	ICP-ES	2.00E+01	2.34E+01	2.03E+01	2.27E+01	1.74E+01	1.87E+01	2.10E+01	2.31E+01	4.06E+01 *	2.34E+01
P	wt %	ICP-ES	9.57E-02	7.44E-02	<2.89E-02	<3.18E-02	7.60E-02	1.19E-01	<3.50E-02	4.67E-02	9.19E-02	5.22E-02
S	wt %	ICP-ES	1.49E-01	1.50E-01	1.80E-01	1.89E-01	1.62E-01	2.34E-01	1.19E+00	1.38E+00	2.76E+00	1.62E+00
Sb	wt %	ICP-ES	<1.59E-02	<1.95E-02	<1.65E-02	<1.82E-02	<1.90E-02	<1.67E-02	<2.00E-02	<1.96E-02	<1.69E-02	<1.63E-02
Si	wt %	ICP-ES	<4.52E-03	3.79E-02	<4.71E-03	3.21E-02	<5.43E-03	3.40E-02	<5.70E-03	<5.59E-03	<4.81E-03	<4.65E-03
Ti	wt %	ICP-ES	<1.36E-04	<1.67E-04	<1.42E-04	<1.56E-04	<1.63E-04	<1.43E-04	4.17E-04	<1.68E-04	<1.45E-04	<1.40E-04
Zn	wt %	ICP-ES	4.78E-03	4.68E-03	<1.17E-03	<1.29E-03	2.61E-03	2.26E-03	2.51E-03	2.28E-03	2.50E-03	<1.16E-03
Cs-133	wt %	ICP-MS	4.68E-04	4.83E-04	5.31E-04	4.05E-04	1.89E-03	1.72E-03	4.68E-04	5.23E-04	1.16E-03	8.94E-04
Mass-135	wt %	ICP-MS	<7.94E-05	1.33E-04	<8.26E-05	8.06E-05	2.87E-04	2.72E-04	1.22E-04	8.82E-05	1.47E-04	1.25E-04
Mass-137	wt %	ICP-MS	6.93E-04	4.45E-04	3.05E-04	2.78E-04	9.13E-04	9.72E-04	3.75E-04	3.70E-04	5.11E-04	4.69E-04
U-235	wt %	ICP-MS	<3.97E-05	<4.88E-05	<4.13E-05	<4.55E-05	<4.76E-05	<4.17E-05	<5.00E-05	<4.90E-05	<4.22E-05	<4.08E-05
U-238	wt %	ICP-MS	2.82E-03	2.17E-03	1.64E-03	1.53E-03	7.53E-04	8.94E-04	4.08E-03	4.34E-03	1.95E-03	2.30E-03

* indicates values discounted and not used in further analyses (Pu-238 , one Na^+, and two NO_3^- results).

Table 7: Analysis of Bulk Undrained Saltcake in Tank 28F Core Sample Segments, Part 2 of 2. Right-Most Sample is Free Liquid from Segment FTF-456.

			Saltcake Segments								Free Liquid	
Analyte	Units	Method	FTF-462		FTF-463		FTF-464		FTF-465		FTF-456	
			Prep 1	Prep 2	Prep 1	Prep 2	Prep 1	Prep 2	Prep 1	Prep 2	Prep 1	Prep 2
Cs-137	pCi/g	γ	6.17E+08	6.31E+08	5.05E+08	3.67E+08	5.36E+08	7.21E+08	2.72E+08	3.10E+08	5.45E+08	4.73E+08
Pu-238 *	pCi/g	PuTTA	2.23E+03	6.76E+02	1.55E+04	2.72E+04	3.69E+03	1.09E+03	1.67E+04	2.55E+03	1.00E+04	1.66E+04
Pu-239/240	pCi/g	PuTTA	3.88E+03	3.55E+03	7.70E+03	1.04E+04	4.55E+03	2.05E+03	1.11E+04	1.54E+04	1.37E+03	8.15E+02
Co-60	pCi/g	Cs-rem γ	<1.65E+02	<1.37E+02	<1.02E+02	<1.83E+02	1.58E+02	<1.98E+02	<1.29E+02	2.54E+02	<1.65E+02	<1.58E+02
Sb-126	pCi/g	Cs-rem γ	4.22E+03	4.38E+03	1.23E+03	2.38E+03	3.47E+03	1.52E+03	2.28E+03	3.01E+03	9.46E+02	7.97E+02
Sn-126	pCi/g	Cs-rem γ	4.23E+03	<6.22E+03	1.65E+03	3.27E+03	3.02E+03	2.44E+03	<3.12E+03	3.30E+03	1.24E+03	1.04E+03
Eu-154	pCi/g	Cs-rem γ	<1.50E+02	<1.67E+02	<1.18E+02	<2.21E+02	<2.78E+02	<2.61E+02	<2.58E+02	<2.73E+02	<2.55E+02	<2.36E+02
Am-241	pCi/g	Cs-rem γ	1.09E+03	2.88E+03	1.13E+03	2.90E+03	1.64E+03	<8.69E+02	2.26E+03	2.70E+03	3.42E+03	<1.01E+03
Cs-rem beta	pCi/g	Cs-rem β	5.50E+05	5.68E+05	3.62E+05	3.77E+05	4.64E+05	2.91E+05	3.62E+05	4.27E+05	2.13E+05	1.77E+05
Tc-99	pCi/g	ICP-MS	1.82E+05	1.58E+05	1.45E+05	1.30E+05	1.54E+05	1.59E+05	9.58E+04	1.06E+05	1.07E+05	9.87E+04
F^-	wt %	IC	4.81E-02	4.29E-02	<8.30E-02	3.48E-02	<8.16E-02	2.94E-02	1.03E-01	1.02E-01	<8.26E-02	<8.23E-03
CHO_2^-	wt %	IC	<4.81E-01	2.15E-02	<4.15E-01	1.74E-02	<4.08E-01	1.96E-02	<4.31E-01	1.78E-02	<4.13E-01	2.06E-02
Cl^-	wt %	IC	<9.62E-02	1.72E-02	<8.30E-02	1.74E-02	<8.16E-02	1.96E-02	<8.62E-02	1.78E-02	<8.26E-02	2.88E-02
NO_2^-	wt %	IC	2.92E+00	3.42E+00	2.98E+00	2.28E+00	3.33E+00	3.17E+00	2.35E+00	2.19E+00	4.04E+00	4.05E+00
Br^-	wt %	IC	<4.81E-01	<3.00E-02	<4.15E-01	<3.04E-02	<4.08E-01	<3.43E-02	5.17E-02	4.44E-02	1.65E-01	1.60E-01
NO_3^-	wt %	IC	3.08E+01	2.19E+01	6.10E+00	1.08E+01	5.67E+00	9.31E+00	1.30E+01	1.97E+01	9.55E+00	1.16E+01
PO_4^{3-}	wt %	IC	<4.81E-01	<4.29E-01	<4.15E-01	<4.35E-01	<4.08E-01	<4.90E-01	<4.31E-01	<4.44E-01	<4.13E-01	<4.12E-01
SO_4^{2-}	wt %	IC	4.40E+00	4.01E+00	2.49E+00	2.41E+00	2.29E+00	1.78E+00	6.08E+00	1.78E-01	1.65E-01	1.65E-01
$C_2O_4^{2-}$	wt %	IC	6.25E-02	6.01E-02	1.58E-01	1.48E-01	1.67E-01	1.32E-01	3.10E-01	2.44E-01	<4.13E-01	<2.88E-02
CO_3^{2-}	wt %	TIC	1.92E+00	2.07E+00	1.59E+00	1.55E+00	1.36E+00	1.32E+00	2.69E+00	2.36E+00	9.50E-01	1.05E+00
OH^-	wt %	Titration	3.92E+00	4.89E+00	4.51E+00	3.33E+00	5.13E+00	5.58E+00	3.81E+00	3.40E+00	6.88E+00	7.14E+00
AlO_2^-	wt %	Titration	8.79E+00	9.62E+00	2.74E+01	2.72E+01	2.41E+01	2.20E+01	1.73E+01	1.49E+01	2.68E+00	2.91E+00
AlO_2^-	wt %	ICP-ES	8.13E+00	8.46E+00	2.01E+01	2.71E+01	1.84E+01	8.54E+00	7.19E+00	9.35E+00	2.09E+00	1.86E+00
Ag	wt %	ICP-ES	<4.90E-04	6.01E-04	<5.46E-04	7.54E-04	<5.35E-04	6.37E-04	<4.98E-04	5.72E-04	<5.02E-04	6.07E-04
Al	wt %	ICP-ES	3.72E+00	3.87E+00	9.19E+00	1.24E+01	8.43E+00	3.91E+00	3.29E+00	4.28E+00	9.57E-01	8.52E-01
Ba	wt %	ICP-ES	<7.90E-04	<8.47E-04	<8.81E-04	9.15E-04	8.91E-04	<8.23E-04	8.11E-04	1.10E-03	<8.10E-04	<7.75E-04
Ca	wt %	ICP-ES	<1.41E-03	<1.51E-03	<1.57E-03	<1.43E-03	<1.54E-03	<1.47E-03	<1.43E-03	1.74E-03	<1.44E-03	<1.38E-03
Ce	wt %	ICP-ES	<1.53E-02	1.93E-02	<1.70E-02	1.84E-02	<1.66E-02	1.72E-02	<1.55E-02	2.02E-02	<1.56E-02	1.86E-02
Cr	wt %	ICP-ES	1.67E-02	1.77E-02	1.08E-02	1.51E-02	1.59E-02	8.90E-03	1.02E-02	1.38E-02	7.09E-03	7.50E-03
Cu	wt %	ICP-ES	<2.55E-04	<2.74E-04	<2.84E-04	2.80E-04	<2.78E-04	<2.66E-04	<2.59E-04	<2.63E-04	<2.62E-04	<2.50E-04
Fe	wt %	ICP-ES	5.90E-03	5.33E-03	1.25E-02	1.60E-02	1.21E-02	4.87E-03	1.21E-02	1.19E-02	3.76E-03	2.94E-03
Gd	wt %	ICP-ES	<4.91E-04	6.95E-04	<5.47E-04	8.49E-04	<5.35E-04	7.09E-04	<4.98E-04	7.08E-04	<5.02E-04	7.52E-04
K	wt %	ICP-ES	2.90E-01	<2.87E-01	<2.98E-01	<2.71E-01	<2.92E-01	3.50E-01	<2.72E-01	<2.75E-01	<2.74E-01	<2.63E-01
Li	wt %	ICP-ES	4.99E-02	7.35E-02	5.43E-02	8.34E-02	5.40E-02	7.51E-02	4.62E-02	7.89E-02	4.84E-02	6.14E-02
Mn	wt %	ICP-ES	1.98E-04	<9.95E-05	4.48E-04	<9.39E-05	3.60E-04	<9.66E-05	3.75E-04	<9.55E-05	6.16E-04	<9.10E-05
Na	wt %	ICP-ES	2.00E+01	2.14E+01	1.93E+01	2.13E+01	1.86E+01	1.93E+01	1.48E+01	2.26E+01	1.49E+01	1.39E+01
P	wt %	ICP-ES	1.30E-01	1.38E-01	6.06E-02	6.18E-02	1.11E-01	5.07E-02	5.72E-02	8.29E-02	<2.82E-02	<2.70E-02
S	wt %	ICP-ES	1.10E+00	1.12E+00	7.10E-01	1.14E+00	6.43E-01	1.73E-01	1.22E+00	1.51E+00	7.08E-02	6.96E-02
Sb	wt %	ICP-ES	<1.57E-02	<1.69E-02	1.84E-02	2.52E-02	<1.72E-02	<1.64E-02	<1.60E-02	<1.62E-02	<1.61E-02	<1.54E-02
Si	wt %	ICP-ES	<4.49E-03	1.20E-02	<5.00E-03	7.39E-03	<4.89E-03	1.02E-02	<4.56E-03	<4.61E-03	<4.60E-03	<4.40E-03
Ti	wt %	ICP-ES	<1.35E-04	<1.45E-04	<1.50E-04	<1.36E-04	<1.47E-04	<1.40E-04	<1.37E-04	<1.39E-04	<1.38E-04	<1.32E-04
Zn	wt %	ICP-ES	1.53E-03	1.53E-03	<1.24E-03	<1.13E-03	1.94E-03	2.00E-03	1.55E-03	1.72E-03	1.73E-02	1.56E-02
Cs-133	wt %	ICP-MS	2.11E-03	1.96E-03	1.62E-03	1.22E-03	1.78E-03	2.37E-03	9.07E-04	1.00E-03	1.78E-03	1.54E-03
Mass-135	wt %	ICP-MS	2.86E-04	3.14E-04	1.96E-04	1.81E-04	2.72E-04	3.29E-04	1.32E-04	2.57E-04	2.57E-04	2.47E-04
Mass-137	wt %	ICP-MS	9.59E-04	9.85E-04	1.12E-03	1.12E-03	1.21E-03	1.12E-03	9.06E-04	1.32E-03	6.89E-04	6.97E-04
U-235	wt %	ICP-MS	<3.97E-05	<4.22E-05	<4.13E-05	<3.98E-05	<4.76E-05	<4.10E-05	<4.00E-05	<4.05E-05	<5.00E-05	<3.86E-05
U-238	wt %	ICP-MS	1.73E-03	1.59E-03	3.68E-03	5.11E-03	2.79E-03	1.15E-03	4.50E-03	5.85E-03	6.23E-04	4.77E-04

* indicates values discounted and not used in further analyses (Pu-238)

Table 8: Average or Best Value for Saltcake Segment Analysis.

Analyte	Units	Method	FTF-456	FTF-457	FTF-459	FTF-460	FTF-461	FTF-462	FTF-463	FTF-464	FTF-465	FTF-456 FL
Cs-137	pCi/g	γ	1.43E+08	1.41E+08	5.72E+08	1.48E+08	2.92E+08	6.24E+08	4.36E+08	6.28E+08	2.91E+08	5.09E+08
Pu-238 *	pCi/g	PuTTA	4.02E+03	2.77E+03	3.39E+03	8.07E+03	4.95E+03	1.45E+03	2.13E+04	2.39E+03	9.63E+03	1.33E+04
Pu-239/240	pCi/g	PuTTA	6.20E+03	4.33E+03	5.21E+03	1.05E+04	5.20E+03	3.71E+03	9.03E+03	3.30E+03	1.32E+04	1.09E+03
Co-60	pCi/g	Cs-rem γ	2.23E+02	<1.85E+02	<1.99E+02	<2.23E+02	<1.91E+02	<1.51E+02	<1.43E+02	1.78E+02	<1.91E+02	<1.61E+02
Sb-126	pCi/g	Cs-rem γ	1.83E+03	4.25E+02	3.20E+03	2.05E+03	1.49E+03	4.30E+03	1.81E+03	2.50E+03	2.65E+03	8.72E+02
Sn-126	pCi/g	Cs-rem γ	2.68E+03	4.64E+02	3.37E+03	2.99E+03	2.30E+03	4.23E+03	2.46E+03	2.73E+03	3.30E+03	1.14E+03
Eu-154	pCi/g	Cs-rem γ	4.14E+02	<2.78E+02	<3.13E+02	<3.42E+02	<2.57E+02	<1.59E+02	<1.69E+02	<2.70E+02	<2.65E+02	<2.45E+02
Am-241	pCi/g	Cs-rem γ	<=1.51E+03	1.09E+03	<1.21E+03	<=1.79E+03	<=1.19E+03	1.98E+03	2.01E+03	<=1.26E+03	2.48E+03	<=2.22E+03
Cs-rem beta	pCi/g	Cs-rem β	2.97E+05	8.65E+04	4.31E+05	2.78E+05	2.50E+05	5.59E+05	3.69E+05	3.77E+05	3.94E+05	1.95E+05
Tc-99	pCi/g	ICP-MS	7.95E+04	5.52E+04	1.36E+05	4.50E+04	6.87E+04	1.70E+05	1.37E+05	1.56E+05	1.01E+05	1.03E+05
F^-	wt %	IC	2.19E-02	1.40E-02	9.62E-03	7.77E-02	4.70E-02	4.55E-02	3.48E-02	2.94E-02	1.03E-01	<4.54E-02
CHO_2^-	wt %	IC	<2.30E-01	<2.37E-01	2.40E-02	<4.44E-01	2.25E-02	2.15E-02	1.74E-02	1.96E-02	1.78E-02	2.06E-02
Cl^-	wt %	IC	<5.30E-02	<5.48E-02	2.88E-02	<8.89E-02	2.04E-02	1.72E-02	1.74E-02	1.96E-02	1.78E-02	2.88E-02
NO_2^-	wt %	IC	1.17E+00	9.54E-01	3.84E+00	2.54E+00	3.00E+00	3.17E+00	2.63E+00	3.25E+00	2.27E+00	4.05E+00
Br^-	wt %	IC	3.51E-02	<2.44E-01	6.73E-02	1.71E-01	3.15E-02	<2.55E-01	<2.23E-01	<2.21E-01	4.81E-02	1.63E-01
NO_3^-	wt %	IC	4.32E+01	5.36E+01	9.60E+00	1.92E+01	2.21E+01	2.64E+01	8.44E+00	7.49E+00	1.64E+01	1.06E+01
PO_4^{3-}	wt %	IC	<4.41E-01	<4.61E-01	<4.78E-01	<4.44E-01	<4.51E-01	<4.55E-01	<4.25E-01	<4.49E-01	<4.38E-01	<4.12E-01
SO_4^{2-}	wt %	IC	3.72E-01	4.52E-01	4.57E-01	5.82E+00	4.22E+00	4.21E+00	2.45E+00	2.04E+00	3.13E+00	1.65E-01
$C_2O_4^{2-}$	wt %	IC	7.70E-02	3.23E-02	3.37E-02	1.84E-01	7.85E-02	6.13E-02	1.53E-01	1.50E-01	2.77E-01	<2.21E-01
CO_3^{2-}	wt %	TIC	3.43E+00	8.34E-01	7.88E-01	2.61E+00	2.32E+00	2.00E+00	1.57E+00	1.34E+00	2.52E+00	9.98E-01
OH^-	wt %	Titration	1.46E+00	1.22E+00	6.31E+00	3.63E+00	5.07E+00	4.41E+00	3.92E+00	5.36E+00	3.61E+00	7.01E+00
AlO_2^-	wt %	Titration	1.56E+00	6.53E+00	1.43E+01	4.32E+00	6.49E+00	9.21E+00	2.73E+01	2.30E+01	1.61E+01	2.80E+00
AlO_2^-	wt %	ICP-ES	6.13E-01	5.62E+00	1.28E+01	1.43E+00	6.61E+00	8.29E+00	2.36E+01	1.35E+01	8.27E+00	1.98E+00
Ag	wt %	ICP-ES	<=5.84E-04	<=5.83E-04	<=5.88E-04	<=6.83E-04	6.32E-04	<=5.46E-04	<=6.50E-04	<=5.86E-04	<=5.35E-04	<=5.55E-04
Al	wt %	ICP-ES	2.81E-01	2.57E+00	5.88E+00	6.55E-01	3.03E+00	3.80E+00	1.08E+01	6.17E+00	3.79E+00	9.05E-01
Ba	wt %	ICP-ES	<8.88E-04	<8.72E-04	<8.97E-04	<9.92E-04	<8.33E-04	<8.19E-04	<=8.98E-04	<=8.57E-04	9.56E-04	<7.93E-04
Ca	wt %	ICP-ES	<1.59E-03	<1.56E-03	<1.60E-03	<1.78E-03	<1.49E-03	<1.46E-03	<1.50E-03	<1.51E-03	<=1.59E-03	<1.41E-03
Ce	wt %	ICP-ES	<=1.78E-02	<=1.87E-02	<=1.89E-02	<=2.14E-02	<=1.77E-02	<=1.73E-02	<=1.77E-02	<=1.69E-02	<=1.79E-02	<=1.71E-02
Cr	wt %	ICP-ES	<7.35E-03	<7.21E-03	1.23E-02	<8.22E-03	1.04E-02	1.72E-02	1.30E-02	1.24E-02	1.20E-02	7.30E-03
Cu	wt %	ICP-ES	<2.87E-04	<2.82E-04	<2.90E-04	<3.21E-04	<2.70E-04	<2.65E-04	<=2.82E-04	<2.72E-04	<2.61E-04	<2.56E-04
Fe	wt %	ICP-ES	3.14E-02	9.48E-03	7.74E-03	1.02E-02	4.96E-03	5.62E-03	1.43E-02	8.49E-03	1.20E-02	3.35E-03
Gd	wt %	ICP-ES	<=6.00E-04	<=6.06E-04	<=6.11E-04	<=6.78E-04	<=6.30E-04	<=5.93E-04	<=6.98E-04	<=6.22E-04	<=6.03E-04	<=6.27E-04
K	wt %	ICP-ES	<3.01E-01	<2.95E-01	<3.04E-01	<3.37E-01	<=3.28E-01	<=2.89E-01	<2.85E-01	<=3.21E-01	<2.74E-01	<2.69E-01
Li	wt %	ICP-ES	4.25E-02	4.68E-02	5.16E-02	5.75E-02	7.05E-02	6.17E-02	6.89E-02	6.46E-02	6.26E-02	5.49E-02
Mn	wt %	ICP-ES	1.54E-03	<=1.88E-04	<=1.66E-04	<=1.48E-04	<=1.59E-04	<=1.49E-04	<=2.71E-04	<=2.28E-04	<=2.35E-04	<=3.54E-04
Na	wt %	ICP-ES	2.17E+01	2.15E+01	1.81E+01	2.21E+01	2.34E+01	2.07E+01	2.03E+01	1.90E+01	1.87E+01	1.44E+01
P	wt %	ICP-ES	8.51E-02	<3.04E-02	9.75E-02	<=4.09E-02	7.21E-02	1.34E-01	6.12E-02	8.09E-02	7.01E-02	<2.76E-02
S	wt %	ICP-ES	1.50E-01	1.85E-01	1.98E-01	1.29E+00	2.19E+00	1.11E+00	9.25E-01	4.08E-01	1.37E+00	7.02E-02
Sb	wt %	ICP-ES	<1.77E-02	<1.74E-02	<1.79E-02	<1.98E-02	<1.66E-02	<1.63E-02	2.18E-02	<1.68E-02	<1.61E-02	<1.58E-02
Si	wt %	ICP-ES	<=2.12E-02	<=1.84E-02	<=1.97E-02	<5.65E-03	<4.73E-03	<=8.25E-03	<=6.20E-03	<=7.55E-03	<4.59E-03	<4.50E-03
Ti	wt %	ICP-ES	<1.52E-04	<1.49E-04	<1.53E-04	<=2.93E-04	<1.43E-04	<1.40E-04	<1.43E-04	<1.44E-04	<1.38E-04	<1.35E-04
Zn	wt %	ICP-ES	4.73E-03	<1.23E-03	2.44E-03	2.40E-03	<=1.83E-03	1.53E-03	<1.19E-03	1.97E-03	1.64E-03	1.65E-02
Cs-133	wt %	ICP-MS	4.75E-04	4.68E-04	1.80E-03	4.96E-04	1.03E-03	2.04E-03	1.42E-03	2.08E-03	9.56E-04	1.66E-03
Mass-135	wt %	ICP-MS	1.33E-04	8.06E-05	2.79E-04	1.05E-04	1.36E-04	3.00E-04	1.88E-04	3.01E-04	1.94E-04	2.52E-04
Mass-137	wt %	ICP-MS	5.69E-04	2.92E-04	9.42E-04	3.73E-04	4.90E-04	9.72E-04	1.12E-03	1.17E-03	1.11E-03	6.93E-04
U-235	wt %	ICP-MS	<4.42E-05	<4.34E-05	<4.46E-05	<4.95E-05	<4.15E-05	<4.09E-05	<4.06E-05	<4.43E-05	<4.02E-05	<4.43E-05
U-238	wt %	ICP-MS	2.49E-03	1.58E-03	8.23E-04	4.21E-03	2.13E-03	1.66E-03	4.40E-03	1.97E-03	5.17E-03	5.50E-04

Figure 8 and Figure 9 contain plots of the results of several of the more significant analytes presented with the vertical axis corresponding to the tank height. This representation uses the data for the "average/best" values listed in Table 8, and the error bars correspond to the standard deviation of repeated analyses. For the saltcake in these undrained segments, soluble components in the as-received saltcake (such as Cs-137 and OH^-) roughly follow the trend in sample moisture content. Also of interest is the relatively high levels of aluminum (reported here as AlO_2^-), with the two analytical methods measuring 13 to 28 wt% AlO_2^- in the two salt slurry samples (FTF-463 and FTF-464). Note again that an underlying assumption is that only the saltcake contained in the samplers represents the tank height, because the free liquid contained in the samplers was not included in this analysis.

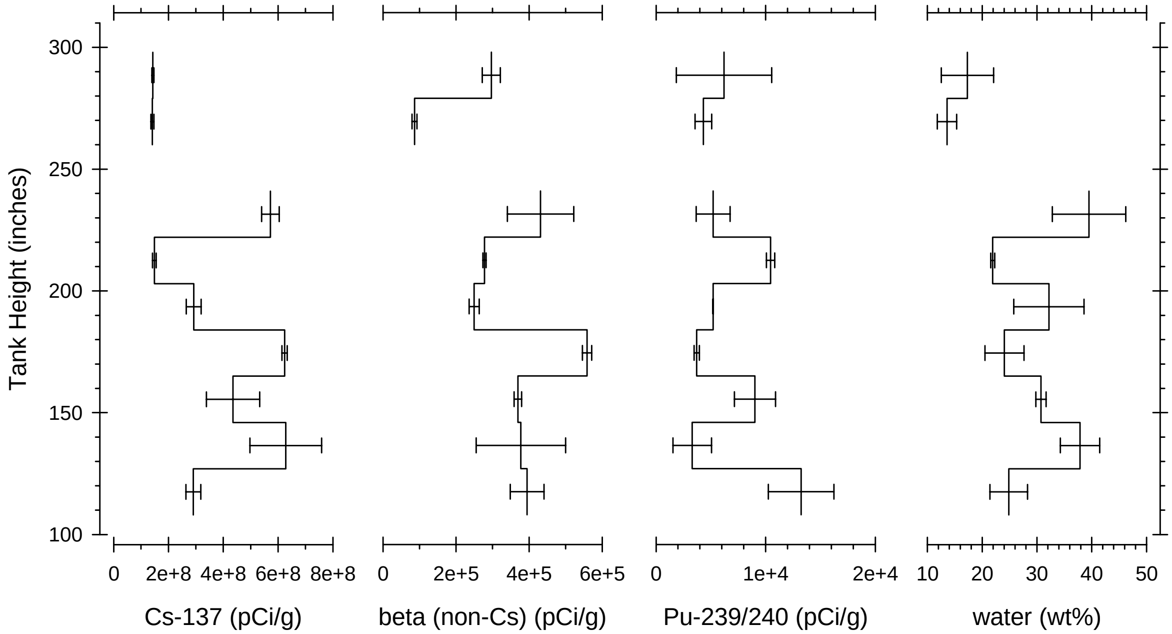

Figure 8: Tank 28F Saltcake Depth Profile of Selected Radioactive Components and Moisture Content.

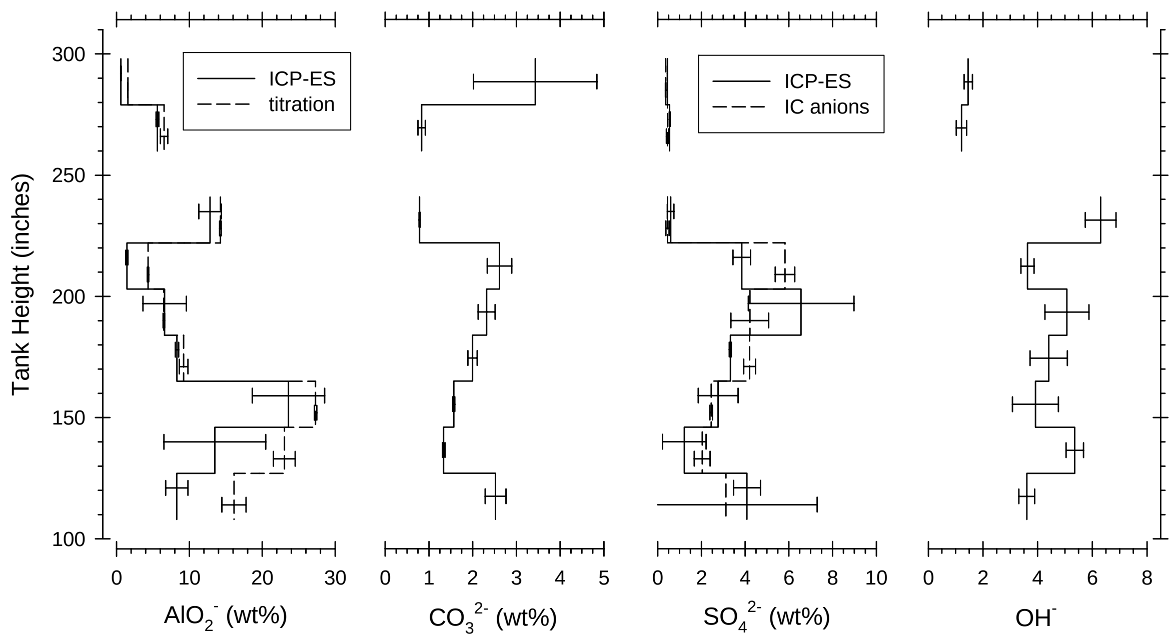

Figure 9: Tank 28F Saltcake Depth Profile of Selected Anions.

The variability charts for each analyte in Appendix A.3 contain additional graphical representations of the data in Table 6 and Table 7, without regard for whether individual results are above or below the lower detection limit. Values for the blanks submitted with samples are also included in the variability charts. For most cases, the reported levels for the blanks correspond to the detection limits and, with comparison to the sample results, indicate how close to the detection limits the actual sample results were.

5.2 Saltcake Segment Statistics

Table 9 and Table 10 contain analyte-by-analyte statistics for the set of saltcake core samples, with each saltcake segment weighted evenly. For each analyte there are two rows: the first, indicated by a 1 in the second column, considers all detectable and below-detectable-level results together; while the second, indicated by a 2 in the second column, considers only the detectable values. For some analytes, which appear grey in the tables, there were not enough above-detectable-level results to determine the statistics. The total variance in analyte measurements are split into two categories, the sample-to-sample (segment-to-segment) variance and the residual (sample preparation and analytical measurement) variance. For the majority of the cases where significant amounts of the data were above the detection limits, the segment-to-segment variance exceeded the preparation/measurement variance. This result can be interpreted that the in-tank variation of most analytes, based on this sample set, is observable and separable from the analytical uncertainty. Some analytes that had a more prominent preparation and measurement variance, such as Na^+, did so because of their consistent level in saltcake.

Appendix A.4 contains a set of analyte-to-analyte bivariate regressions for selected analyte pairings. These data were based on the sample results of Table 8 and include bdl values at their detection limits. For each sample segment, the result for an analyte is plotted against that of another analyte and a linear regression is attempted. Analyte-to-analyte pairings were selected by rejecting pairings that either 1) had >50% of the analyte pairings at bdl, or 2) had |prob| > F values in the F-test of >0.1. Situations with too many bdl values in the regression would indicate false-positive analyte correlations because detection limits for analytes run by the same analytical method or from the same dilution preparation would exhibit a correlation. Several metals are included even though most of the results are bdl due to the presence of a large leverage point that facilitates correlation. For the F-test, the probability that there is not a correlation decreases as the fit gets better. The linear regression equation is provided for each accepted case. Assuming that the same underlying mechanism is present, these equations can be used to infer the quantity of an unknown analyte in future Tank 28F samples if an acceptably correlated analyte is measured. The bivariate cases that are inverse to those shown are not included due to space considerations but would have the same F-test result. For example, both Cs-137 vs. Tc-99 and Tc-99 vs. Cs-137 had identical values for |prob| > F of <0.0001. The equation for Cs-137 as a function of Tc-99 can be determined from the provided equation for Tc-99 as a function of Cs-137.

Several analyte-to-analyte pairings exhibited excellent correlations (e.g. Tc-99 vs. Cs-137). When all samples were examined, there was a large group of analytes that exhibited inter-correlation (Cs-137, Tc-99, Cs-removed Beta, Sb-126, Sn-126, Mass 133, Mass 135, Mass 137, Cr, P, NO_2^-, OH^-, NO_3^-, and moisture content). Other correlations are observed as expected: sulfur (by ICP-ES) with sulfate (by IC), aluminum (by ICP-ES) with aluminate (by titration). Other noteworthy correlations exist between Pu-239/240 and fluoride and between Pu-239/240 and U-238.

The first set of correlations indicate that the highly soluble species tracked together in waste processing operations. The Cs-removed beta appears to be about one-third Tc-99, and the remainder is probably mostly Sr-90. While strontium is considered primarily a sludge component, its total (radioactive + non-radioactive) solubility[5] in salt solution at 5.6 M [Na^+] is around 9 mg/L, so it is conceivable that Sr-90 solubilizes in samples with higher liquid content and contributes to the remaining beta-emitting mixture. Elements at masses 133, 135, and 137 are predominately cesium, with some contribution from barium. These are either currently soluble cesium or were soluble cesium when the waste was disposed in the tank and subsequently converted to barium by decay. The correlation between Cs-137 gamma and mass 133 by ICP-MS is extremely good, and is much better than the correlation with masses 135 or 137. This observation is attributable to the mass 133 contribution being entirely due to cesium, whereas masses 135 and 137 could have some contribution from barium. Although the influent to the tank may have had a variable cesium isotopic ratio due to varying waste age, since both cesium isotopes (137 and 133) are completely soluble, they would have equally distributed in the ~20 years that the tank has been stagnant, as long as there are no pools of liquid that are physically isolated. The mass 135 and 137 would have both cesium and barium contributions, with the barium precipitating in inhomogeneous layers, so the correlation with Cs-137 would never reach a constant ratio.

Antimony (Sb-126) and tin (Sn-126) apparently have a sufficient solubility to track with the other soluble species as well. Chromium is probably present as chromate, which is soluble. Nitrite is soluble in the aqueous phase, even though it could partially crystallize out in some conditions, it is expected to continue to track with the other soluble components. Evidence that nitrite is soluble derives from its linear inverse proportionality to bromide in the free liquid phase. Hydroxide is very soluble, and is present in the interstitial liquid, so it would track with soluble components. A correlation of the soluble species with phosphate is somewhat surprising. This anion is generally insoluble in the highly concentrated salt solutions, and would be expected to be more closely correlated with sludge-like species. The inverse correlation of nitrate with Cs-137 is interesting, but is explained as essentially the opposite of moisture content. As the amount of solids increases (which is mostly sodium nitrate), the amount of liquid phase decreases (which contains most of the cesium).

The nitrite ion concentration is lower (~1 wt%) near the top of the tank than deeper (~3 wt%), and is similar to hydroxide behavior. This observation may be an artifact specific to this tank or caused by the dilution by DSF (see Table 8). As other tanks are sampled, this should be examined to see if it is consistent. It is also seen that there is a surprising amount of aluminate in the samples, particularly the bottom three, which average around 20 wt%. Another observation is that the dark color of FTF-456 is consistent with the analysis showing higher concentrations of Mn and Fe.

Correlations were also observed between Pu-239/240 and fluoride and between Pu-239/240 and U-238. The fluoride correlation is fairly weak and the range of fluoride concentration spans only a factor of about two, so this correlation may or may not be related to a real phenomena. More data would be needed to fully assess. The Pu-238/240 to U-238 correlation is evidently due to their presence together during canyon processing.

It is also interesting to note what is not correlated. There is no correlation between actinides, as measured by ICP-MS or PuTTA and sludge components (Fe, Mn). At this scale, and with an inhomogeneous mixture, there does not appear to be a constant ratio.

The effect of DSF on these results is 2-fold. As can be seen from the bromide analysis, the contamination of the saltcake segment samples by DSF is moderate, with 0.03 to 0.17 wt% versus pure DSF which is 1 wt%. However, this analysis does not convey the amount of solids that were dissolved by the DSF and removed during the free liquid removal step prior to preparing these saltcake samples for analysis.

Table 9: Overall Statistics for Saltcake Segments, Part 1 of 2

Analyte	All Values (1) bdl's Deleted (2)	n	Measured Value	Sample-to-Sample Variance	Residual Variance	Total Variance	% Relative Total Std. Dev.	MS	DoF	95% Confidence Interval for the Mean Lower Limit	95% Confidence Interval for the Mean Upper Limit
Ag (wt%)	1	18	5.98E-04	0.00E+00	6.10E-09	6.10E-09	13.1%	4.59E-09	8	5.61E-04	6.35E-04
Ag (wt%)	2										
Al (wt%)	1	18	4.11E+00	9.29E+00	2.03E+00	1.13E+01	81.9%	2.06E+01	8	1.64E+00	6.57E+00
Al (wt%)	2	18	4.11E+00	9.29E+00	2.03E+00	1.13E+01	81.9%	2.06E+01	8	1.64E+00	6.57E+00
AlO2 (ICP-ES) wt %	1	18	8.97E+00	4.44E+01	9.63E+00	5.40E+01	81.9%	9.84E+01	8	3.58E+00	1.44E+01
AlO2 (ICP-ES) wt %	2	18	8.97E+00	4.44E+01	9.63E+00	5.40E+01	81.9%	9.84E+01	8	3.58E+00	1.44E+01
AlO2 (titration) wt %	1	18	1.21E+01	7.64E+01	6.37E-01	7.71E+01	72.6%	1.54E+02	8	5.36E+00	1.88E+01
AlO2 (titration) wt %	2	18	1.21E+01	7.64E+01	6.37E-01	7.71E+01	72.6%	1.54E+02	8	5.36E+00	1.88E+01
Am-241 (pCi/g)	1	18	1.61E+03	0.00E+00	4.66E+05	4.66E+05	42.3%	4.60E+05	8	1.24E+03	1.98E+03
Am-241 (pCi/g)	2	6	2.16E+03	0.00E+00	6.21E+05	6.21E+05	36.5%	1.54E+05	2	1.47E+03	2.85E+03
Ba (wt%)	1	18	8.90E-04	0.00E+00	7.18E-09	7.18E-09	9.5%	6.15E-09	8	8.47E-04	9.33E-04
Ba (wt%)	2										
Br (wt%)	1	18	1.89E-01	0.00E+00	3.58E-02	3.58E-02	100.0%	1.60E-02	8	1.21E-01	2.58E-01
Br (wt%)	2	6	8.34E-02	5.76E-03	1.22E-05	5.77E-03	91.1%	1.15E-02	2	-1.05E-01	2.72E-01
C2O4 (wt%)	1	18	1.41E-01	1.83E-03	1.13E-02	1.31E-02	81.3%	1.49E-02	8	7.44E-02	2.07E-01
C2O4 (wt%)	2	16	1.27E-01	6.22E-03	4.63E-04	6.68E-03	64.5%	1.29E-02	7	5.95E-02	1.94E-01
Ca (wt%)	1	18	1.56E-03	2.01E-10	1.74E-08	1.76E-08	8.5%	1.78E-08	8	1.49E-03	1.63E-03
Ca (wt%)	2										
Ce (wt%)	1	18	1.82E-02	0.00E+00	4.94E-06	4.94E-06	12.2%	3.48E-06	8	1.72E-02	1.93E-02
Ce (wt%)	2										
CHO2 (wt%)	1	18	2.32E-01	0.00E+00	4.66E-02	4.66E-02	92.9%	2.26E-02	8	1.50E-01	3.14E-01
CHO2 (wt%)	2	2									
Cl (wt%)	1	18	5.43E-02	0.00E+00	1.25E-03	1.25E-03	65.0%	6.10E-04	8	4.09E-02	6.77E-02
Cl (wt%)	2	2									
CO3 (TIC) wt %	1	18	1.94E+00	6.55E-01	2.43E-01	8.98E-01	49.0%	1.55E+00	8	1.26E+00	2.61E+00
CO3 (TIC) wt %	2	18	1.94E+00	6.55E-01	2.43E-01	8.98E-01	49.0%	1.55E+00	8	1.26E+00	2.61E+00
Co-60 (pCi/g)	1	18	1.90E+02	1.99E+02	1.76E+03	1.96E+03	23.3%	2.15E+03	8	1.65E+02	2.15E+02
Co-60 (pCi/g)	2										
Cr (wt%)	1	18	1.11E-02	7.00E-06	6.69E-06	1.37E-05	33.3%	2.00E-05	8	8.68E-03	1.35E-02
Cr (wt%)	2	12	1.29E-02	3.78E-07	9.81E-06	1.02E-05	24.8%	1.00E-05	5	1.05E-02	1.52E-02
Cs-137 (pCi/g)	1	18	3.64E+08	4.11E+16	3.26E+15	4.44E+16	57.8%	8.50E+16	8	2.06E+08	5.23E+08
Cs-137 (pCi/g)	2	18	3.64E+08	4.11E+16	3.26E+15	4.44E+16	57.8%	8.50E+16	8	2.06E+08	5.23E+08
Cs-rem beta (pCi/g)	1	18	3.38E+05	1.60E+10	2.93E+09	1.89E+10	40.7%	3.50E+10	8	2.36E+05	4.40E+05
Cs-rem beta (pCi/g)	2	18	3.38E+05	1.60E+10	2.93E+09	1.89E+10	40.7%	3.50E+10	8	2.36E+05	4.40E+05
Cu (wt%)	1	18	2.81E-04	1.46E-10	3.55E-10	5.01E-10	8.0%	6.50E-10	8	2.67E-04	2.95E-04
Cu (wt%)	2										
Eu-154 (pCi/g)	1	18	2.72E+02	5.06E+03	1.40E+03	6.47E+03	29.5%	1.15E+04	8	2.14E+02	3.31E+02
Eu-154 (pCi/g)	2										
F (wt%)	1	18	6.08E-02	0.00E+00	9.66E-04	9.66E-04	51.1%	6.60E-04	8	4.68E-02	7.48E-02
F (wt%)	2	8	6.82E-02	7.37E-04	1.37E-05	7.51E-04	40.2%	1.49E-03	3	2.47E-02	1.12E-01
Fe (wt%)	1	18	1.16E-02	4.82E-05	3.08E-05	7.89E-05	76.9%	1.30E-04	8	5.36E-03	1.78E-02
Fe (wt%)	2	18	1.16E-02	4.82E-05	3.08E-05	7.89E-05	76.9%	1.30E-04	8	5.36E-03	1.78E-02
Gd (wt%)	1	18	6.27E-04	0.00E+00	1.08E-08	1.08E-08	16.6%	2.72E-09	8	5.99E-04	6.55E-04
Gd (wt%)	2										
K (wt%)	1	18	3.04E-01	0.00E+00	1.01E-03	1.01E-03	10.5%	8.90E-04	8	2.87E-01	3.20E-01
K (wt%)	2										
Li (wt%)	1	18	5.85E-02	0.00E+00	2.13E-04	2.13E-04	25.0%	1.90E-04	8	5.10E-02	6.60E-02
Li (wt%)	2	18	5.85E-02	0.00E+00	2.13E-04	2.13E-04	25.0%	1.90E-04	8	5.10E-02	6.60E-02

Table 10: Overall Statistics for Saltcake Segments, Part 2 of 2

Analyte	All Values (1) DLs Deleted (2)	n	Measured Value	Sample-to-Sample Variance	Residual Variance	Total Variance	% Relative Total Std. Dev.	MS	DoF	95% Confidence Interval for the Mean Lower Limit	Upper Limit
Cs-133 (wt%)	1	18	1.20E-03	4.22E-07	3.66E-08	4.59E-07	56.7%	8.81E-07	8	6.85E-04	1.71E-03
Cs-133 (wt%)	2	18	1.20E-03	4.22E-07	3.66E-08	4.59E-07	56.7%	8.81E-07	8	6.85E-04	1.71E-03
Mass-135 (wt%)	1	18	1.88E-04	6.97E-09	1.37E-09	8.33E-09	48.6%	1.53E-08	8	1.21E-04	2.55E-04
Mass-135 (wt%)	2	14	2.15E-04	5.58E-09	1.55E-09	7.13E-09	39.3%	1.27E-08	6	1.41E-04	2.89E-04
Mass-137 (wt%)	1	16	8.08E-04	1.26E-07	1.16E-08	1.37E-07	45.9%	2.63E-07	7	5.05E-04	1.11E-03
Mass-137 (wt%)	2	16	8.08E-04	1.26E-07	1.16E-08	1.37E-07	45.9%	2.63E-07	7	5.05E-04	1.11E-03
U-235 (wt%)	1	18	4.33E-05	3.18E-12	1.06E-11	1.38E-11	8.6%	1.70E-11	8	4.10E-05	4.55E-05
U-235 (wt%)	2										
U-238 (wt%)	1	18	2.72E-03	2.05E-06	4.01E-07	2.45E-06	57.7%	4.51E-06	8	1.56E-03	3.87E-03
U-238 (wt%)	2	18	2.72E-03	2.05E-06	4.01E-07	2.45E-06	57.7%	4.51E-06	8	1.56E-03	3.87E-03
Mn (wt%)	1	18	3.42E-04	1.63E-07	7.82E-08	2.41E-07	143.6%	4.04E-07	8	-3.47E-06	6.87E-04
Mn (wt%)	2	2									
Na (wt%)	1	16	2.02E+01	0.00E+00	5.13E+00	5.13E+00	11.2%	4.58E+00	7	1.90E+01	2.15E+01
Na (wt%)	2	16	2.02E+01	0.00E+00	5.13E+00	5.13E+00	11.2%	4.58E+00	7	1.90E+01	2.15E+01
NO2 (wt%)	1	18	2.54E+00	8.79E-01	5.91E-02	9.38E-01	38.2%	1.82E+00	8	1.80E+00	3.27E+00
NO2 (wt%)	2	18	2.54E+00	8.79E-01	5.91E-02	9.38E-01	38.2%	1.82E+00	8	1.80E+00	3.27E+00
NO3 (wt%)	1	14	1.56E+01	4.74E+01	1.33E+01	6.07E+01	49.8%	1.08E+02	6	8.85E+00	2.24E+01
NO3 (wt%)	2	14	1.56E+01	4.74E+01	1.33E+01	6.07E+01	49.8%	1.08E+02	6	8.85E+00	2.24E+01
OH (wt%)	1	18	3.89E+00	2.72E+00	2.70E-01	2.99E+00	44.5%	5.71E+00	8	2.59E+00	5.18E+00
OH (wt%)	2	18	3.89E+00	2.72E+00	2.70E-01	2.99E+00	44.5%	5.71E+00	8	2.59E+00	5.18E+00
P (wt%)	1	18	7.47E-02	7.05E-04	4.66E-04	1.17E-03	45.8%	1.88E-03	8	5.11E-02	9.82E-02
P (wt%)	2	14	8.58E-02	2.94E-04	5.89E-04	8.83E-04	34.6%	1.18E-03	6	6.33E-02	1.08E-01
PO4 (wt%)	1	18	4.49E-01	0.00E+00	6.22E-04	6.22E-04	5.6%	4.60E-04	8	4.37E-01	4.61E-01
PO4 (wt%)	2										
Pu-238 (pCi/g)	1										
Pu-238 (pCi/g)	2										
Pu-239/240 (pCi/g)	1	18	6.75E+03	9.54E+06	4.23E+06	1.38E+07	55.0%	2.33E+07	8	4.12E+03	9.37E+03
Pu-239/240 (pCi/g)	2	18	6.75E+03	9.54E+06	4.23E+06	1.38E+07	55.0%	2.33E+07	8	4.12E+03	9.37E+03
S (wt%)	1	18	8.68E-01	4.33E-01	1.02E-01	5.35E-01	84.2%	9.69E-01	8	3.33E-01	1.40E+00
S (wt%)	2	18	8.68E-01	4.33E-01	1.02E-01	5.35E-01	84.2%	9.69E-01	8	3.33E-01	1.40E+00
Sb (wt%)	1	18	1.78E-02	1.53E-06	3.89E-06	5.42E-06	13.1%	6.95E-06	8	1.64E-02	1.92E-02
Sb (wt%)	2	2									
Sb-126 (pCi/g)	1	18	2.25E+03	9.80E+05	4.49E+05	1.43E+06	53.2%	2.41E+06	8	1.40E+03	3.09E+03
Sb-126 (pCi/g)	2	18	2.25E+03	9.80E+05	4.49E+05	1.43E+06	53.2%	2.41E+06	8	1.40E+03	3.09E+03
Si (wt%)	1	18	1.07E-02	0.00E+00	1.25E-04	1.25E-04	104.5%	1.00E-04	8	5.26E-03	1.61E-02
Si (wt%)	2										
Sn-126 (pCi/g)	1	18	2.82E+03	1.34E+06	4.31E+05	1.77E+06	47.2%	3.11E+06	8	1.86E+03	3.78E+03
Sn-126 (pCi/g)	2	12	2.76E+03	0.00E+00	3.04E+05	3.04E+05	20.0%	2.95E+05	5	2.35E+03	3.16E+03
SO4 (wt%)	1	18	2.57E+00	2.77E+00	2.06E+00	4.83E+00	85.5%	7.60E+00	8	1.07E+00	4.07E+00
SO4 (wt%)	2	18	2.57E+00	2.77E+00	2.06E+00	4.83E+00	85.5%	7.60E+00	8	1.07E+00	4.07E+00
Tc (pCi/g)	1	18	1.18E+05	6.27E+08	8.52E+08	1.48E+09	32.6%	2.11E+09	8	9.28E+04	1.43E+05
Tc (pCi/g)	2	10	1.40E+05	6.33E+08	9.66E+07	7.29E+08	19.3%	1.36E+09	4	1.08E+05	1.73E+05
Ti (wt%)	1	18	1.61E-04	6.66E-10	3.55E-09	4.22E-09	40.3%	4.88E-07	8	-2.19E-04	5.41E-04
Ti (wt%)	2										
Zn (wt%)	1	18	2.10E-03	1.11E-06	1.13E-07	1.22E-06	52.6%	2.34E-06	8	1.27E-03	2.94E-03
Zn (wt%)	2	12	2.45E-03	1.38E-06	1.82E-08	1.40E-06	48.3%	2.78E-06	5	1.21E-03	3.69E-03

5.3 Implication to Tank Characterization

The contents of the samples lead to questions about the proper application of this data set to characterize the in-tank contents. No adjustment is made to the data to account for two factors: 1) the free liquid in the samples and 2) the possibility of salt dissolution or dilution by contact with DSF during sampling.

Many of the samples contained large amounts of FL. Of the samplers that contained saltcake, Sample FTF-457 contained the least contribution of FL (12%) to the over all segment mass. Seven of the other eight samplers that contained saltcake had FL contributions of 50% to 90% of the segment mass. The analysis in this report assumes that only the salt contained in the as-received samples represents the in-tank state of the material at a specific tank level. The presence of FL is assumed to be caused by a partial blockage of the sampler tip and difficulty sampling a loose salt material. The sampler could act as a straw as the piston is drawn up, sucking interstitial liquid and drill string materials into the sampler instead of saltcake. Based on this assumption, the FL is entering the sampler instead of saltcake that existed at the point of sampling. Thus, we are justified in ignoring the relatively large amount of liquid in our characterization analysis.

An alternative explanation for the FL in the samples, which cannot be proved or disproved by the sample analysis, is that pockets of liquid exist within the saltcake. Tank 28F may contain subsurface horizontal lenses of liquid. Tank 28F saltcake may contain vertical regions, perhaps far away from cooling coils, that never formed a consolidated saltcake material over. Both of these behaviors would likely be localized. If liquid regions span the entire tank, it would be appropriate to combine the FL analysis with the saltcake segment analysis, resulting in saltcake characterization that would more closely resemble tank supernate. Adding the FL results back to the saltcake segment analysis would result in levels of soluble radionuclides (Cs-137 and Tc-99) that are significantly higher than those reported herein. This alternative explanation, however, differs conceptually from how saltcake is envisioned at SRS. Information from different characterization methods, such as a tank-well gamma monitor, would be required to determine in-tank levels of soluble radionuclides if such liquid regions exist.

The effect of the DSF on the Cs-137 content is difficult to quantify. Each sample has a varying quantity of DSF, and the original composition of each can only be estimated based on assumptions about the initial concentration of one species or the expansion volume upon dissolution of saltcake. It is also not known where the free liquid in each segment came from, or whether it dissolved saltcake in the tank prior to sampling or after the sample was collected. It is clear that DSF has potential to dilute the interstitial liquid, dissolve saltcake, and change the % liquid in the saltcake samples. See Appendix A.2 for further discussion of the effect of the DSF on sample results and potential methods for adjusting the results contained in this report.

6 Saltcake Composite Dissolution Test and Analysis

6.1 Saltcake Composite Formulation

Due to the varied amounts of saltcake contained within the individual saltcake segments, the task plan called for the composite to be made from approximately equal percentages of the saltcake contained within each segment. In order to create a composite of near the desired size in the absence of completely filled samples, approximately 50% of the saltcake in each sample segment was used. Table 11 contains the mass of each segment added to the composite and the corresponding percentage of the composite attributable to each segment. Upon homogenizing and equilibration of the composite (see Figure 10), additional liquid was supernatant to the saltcake. This supernatant liquid was decanted and held for analysis separately as the composite supernatant material. From the 416.5 grams of Tank 28F saltcake composite originally formulated, 81.9 grams were removed as supernatant liquid, resulting in the final saltcake composite mass of 334.6 grams.

Table 11: Contribution of Each Tank 28F Saltcake Segment to the Overall Composite

Sample	Composite Mass (g)	% of Composite
FTF-456	15.2	3.7%
FTF-457	118.1	28.4%
FTF-459	11.6	2.8%
FTF-460	31.0	7.4%
FTF-461	118.5	28.5%
FTF-462	35.1	8.4%
FTF-463	7.0	1.7%
FTF-464	16.5	4.0%
FTF-465	63.4	15.2%

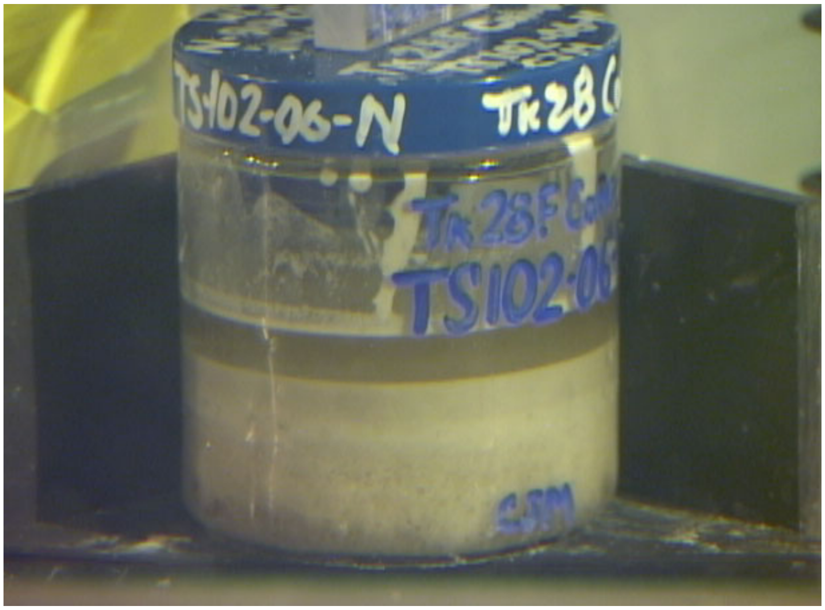

Figure 10: Tank 28F Overall Undrained Saltcake composite, Prior To Decanting Supernatant Liquid and Re-Homogenizing Salt

6.2 Dissolution Test

The dissolution test was a single-batch test where de-ionized water was added to the saltcake composite at a 4:1 mass ratio of water to salt. Nominally, 50 gram portions of the undrained, homogenized saltcake composite followed by 200 grams of water were added to each of three 25- mL centrifuge tubes. This mixture was shaken and allowed to equilibrate for approximately one day, with the majority of the salt dissolution evident within the first hour. The dissolution period was followed by centrifuging of the 250-mL tubes, but the solid-liquid separation appeared incomplete due to the cloudiness of the supernate after several periods of centrifuging. We determined the cause of the incomplete separation to be the first time use of this centrifuge rotor/bucket/250-mL-tube combination. Each of the three sets of material in the 250-mL tubes was split out into five 50-mL tubes, for a total of fifteen subsamples. The solid-liquid separation was accomplished and clear supernatant solutions were decanted and recombined into the three original dissolution batches. The nominal cell temperature during salt dissolution was 25 to 30 °C. The total equilibration time, due to the delay in solid-liquid separation, was five days. Table 12 contains a summary of the materials used and formed during the dissolution testing of the Tank 28F saltcake composite.

Table 12: Summary of Dissolution Test of Undrained Tank 28F Saltcake Composite

Saltcake Used	151.3	grams
Water Used	612.0	grams
Dissolved Salt	762.7	grams
Residual Solids	0.721	grams
Water/Salt	4.04	g/g
Solids/Salt	0.0048	g/g
Solution/Salt	5.04	g/g

6.3 Analysis of Soluble Fraction (Suite SC)

Table 13, Table 14, and Table 15 contain the analytical results for the preparations of each of the three as-dissolved saltcake solutions (see the previous section for dissolution details). The averages and standard deviations of the analytes are presented for the as-dissolved solution. Due to the relatively large water-to-salt ratio used in the dissolution testing, the as-dissolved solution had a sodium content of only 2.21 M, which is far below the solution concentration that will be sent to down-stream processes. To adjust for the low sodium content of this solution, the tables contain a second set of average results adjusted to a 6.0 M sodium solution. The conversion to a 6.0 M sodium stream is performed mathematically only, thus the results for the 6.0 M stream will indicate some components at levels above their solubility. This set of results is, however, useful for comparison to the requirements of down stream processes. Additionally, the average results are presented on the basis of the original saltcake composite material prior to the dissolution testing. These results are useful for setting in-tank average concentrations of saltcake components and for comparison with the saltcake segment results presented in Section 5.

The two right-most columns in Table 13, Table 14, and Table 15 correspond to two separate materials that should most closely represent interstitial liquid within the tank. The first of these two columns is the single result for the analysis of the supernate that formed upon homogenization of the saltcake composite. This material would likely be identical to the interstitial liquid contained in the saltcake composite. No interstitial-liquid draining was performed for the Tank 28F saltcake composite, so the results for this material will give insight into the interpretation of the composite dissolution data. The second column is the FL contained in sample FTF-462. This material had the lowest Br^- and highest Cs-137 content of all the FL samples analyzed in this set, and thus it is the most representative of Tank 28F interstitial liquid. As seen in Table 3, the FL from FTF-462 was estimated to have only 2 wt% drill-sting fluid as determined by Br^- tracer content, indicating that it is likely mostly saltcake interstitial liquid that drained into the drill-string or the sampler itself during the sampling process.

The dissolved saltcake samples contained small amounts of Br^- (average of 112 mg/L), which likely originated from drill string tracer fluid. Note that the results in the tables of this section do not contain any adjustment for the amount of drill-string fluid that might have been contained in the samples. Appendix A.2 contains a discussion of potential methods to back-calculate saltcake sample component results when drill string fluid has apparently dissolved a portion of the sample.

The soluble portion of the saltcake had few quantifiable radionuclides present for the analytical methods that were used in this testing. Adjusted to a 6 M sodium solution basis, the dissolved salt averaged 9.94E+07pCi/mL (0.38 Ci/gal) Cs-137 and 2.38E+4 pCi/mL of Tc-99. The Cs-removed Beta measurement averaged 1.41E+05 pCi/mL, which is not supported by the results of other individual radionuclides. The other measured isotopes were smaller quantities of Sr-90, Sb-126, Sn-126, U-238, Pu-238, and Cm-244. The Cm-244 result was highly variable, indicating that its source might be either contamination or incomplete solid-liquid separation. The soluble alpha activity, taken as the sum of the above and below detectable quantities of Pu-238, Pu-239/240, Am-241, and Cm-244, totaled 8.87E+03 pCi/mL. Note that the highly variable Cm-244 value contributed to over half of this total alpha value.

The use of data for the soluble radionuclides (Cs-137 and Tc-99) in the saltcake composite relies on the same assumptions and has the same implications as those discussed in Section 5.3. First, if pockets of liquid exist within the actual tank saltcake, the reported values for Cs-137 and Tc-99 would under predict the actual levels that would be obtained during in-tank dissolution. Second, contact of DSF with the sample during sampling may have washed or diluted some Cs-137 and Tc-99 from the remaining portion of solid salts, again biasing our dissolution results low. Appendix A.2 contains a discussion of the application of the DSF estimates to adjust the data of this report. Third, there is an important additional circumstance specific to the composite dissolution test that is separate from those discussed in Section 5.3. The supernate that formed during sample compositing and that was subsequently removed effectively lowered the moisture content (and thus the interstitial liquid content) of the remaining saltcake composite. As seen in Table 5, moisture content for the Tank 28F saltcake composite was 15.4 wt% (st. dev. = 1.2 wt%, n = 6), which is in line with previous saltcake samples from other tanks[4] but is relatively low when compared with the Tank 28F saltcake segments. If the supernatant liquid formed during compositing would have been mixed into the saltcake and included in the analysis, the moisture content would have been 22.6 wt%. Likewise, the results for all soluble components, such as Cs-137, would need to be multiplied by a factor of 1.47 to reflect the inclusion of the supernatant liquid.

The FL in sample FTF-462 had a Cs-137 content of 1.33E+09 pCi/mL (5.03 Ci/gal). The supernate that formed on the saltcake composite had a Cs-137 content of 1.04E+09 pCi/mL (3.95 Ci/gal). The more in-depth analysis of the FL from FTF-462 is consistent with the initial Cs-137 and anions characterization in Section 4.

Table 13: Radionuclide Analysis of the Soluble Portion of the Tank 28F Composite

Analyte	Method	pCi/mL in As-Dissolved Solution					pCi/mL Adjusted to 6M Na^+ Solution		pCi/g of Saltcake		Free Liquid (pCi/mL)	
		Prep 1	Prep 2	Prep 3	Average	St.Dev.	Average	St.Dev.	Average	St.Dev.	FTF-462	Composite
C-14	C-14	<1.29E+03	<1.40E+03	<1.90E+03	<1.53E+03	--	<4.15E+03	--	<6.81E+03	--	<1.56E+04	--
Al-26	Cs-rem. Gamma	<5.28E+01	<3.13E+01	<3.47E+01	<3.96E+01	--	<1.07E+02	--	<1.76E+02	--	<1.76E+02	<1.99E+02
Co-60	Cs-rem. Gamma	<9.06E+01	<4.13E+01	<5.01E+01	<6.07E+01	--	<1.64E+02	--	<2.70E+02	--	<2.83E+02	<2.31E+02
Se-79	Se-79	<1.24E+03	<2.44E+03	<6.13E+02	<1.43E+03	--	<3.87E+03	--	<6.36E+03	--	<1.76E+04	--
Sr-90	Sr-90	6.82E+02	1.91E+03	6.91E+02	1.09E+03	7.0E+02	2.95E+03	1.88E+03	4.85E+03	3.09E+03	6.42E+03	--
Nb-94	Cs-rem. Gamma	<7.86E+01	<4.46E+01	<4.71E+01	<5.68E+01	--	<1.54E+02	--	<2.53E+02	--	<2.23E+02	<1.96E+02
Tc-99	ICP-MS	9.58E+03	8.10E+03	8.70E+03	8.79E+03	7.5E+02	2.38E+04	2.1E+03	3.92E+04	3.4E+03	2.32E+05	1.99E+05
Ru-106	Cs-rem. Gamma	<4.70E+02	<2.91E+02	<3.20E+02	<3.60E+02	--	<9.76E+02	--	<1.60E+03	--	<1.62E+03	<1.38E+03
Sb-125	Cs-rem. Gamma	<2.32E+02	<1.30E+02	<1.31E+02	<1.64E+02	--	<4.45E+02	--	<7.32E+02	--	<6.68E+02	<6.37E+02
Sb-126	Cs-rem. Gamma	4.45E+02	4.61E+02	4.30E+02	4.45E+02	1.6E+01	1.21E+03	3E+01	1.98E+03	5E+01	2.66E+03	1.24E+03
Sn-126	Cs-rem. Gamma	5.13E+02	5.87E+02	5.15E+02	5.38E+02	4.2E+01	1.46E+03	1.0E+02	2.40E+03	1.7E+02	3.73E+03	1.33E+03
I-129	I-129	<4.45E+01	<1.07E+02	<4.76E+01	<6.64E+01	--	<1.79E+02	--	<2.95E+02	--	1.36E+02	--
Cs-134	Gamma	<1.80E+04	<1.96E+04	<1.96E+04	<1.91E+04	--	<5.17E+04	--	<8.49E+04	--	<1.32E+05	<1.28E+05
Cs-137	Gamma	3.82E+07	3.57E+07	3.62E+07	3.67E+07	1.3E+06	9.94E+07	3.7E+06	1.63E+08	6E+06	1.33E+09	1.04E+09
Ce-144	Cs-rem. Gamma	<5.08E+02	<2.16E+02	<2.20E+02	<3.15E+02	--	<8.52E+02	--	<1.40E+03	--	<1.43E+03	<9.97E+02
Eu-154	Cs-rem. Gamma	<1.46E+02	<6.30E+01	<6.61E+01	<9.18E+01	--	<2.49E+02	--	<4.09E+02	--	<3.90E+02	<2.85E+02
Eu-155	Cs-rem. Gamma	<2.81E+02	<1.13E+02	<1.18E+02	<1.70E+02	--	<4.61E+02	--	<7.58E+02	--	<7.69E+02	<4.34E+02
Th-230	ICP-MS	<4.66E+02	<4.54E+02	<4.55E+02	<4.59E+02	--	<1.24E+03	--	<2.04E+03	--	<2.65E+03	<2.41E+03
Th-232	ICP-MS	<6.06E-03	<5.90E-03	<5.92E-03	<5.96E-03	--	<1.62E-02	--	<2.65E-02	--	<3.44E-02	<3.13E-02
U-233	ICP-MS	<2.14E+02	<2.08E+02	<2.09E+02	<2.10E+02	--	<5.70E+02	--	<9.37E+02	--	<1.22E+03	<1.10E+03
U-234	ICP-MS	<1.38E+02	<1.35E+02	<1.35E+02	<1.36E+02	--	<3.68E+02	--	<6.05E+02	--	<7.85E+02	<7.13E+02
U-235	ICP-MS	<4.78E-02	<4.65E-02	<4.67E-02	<4.70E-02	--	<1.27E-01	--	<2.09E-01	--	<2.71E-01	<2.47E-01
U-236	ICP-MS	<1.43E+00	<1.39E+00	<1.40E+00	<1.41E+00	--	<3.81E+00	--	<6.26E+00	--	<8.12E+00	<7.38E+00
Np-237	ICP-MS	<1.56E+01	<1.52E+01	<1.52E+01	<1.53E+01	--	<4.15E+01	--	<6.82E+01	--	<8.85E+01	<8.04E+01
U-238	ICP-MS	7.71E-02	6.75E-02	8.02E-02	7.49E-02	6.7E-03	2.03E-01	2.0E-02	3.34E-01	3.2E-02	2.75E-01	5.23E-01
Pu-238	PuTTA	<3.95E+01	1.70E+03	<3.04E+02	<=6.82E+02	--	<=1.84E+03	--	<=3.02E+03	--	<2.94E+03	<1.90E+03
Pu-239/240	PuTTA	<5.13E+01	<2.07E+02	<5.11E+02	<2.56E+02	--	<6.97E+02	--	<1.15E+03	--	<7.16E+02	<2.62E+03
Pu-239	ICP-MS	<1.37E+03	<1.34E+03	<1.34E+03	<1.35E+03	--	<3.66E+03	--	<6.02E+03	--	<7.81E+03	<7.09E+03
Pu-240	ICP-MS	<5.04E+03	<4.91E+03	<4.92E+03	<4.95E+03	--	<1.34E+04	--	<2.21E+04	--	<2.86E+04	<2.60E+04
Pu-241	Pu-241	<5.48E+04	<1.84E+04	<1.09E+04	<2.80E+04	--	<7.57E+04	--	<1.24E+05	--	<1.12E+05	<1.15E+05
Pu-242	ICP-MS	<8.44E+01	<8.22E+01	<8.24E+01	<8.30E+01	--	<2.25E+02	--	<3.70E+02	--	<4.80E+02	<4.36E+02
Am-241	Am/Cm	<2.06E+02	<1.25E+03	<3.34E+02	<5.95E+02	--	<1.61E+03	--	<2.64E+03	--	<6.00E+03	--
Am-241	Cs-rem. Gamma	<4.40E+02	<5.58E+02	<2.50E+02	<4.16E+02	--	<1.12E+03	--	<1.85E+03	--	<1.33E+03	<1.12E+03
Am-243	Am/Cm	<9.16E+01	<3.51E+02	<1.61E+02	<2.01E+02	--	<5.44E+02	--	<8.94E+02	--	<2.45E+03	--
Am-243	Cs-rem. Gamma	<1.77E+02	<6.59E+01	<6.52E+01	<1.03E+02	--	<2.78E+02	--	<4.57E+02	--	<4.38E+02	<3.85E+02
Am-242m	Am/Cm	<1.18E+03	<4.90E+03	<1.89E+03	<2.66E+03	--	<7.18E+03	--	<1.18E+04	--	<3.59E+04	--
Cm-243	Am/Cm	<3.02E+02	<1.26E+03	<4.85E+02	<6.81E+02	--	<1.84E+03	--	<3.02E+03	--	<9.17E+03	--
Cm-245	Am/Cm	<2.47E+02	<1.03E+03	<3.99E+02	<5.58E+02	--	<1.51E+03	--	<2.48E+03	--	<7.52E+03	--
Cm-247	Am/Cm	<3.19E+02	<1.68E+03	<5.35E+02	<8.46E+02	--	<2.28E+03	--	<3.75E+03	--	<1.17E+04	--
Cf-249	Am/Cm	<2.84E+02	<1.78E+03	<4.78E+02	<8.49E+02	--	<2.29E+03	--	<3.76E+03	--	<1.19E+04	--
Cf-251	Am/Cm	<3.10E+02	<1.30E+03	<5.40E+02	<7.17E+02	--	<1.94E+03	--	<3.18E+03	--	<8.63E+03	--
Cm-242	Am/Cm	<5.08E+00	<9.55E+00	<8.66E+00	<7.76E+00	--	<2.10E+01	--	<3.46E+01	--	<1.93E+02	--
Cm-244	Am/Cm	<5.13E+01	4.62E+03	5.93E+02	<=1.75E+03	--	<=4.72E+03	--	<=7.77E+03	--	2.97E+03	--
Cm-245	Cs-rem. Gamma	<6.87E+02	<2.89E+02	<2.97E+02	<4.24E+02	--	<1.15E+03	--	<1.89E+03	--	<1.79E+03	<1.35E+03
non-Cs Beta	Cs-rem. Beta	5.18E+04	5.43E+04	5.01E+04	5.21E+04	2.1E+03	1.41E+05	5E+03	2.32E+05	8E+03	5.12E+05	3.49E+05

Table 14: Other Metal and Mass Analysis of the Soluble Portion of the Tank 28F Composite

Analyte	Method	mg/L in As-Dissolved Solution					mg/L Adjusted to 6M Na^+ Solution		g/100g of Saltcake		Free Liquid (mg/L)	
		Prep 1	Prep 2	Prep 3	Average	St.Dev.	Average	St.Dev.	Average	St.Dev.	FTF-462	Composite
Ag	ICP-ES	<4.72E+00	<4.60E+00	<4.61E+00	<4.64E+00	--	<1.26E+01	--	<2.07E-03	--	<2.44E+01	<2.68E+01
Al	ICP-ES	5.38E+03	5.45E+03	5.20E+03	5.34E+03	1.3E+02	1.45E+04	2E+02	2.38E+00	4E-02	2.62E+04	1.49E+04
As	AA	<3.05E-01	<2.95E-01	<2.98E-01	<2.99E-01	--	<8.11E-01	--	<1.33E-04	--	<1.65E+00	<1.69E+00
B	ICP-ES	<1.02E+01	<9.94E+00	<9.96E+00	<1.00E+01	--	<2.72E+01	--	<4.47E-03	--	<5.26E+01	<5.80E+01
Ba	ICP-ES	<2.52E+00	<2.45E+00	<2.46E+00	<2.48E+00	--	<6.71E+00	--	<1.10E-03	--	<1.30E+01	<1.43E+01
Ca	ICP-ES	<6.48E+00	<6.31E+00	<6.33E+00	<6.37E+00	--	<1.73E+01	--	<2.84E-03	--	<3.34E+01	<3.68E+01
Cd	ICP-ES	<6.75E+00	<6.58E+00	<6.60E+00	<6.64E+00	--	<1.80E+01	--	<2.96E-03	--	<3.49E+01	<3.84E+01
Ce	ICP-ES	<3.35E+01	<3.26E+01	<3.27E+01	<3.29E+01	--	<8.92E+01	--	<1.47E-02	--	<1.73E+02	<1.90E+02
Co	ICP-MS	<2.21E-02	<2.15E-02	<2.16E-02	<2.17E-02	--	<5.89E-02	--	<9.68E-06	--	<1.14E-01	<1.26E-01
Cr	ICP-ES	<1.20E+01	<1.17E+01	<1.18E+01	<1.18E+01	--	<3.21E+01	--	<5.28E-03	--	6.56E+01	1.72E+02
Cs-133	ICP-MS	1.17E+00	1.20E+00	1.16E+00	1.18E+00	2E-02	3.19E+00	4E-02	5.25E-04	7E-06	4.10E+01	3.35E+01
Cu	ICP-ES	<3.79E+00	<3.69E+00	<3.70E+00	<3.73E+00	--	<1.01E+01	--	<1.66E-03	--	<1.96E+01	<2.15E+01
Fe	ICP-ES	<4.75E+00	<4.63E+00	<4.64E+00	<4.67E+00	--	<1.27E+01	--	<2.08E-03	--	2.62E+01	3.60E+01
Gd	ICP-ES	<5.61E+00	<5.47E+00	<5.48E+00	<5.52E+00	--	<1.50E+01	--	<2.46E-03	--	<2.90E+01	<3.19E+01
Hg	CVAA	<1.22E+00	<1.18E+00	<1.19E+00	<1.20E+00	--	<3.24E+00	--	<5.33E-04	--	<6.61E+00	<6.74E+00
K	ICP-ES	2.31E+02	1.66E+02	1.65E+02	1.87E+02	3.8E+01	5.07E+02	1.01E+02	8.34E-02	1.66E-02	4.47E+03	5.53E+03
K	AA	1.83E+02	1.57E+02	1.60E+02	1.67E+02	1.4E+01	4.52E+02	3.8E+01	7.42E-02	6.2E-03	4.23E+03	4.68E+03
La	ICP-ES	<1.10E+01	<1.07E+01	<1.07E+01	<1.08E+01	--	<2.93E+01	--	<4.81E-03	--	<5.67E+01	<6.24E+01
Li	ICP-ES	<5.33E+00	<5.19E+00	<5.20E+00	<5.24E+00	--	<1.42E+01	--	<2.33E-03	--	<2.75E+01	<3.03E+01
Mg	ICP-ES	<9.45E+00	<9.20E+00	<9.23E+00	<9.29E+00	--	<2.52E+01	--	<4.14E-03	--	<4.88E+01	<5.37E+01
Mn	ICP-ES	<5.82E+00	<5.67E+00	<5.69E+00	<5.73E+00	--	<1.55E+01	--	<2.55E-03	--	<3.01E+01	<3.31E+01
Mo	ICP-ES	<3.47E+01	<3.38E+01	<3.39E+01	<3.41E+01	--	<9.25E+01	--	<1.52E-02	--	<1.79E+02	<1.97E+02
Na	ICP-ES	5.11E+04	5.14E+04	5.04E+04	5.09E+04	5E+02	1.38E+05	0E+00	2.27E+01	1E-02	2.49E+05	2.78E+05
Na	AA	5.22E+04	5.45E+04	5.10E+04	5.26E+04	1.7E+03	1.42E+05	4E+03	2.34E+01	6E-01	2.61E+05	2.59E+05
Ni	ICP-ES	<2.24E+01	<2.19E+01	<2.19E+01	<2.21E+01	--	<5.98E+01	--	<9.83E-03	--	<1.16E+02	<1.27E+02
P	ICP-ES	1.35E+02	1.39E+02	1.30E+02	1.34E+02	5E+00	3.64E+02	9E+00	5.98E-02	1.6E-03	7.07E+02	8.73E+02
Pb	ICP-ES	<6.43E+01	<6.27E+01	<6.28E+01	<6.33E+01	--	<1.71E+02	--	<2.82E-02	--	<3.32E+02	<3.65E+02
Pb	ICP-MS	<9.95E-02	1.48E-01	<9.72E-02	<=1.15E-01	--	<=3.11E-01	--	<=5.10E-05	--	2.38E+00	2.71E+00
Pd	ICP-MS	<9.90E-02	<9.64E-02	<9.67E-02	<9.74E-02	--	<2.64E-01	--	<4.34E-05	--	<6.27E-01	<5.62E-01
Rb	ICP-MS	4.61E-01	4.21E-01	4.05E-01	4.29E-01	2.9E-02	1.16E+00	7E-02	1.91E-04	1.2E-05	1.21E+01	1.52E+01
S	ICP-ES	2.49E+03	2.55E+03	2.52E+03	2.52E+03	3E+01	6.82E+03	9E+01	1.12E+00	1E-02	6.79E+02	5.20E+02
Sb	ICP-ES	<3.07E+02	<2.99E+02	<3.00E+02	<3.02E+02	--	<8.19E+02	--	<1.35E-01	--	<1.59E+03	<1.75E+03
Se	AA	<6.10E-01	<5.91E-01	<5.96E-01	<5.99E-01	--	<1.62E+00	--	<2.67E-04	--	<3.30E+00	<3.37E+00
Si	ICP-ES	<8.09E+01	<7.88E+01	<7.90E+01	<7.96E+01	--	<2.16E+02	--	<3.54E-02	--	<5.57E+02	4.60E+02
Sn	ICP-ES	<5.40E+01	<5.26E+01	<5.28E+01	<5.32E+01	--	<1.44E+02	--	<2.37E-02	--	<2.79E+02	<3.07E+02
Sn	ICP-MS	1.22E+00	1.21E+00	1.16E+00	1.20E+00	3E-02	3.24E+00	6E-02	5.33E-04	1.1E-05	3.78E+00	7.56E+00
Sr	ICP-ES	<4.71E+00	<4.59E+00	<4.60E+00	<4.63E+00	--	<1.25E+01	--	<2.06E-03	--	<2.43E+01	<2.68E+01
Ti	ICP-ES	<5.81E+00	<5.66E+00	<5.68E+00	<5.72E+00	--	<1.55E+01	--	<2.55E-03	--	<3.00E+01	<3.30E+01
U	ICP-MS	2.29E-01	2.01E-01	2.39E-01	2.23E-01	2.0E-02	6.04E-01	5.9E-02	9.93E-05	9.6E-06	1.56E+00	8.18E-01
V	ICP-ES	<3.18E+01	<3.10E+01	<3.11E+01	<3.13E+01	--	<8.48E+01	--	<1.39E-02	--	<1.64E+02	<1.81E+02
W	ICP-MS	9.94E-01	9.91E-01	9.61E-01	9.82E-01	1.8E-02	2.66E+00	3E-02	4.37E-04	5E-06	1.36E+01	8.33E+00
Zn	ICP-ES	<1.31E+01	<1.28E+01	<1.28E+01	<1.29E+01	--	<3.50E+01	--	<5.76E-03	--	<6.79E+01	<7.47E+01
Zr	ICP-ES	<1.89E+01	<1.84E+01	<1.85E+01	<1.86E+01	--	<5.04E+01	--	<8.28E-03	--	<9.75E+01	<1.07E+02
Mass 93	ICP-MS	<8.84E-02	<8.61E-02	<8.64E-02	<8.70E-02	--	<2.36E-01	--	<3.87E-05	--	<5.02E-01	<4.56E-01
Mass 135	ICP-MS	1.67E-01	1.80E-01	1.64E-01	1.70E-01	8E-03	4.61E-01	1.9E-02	7.58E-05	3.1E-06	5.79E+00	4.80E+00
Mass 137	ICP-MS	4.42E-01	4.55E-01	4.25E-01	4.40E-01	1.5E-02	1.19E+00	3E-02	1.96E-04	5E-06	1.57E+01	1.29E+01
Mass 138	ICP-MS	4.91E-02	<3.23E-02	<3.24E-02	<=3.79E-02	--	<=1.03E-01	--	<=1.69E-05	--	<1.88E-01	2.24E-01

Table 15: Anion Analysis of the Soluble Portion of the Tank 28F Composite

Analyte	Method	mg/L in As-Dissolved Solution					mg/L Adjusted to 6M Na^+ Solution		g/100g of Saltcake		Free Liquid (mg/L)	
		Prep 1	Prep 2	Prep 3	Average	St.Dev.	Average	St.Dev.	Average	St.Dev.	FTF-462	Composite
NO_3^-	IC	1.07E+05	1.07E+05	1.07E+05	1.07E+05	2E+02	2.90E+05	2E+03	4.77E+01	3E-01	8.40E+04	1.17E+05
NO_2^-	IC	2.96E+03	3.49E+03	2.88E+03	3.11E+03	3.3E+02	8.42E+03	8.3E+02	1.38E+00	1.4E-01	8.22E+04	7.09E+04
OH^-	Titration	<1.88E+03	<1.83E+03	<1.84E+03	<1.85E+03	--	<5.01E+03	--	<8.24E-01	--	1.56E+05	1.12E+05
AlO_2^-	ICP-ES	1.18E+04	1.19E+04	1.14E+04	1.17E+04	3E+02	3.16E+04	5E+02	5.20E+00	8E-02	5.72E+04	3.25E+04
AlO_2^-	Titration	<6.54E+03	<6.34E+03	<6.39E+03	<6.42E+03	--	<1.74E+04	--	<2.86E+00	--	4.70E+04	7.80E+04
CO_3^{2-}	TIC/TOC	<5.54E+02	<5.37E+02	<5.42E+02	<5.44E+02	--	<1.47E+03	--	<2.42E-01	--	<3.07E+03	<3.00E+03
SO_4^{2-}	IC	5.94E+03	6.37E+03	6.09E+03	6.13E+03	2.2E+02	1.66E+04	5E+02	2.73E+00	9E-02	<3.07E+02	1.20E+03
SO_4^{2-}	ICP-ES	6.21E+03	6.37E+03	6.28E+03	6.29E+03	8.1E+01	1.70E+04	2E+02	2.80E+00	4E-02	1.69E+03	1.30E+03
PO_4^{3-}	IC	<1.11E+02	<1.07E+02	<1.08E+02	<1.09E+02	--	<2.95E+02	--	<4.85E-02	--	<6.13E+02	<6.01E+02
PO_4^{3-}	ICP-ES	3.44E+02	3.54E+02	3.30E+02	3.43E+02	1.2E+01	9.28E+02	2.4E+01	1.53E-01	4E-03	1.80E+03	2.23E+03
Cl^-	IC	<2.22E+01	2.15E+01	<2.17E+01	<=2.18E+01	--	<=5.90E+01	--	<=9.70E-03	--	1.84E+02	1.62E+03
F^-	IC	3.32E+01	3.22E+01	3.25E+01	3.27E+01	5.3E-01	8.85E+01	1.7E+00	1.45E-02	3E-04	<1.23E+02	<1.20E+02
Br^-	IC	1.11E+02	1.18E+02	1.08E+02	1.12E+02	5E+00	3.05E+02	1.1E+01	5.01E-02	1.9E-03	5.52E+02	2.46E+03
$C_2O_4^{2-}$	IC	2.44E+02	3.01E+02	2.60E+02	2.68E+02	2.9E+01	7.26E+02	7.6E+01	1.19E-01	1.3E-02	<6.13E+02	<6.01E+02
CHO_2^-	IC	3.32E+01	3.22E+01	3.25E+01	3.27E+01	5E-01	8.85E+01	1.7E+00	1.45E-02	3E-04	2.45E+02	3.00E+02
TOC	TIC/TOC	1.73E+03	1.54E+03	1.64E+03	1.63E+03	9.6E+01	4.43E+03	2.8E+02	7.28E-01	4.5E-02	3.49E+03	4.02E+03

6.4 Analysis of Insoluble Fraction (Suite SCI)

We analyzed the residual insoluble solids that remained in the centrifuge tubes after the Tank 28F saltcake composite dissolution testing. Table 16 and Table 17 contain the radiochemical and metals analysis of the prepared residual insoluble solids. Results are presented on the two individual preparations, as well as the average and standard deviation of the results, based on the dried insoluble solids. These results are then converted to the basis of the original saltcake composite by using the Solids/Salt value from Table 12.

Uranium-235 was present in quantifiable amounts in the residual insoluble solids from the Tank 28F saltcake composite dissolution. The U-235 in the residual insoluble solids averaged 0.243% (st. dev. = 0.018%, *n* = 3).

Figure 11 contains the scanning electron microscope (SEM) backscattered micrographs for a portion of the residual insoluble solids. Figure 12 contains the X-ray energy dispersive spectroscopy (XEDS) images that correspond to the regions and spots identified in Figure 11. Figure 13 contains the X-ray diffraction (XRD) analysis of a portion of the solids. All these spectroscopy results support the presence of sodium salts (sodium nitrate), aluminum hydroxide (gibbsite and bayerite), and particles more similar to sludge (U, Fe, Cr, Mn, Ru, Si, etc.). The morphology of individual crystals is difficult to ascertain from the SEM images due to the cake-like nature of this salt and aluminum hydroxide mixture. Sludge particles, however, are easily discernable as bright areas on the backscattered images.

The presence of bayerite suggests that the insoluble aluminum hydroxide phase was formed recently (during the dissolution test). The bayerite and all or a portion of the gibbsite were likely formed from the aluminum contained in the interstitial liquid and in solid sodium aluminate as the bulk salt (including sodium aluminate) was dissolved and the pH (or free hydroxide) was lowered.

Table 16: Radionuclide Analysis of the Residual Insoluble Solids from the Tank 28F Saltcake Composite Dissolution Test

Analyte	Method	pCi/g of insoluble solids				pC/g of saltcake	
		Prep 1	Prep 2	Average	St.Dev	Average	St.Dev
Al-26	Cs-rem. Gamma	*<1.91E+03*	*<1.65E+03*	*<1.78E+03*	--	*<8.47E+00*	--
Co-60	Cs-rem. Gamma	*<1.73E+03*	*<1.86E+03*	*<1.80E+03*	--	*<8.56E+00*	--
Se-79	Se-79	*<4.14E+03*	*<3.29E+03*	*<3.72E+03*	--	*<1.77E+01*	--
Sr-90	Sr-90	2.71E+06	2.64E+06	2.67E+06	5E+04	1.27E+04	2E+02
Nb-94	Cs-rem. Gamma	*<1.73E+03*	*<1.61E+03*	*<1.67E+03*	--	*<7.96E+00*	--
Tc-99	ICP-MS	1.40E+06	1.50E+06	1.45E+06	7E+04	6.89E+03	3.3E+02
Ru-106	Cs-rem. Gamma	*<2.13E+04*	*<2.21E+04*	*<2.17E+04*	--	*<1.03E+02*	--
Sb-125	Cs-rem. Gamma	*<1.59E+04*	*<1.61E+04*	*<1.60E+04*	--	*<7.62E+01*	--
Sn-126	Cs-rem. Gamma	*<6.31E+03*	*<6.35E+03*	*<6.33E+03*	--	*<3.02E+01*	--
Cs-137	Gamma	3.30E+08	3.41E+08	3.35E+08	8E+06	1.60E+06	4E+04
Ce-144	Cs-rem. Gamma	*<1.82E+04*	*<1.89E+04*	*<1.86E+04*	--	*<8.85E+01*	--
Eu-154	Cs-rem. Gamma	*<5.18E+03*	*<5.27E+03*	*<5.23E+03*	--	*<2.49E+01*	--
Eu-155	Cs-rem. Gamma	*<7.30E+03*	*<7.34E+03*	*<7.32E+03*	--	*<3.49E+01*	--
Th-230	ICP-MS	*<2.57E+04*	*<2.58E+04*	*<2.58E+04*	--	*<1.23E+02*	--
Th-232	ICP-MS	*<2.01E-01*	*<2.02E-01*	*<2.01E-01*	--	*<9.58E-04*	--
U-233	ICP-MS	*<1.18E+04*	*<1.19E+04*	*<1.18E+04*	--	*<5.64E+01*	--
U-234	ICP-MS	*<7.62E+03*	*<7.66E+03*	*<7.64E+03*	--	*<3.64E+01*	--
U-235	ICP-MS	1.82E+01	2.16E+01	1.99E+01	2.4E+00	9.49E-02	1.14E-02
U-236	ICP-MS	8.39E+01	9.32E+01	8.85E+01	6.5E+00	4.22E-01	3.1E-02
Np-237	ICP-MS	*<8.60E+02*	*<8.64E+02*	*<8.62E+02*	--	*<4.11E+00*	--
U-238	ICP-MS	1.23E+03	1.31E+03	1.27E+03	6E+01	6.06E+00	2.8E-01
Pu-238	PuTTA	1.82E+06	2.17E+06	1.99E+06	2.5E+05	9.50E+03	1.17E+03
Pu-239/240	PuTTA	9.50E+05	1.06E+06	1.01E+06	8E+04	4.80E+03	3.8E+02
Pu-239	ICP-MS	8.24E+05	8.97E+05	8.60E+05	5E+04	4.10E+03	2E+02
Pu-240	ICP-MS	2.92E+05	*<2.79E+05*	*<=2.86E+05*	--	*<1.36E+03*	--
Pu-241	Pu-241	3.02E+05	3.41E+05	3.22E+05	2.8E+04	1.53E+03	1.3E+02
Pu-242	ICP-MS	*<4.66E+03*	*<4.68E+03*	*<4.67E+03*	--	*<2.22E+01*	--
Am-241	Am/Cm	2.80E+05	2.97E+05	2.89E+05	1.2E+04	1.37E+03	6E+01
Am-243	Am/Cm	*<4.06E+03*	*<4.55E+04*	*<2.48E+04*	--	*<1.18E+02*	--
Am-242m	Am/Cm	*<7.12E+02*	*<4.40E+03*	*<2.56E+03*	--	*<1.22E+01*	--
Cm-243	Am/Cm	*<1.57E+04*	*<4.33E+04*	*<2.95E+04*	--	*<1.41E+02*	--
Cm-245	Am/Cm	*<1.29E+04*	*<3.64E+04*	*<2.47E+04*	--	*<1.18E+02*	--
Cm-247	Am/Cm	*<1.85E+04*	*<1.59E+04*	*<1.72E+04*	--	*<8.20E+01*	--
Cf-249	Am/Cm	*<1.88E+04*	*<1.85E+04*	*<1.87E+04*	--	*<8.90E+01*	--
Cf-251	Am/Cm	*<1.43E+04*	*<1.40E+04*	*<1.42E+04*	--	*<6.75E+01*	--
Cm-242	Am/Cm	*<5.90E+02*	*<3.64E+03*	*<2.11E+03*	--	*<1.01E+01*	--
Cm-244	Am/Cm	9.28E+04	5.90E+04	7.59E+04	2.39E+04	3.62E+02	1.14E+02
non-Cs Beta	Cs-rem. Beta	6.71E+06	7.48E+06	7.09E+06	5.4E+05	3.38E+04	2.6E+03

Table 17: Metals Analysis of the Residual Insoluble Solids from the Tank 28F Saltcake Composite Dissolution Test

Analyte	Method	g/100g of insoluble solids				g/100g of saltcake	
		Prep 1	Prep 2	Average	St.Dev	Average	St.Dev
Ag	ICP-ES	<4.17E-02	<4.19E-02	<4.18E-02	--	<1.99E-04	--
Ag	ICP-MS	3.77E-03	5.01E-03	4.39E-03	8.7E-04	2.09E-05	4.2E-06
Al	ICP-ES	4.81E+00	6.42E+00	5.62E+00	1.14E+00	2.68E-02	5.4E-03
As	AA	<1.34E-03	<1.35E-03	<1.35E-03	--	<6.41E-06	--
B	ICP-ES	<9.02E-02	<9.07E-02	<9.05E-02	--	<4.31E-04	--
Ba	ICP-ES	3.27E-02	3.62E-02	3.45E-02	2.5E-03	1.64E-04	1.2E-05
Be	ICP-ES	<3.41E-03	<3.43E-03	<3.42E-03	--	<1.63E-05	--
Ca	ICP-ES	1.37E-01	1.51E-01	1.44E-01	1.0E-02	6.85E-04	4.8E-05
Cd	ICP-ES	<5.95E-02	<5.98E-02	<5.97E-02	--	<2.84E-04	--
Cd	ICP-MS	1.31E-03	1.57E-03	1.44E-03	1.8E-04	6.86E-06	8.4E-07
Ce	ICP-ES	<2.96E-01	<2.98E-01	<2.97E-01	--	<1.41E-03	--
Co	ICP-MS	<2.44E-04	<2.45E-04	<2.45E-04	--	<1.16E-06	--
Cr	ICP-ES	6.93E-01	7.75E-01	7.34E-01	5.8E-02	3.50E-03	2.8E-04
Cs-133	ICP-MS	3.36E-04	3.31E-04	3.34E-04	4E-06	1.59E-06	2E-08
Cu	ICP-ES	<3.34E-02	<3.36E-02	<3.35E-02	--	<1.60E-04	--
Fe	ICP-ES	8.93E-01	1.03E+00	9.61E-01	9.7E-02	4.58E-03	4.6E-04
Gd	ICP-ES	<4.98E-02	<5.00E-02	<4.99E-02	--	<2.38E-04	--
Hg	CVAA	<2.93E-03	<2.94E-03	<2.94E-03	--	<1.40E-05	--
K	ICP-ES	<1.09E+00	<1.09E+00	<1.09E+00	--	<5.20E-03	--
K	AA	4.19E-02	3.81E-02	4.00E-02	2.7E-03	1.91E-04	1.3E-05
La	ICP-ES	<9.71E-02	<9.75E-02	<9.73E-02	--	<4.64E-04	--
Li	ICP-ES	<4.70E-02	<4.73E-02	<4.71E-02	--	<2.25E-04	--
Mg	ICP-ES	<8.34E-02	<8.38E-02	<8.36E-02	--	<3.98E-04	--
Mn	ICP-ES	<5.12E-02	<5.15E-02	<5.13E-02	--	<2.45E-04	--
Mo	ICP-ES	<3.07E-01	<3.08E-01	<3.08E-01	--	<1.47E-03	--
Na	ICP-ES	1.61E+01	1.55E+01	1.58E+01	4E-01	7.52E-02	2.0E-03
Na	AA	1.52E+01	1.45E+01	1.49E+01	5E-01	7.08E-02	2.4E-03
Ni	ICP-ES	<1.98E-01	<1.99E-01	<1.99E-01	--	<9.46E-04	--
P	ICP-ES	<3.56E-01	<3.57E-01	<3.56E-01	--	<1.70E-03	--
Pb	ICP-ES	<5.66E-01	<5.69E-01	<5.67E-01	--	<2.70E-03	--
Pb	ICP-MS	6.08E-03	6.98E-03	6.53E-03	6.3E-04	3.11E-05	3.0E-06
Pd	ICP-MS	1.90E-02	2.76E-02	2.33E-02	6.1E-03	1.11E-04	2.9E-05
S	ICP-ES	5.61E-01	5.10E-01	5.35E-01	3.6E-02	2.55E-03	1.7E-04
Sb	ICP-ES	<2.71E+00	<2.72E+00	<2.71E+00	--	<1.29E-02	--
Se	AA	<2.68E-03	<2.70E-03	<2.69E-03	--	<1.28E-05	--
Si	ICP-ES	<7.12E-01	<7.16E-01	<7.14E-01	--	<3.40E-03	--
Sn	ICP-ES	<4.77E-01	<4.79E-01	<4.78E-01	--	<2.28E-03	--
Sr	ICP-ES	<4.15E-02	<4.17E-02	<4.16E-02	--	<1.98E-04	--
Ti	ICP-ES	<5.12E-02	<5.15E-02	<5.13E-02	--	<2.45E-04	--
U	ICP-MS	3.67E-01	3.92E-01	3.79E-01	1.8E-02	1.81E-03	8E-05
V	ICP-ES	<2.81E-01	<2.82E-01	<2.82E-01	--	<1.34E-03	--
W	ICP-MS	2.84E-03	3.01E-03	2.92E-03	1.2E-04	1.39E-05	6E-07
Zn	ICP-ES	<1.16E-01	<1.16E-01	<1.16E-01	--	<5.52E-04	--
Zr	ICP-ES	<1.67E-01	<1.68E-01	<1.67E-01	--	<7.97E-04	--
Mass 93	ICP-MS	<2.44E-04	2.76E-04	<=2.60E-04	--	<1.24E-06	--
Mass 135	ICP-MS	1.53E-04	1.42E-04	1.48E-04	8E-06	7.04E-07	3.8E-08
Mass 137	ICP-MS	3.20E-02	3.52E-02	3.36E-02	2.3E-03	1.60E-04	1.1E-05
Mass 138	ICP-MS	2.76E-04	2.73E-04	2.75E-04	2E-06	1.31E-06	1E-08

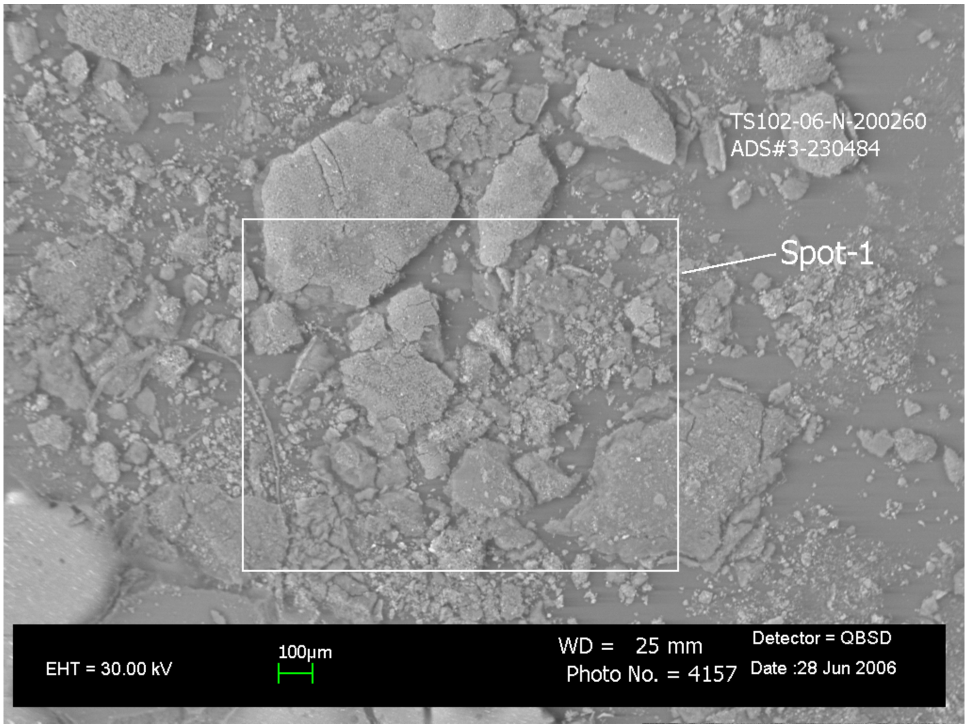

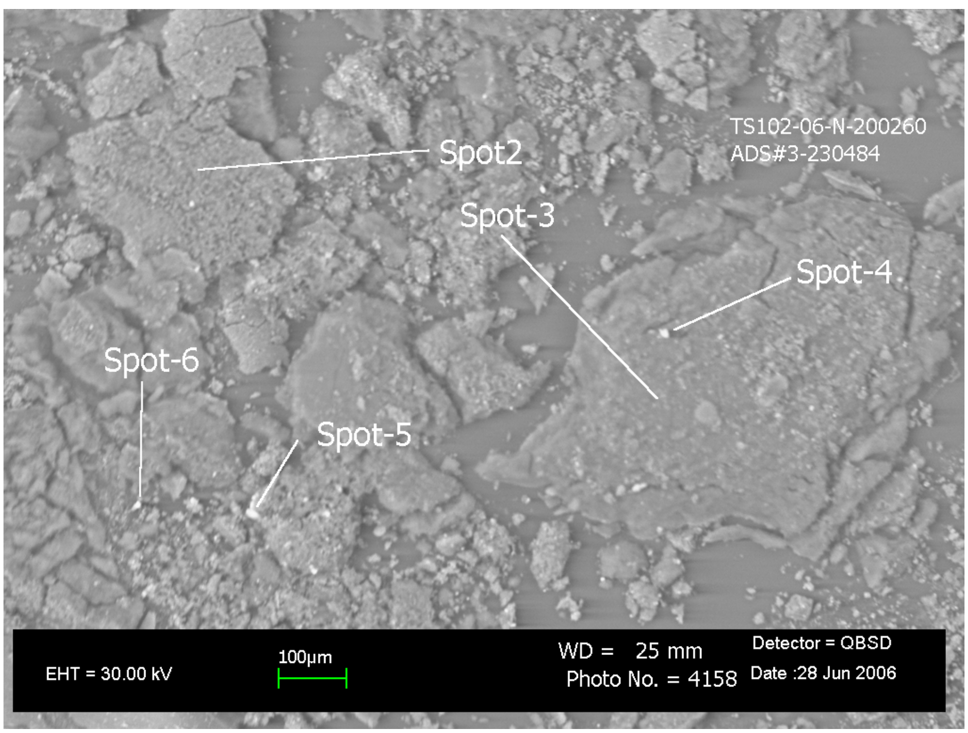

Figure 11: SEM Backscattering Micrographs for Tank 28 Residual Solids.

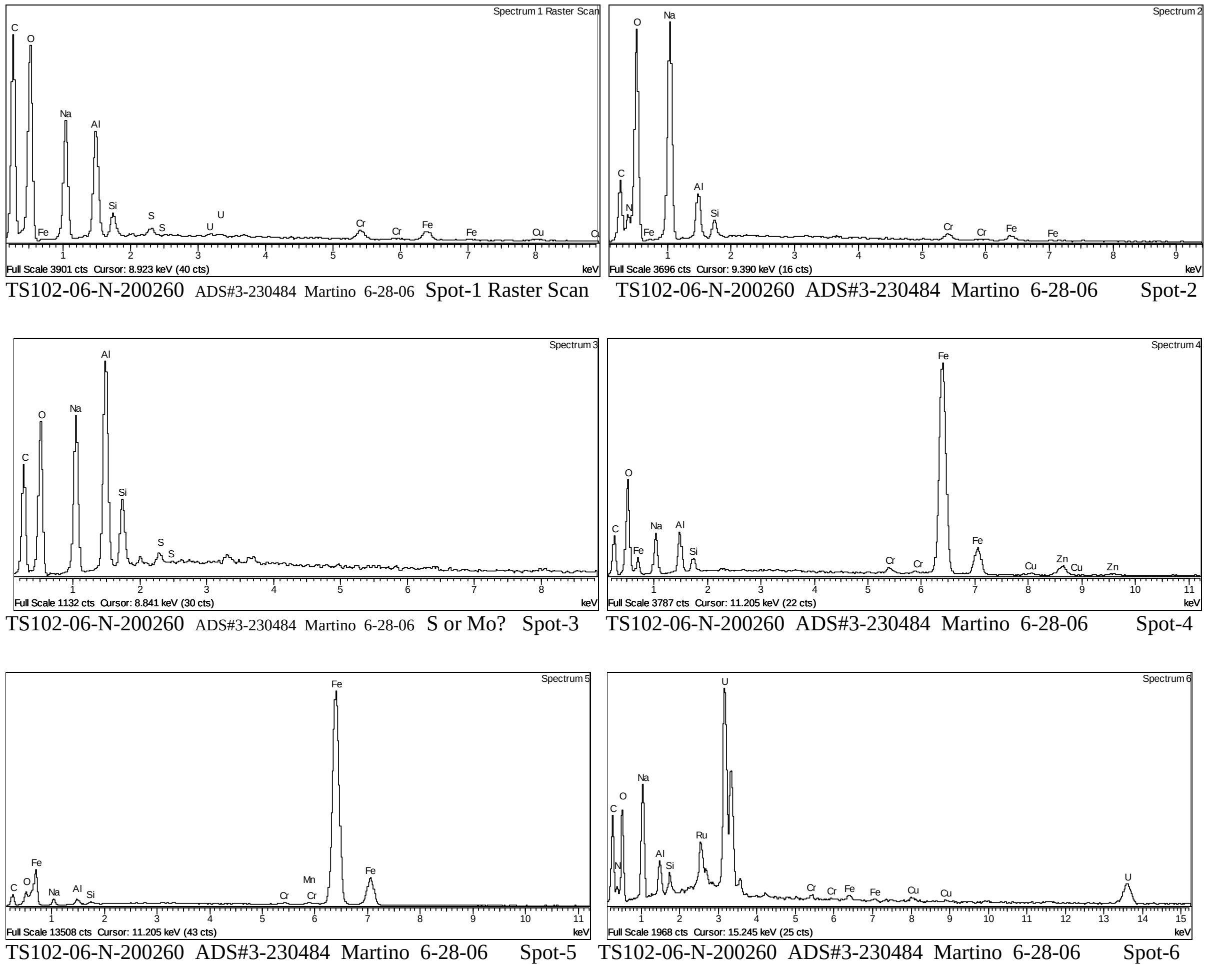

Figure 12: XEDS Spectra for Regions Identified in SEM of Tank 28F Residual Solids

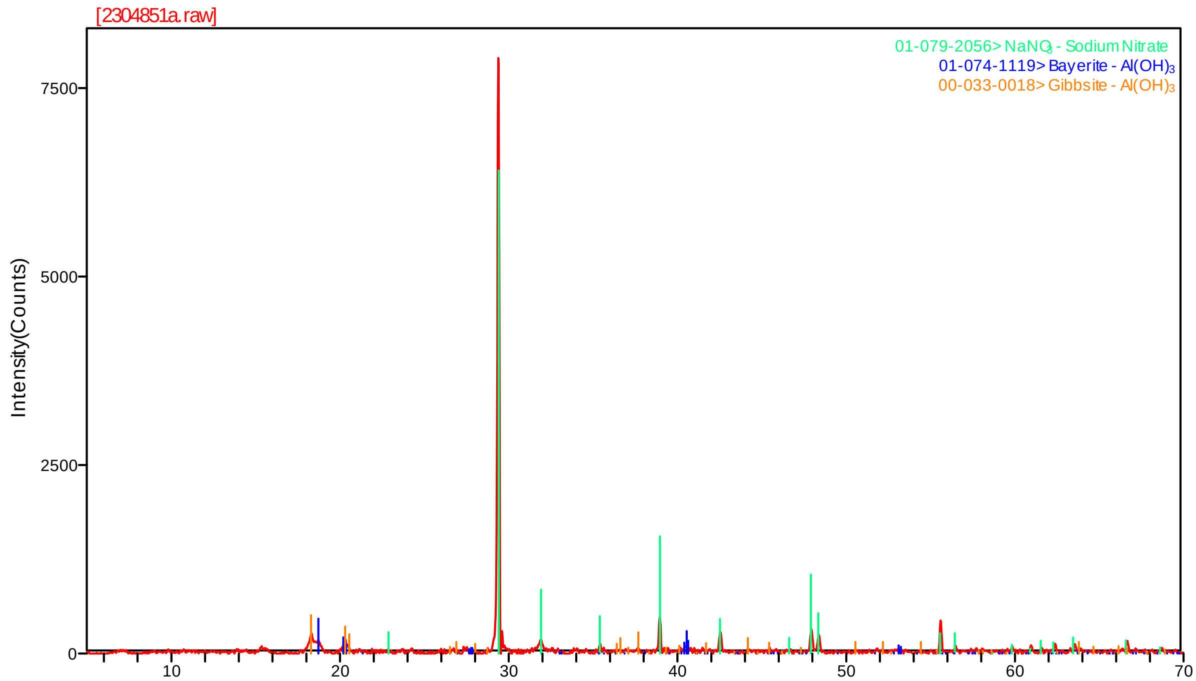

Figure 13: XRD Analysis of Tank 28F Residual Insoluble Solids from Dissolution Test.

6.5 Overall Tank 28F Saltcake Characterization

Table 18, Table 19, and Table 20 contain comparisons of the results for the saltcake composite composition from both the dissolution testing and estimates from the segment analyses. Results are reported on a per-mass-of-saltcake basis. The dissolution test analysis results are compiled from the soluble and insoluble portions reported in the previous section, and a sum of those portions is included as a total. The columns labeled bulk segment analysis rely on the results from the individual saltcake segments. The average concentration and upper and lower 95% CI bounds on the average concentration of analytes in the composite were calculated from the segment results. This calculation differs from the evenly weighted sample results reported in Table 9 and Table 10 because it is weighted using the mass of each segment that was contributed to the saltcake composite. This methodology for using individual segment data to determine the weighted content in the composite is not applicable for analytes with primarily bdl values. Thus, many of the rows in the bulk segment analysis section have been left blank.

Table 18: Radionuclides Results from Dissolution Test and Segment Analysis (pCi/g)

Analyte	Method	Dissolution Test Analysis			Bulk Segment Analysis		
		Soluble	Insoluble	Total	Average	Lower CI	Upper CI
C-14	C-14	<6.81E+03	--	<6.81E+03	--	--	--
Al-26	Cs-rem. Gamma	<1.76E+02	<8.47E+00	<1.85E+02	--	--	--
Co-60	Cs-rem. Gamma	<2.70E+02	<8.56E+00	<2.79E+02	--	--	--
Se-79	Se-79	<6.36E+03	<1.77E+01	<6.38E+03	--	--	--
Sr-90	Sr-90	4.85E+03	1.27E+04	1.76E+04	--	--	--
Nb-94	Cs-rem. Gamma	<2.53E+02	<7.96E+00	<2.61E+02	--	--	--
Tc-99	ICP-MS	3.92E+04	6.89E+03	4.61E+04	8.36E+04	3.95E+04	1.28E+05
Ru-106	Cs-rem. Gamma	<1.60E+03	<1.03E+02	<1.71E+03	--	--	--
Sb-125	Cs-rem. Gamma	<7.32E+02	<7.62E+01	<8.08E+02	--	--	--
Sb-126	Cs-rem. Gamma	1.98E+03	--	1.98E+03	1.75E+03	6.12E+02	2.88E+03
Sn-126	Cs-rem. Gamma	2.40E+03	<3.02E+01	<=2.43E+03	2.21E+03	1.66E+03	2.76E+03
I-129	I-129	<2.95E+02	--	<2.95E+02	--	--	--
Cs-134	Gamma	<8.49E+04	--	<8.49E+04	--	--	--
Cs-137	Gamma	1.63E+08	1.60E+06	1.65E+08	2.85E+08	7.15E+07	4.98E+08
Ce-144	Cs-rem. Gamma	<1.40E+03	<8.85E+01	<1.49E+03	--	--	--
Eu-154	Cs-rem. Gamma	<4.09E+02	<2.49E+01	<4.34E+02	--	--	--
Eu-155	Cs-rem. Gamma	<7.58E+02	<3.49E+01	<7.93E+02	--	--	--
Th-230	ICP-MS	<2.04E+03	<1.23E+02	<2.16E+03	--	--	--
Th-232	ICP-MS	<2.65E-02	<9.58E-04	<2.75E-02	--	--	--
U-233	ICP-MS	<9.37E+02	<5.64E+01	<9.93E+02	--	--	--
U-234	ICP-MS	<6.05E+02	<3.64E+01	<6.41E+02	--	--	--
U-235	ICP-MS	<2.09E-01	9.49E-02	<=3.04E-01	--	--	--
U-236	ICP-MS	<6.26E+00	4.22E-01	<=6.68E+00	--	--	--
Np-237	ICP-MS	<6.82E+01	<4.11E+00	<7.23E+01	--	--	--
U-238	ICP-MS	3.34E-01	6.06E+00	6.39E+00	--	--	--
Pu-238	PuTTA	<=3.02E+03	9.50E+03	<=1.25E+04	--	--	--
Pu-239/240	PuTTA	<1.15E+03	4.80E+03	<=5.94E+03	6.47E+03	2.94E+03	1.00E+04
Pu-239	ICP-MS	<6.02E+03	4.10E+03	<=1.01E+04	--	--	--
Pu-240	ICP-MS	<2.21E+04	<1.36E+03	<2.34E+04	--	--	--
Pu-241	Pu-241	<1.24E+05	1.53E+03	<=1.26E+05	--	--	--
Pu-242	ICP-MS	<3.70E+02	<2.22E+01	<3.92E+02	--	--	--
Am-241	Am/Cm	<2.64E+03	1.37E+03	<=4.02E+03	--	--	--
Am-241	Cs-rem. Gamma	<1.85E+03	--	<1.85E+03	1.64E+03	9.10E+02	2.37E+03
Am-243	Am/Cm	<8.94E+02	<1.18E+02	<1.01E+03	--	--	--
Am-243	Cs-rem. Gamma	<4.57E+02	--	<4.57E+02	--	--	--
Am-242m	Am/Cm	<1.18E+04	<1.22E+01	<1.18E+04	--	--	--
Cm-243	Am/Cm	<3.02E+03	<1.41E+02	<3.16E+03	--	--	--
Cm-245	Am/Cm	<2.48E+03	<1.18E+02	<2.60E+03	--	--	--
Cm-247	Am/Cm	<3.75E+03	<8.20E+01	<3.84E+03	--	--	--
Cf-249	Am/Cm	<3.76E+03	<8.90E+01	<3.85E+03	--	--	--
Cf-251	Am/Cm	<3.18E+03	<6.75E+01	<3.25E+03	--	--	--
Cm-242	Am/Cm	<3.46E+01	<1.01E+01	<4.46E+01	--	--	--
Cm-244	Am/Cm	<=7.77E+03	3.62E+02	<=8.13E+03	--	--	--
Cm-245	Cs-rem. Gamma	<1.89E+03	--	<1.89E+03	--	--	--
non-Cs Beta	Cs-rem. Beta	2.32E+05	3.38E+04	2.66E+05	2.68E+05	1.31E+05	4.05E+05

Table 19: Metals Results from Dissolution Test and Segment Analysis (wt%)

Analyte	Method	Dissolution Test Analysis			Bulk Segment Analysis		
		Soluble	Insoluble	Total	Average	Lower CI	Upper CI
Ag	ICP-ES	*<2.07E-03*	*<1.99E-04*	*<2.27E-03*	--	--	--
Ag	ICP-MS	--	2.09E-05	2.09E-05	--	--	--
Al	ICP-ES	2.38E+00	2.68E-02	2.41E+00	3.14E+00	-1.83E-01	6.46E+00
As	AA	*<1.33E-04*	*<6.41E-06*	*<1.40E-04*	--	--	--
B	ICP-ES	*<4.47E-03*	*<4.31E-04*	*<4.90E-03*	--	--	--
Ba	ICP-ES	*<1.10E-03*	1.64E-04	*<=1.27E-03*	--	--	--
Be	ICP-ES	--	*<1.63E-05*	*<1.63E-05*	--	--	--
Ca	ICP-ES	*<2.84E-03*	6.85E-04	*<=3.52E-03*	--	--	--
Cd	ICP-ES	*<2.96E-03*	*<2.84E-04*	*<3.24E-03*	--	--	--
Cd	ICP-MS	--	6.86E-06	6.86E-06	--	--	--
Ce	ICP-ES	*<1.47E-02*	*<1.41E-03*	*<1.61E-02*	--	--	--
Co	ICP-MS	*<9.68E-06*	*<1.16E-06*	*<1.08E-05*	--	--	--
Cr	ICP-ES	*<5.28E-03*	3.50E-03	*<=8.77E-03*	--	--	--
Cs-133	ICP-MS	5.25E-04	1.59E-06	5.26E-04	9.53E-04	2.66E-04	1.64E-03
Cu	ICP-ES	*<1.66E-03*	*<1.60E-04*	*<1.82E-03*	--	--	--
Fe	ICP-ES	*<2.08E-03*	4.58E-03	*<=6.66E-03*	9.11E-03	7.64E-04	1.75E-02
Gd	ICP-ES	*<2.46E-03*	*<2.38E-04*	*<2.70E-03*	--	--	--
Hg	CVAA	*<5.33E-04*	*<1.40E-05*	*<5.47E-04*	--	--	--
K	ICP-ES	8.34E-02	*<5.20E-03*	*<=8.86E-02*	--	--	--
K	AA	7.42E-02	1.91E-04	7.44E-02	--	--	--
La	ICP-ES	*<4.81E-03*	*<4.64E-04*	*<5.27E-03*	--	--	--
Li	ICP-ES	*<2.33E-03*	*<2.25E-04*	*<2.56E-03*	5.91E-02	4.90E-02	6.92E-02
Mg	ICP-ES	*<4.14E-03*	*<3.98E-04*	*<4.54E-03*	--	--	--
Mn	ICP-ES	*<2.55E-03*	*<2.45E-04*	*<2.80E-03*	--	--	--
Mo	ICP-ES	*<1.52E-02*	*<1.47E-03*	*<1.67E-02*	--	--	--
Na	ICP-ES	2.27E+01	7.52E-02	2.28E+01	2.14E+01	1.95E+01	2.33E+01
Na	AA	2.34E+01	7.08E-02	2.35E+01	--	--	--
Ni	ICP-ES	*<9.83E-03*	*<9.46E-04*	*<1.08E-02*	--	--	--
P	ICP-ES	5.98E-02	*<1.70E-03*	*<=6.15E-02*	--	--	--
Pb	ICP-ES	*<2.82E-02*	*<2.70E-03*	*<3.09E-02*	--	--	--
Pb	ICP-MS	*<=5.10E-05*	3.11E-05	*<=8.22E-05*	--	--	--
Pd	ICP-MS	*<4.34E-05*	1.11E-04	*<=1.54E-04*	--	--	--
Rb	ICP-MS	1.91E-04	--	1.91E-04	--	--	--
S	ICP-ES	1.12E+00	2.55E-03	1.12E+00	1.12E+00	3.95E-01	1.84E+00
Sb	ICP-ES	*<1.35E-01*	*<1.29E-02*	*<1.47E-01*	--	--	--
Se	AA	*<2.67E-04*	*<1.28E-05*	*<2.79E-04*	--	--	--
Si	ICP-ES	*<3.54E-02*	*<3.40E-03*	*<3.88E-02*	--	--	--
Sn	ICP-ES	*<2.37E-02*	*<2.28E-03*	*<2.59E-02*	--	--	--
Sn	ICP-MS	5.33E-04	--	5.33E-04	--	--	--
Sr	ICP-ES	*<2.06E-03*	*<1.98E-04*	*<2.26E-03*	--	--	--
Ti	ICP-ES	*<2.55E-03*	*<2.45E-04*	*<2.79E-03*	--	--	--
U	ICP-MS	9.93E-05	1.81E-03	1.91E-03	2.56E-03	1.01E-03	4.12E-03
V	ICP-ES	*<1.39E-02*	*<1.34E-03*	*<1.53E-02*	--	--	--
W	ICP-MS	4.37E-04	1.39E-05	4.51E-04	--	--	--
Zn	ICP-ES	*<5.76E-03*	*<5.52E-04*	*<6.31E-03*	--	--	--
Zr	ICP-ES	*<8.28E-03*	*<7.97E-04*	*<9.07E-03*	--	--	--
Mass 93	ICP-MS	*<3.87E-05*	*<1.24E-02*	*<1.24E-02*	--	--	--
Mass 135	ICP-MS	7.58E-05	7.04E-03	7.11E-03	1.52E-04	4.83E-05	2.56E-04
Mass 137	ICP-MS	1.96E-04	1.60E+00	1.60E+00	6.09E-04	2.23E-04	9.96E-04
Mass 138	ICP-MS	*<=1.69E-05*	1.31E-02	*<=1.31E-02*	--	--	--

Table 20: Anion Results from Dissolution Test and Segment Analysis (wt%)

Analyte	Method	Dissolution Test Analysis			Bulk Segment Analysis		
		Soluble	Insoluble	Total	Average	Lower CI	Upper CI
NO_3^-	IC	4.77E+01	--	4.77E+01	3.00E+01	2.04E+01	3.95E+01
NO_2^-	IC	1.38E+00	--	1.38E+00	2.25E+00	1.27E+00	3.24E+00
OH^-	Titration	*<8.24E-01*	--	*<8.24E-01*	3.49E+00	1.74E+00	5.24E+00
AlO_2^-	ICP-ES	5.20E+00	--	5.20E+00	6.86E+00	-4.02E-01	1.41E+01
AlO_2^-	Titration	*<2.86E+00*	--	*<2.86E+00*	9.09E+00	1.86E-02	1.82E+01
CO_3^{2-}	TIC/TOC	*<2.42E-01*	--	*<2.42E-01*	1.87E+00	9.60E-01	2.78E+00
SO_4^{2-}	IC	2.73E+00	--	2.73E+00	2.74E+00	7.23E-01	4.76E+00
SO_4^{2-}	ICP-ES	2.80E+00	--	2.80E+00	--	--	--
PO_4^{3-}	IC	*<4.85E-02*	--	*<4.85E-02*	--	--	--
PO_4^{3-}	ICP-ES	1.53E-01	--	1.53E-01	--	--	--
Cl^-	IC	*<=9.70E-03*	--	*<=9.70E-03*	--	--	--
F^-	IC	1.45E-02	--	1.45E-02	4.54E-02	-1.10E-03	9.18E-02
Br^-	IC	5.01E-02	--	5.01E-02	--	--	--
$C_2O_4^{2-}$	IC	1.19E-01	--	1.19E-01	1.05E-01	1.94E-02	1.90E-01
CHO_2^-	IC	1.45E-02	--	1.45E-02	--	--	--
TOC	TIC/TOC	7.28E-01	--	7.28E-01	--	--	--

7 Conclusions

- Twelve LM-75 core samplers from Tank 28F sampling were received by SRNL for saltcake characterization. Of these, nine samplers contained mixtures of free liquid and saltcake, two contained only liquid, and one was empty. The saltcake contents generally appeared wet
- The dissolved fraction of the undrained composite adjusting to a basis of a 6 M sodium solution, averaged 9.94E+07pCi/mL (0.38 Ci/gal) Cs-137 and 2.38E+04 pCi/mL of Tc-99. These results do not reflect three key aspects of sampling and sample handling: the large amount of free liquid received in the samplers was separated before sample homogenization, the supernatant liquid formed upon creation of the composite was separated prior to dissolution testing, and the analysis of free liquid indicates partial dilution and dissolution of the sample by drill string fluid. Adjustment to account for these effects would lead to higher estimated concentrations of the soluble radionuclides than those measured in the dissolution test solutions.
- Comparing pairs of analytes within all of the individual sample segments, there was a large group of analytes that exhibited inter-correlation (Cs-137, Tc-99, Cs-removed Beta, Sb-126, Sn-126, Mass 133, Mass 135, Mass 137, Cr, P, NO_2^-, OH^-, NO_3^-, and moisture content).
- Residual insoluble material remaining after the dissolution testing was primarily sodium nitrate and aluminum hydroxide. The aluminum hydroxide phases identified were the $Al(OH)_3$ polymorphs bayerite and gibbsite.

8 Quality Assurance

This work was performed in accordance with the requirements of the task technical and quality assurance plan.[3] Laboratory Notebook WSRC-NB-2006-00051 and various Analytical Development Section notebooks contain the experimental data.

9 References

[1] J. R. Sessions, "Enhanced Characterization Project Execution Plan," CBU-SPT-2004-00119, Rev. 0, July 2004.

[2] P. J. Hill, "Basis for Obtaining Full Length Salt Core Samples," CBU-PIT-2005-00292, Rev. 0, December 21, 2005.

[3] C. J. Martino, D. J. McCabe, R. L. Nichols, and T. B. Edwards, "Task Technical and Quality Assurance Plan for the Characterization of Tank 28F Saltcake Core Samples," WSRC-RP-2004-00513, Rev. 1, March 20, 2006.

[4] C. J. Martino, R. L. Nichols, D. J. McCabe, and M. R. Millings, "Tank 10H Saltcake Core Sample Analysis," WSRC-TR-2004-00164, Rev. 0, April 19, 2004.

[5] T.B. Peters, D.T. Hobbs, S.D. Fink, "Results of Supplemental MST Studies," WSRC-STI-2006-00012, Rev. 0, July 24, 2006.

A Appendix

A.1 <u>Sampler Extrusion Observations</u>

FTF-456; segment 28-1

As the sleeving material containing the sampler was removed from the PVC shipping tube, it was noted that the sleeving material was breached. Prior to the sample being opened, the ball valve was clean and free of debris. During sampler disassembly, the release disk came out before the spring stops were removed, indicating that the piston was not fully retracted and not tight against the spring stops. When the ball valve was opened, approximately 195 mL of dark cloudy liquid flowed out. The sample was placed in the extruder, and the extruder was run without resistance from 75 cm to 16 cm. Wet salt came out with little additional resistance from 16 cm to 9 cm. The salt was large grained wet solids and appeared medium-gray.

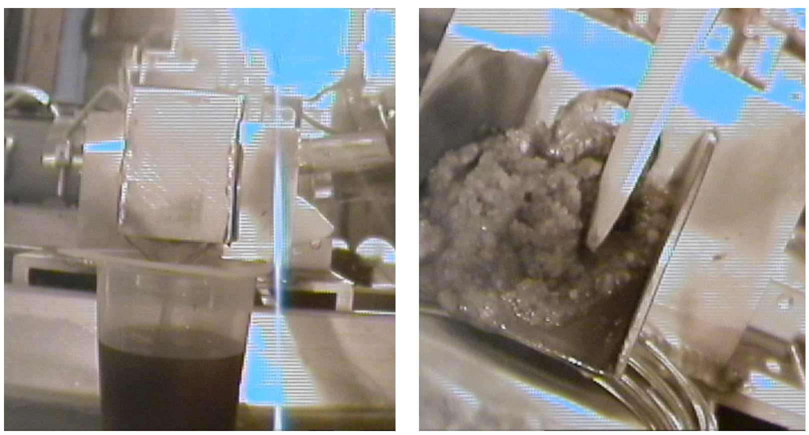

Figure 14: Extrusion of Sample FTF-456

FTF-457; segment 28-2

Prior to the sample being opened, the ball valve was clean and free of debris, and the sampler tip was slightly dented. There was no free liquid initially, but some was removed upon extrusion. The sample was placed in the extruder, and the extruder was run without resistance from 75 cm to 56 cm. As the extruder was run from 56 cm to 9 cm at the minimum push force, the following regions were encountered, in order: a region of moist white salt, an empty region, a region of free liquid, and a region of slightly darker wet salt. Note that solid material extruded from a sample first corresponds to the lowest in-tank level and that extruded last corresponds to the highest in-tank level.

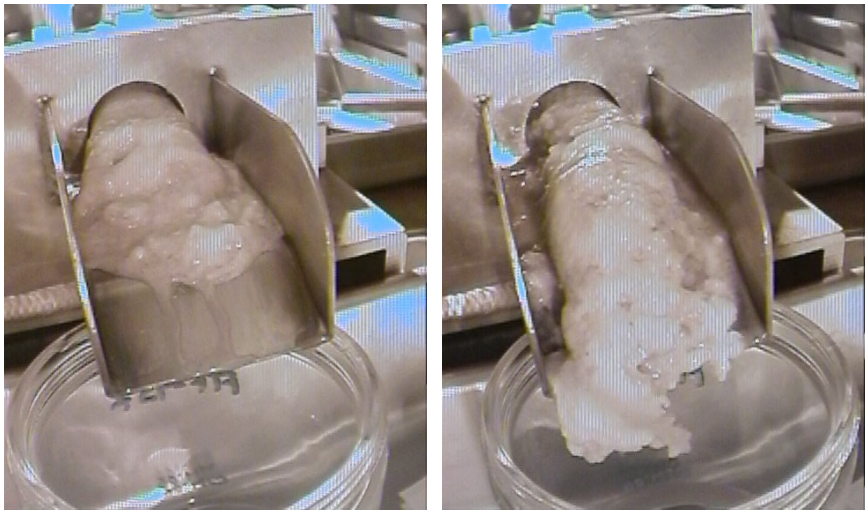

Figure 15: Extrusion of Sample FTF-457

FTF-458; segment 28-3

As the sampler was removed from the sleeving material, approximately 25 mL of liquid was collected from the bag. Prior to the sample being opened, the ball valve was clean and free of debris. During sampler disassembly, the release disk came out before the spring stops were removed, indicating that the piston was not fully retracted and not tight against the spring stops. When the ball valve was opened, approximately 75 mL of light colored clear liquid with a small amount of floating black solids flowed out. The sample was placed in the extruder, and the extruder was run without resistance from 75 cm to 8 cm. The sample contained no significant saltcake solids.

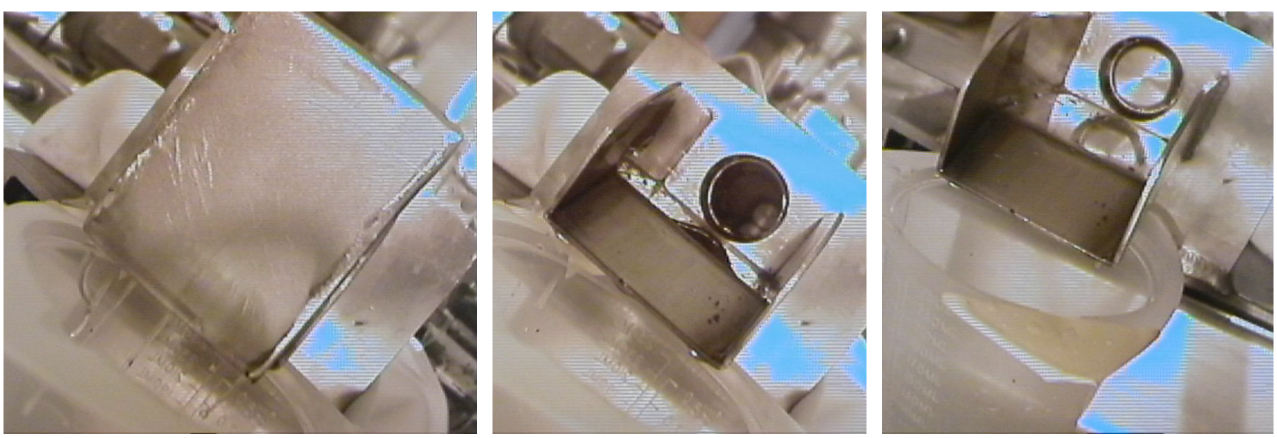

Figure 16: Extrusion of Sample FTF-458

FTF-459; segment 28-4

As the sampler was removed from the sleeving material, approximately 60 mL of liquid was collected from the bag. Prior to the sample being opened, the ball valve was clean and free of debris. During sampler disassembly, the release disk came out before the spring stops were removed, indicating that the piston was not fully retracted and not tight against the spring stops. When the ball valve was opened, approximately 110 mL of white (cloudy) soupy liquid with a small amount of floating black solids flowed out. The sample was placed in the extruder, and the extruder was run without resistance from 75 cm to 8 cm. Approximately 15 mL of slushy/soupy salt was obtained.

Figure 17: Extrusion of Sample FTF-459

FTF-460; segment 28-5

Prior to the sample being opened, the ball valve was clean and free of debris. During sampler disassembly, the release disk came out before the spring stops were removed, indicating that the piston was not fully retracted and not tight against the spring stops. When the ball valve was opened, approximately 110 mL of murky gray liquid flowed out. As this free liquid was being transferred into a bottle for storage, some larger grained solids had settled out. Those solids were transferred to the saltcake sample jar. The sample was placed in the extruder, and the extruder was run without resistance from 75 cm to 8 cm. Slushy large-grained salt was obtained when the extruder had reached 30 cm.

Figure 18: Extrusion of Sample FTF-460

FTF-461; segment 28-6

Prior to the sample being opened, a small amount of salt was evident on the ball valve and gasket. There was no free liquid initially, but some was removed upon extrusion. The sample was placed in the extruder, and the extruder was run at the minimum push force. During extrusion, white salt came out initially to about the length of the extruder chute. This was followed by approximately 170 mL of viscous fluid that flowed into the sample jar. The liquid was transferred into a bottle for storage, and additional salt was extruded from the sampler. The salt was white and moist in appearance.

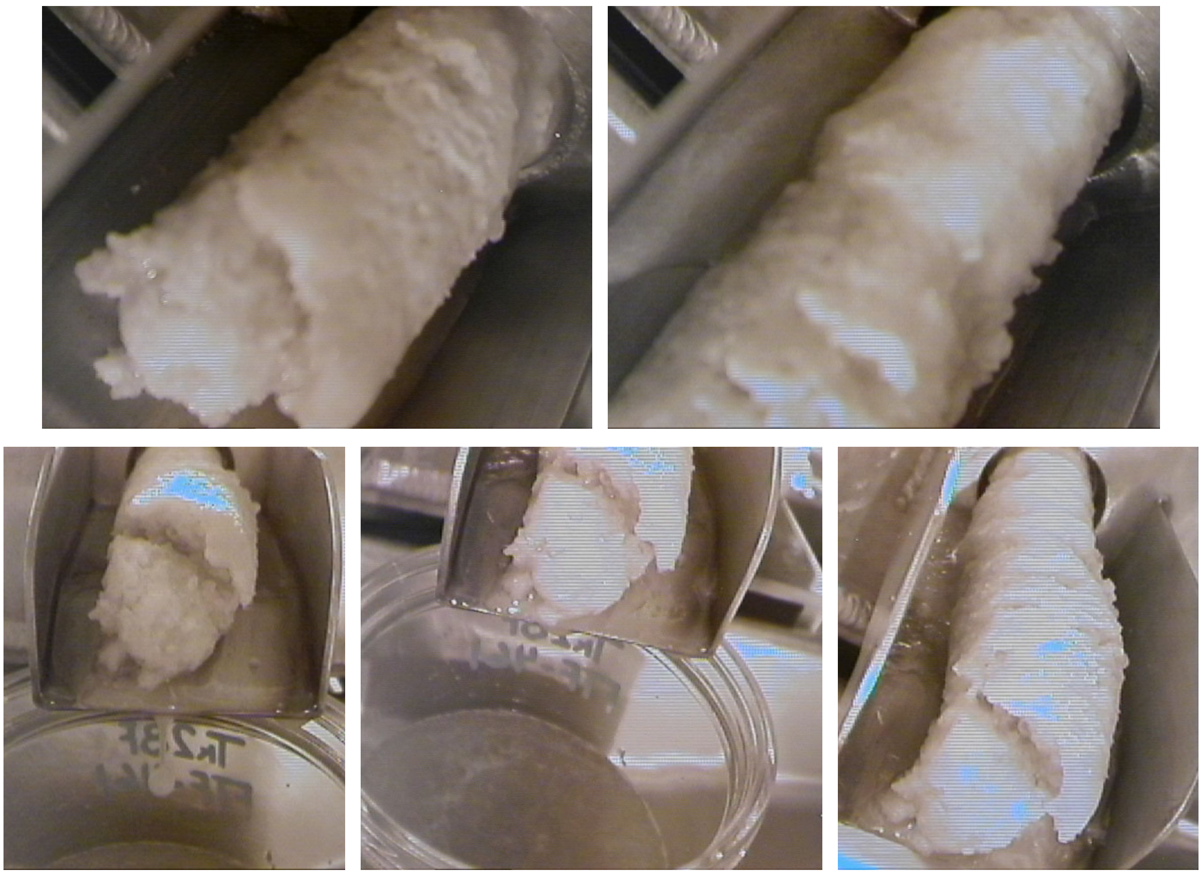

Figure 19: Extrusion of Sample FTF-461

FTF-462; segment 28-7

Prior to the sample being opened, the ball valve was clean and free of debris. When the ball valve was opened, approximately 175 mL of murky gray liquid flowed out. The sample was placed in the extruder, and the extruder was run at the minimum push force. During extrusion, a small amount (approximately 80 mL) of wet white salt slurry flowed out of the sampler and off the extruder chute.

Figure 20: Extrusion of Sample FTF-462

FTF-463; segment 28-8

Originally, the sleeving material was dripping a small amount of liquid as the sample was handled. As the sleeving was removed, approximately 80 mL of clear liquid with a slight brown color was collected. Prior to the sample being opened, the sampler was wet, but the ball valve was clean and free of debris. During sampler disassembly, the release disk came out before the spring stops were removed, indicating that the piston was not fully retracted and not tight against the spring stops. Little free liquid was removed upon the initial opening of the ball valve. The sample was placed in the extruder, and the extruder was run using the minimum push force. Near the completion of extrusion, creamy white slurry was extruded. This material was reminiscent of a thick flour/water mixture or melting ice-cream, and was not typical of previous saltcake samples.

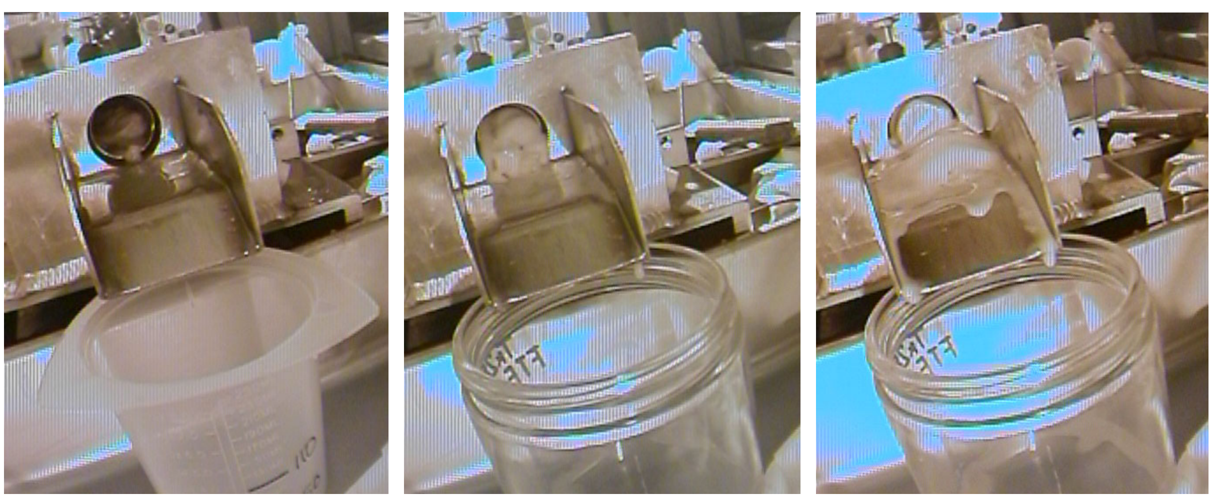

Figure 21: Extrusion of Sample FTF-463

FTF-464; segment 28-9

A small amount of liquid was contained in the sample sleeving, but was not collected. Prior to the sample being opened, the ball valve was clean and free of debris. During sampler disassembly, the release disk came out before the spring stops were removed, indicating that the piston was not fully retracted and not tight against the spring stops. As the ball valve was opened, 55 to 60 mL of thick grayish-white salt slurry or cloudy liquid flowed out. The sample was placed in the extruder, and the extruder was run using the minimum push force. Less than 100 mL of material was extruded, which appeared similar to that of sample FTF463. The material was a very moist, white, fine-grained, "creamy" salt slurry.

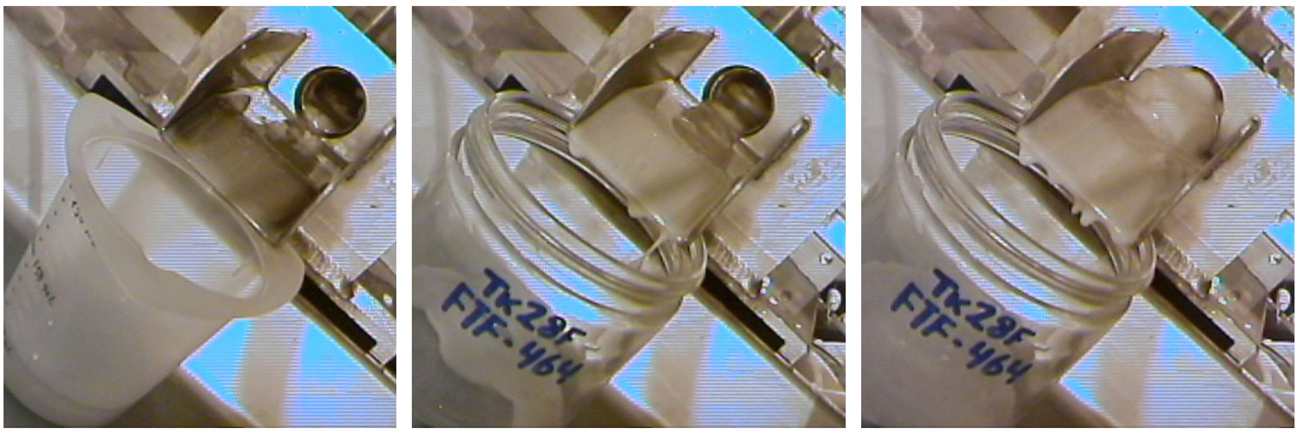

Figure 22: Extrusion of Sample FTF-464

FTF-465; segment 28-10

A small amount of liquid was contained in the sample sleeving, but was not collected. Prior to the sample being opened, the ball valve was clean and free of debris. As the ball valve was opened, approximately 200 mL of murky gray liquid or salt slurry flowed out. This free liquid appeared darker than that obtained in the previous several samples (FTF-462 through FTF-464). The sample was placed in the extruder, and the extruder was run using the minimum push force. A light-shaded wet salt was extruded, with much larger grains (similar to FTF-456) when compared to the previous "creamy" salt slurries (FTF-463 and FTF-464).

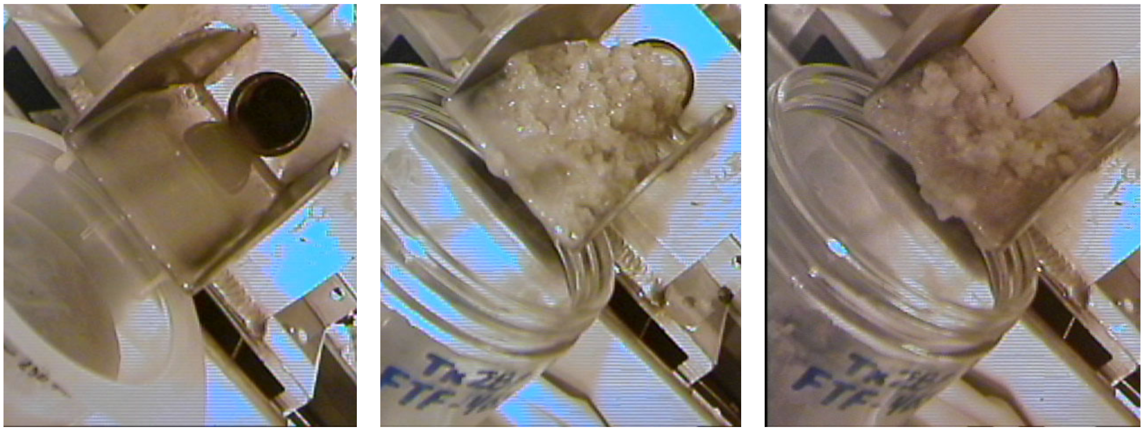

Figure 23: Extrusion of Sample FTF-465

FTF-466; segment 28-11

The sleeving material was dripping on the outside, but no liquid was evident inside the sleeving when the sampler was removed. Prior to the sample being opened, the ball valve was clean and free of debris. As the ball valve was opened, approximately 220 mL of low viscosity fluid (similar to that of water) flowed out. The liquid had a slight tint and cloudiness, but no saltcake was evident in this sample.

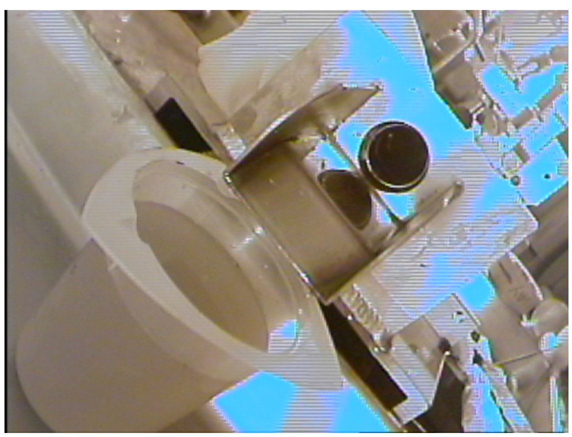

Figure 24: Extrusion of Sample FTF-466

FTF-467; segment 28-12

The sampler was clean and dry, with several small dents in the tip. During sampler disassembly, the release disk came out before the spring stops were removed, indicating that the piston was not fully retracted and not tight against the spring stops. As the ball valve was opened, it was evident that the sampler contained no liquid or solid material.

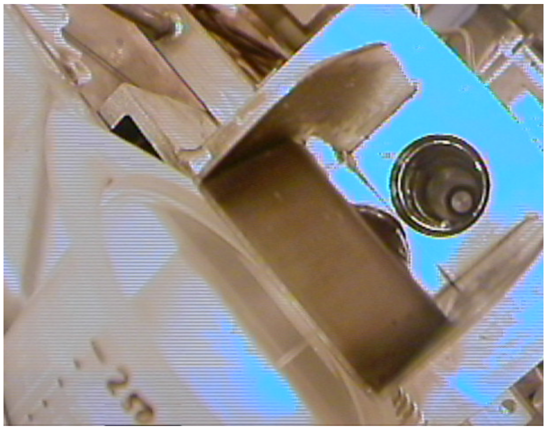

Figure 25: Extrusion of Sample FTF-467

A.2 Adjustment of Saltcake Measurements for Drill-String Fluid Content

The effect of DSF on the saltcake segment concentration is assumed to be due to two phenomena, one is dilution and removal of interstitial liquid and any soluble species, and the other is concentration of insoluble species in the remaining saltcake due to dissolution and removal of sodium nitrate. When liquid is found in the samplers, there is no way to actually know where it came from. Possible origins are: (1) in-leakage of drill string fluid from the drill string during sampling; (2) percolation of interstitial liquid from the tank into the sampler; or (3) in-leakage of drill string fluid before or after sampling as the sampler is being raised or lowered. The presence of bromide in the samples indicates that some of the DSF entered the samplers, but it is not known if the DSF was unsaturated and thereby dissolved some of the saltcake in the samples, or if the DSF intermingled with the tank supernate prior to entering the samplers and thereby did not dissolve saltcake in the samplers. The fit of the correlation between bromide ion concentration and Cs-137 concentration (Figure 6) indicates a slight upward curvature, and the linear fit does not pass through 0.125 M on the y-axis, which corresponds to 1.0 wt% bromide. This indicates that the DSF partially dissolved the saltcake in the sampler because this would have caused an expansion of the liquid due to dissolution of sodium nitrate, and non-linearity of the correlation. Most likely, both mixing of DSF with supernate, and dissolution of some saltcake occurred. To bracket the possible effect of DSF, calculations are performed to yield a maximum correction factor for both soluble and insoluble species.

To illustrate the estimated effect of DSF on soluble species in the liquid phase, a sample calculation is shown, using analysis results from sample FTF-456 and assuming that the liquid in FTF-462 is representative of the original interstitial liquid in all the samples. Also, the estimated expansion of the DSF is approximately 30% upon dissolution of sodium nitrate. This has the effect of lowering the concentration of bromide to 7000 mg/L.

	Liquid gamma (Ci/gal)	Br (mg/L)	vol fract DSF b/o Br	DSF-corrected Cs-137 (Ci/gal)
#1; FTF-456	3.10	3250	0.46	5.8
#2; FTF-457	2.70	3767	0.54	5.8
#3; FTF-458	1.80	6475	0.93	24.0
#4; FTF-459	4.10	2500	0.36	6.4
#5; FTF-460	2.80	4124	0.59	6.8
#6; FTF-461	4.50	2155	0.31	6.5
#7; FTF-462	5.40	300	0.04	5.6
#8; FTF-463	5.20	687	0.10	5.8
#9; FTF-464	5.30	1475	0.21	6.7
#10; FTF-465	4.40	2653	0.38	7.1
#11; FTF-466	0.87	8477	1.21	

% DSF based on Br = 100 x [Br]/7000 mg/L = 100 x 3250 mg/L/7000 mg/L = 46 vol%

DSF-dilution corrected Cs content = [Cs-137]/(1-vol fraction DSF) = 3.1 Ci/gal/0.54 = 5.7 Ci/gal

The result for FTF-458 is not consistent and is not readily explained. The result for FTF-466 indicates that the volume fraction of DSF is >100%; however, what appears to have happened is that this solution was not fully saturated with dissolved sodium nitrate, so the assumed 30% expansion in the calculation is not valid. This is consistent with the density of this liquid (1.110 g/mL), which indicates it is under-saturated in sodium nitrate.

The remaining estimated values are fairly consistent and indicate that the true Cs-137 content in interstitial liquid is 6.3 Ci/gal. A comparison with data in Table 8 indicates that the Cs-137 content of saltcake segments has a much larger variance. This is evidently because of a varying water content in the saltcake segments which appears proportional to other soluble analytes. For example, Cs-137 in FTF-456 is 1.43E8 pCi/g, and FTF-462 is 6.24E8 pCi/g, a difference of more than 4-fold, although the estimated difference in DSF-corrected free liquid phase Cs concentration is less than 5%. This observation is fairly consistent when viewed along with the water content reported in Table 5.

To illustrate the estimated effect of DSF on insoluble species, a sample calculation is shown, using analysis results from sample FTF-456 and assuming that the liquid in FTF-462 is representative of the original interstitial liquid in all the samples.

Total FL volume = 263.18 g/1.4178 g/mL = 186 mL

Total nitrate in solution = [NO_3^-] x total FL volume = 2.1 M x 0.186 L = 0.390 moles NO_3^-

mL supernate in FL = (Cs-137 vol fraction) x FL volume
= (3.1 Ci/gal/5.4 Ci/gal) x 186 mL =107 mL

Moles nitrate from original supernate in FL = mL supernate x [NO_3^-] = 0.107 L x 1.425 M
= 0.152 moles NO_3^-

Moles NO_3^- dissolved in FL = moles NO_3^- total – moles NO_3^- in supernate
= 0.39 mol – 0.152 mol = 0.24 mol.

Grams sodium nitrate dissolved in sample = 0.24 moles x 84.99 g/m = 20.4 g

% of total sample = 100 x (20.4 g/(20.4 g + 38.81 g)) = 34%

This translates to a maximum 34% “dilution” of insoluble solids in the saltcake segment analysis, where the solid sodium nitrate would have diluted the insoluble species relative to the amount measured.

	Liquid gamma (Ci/gal)	Br (mg/L)	vol fract IL b/o Cs-137	Free Liquid (g)	Wet Solids (g)	density (g/mL)	[NO3] (M)	total NO3 (moles)	moles NO3 in supern.	g NaNO3 diss. in FL	% of total sample
#1; FTF-456	3.10	3250	0.57	263.18	38.81	1.4178	2.1069	0.3911	0.152	20.33	34.4
#2; FTF-457	2.70	3767	0.50	29.68	210.87	1.4800	2.0721	0.0416	0.014	2.32	1.1
#3; FTF-458	1.80	6475	0.33	95.39	0.00	1.3383	2.0934	0.1492	0.034	9.80	100.0
#4; FTF-459	4.10	2500	0.76	125.44	36.41	1.4614	1.7073	0.1465	0.093	4.56	11.1
#5; FTF-460	2.80	4124	0.52	168.98	71.33	1.3913	2.6339	0.3199	0.090	19.56	21.5
#6; FTF-461	4.50	2155	0.83	232.72	221.86	1.4504	1.6290	0.2614	0.191	6.02	2.6
#7; FTF-462	5.40	300	1.00	279.65	81.26	1.4877	1.4250	0.2679	0.268	0.00	0.0
#8; FTF-463	5.20	687	0.96	19.03	25.69	1.4275	1.5525	0.0207	0.018	0.20	0.8
#9; FTF-464	5.30	1475	0.98	101.06	41.90	1.4588	1.4730	0.1020	0.097	0.44	1.0
#10; FTF-465	4.40	2653	0.81	278.88	131.26	1.4522	1.5441	0.2965	0.223	6.25	4.5
#11; FTF-466	0.87	8477	0.16	230.83	0.00	1.1099	0.2362	0.0491	0.048	0.12	100.0

Samples FTF-458 and FTF-466 appear to contain sodium nitrate that can only be attributed to supernate. This is consistent with the observation that neither of these samples contained appreciable insoluble solids when extruded.

To correct for the effect of DSF on a dissolved saltcake sample, data from sample FTF-462 in Table 8 is used. The calculation of the Cs-137 content for a theoretical dissolution of this undrained saltcake to 6.0 M [Na^+] is shown below.

6.0 M [Na^+] = 6.0 mol/L x 22.99 g/mol = 138 g Na/L

[Na^+] = 20.7 g/100 g saltcake

$$\frac{138 \text{ g Na/L}}{0.207 \text{ g Na/g saltcake}} = 666.7 \text{ g saltcake/L}$$

Cs-137 = 6.24E8 pCi/g saltcake

6.24E8 pCi/g saltcake x 666.7 g saltcake/L = 4.16E11 pCi/L = 0.416 Ci/L

0.416 Ci/L x 3.785 L/gal = 1.57 Ci/gal

A.3 Variability Charts of Segment Data

Variability Chart for F wt %

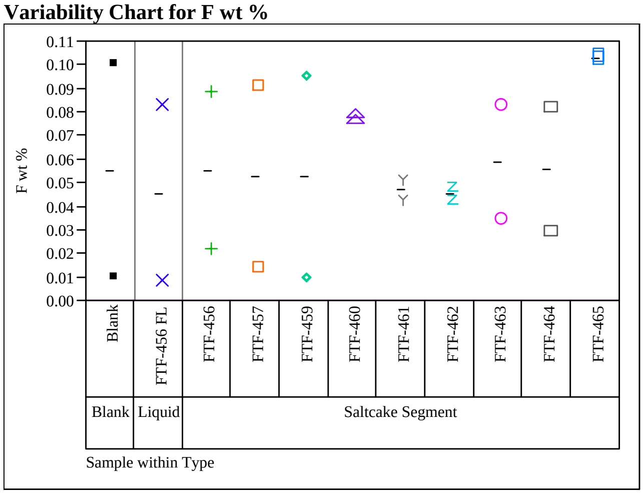

Variability Chart for NO2 wt %

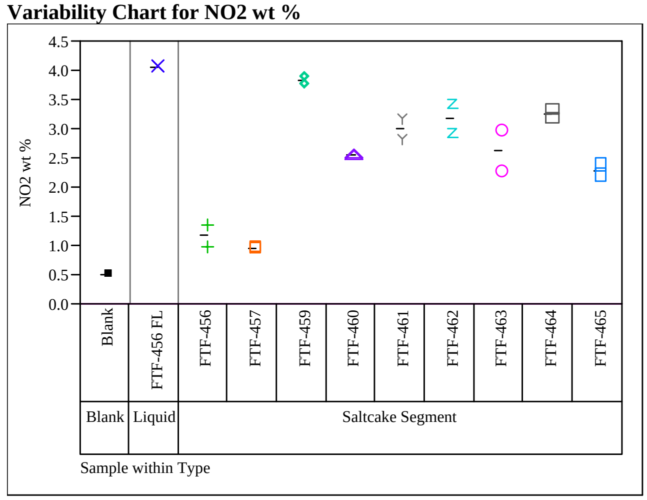

Variability Chart for CHO2 wt %

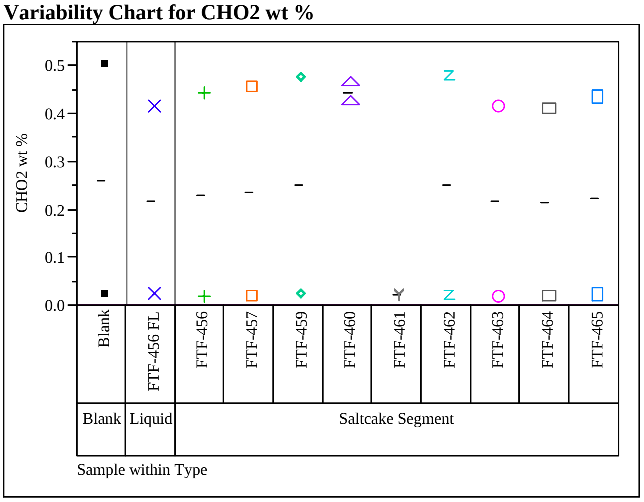

Variability Chart for Br wt %

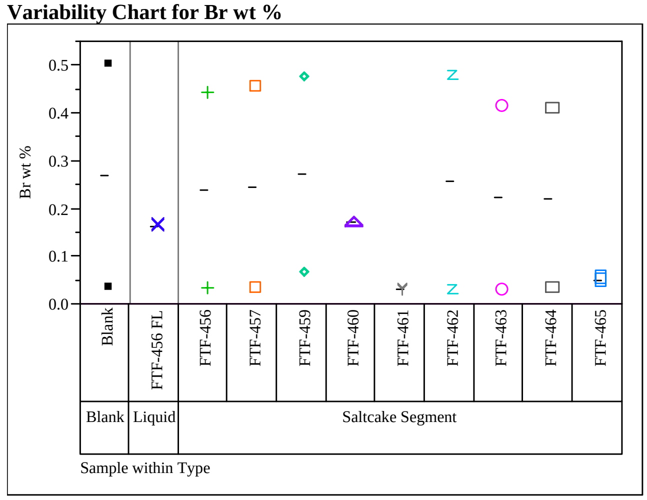

Variability Chart for Cl wt %

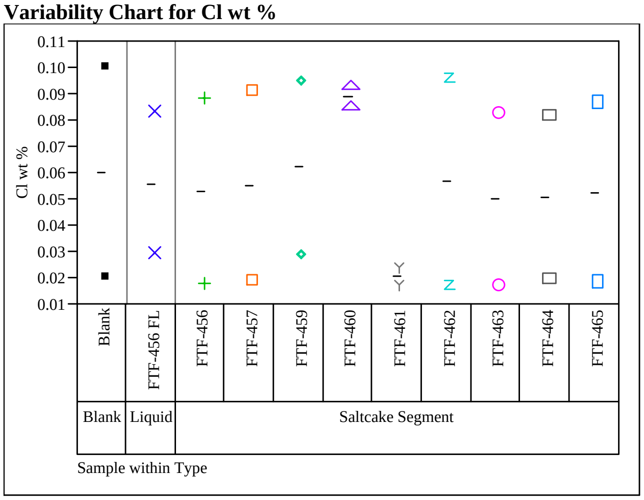

Variability Chart for NO3 wt %

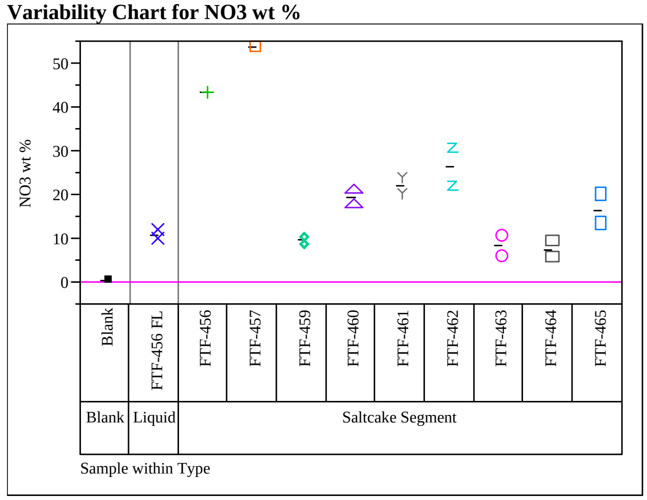

Variability Chart for PO4 wt %

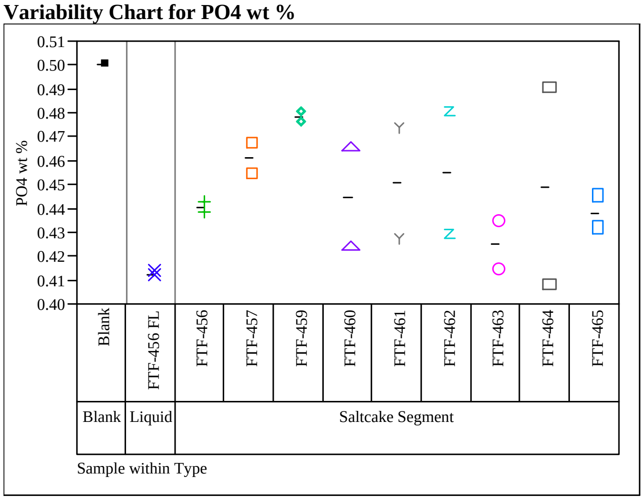

Variability Chart for SO4 wt %

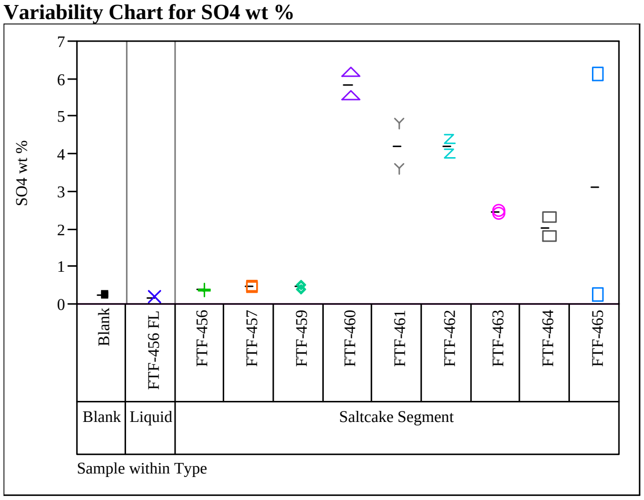

Variability Chart for C2O4 wt %

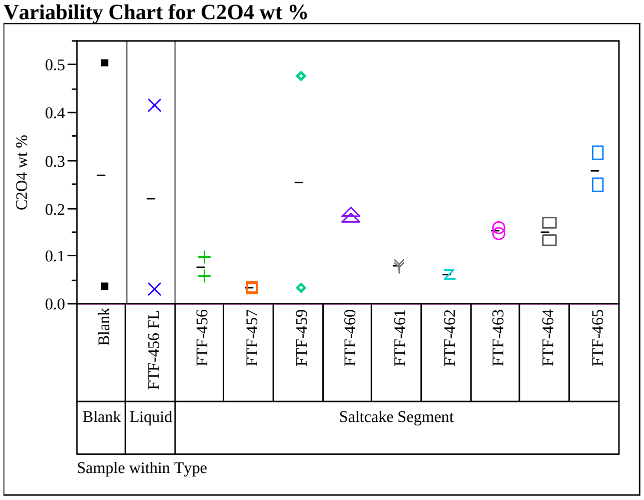

Variability Chart for CO3 (TIC) wt %

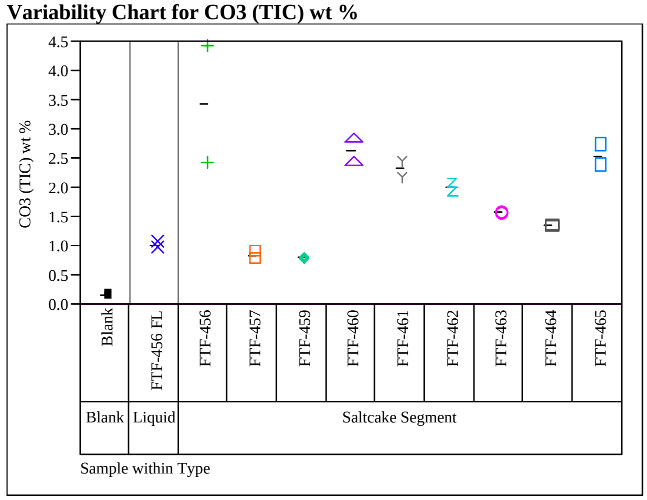

Variability Chart for OH wt %

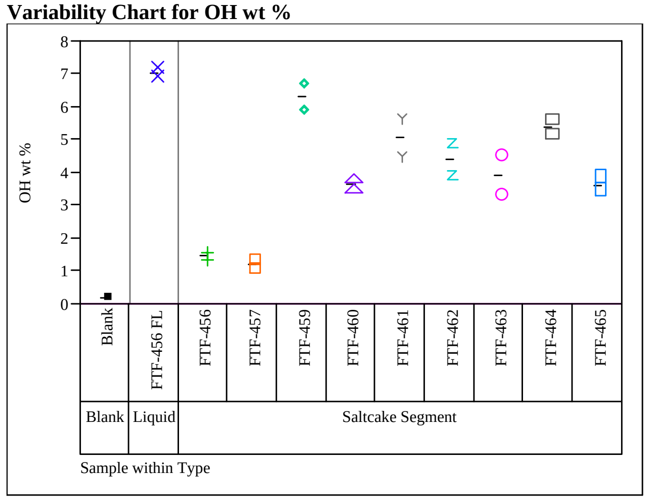

Variability Chart for AlO2 (titration) wt %

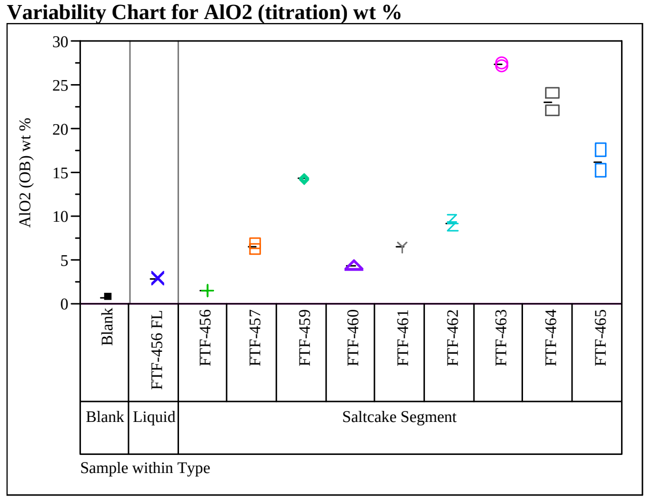

Variability Chart for AlO2 (ICP-ES) wt %

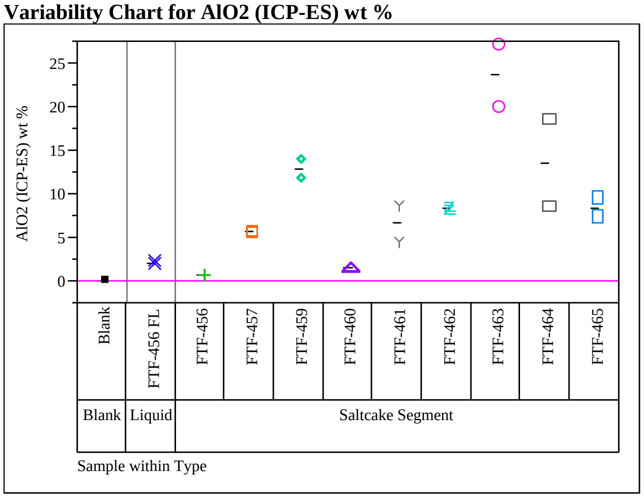

Variability Chart for Ag ICP-ES (wt%)

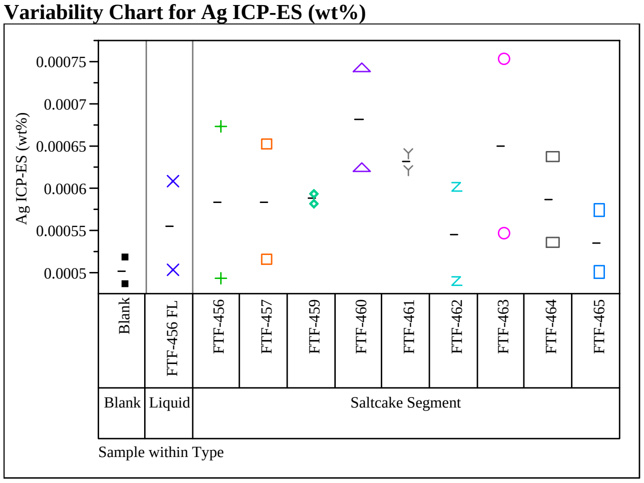

Variability Chart for Al ICP-ES (wt%)

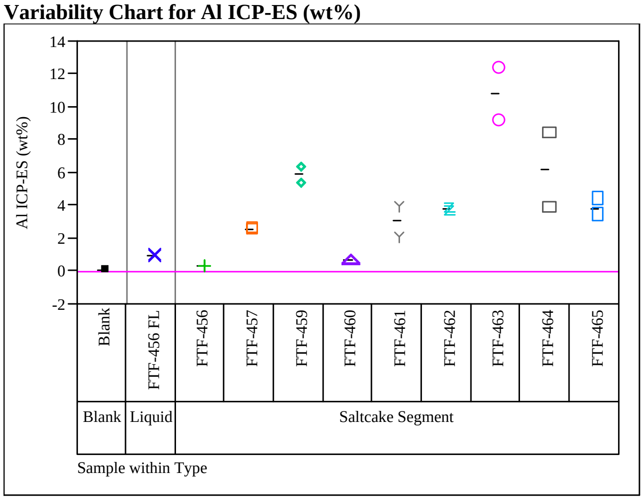

Variability Chart for Ba ICP-ES (wt%)

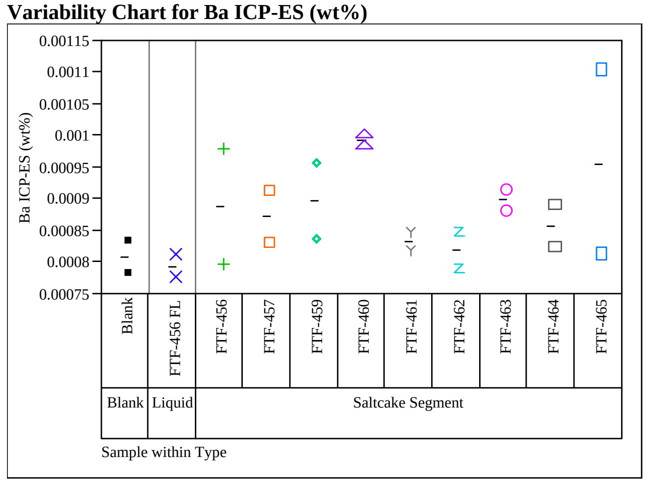

Variability Chart for Ca ICP-ES (wt%)

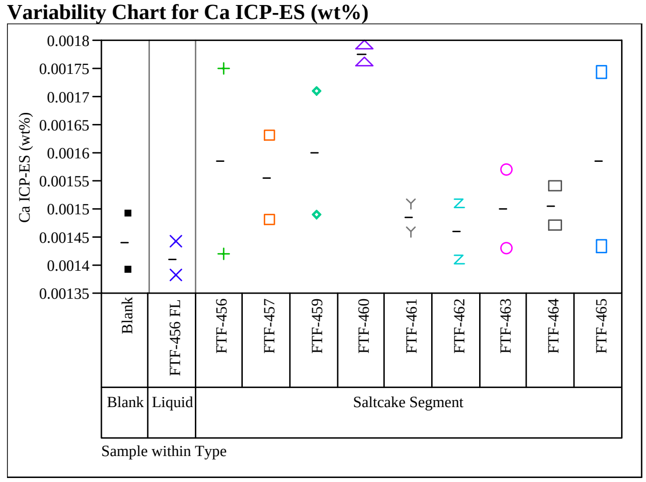

Variability Chart for Ce ICP-ES (wt%)

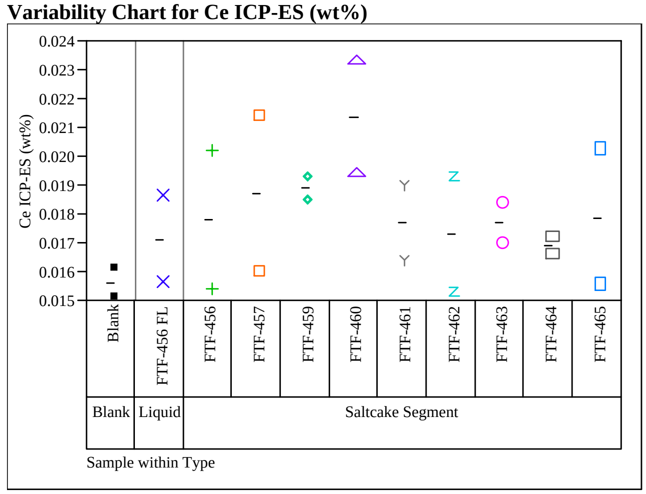

Variability Chart for Cr ICP-ES (wt%)

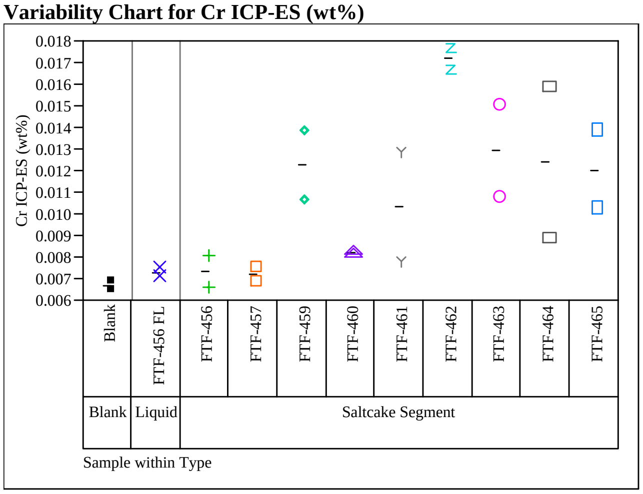

Variability Chart for Gd ICP-ES (wt%)

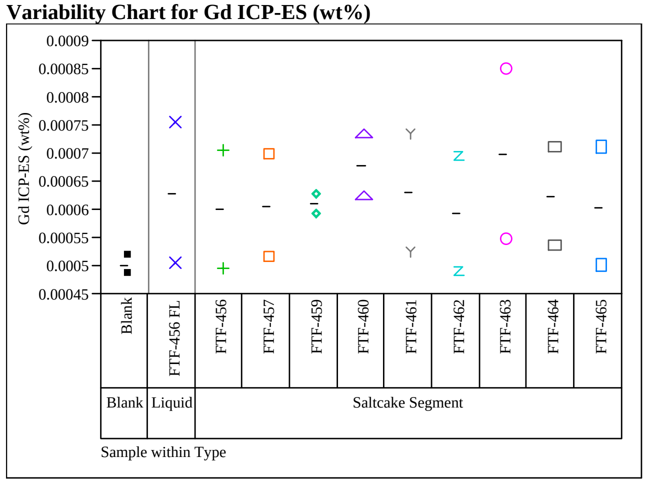

Variability Chart for Cu ICP-ES (wt%)

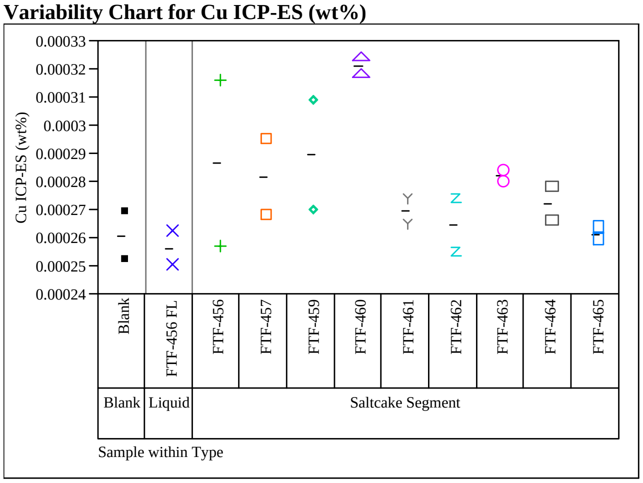

Variability Chart for K ICP-ES (wt%)

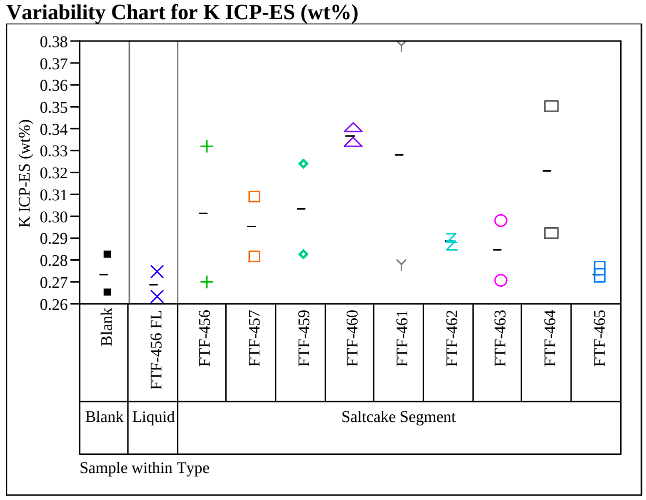

Variability Chart for Fe ICP-ES (wt%)

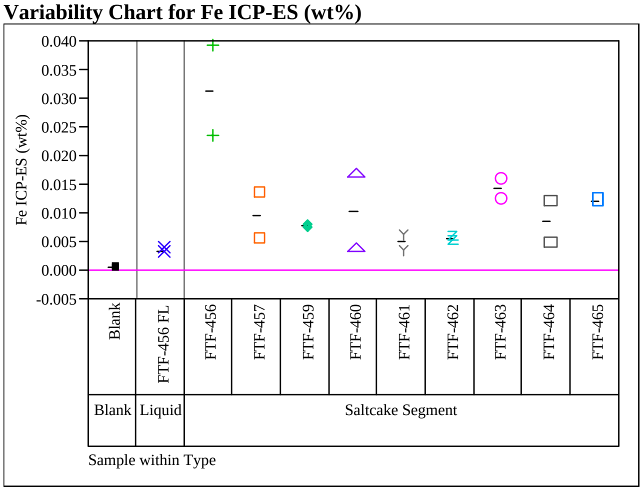

Variability Chart for Li ICP-ES (wt%)

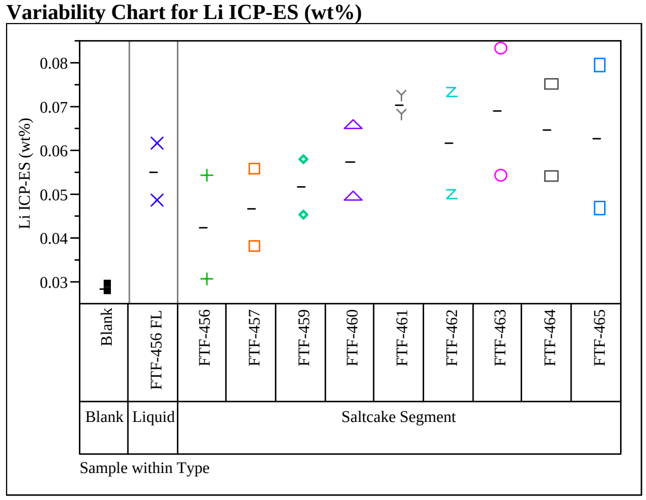

Variability Chart for Mn ICP-ES (wt%)

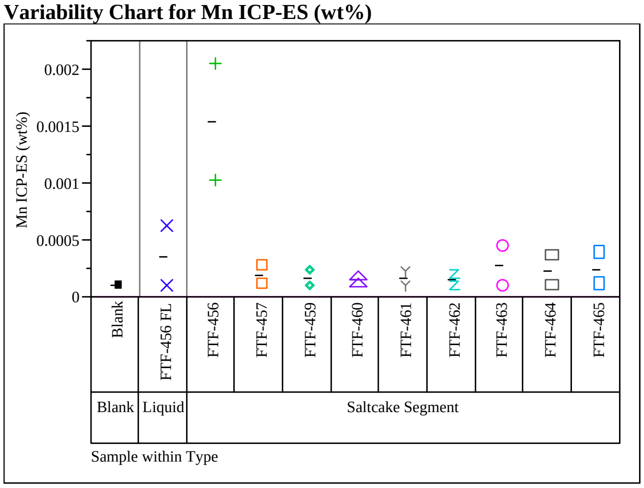

Variability Chart for S ICP-ES (wt%)

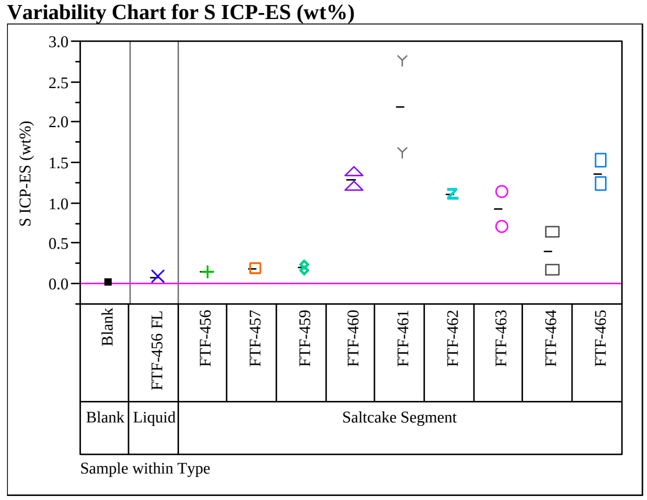

Variability Chart for Na ICP-ES (wt%)

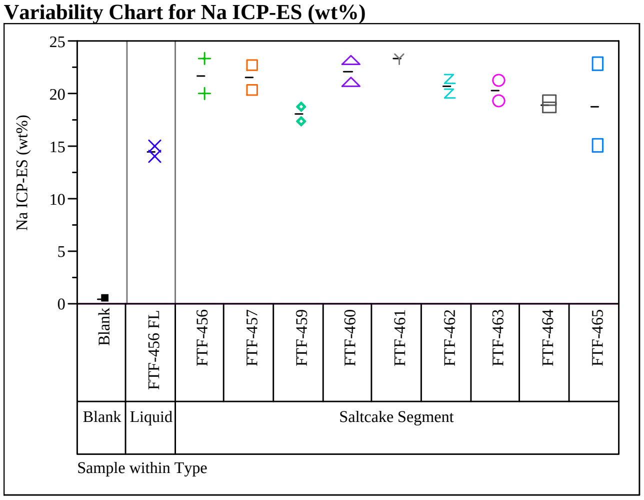

Variability Chart for Sb ICP-ES (wt%)

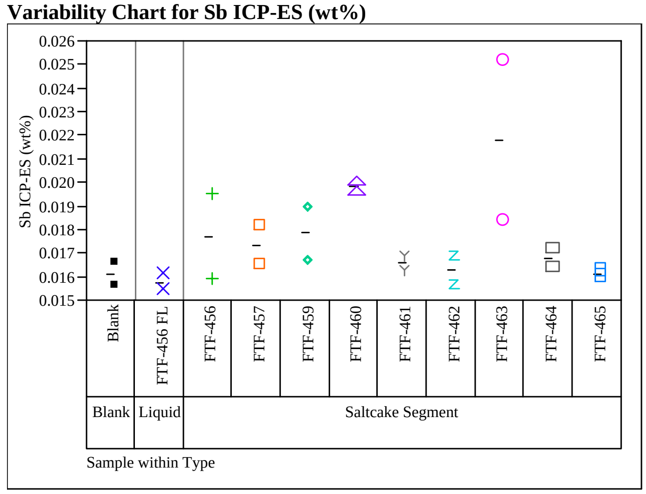

Variability Chart for P ICP-ES (wt%)

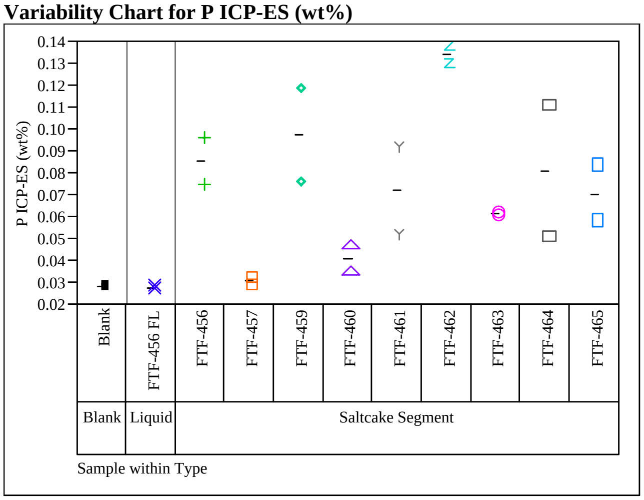

Variability Chart for Si ICP-ES (wt%)

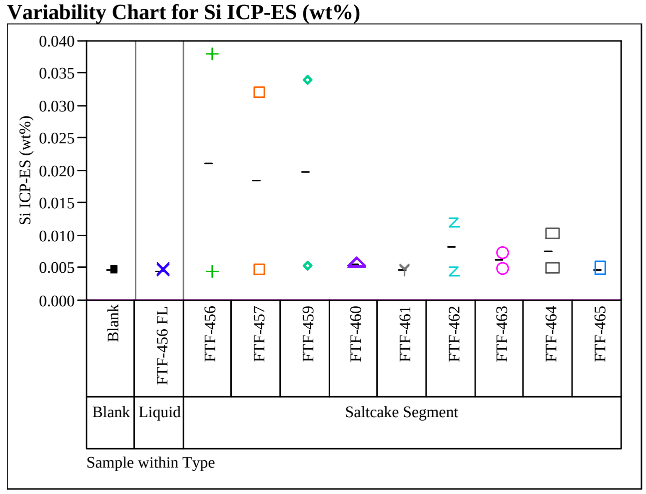

Variability Chart for Ti ICP-ES (wt%)

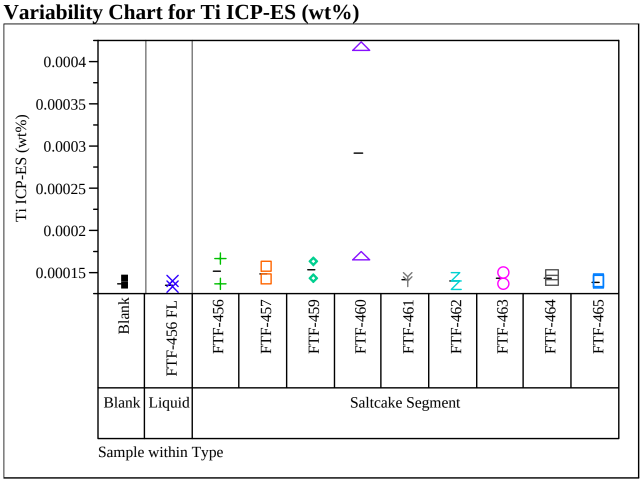

Variability Chart for U ICP-ES (wt%)

Variability Chart for Zn ICP-ES (wt%)

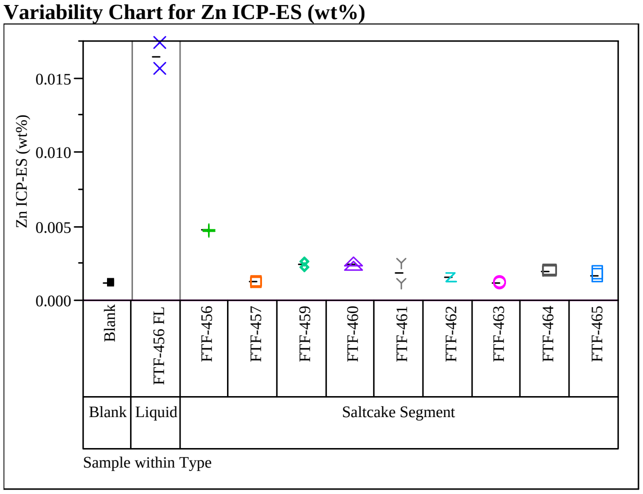

Variability Chart for Cs-137 (pCi/g)

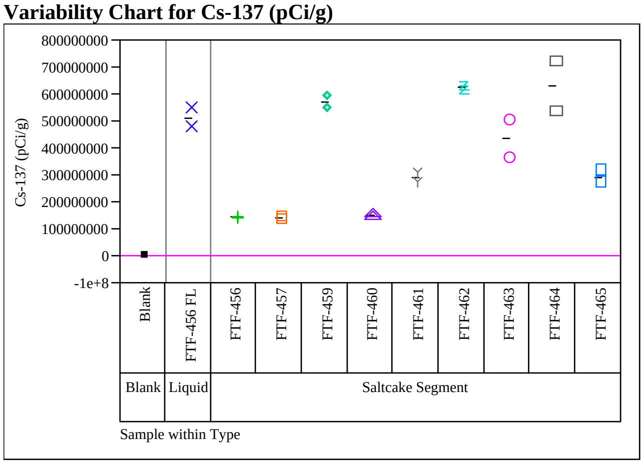

Variability Chart for Pu-239/240 (pCi/g)

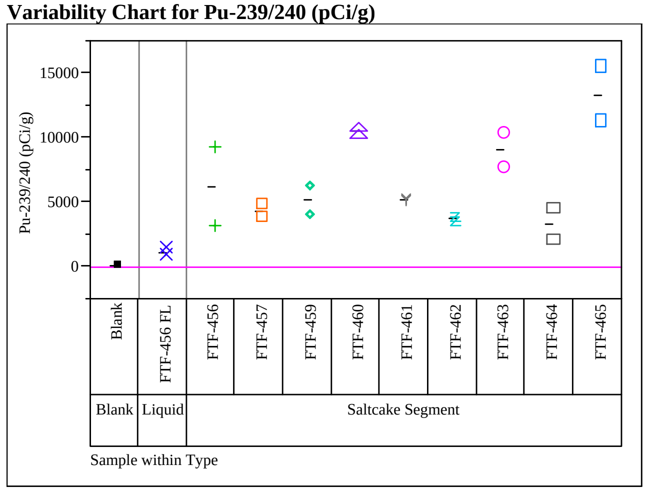

Variability Chart for Co-60 (pCi/g)

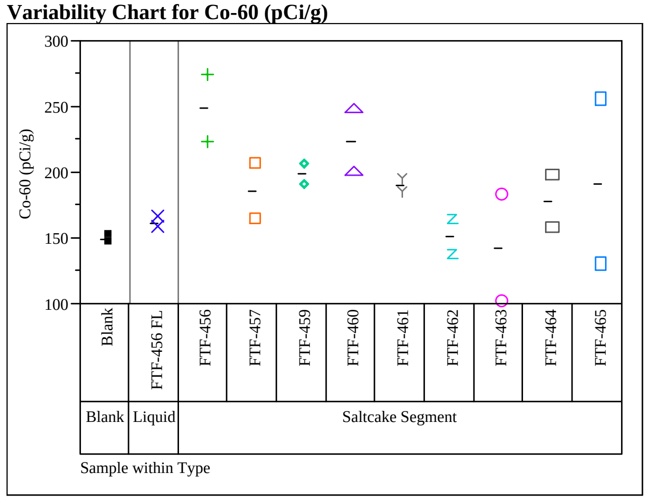

Variability Chart for Sb-126 (pCi/g)

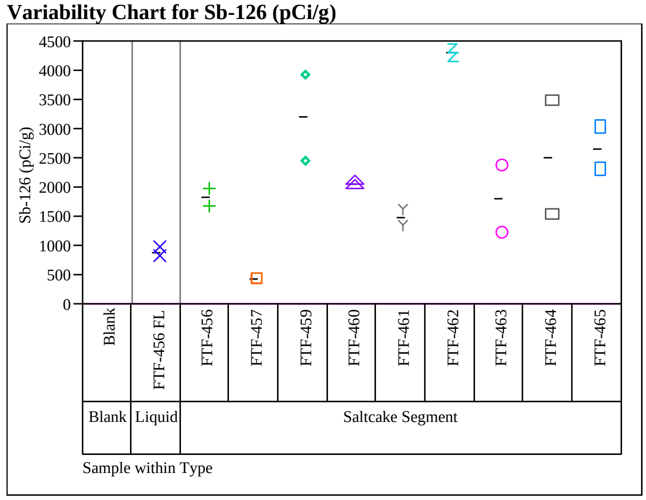

Variability Chart for Sn-126 (pCi/g)

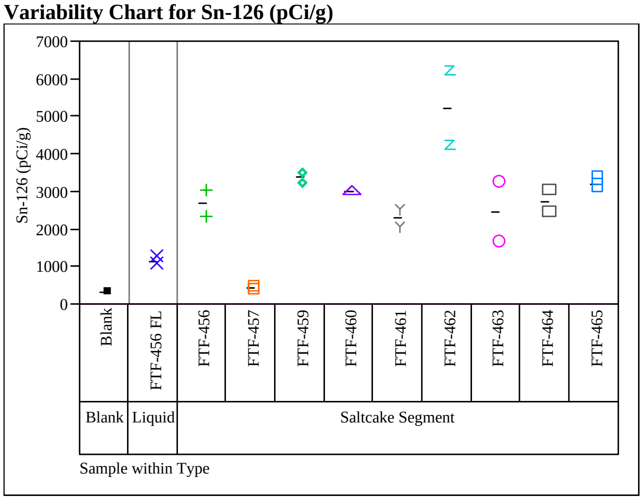

Variability Chart for Cs-rem beta (pCi/g)

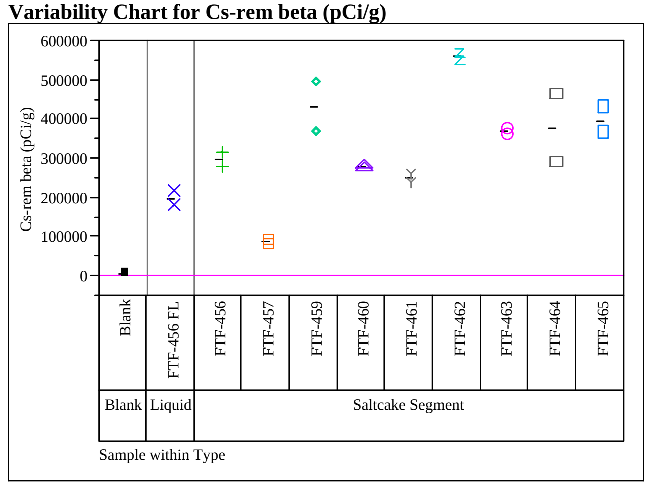

Variability Chart for Eu-154 (pCi/g)

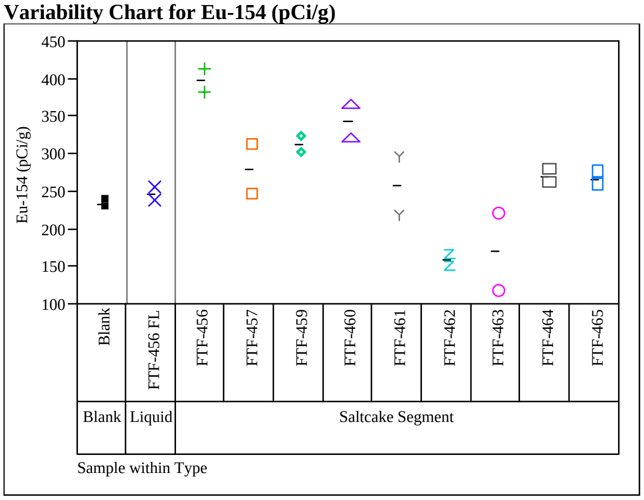

Variability Chart for Tc-99 (ICP-MS) (pCi/g)

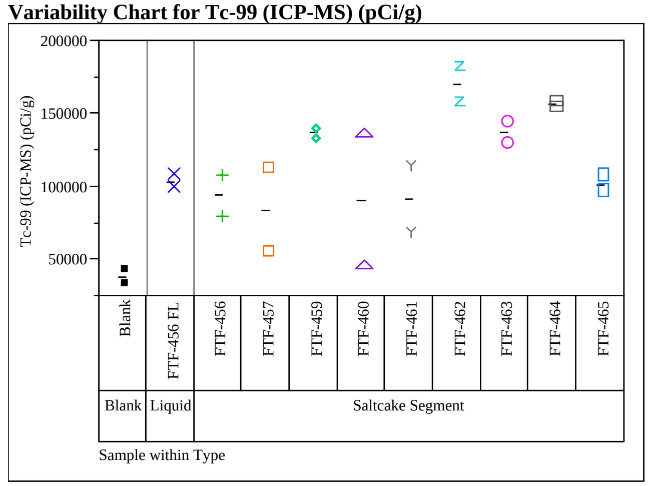

Variability Chart for Am-241 (pCi/g)

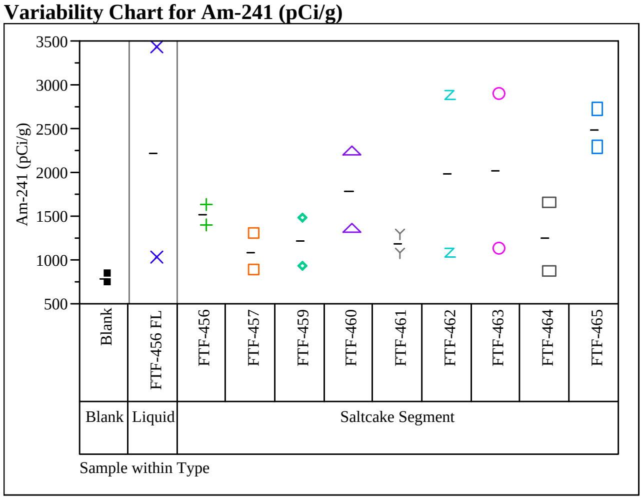

Variability Chart for Mass-133 (Cs) ICP-MS (wt%)

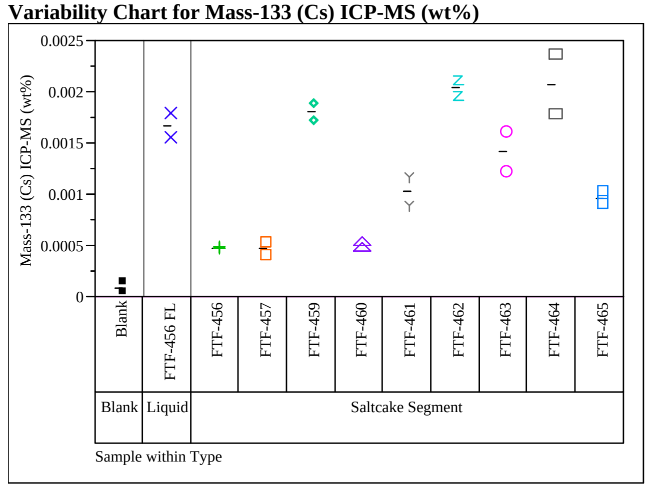

Variability Chart for Mass-135 (Cs,Ba) ICP-MS (wt%)

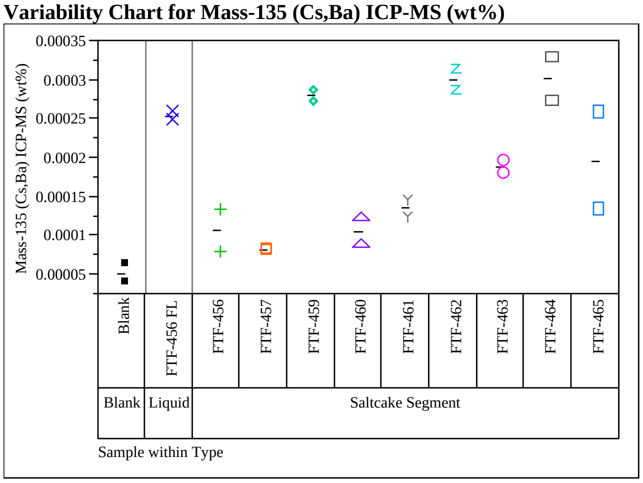

Variability Chart for Mass-238 (U) ICP-MS (wt%)

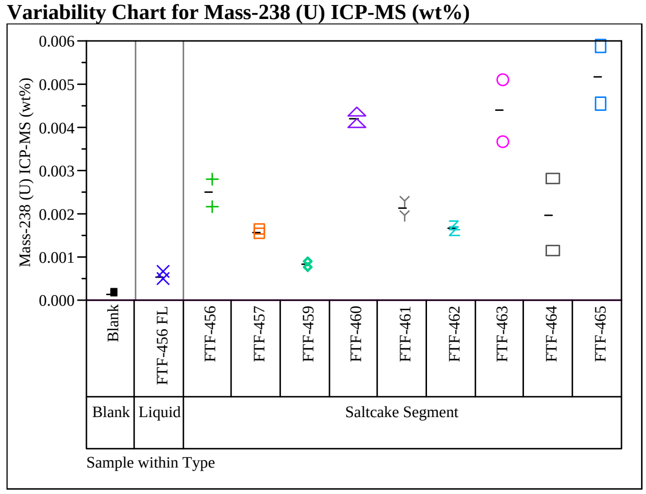

Variability Chart for Mass-137 (Cs,Ba) ICP-MS (wt%)

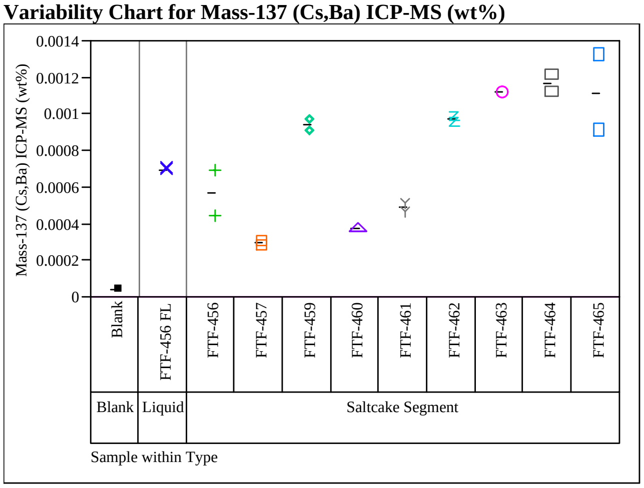

Variability Chart for Mass-235 (U) ICP-MS (wt%)

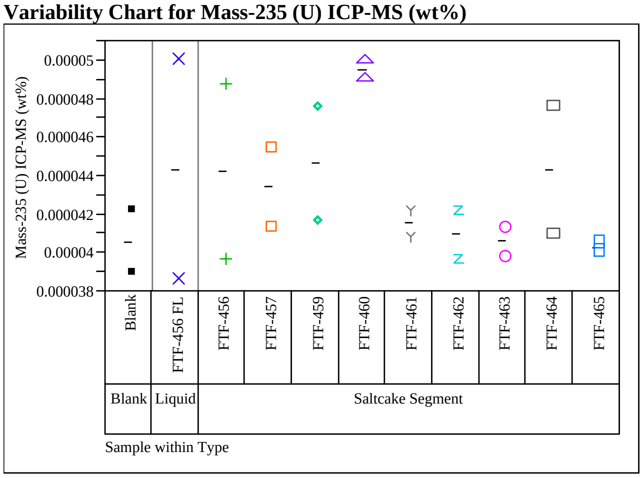

A.4 Bivariate Fits of Segment Data

Bivariate Fit of Cs-137 (pCi/g) By Cr ICP-ES (wt%)

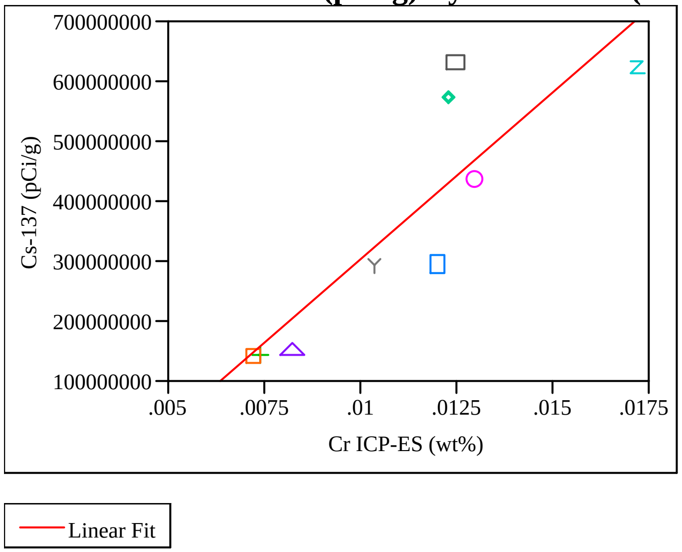

Linear Fit

Cs-137 (pCi/g) = -2.561e+8 + 5.583e+10 Cr ICP-ES (wt%)

Summary of Fit

RSquare	0.755355
RSquare Adj	0.720406
Root Mean Square Error	1.092e+8
Mean of Response	3.64e+8
Observations (or Sum Wgts)	9

Analysis of Variance

Source	DF	Sum of Squares	Mean Square	F Ratio
Model	1	2.5774e+17	2.577e+17	21.6129
Error	7	8.3477e+16	1.193e+16	Prob > F
C. Total	8	3.4122e+17		0.0023

Parameter Estimates

Term	Estimate	Std Error	t Ratio	Prob>|t|
Intercept	-2.561e+8	1.383e+8	-1.85	0.1064
Cr ICP-ES (wt%)	5.583e+10	1.2e+10	4.65	0.0023

Bivariate Fit of Cs-rem beta (pCi/g) By Cr ICP-ES (wt%)

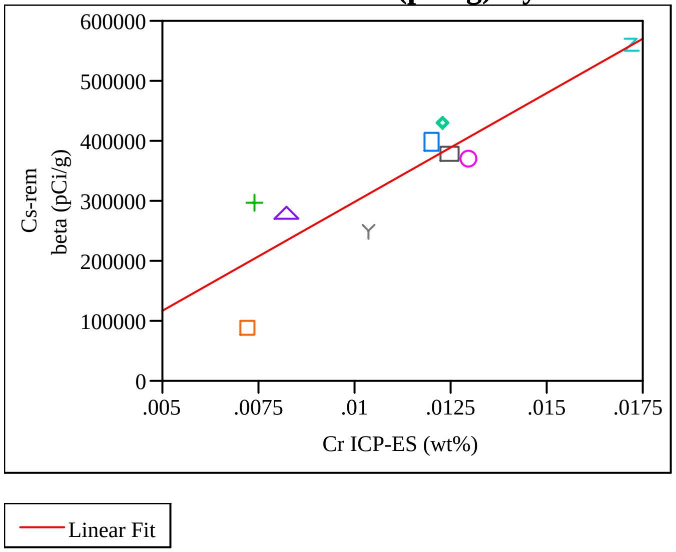

Linear Fit

Cs-rem beta (pCi/g) = -63834.59 + 36174885 Cr ICP-ES (wt%)

Summary of Fit

RSquare	0.776149
RSquare Adj	0.744171
Root Mean Square Error	66775.51
Mean of Response	337988
Observations (or Sum Wgts)	9

Analysis of Variance

Source	DF	Sum of Squares	Mean Square	F Ratio
Model	1	1.0822e+11	1.082e+11	24.2708
Error	7	3.1213e+10	4.459e+9	Prob > F
C. Total	8	1.3944e+11		0.0017

Parameter Estimates

Term	Estimate	Std Error	t Ratio	Prob>|t|
Intercept	-63834.59	84545.4	-0.76	0.4749
Cr ICP-ES (wt%)	36174885	7342851	4.93	0.0017

Bivariate Fit of Mass-133 (Cs) ICP-MS (wt%) By Cr ICP-ES (wt%)

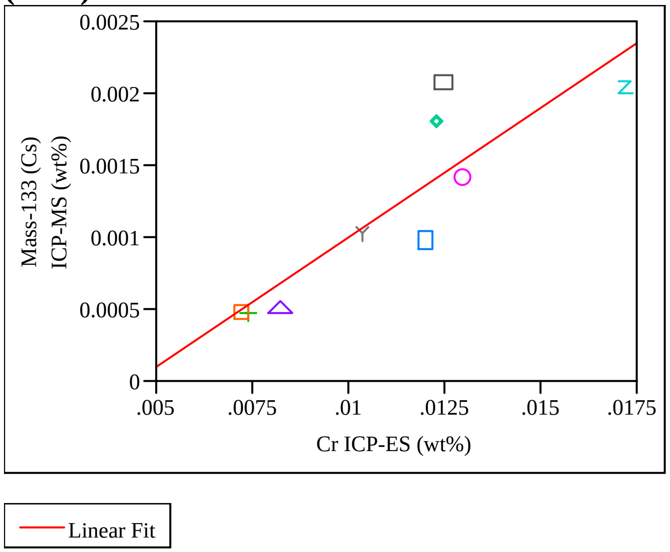

Linear Fit

Mass-133 (Cs) ICP-MS (wt%) = -0.000803 + 0.1798983 Cr ICP-ES (wt%)

Summary of Fit

RSquare	0.759443
RSquare Adj	0.725077
Root Mean Square Error	0.000348
Mean of Response	0.001195
Observations (or Sum Wgts)	9

Analysis of Variance

Source	DF	Sum of Squares	Mean Square	F Ratio
Model	1	2.67645e-6	2.6764e-6	22.0991
Error	7	8.47779e-7	1.2111e-7	Prob > F
C. Total	8	3.52423e-6		0.0022

Parameter Estimates

Term	Estimate	Std Error	t Ratio	Prob>|t|
Intercept	-0.000803	0.000441	-1.82	0.1111
Cr ICP-ES (wt%)	0.1798983	0.038268	4.70	0.0022

Bivariate Fit of Mass-135 (Cs,Ba) ICP-MS (wt%) By Cr ICP-ES (wt%)

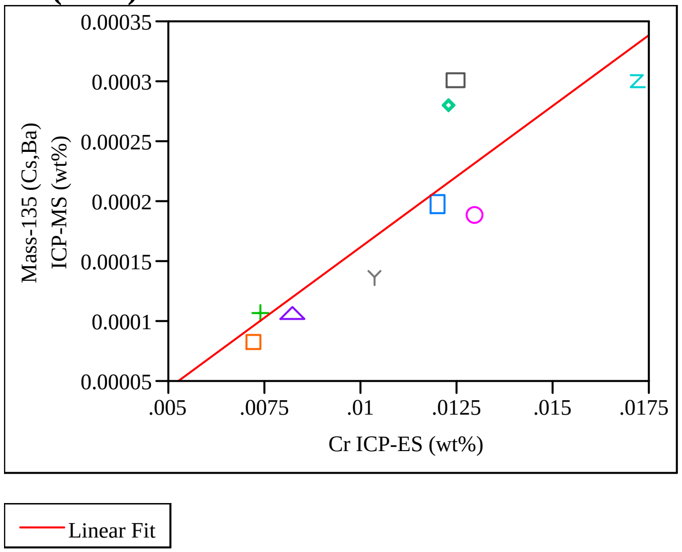

Linear Fit

Mass-135 (Cs,Ba) ICP-MS (wt%) = -0.000073 + 0.0234992 Cr ICP-ES (wt%)

Summary of Fit

RSquare	0.747051
RSquare Adj	0.710915
Root Mean Square Error	0.000047
Mean of Response	0.000188
Observations (or Sum Wgts)	9

Analysis of Variance

Source	DF	Sum of Squares	Mean Square	F Ratio
Model	1	4.5668e-8	4.5668e-8	20.6736
Error	7	1.5463e-8	2.209e-9	Prob > F
C. Total	8	6.1131e-8		0.0026

Parameter Estimates

Term	Estimate	Std Error	t Ratio	Prob>|t|
Intercept	-0.000073	5.951e-5	-1.23	0.2593
Cr ICP-ES (wt%)	0.0234992	0.005168	4.55	0.0026

Bivariate Fit of Mass-137 (Cs,Ba) ICP-MS (wt%) By Cr ICP-ES (wt%)

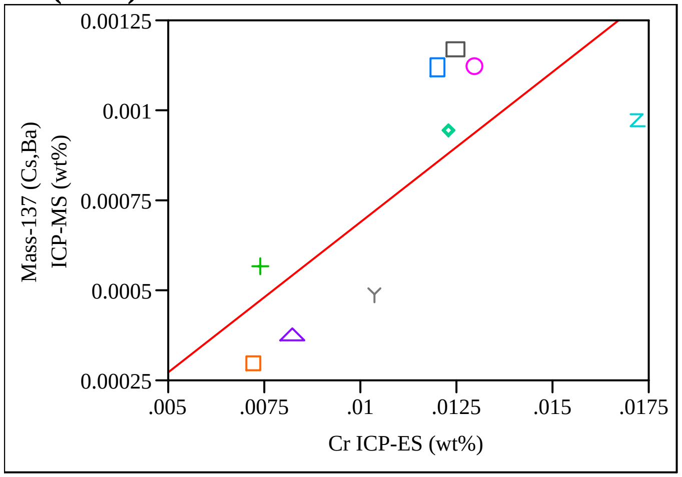

Linear Fit

Linear Fit

Mass-137 (Cs,Ba) ICP-MS (wt%) = -0.000142 + 0.0831716 Cr ICP-ES (wt%)

Summary of Fit

RSquare	0.58966
RSquare Adj	0.53104
Root Mean Square Error	0.000238
Mean of Response	0.000782
Observations (or Sum Wgts)	9

Analysis of Variance

Source	DF	Sum of Squares	Mean Square	F Ratio
Model	1	5.72077e-7	5.7208e-7	10.0590
Error	7	3.98105e-7	5.6872e-8	Prob > F
C. Total	8	9.70182e-7		0.0157

Parameter Estimates

Term	Estimate	Std Error	t Ratio	Prob>|t|
Intercept	-0.000142	0.000302	-0.47	0.6518
Cr ICP-ES (wt%)	0.0831716	0.026224	3.17	0.0157

Bivariate Fit of NO2 wt % By Cr ICP-ES (wt%)

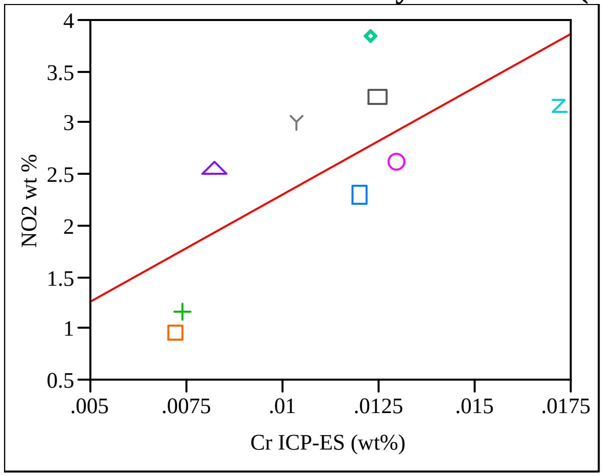

Linear Fit

Linear Fit

NO2 wt % = 0.2280329 + 207.81644 Cr ICP-ES (wt%)

Summary of Fit

RSquare	0.491391
RSquare Adj	0.418733
Root Mean Square Error	0.726711
Mean of Response	2.536412
Observations (or Sum Wgts)	9

Analysis of Variance

Source	DF	Sum of Squares	Mean Square	F Ratio
Model	1	3.5716163	3.57162	6.7630
Error	7	3.6967576	0.52811	Prob > F
C. Total	8	7.2683739		0.0354

Parameter Estimates

Term	Estimate	Std Error	t Ratio	Prob>|t|
Intercept	0.2280329	0.920098	0.25	0.8114
Cr ICP-ES (wt%)	207.81644	79.91144	2.60	0.0354

Bivariate Fit of OH wt % By Cr ICP-ES (wt%)

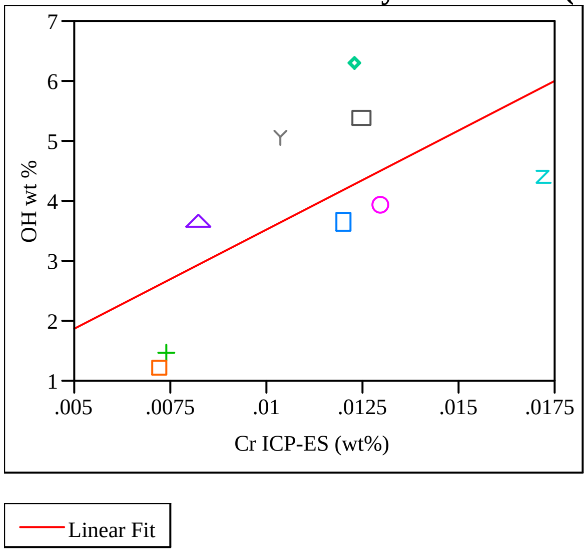

Linear Fit

OH wt % = 0.2367255 + 328.49843 Cr ICP-ES (wt%)

Summary of Fit

RSquare	0.390332
RSquare Adj	0.303237
Root Mean Square Error	1.411128
Mean of Response	3.885613
Observations (or Sum Wgts)	9

Analysis of Variance

Source	DF	Sum of Squares	Mean Square	F Ratio
Model	1	8.924248	8.92425	4.4817
Error	7	13.938967	1.99128	Prob > F
C. Total	8	22.863214		0.0720

Parameter Estimates

Term	Estimate	Std Error	t Ratio	Prob>|t|
Intercept	0.2367255	1.786648	0.13	0.8983
Cr ICP-ES (wt%)	328.49843	155.1721	2.12	0.0720

Bivariate Fit of P ICP-ES (wt%) By Cr ICP-ES (wt%)

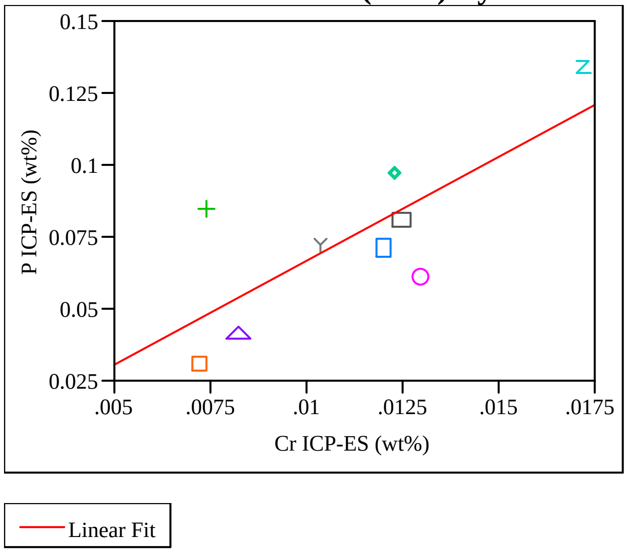

Linear Fit

P ICP-ES (wt%) = -0.006105 + 7.2706566 Cr ICP-ES (wt%)

Summary of Fit

RSquare	0.582516
RSquare Adj	0.522875
Root Mean Square Error	0.021156
Mean of Response	0.074656
Observations (or Sum Wgts)	9

Analysis of Variance

Source	DF	Sum of Squares	Mean Square	F Ratio
Model	1	0.00437172	0.004372	9.7671
Error	7	0.00313318	0.000448	Prob > F
C. Total	8	0.00750490		0.0167

Parameter Estimates

Term	Estimate	Std Error	t Ratio	Prob>|t|
Intercept	-0.006105	0.026787	-0.23	0.8262
Cr ICP-ES (wt%)	7.2706566	2.326435	3.13	0.0167

Bivariate Fit of Sb-126 (pCi/g) By Cr ICP-ES (wt%)

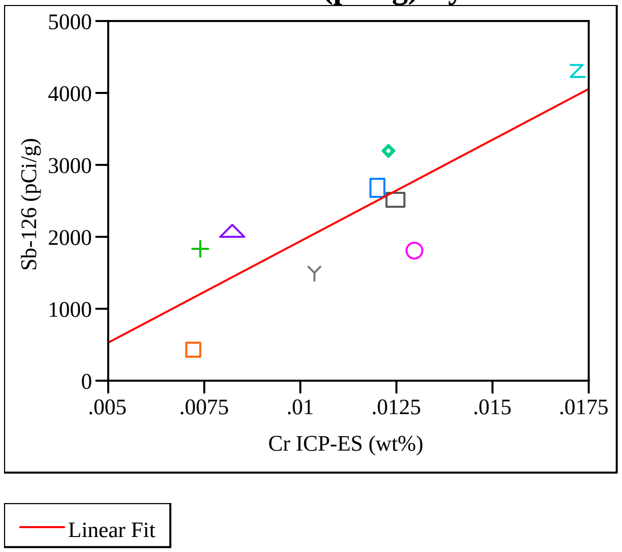

Linear Fit

Sb-126 (pCi/g) = -883.3088 + 281965.27 Cr ICP-ES (wt%)

Summary of Fit

RSquare	0.682179
RSquare Adj	0.636775
Root Mean Square Error	661.518
Mean of Response	2248.699
Observations (or Sum Wgts)	9

Analysis of Variance

Source	DF	Sum of Squares	Mean Square	F Ratio
Model	1	6575007.4	6575007	15.0249
Error	7	3063242.5	437606	Prob > F
C. Total	8	9638249.9		0.0061

Parameter Estimates

Term	Estimate	Std Error	t Ratio	Prob>|t|
Intercept	-883.3088	837.5571	-1.05	0.3266
Cr ICP-ES (wt%)	281965.27	72742.66	3.88	0.0061

Bivariate Fit of Sn-126 (pCi/g) By Cr ICP-ES (wt%)

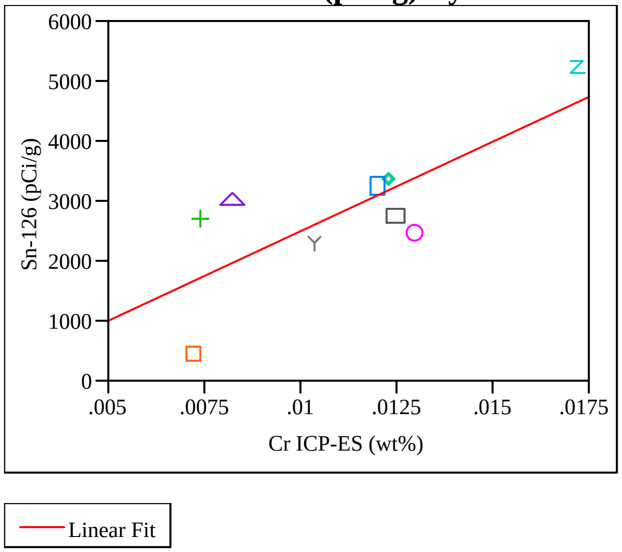

Linear Fit

Sn-126 (pCi/g) = -489.9174 + 298058.11 Cr ICP-ES (wt%)

Summary of Fit

RSquare	0.590101
RSquare Adj	0.531544
Root Mean Square Error	853.8457
Mean of Response	2820.846
Observations (or Sum Wgts)	9

Analysis of Variance

Source	DF	Sum of Squares	Mean Square	F Ratio
Model	1	7346947	7346947	10.0774
Error	7	5103367	729052	Prob > F
C. Total	8	12450314		0.0156

Parameter Estimates

Term	Estimate	Std Error	t Ratio	Prob>|t|
Intercept	-489.9174	1081.066	-0.45	0.6641
Cr ICP-ES (wt%)	298058.11	93891.63	3.17	0.0156

Bivariate Fit of Tc-99 (ICP-MS) (pCi/g) By Cr ICP-ES (wt%)

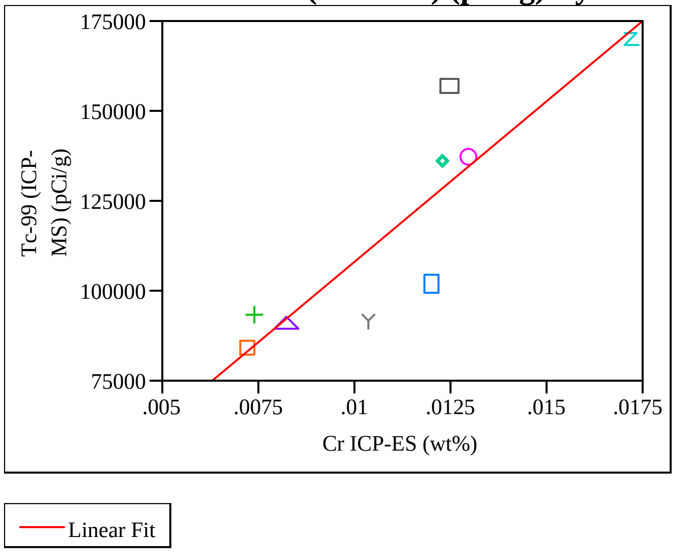

Linear Fit

Tc-99 (ICP-MS) (pCi/g) = 18930.264 + 8904293.3 Cr ICP-ES (wt%)

Summary of Fit

RSquare	0.77658
RSquare Adj	0.744663
Root Mean Square Error	16416.13
Mean of Response	117837.2
Observations (or Sum Wgts)	9

Analysis of Variance

Source	DF	Sum of Squares	Mean Square	F Ratio
Model	1	6556981079	6.557e+9	24.3311
Error	7	1886424221	269489174	Prob > F
C. Total	8	8443405300		0.0017

Parameter Estimates

Term	Estimate	Std Error	t Ratio	Prob>|t|
Intercept	18930.264	20784.68	0.91	0.3927
Cr ICP-ES (wt%)	8904293.3	1805170	4.93	0.0017

Bivariate Fit of Cs-rem beta (pCi/g) By Cs-137 (pCi/g)

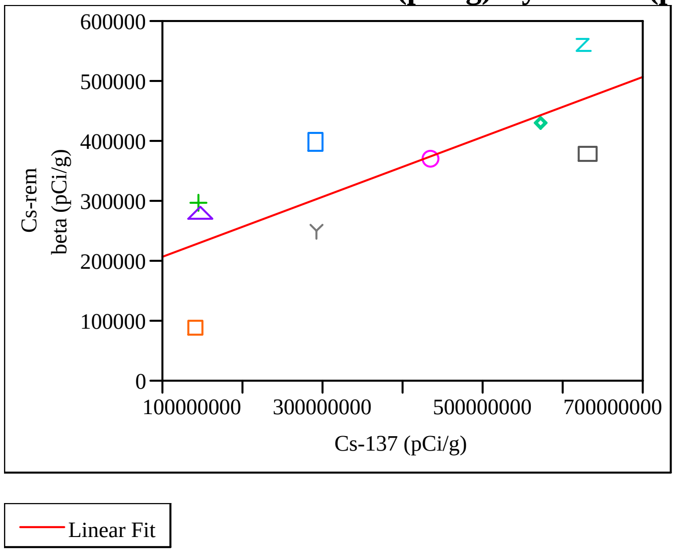

Linear Fit

Cs-rem beta (pCi/g) = 156915.67 + 0.0004974 Cs-137 (pCi/g)

Summary of Fit

RSquare	0.605517
RSquare Adj	0.549163
Root Mean Square Error	88644.53
Mean of Response	337988
Observations (or Sum Wgts)	9

Analysis of Variance

Source	DF	Sum of Squares	Mean Square	F Ratio
Model	1	8.4431e+10	8.443e+10	10.7448
Error	7	5.5005e+10	7.8579e+9	Prob > F
C. Total	8	1.3944e+11		0.0135

Parameter Estimates

Term	Estimate	Std Error	t Ratio	Prob>|t|
Intercept	156915.67	62646.25	2.50	0.0407
Cs-137 (pCi/g)	0.0004974	0.000152	3.28	0.0135

Bivariate Fit of Mass-133 (Cs) ICP-MS (wt%) By Cs-137 (pCi/g)

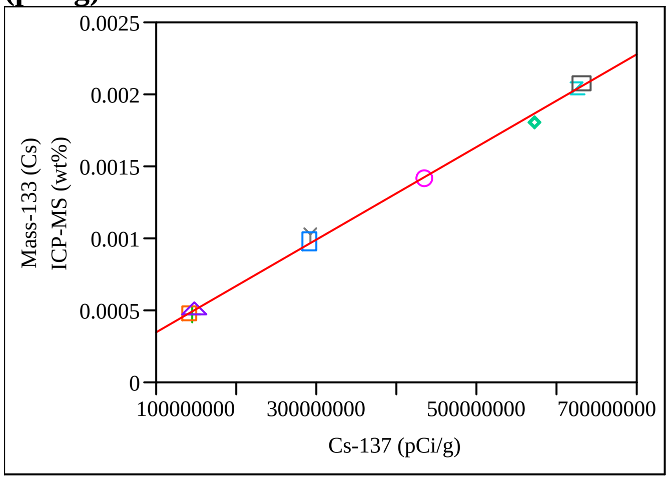

Linear Fit

Linear Fit

Mass-133 (Cs) ICP-MS (wt%) = 2.6748e-5 + 3.21e-12 Cs-137 (pCi/g)

Summary of Fit

RSquare	0.997501
RSquare Adj	0.997144
Root Mean Square Error	3.547e-5
Mean of Response	0.001195
Observations (or Sum Wgts)	9

Analysis of Variance

Source	DF	Sum of Squares	Mean Square	F Ratio
Model	1	3.51542e-6	3.5154e-6	2793.669
Error	7	8.80847e-9	1.2584e-9	Prob > F
C. Total	8	3.52423e-6		<.0001

Parameter Estimates

Term	Estimate	Std Error	t Ratio	Prob>|t|
Intercept	2.6748e-5	0.000025	1.07	0.3214
Cs-137 (pCi/g)	3.21e-12	6.07e-14	52.86	<.0001

Bivariate Fit of Mass-135 (Cs,Ba) ICP-MS (wt%) By Cs-137 (pCi/g)

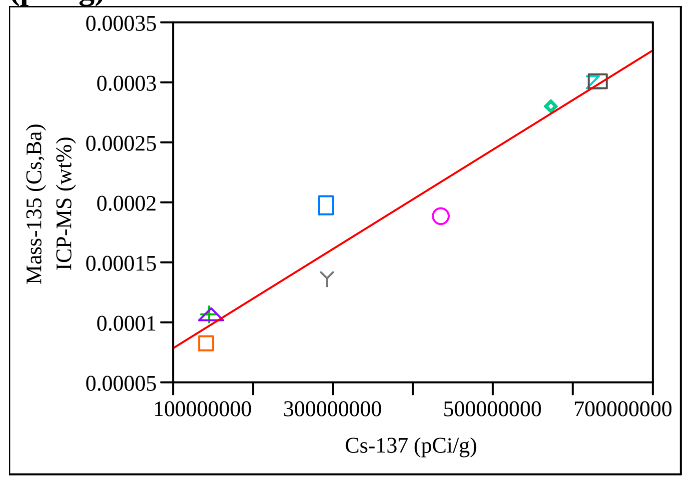

Linear Fit

Linear Fit

Mass-135 (Cs,Ba) ICP-MS (wt%) = 3.7863e-5 + 4.124e-13 Cs-137 (pCi/g)

Summary of Fit

RSquare	0.949186
RSquare Adj	0.941927
Root Mean Square Error	0.000021
Mean of Response	0.000188
Observations (or Sum Wgts)	9

Analysis of Variance

Source	DF	Sum of Squares	Mean Square	F Ratio
Model	1	5.80247e-8	5.8025e-8	130.7575
Error	7	3.10631e-9	4.438e-10	Prob > F
C. Total	8	6.1131e-8		<.0001

Parameter Estimates

Term	Estimate	Std Error	t Ratio	Prob>|t|
Intercept	3.7863e-5	1.489e-5	2.54	0.0385
Cs-137 (pCi/g)	4.124e-13	3.61e-14	11.43	<.0001

Bivariate Fit of Mass-137 (Cs,Ba) ICP-MS (wt%) By Cs-137 (pCi/g)

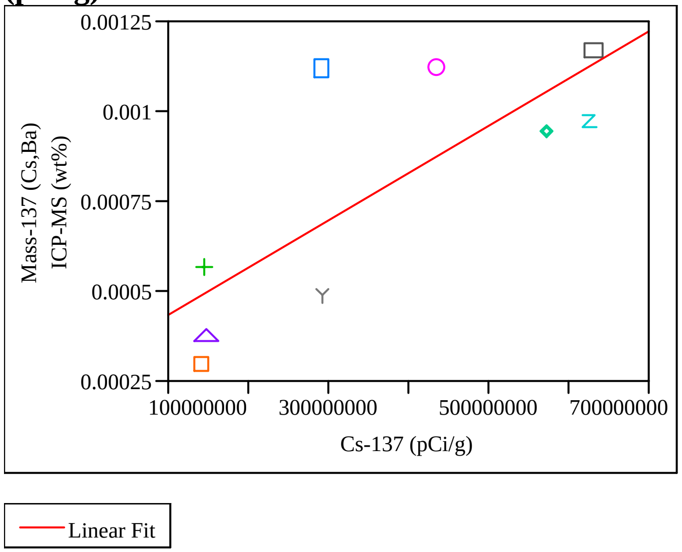

Linear Fit

Mass-137 (Cs,Ba) ICP-MS (wt%) = 0.0003017 + 1.318e-12 Cs-137 (pCi/g)

Summary of Fit

RSquare	0.611114
RSquare Adj	0.555559
Root Mean Square Error	0.000232
Mean of Response	0.000782
Observations (or Sum Wgts)	9

Analysis of Variance

Source	DF	Sum of Squares	Mean Square	F Ratio
Model	1	5.92892e-7	5.9289e-7	11.0001
Error	7	3.7729e-7	5.3899e-8	Prob > F
C. Total	8	9.70182e-7		0.0128

Parameter Estimates

Term	Estimate	Std Error	t Ratio	Prob>|t|
Intercept	0.0003017	0.000164	1.84	0.1085
Cs-137 (pCi/g)	1.318e-12	3.97e-13	3.32	0.0128

Bivariate Fit of Na ICP-ES (wt%) By Cs-137 (pCi/g)

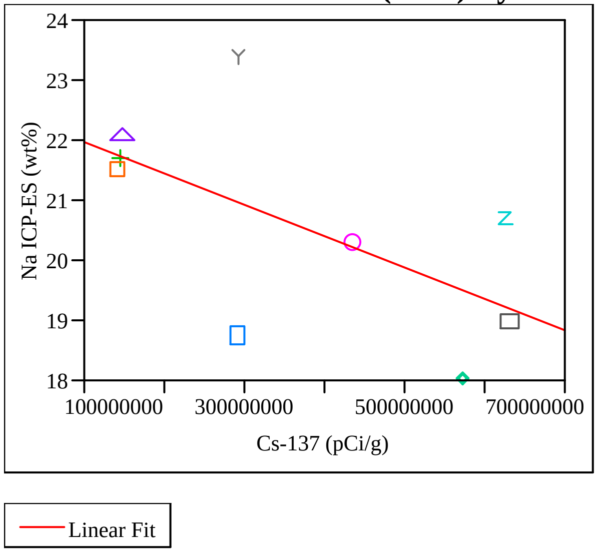

Linear Fit

Na ICP-ES (wt%) = 22.493128 - 5.216e-9 Cs-137 (pCi/g)

Summary of Fit

RSquare	0.372864
RSquare Adj	0.283273
Root Mean Square Error	1.493507
Mean of Response	20.59444
Observations (or Sum Wgts)	9

Analysis of Variance

Source	DF	Sum of Squares	Mean Square	F Ratio
Model	1	9.283284	9.28328	4.1619
Error	7	15.613938	2.23056	Prob > F
C. Total	8	24.897222		0.0807

Parameter Estimates

Term	Estimate	Std Error	t Ratio	Prob>|t|
Intercept	22.493128	1.055481	21.31	<.0001
Cs-137 (pCi/g)	-5.216e-9	2.557e-9	-2.04	0.0807

Bivariate Fit of NO2 wt % By Cs-137 (pCi/g)

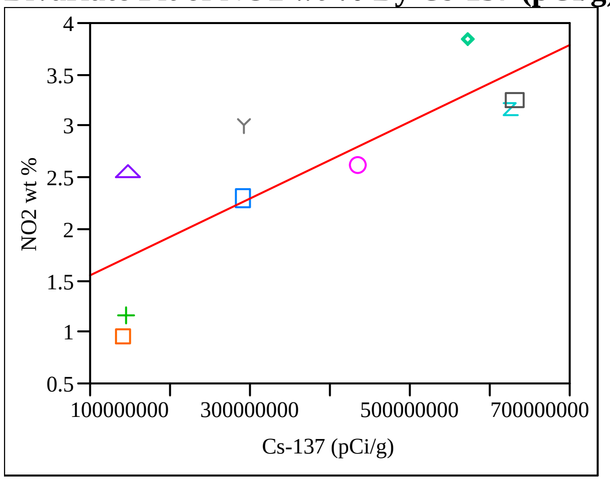

Linear Fit

Linear Fit

NO2 wt % = 1.1834023 + 3.7169e-9 Cs-137 (pCi/g)

Summary of Fit

RSquare	0.648576
RSquare Adj	0.598373
Root Mean Square Error	0.604067
Mean of Response	2.536412
Observations (or Sum Wgts)	9

Analysis of Variance

Source	DF	Sum of Squares	Mean Square	F Ratio
Model	1	4.7140929	4.71409	12.9190
Error	7	2.5542810	0.36490	Prob > F
C. Total	8	7.2683739		0.0088

Parameter Estimates

Term	Estimate	Std Error	t Ratio	Prob>|t|
Intercept	1.1834023	0.426902	2.77	0.0276
Cs-137 (pCi/g)	3.7169e-9	1.034e-9	3.59	0.0088

Bivariate Fit of NO3 wt % By Cs-137 (pCi/g)

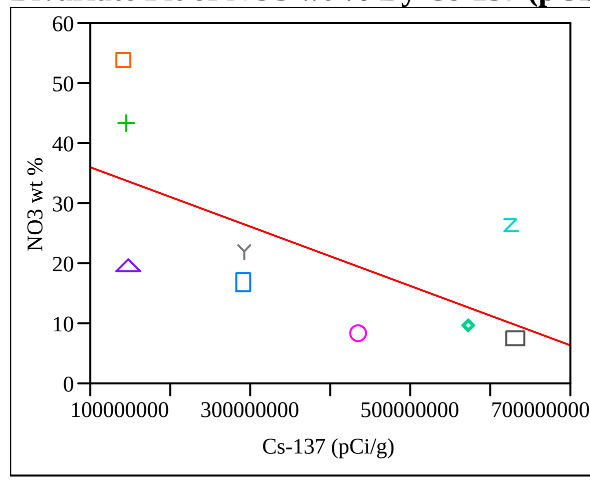

Linear Fit

Linear Fit

NO3 wt % = 41.046996 - 4.9766e-8 Cs-137 (pCi/g)

Summary of Fit

RSquare	0.412554
RSquare Adj	0.328633
Root Mean Square Error	13.11134
Mean of Response	22.93134
Observations (or Sum Wgts)	9

Analysis of Variance

Source	DF	Sum of Squares	Mean Square	F Ratio
Model	1	845.0931	845.093	4.9160
Error	7	1203.3513	171.907	Prob > F
C. Total	8	2048.4444		0.0621

Parameter Estimates

Term	Estimate	Std Error	t Ratio	Prob>|t|
Intercept	41.046996	9.265958	4.43	0.0030
Cs-137 (pCi/g)	-4.977e-8	2.245e-8	-2.22	0.0621

Bivariate Fit of OH wt % By Cs-137 (pCi/g)

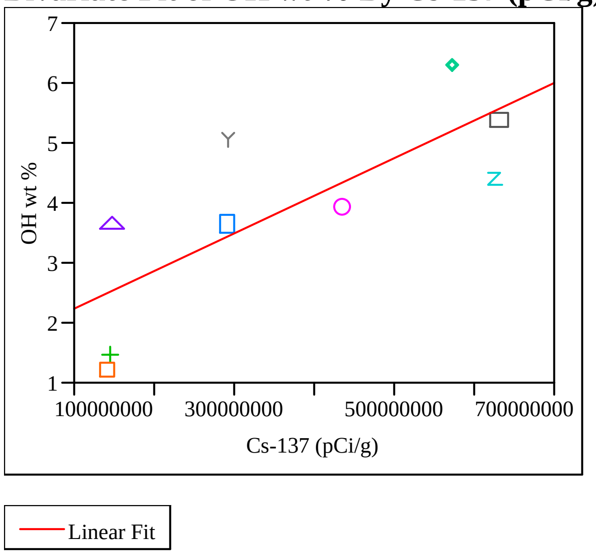

Linear Fit

OH wt % = 1.5894786 + 6.3078e-9 Cs-137 (pCi/g)

Summary of Fit

RSquare	0.593819
RSquare Adj	0.535793
Root Mean Square Error	1.151807
Mean of Response	3.885613
Observations (or Sum Wgts)	9

Analysis of Variance

Source	DF	Sum of Squares	Mean Square	F Ratio
Model	1	13.576604	13.5766	10.2337
Error	7	9.286611	1.3267	Prob > F
C. Total	8	22.863214		0.0151

Parameter Estimates

Term	Estimate	Std Error	t Ratio	Prob>|t|
Intercept	1.5894786	0.813997	1.95	0.0918
Cs-137 (pCi/g)	6.3078e-9	1.972e-9	3.20	0.0151

Bivariate Fit of P ICP-ES (wt%) By Cs-137 (pCi/g)

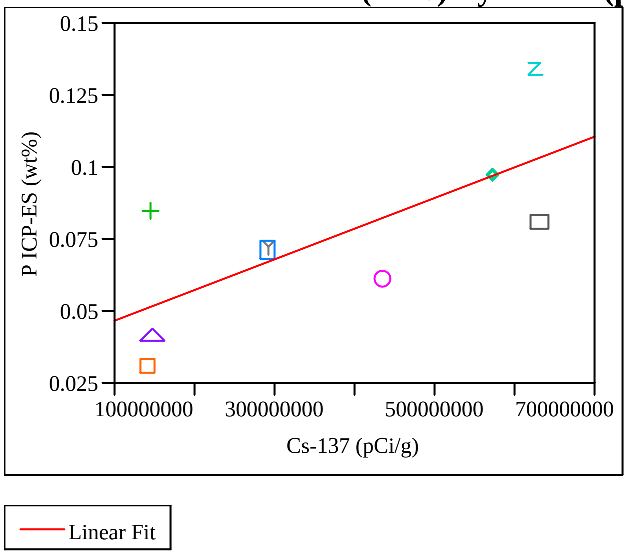

Linear Fit

P ICP-ES (wt%) = 0.0360005 + 1.062e-10 Cs-137 (pCi/g)

Summary of Fit

RSquare	0.512701
RSquare Adj	0.443087
Root Mean Square Error	0.022857
Mean of Response	0.074656
Observations (or Sum Wgts)	9

Analysis of Variance

Source	DF	Sum of Squares	Mean Square	F Ratio
Model	1	0.00384777	0.003848	7.3649
Error	7	0.00365713	0.000522	Prob > F
C. Total	8	0.00750490		0.0300

Parameter Estimates

Term	Estimate	Std Error	t Ratio	Prob>|t|
Intercept	0.0360005	0.016153	2.23	0.0611
Cs-137 (pCi/g)	1.062e-10	3.91e-11	2.71	0.0300

Bivariate Fit of Sb-126 (pCi/g) By Cs-137 (pCi/g)

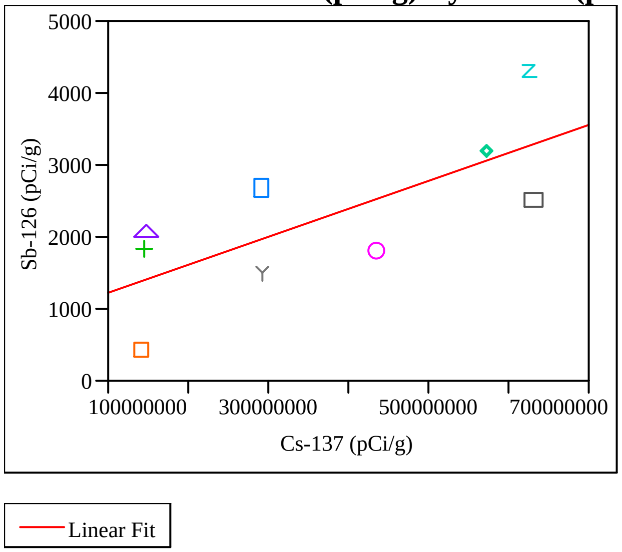

Linear Fit

Sb-126 (pCi/g) = 829.93131 + 3.8976e-6 Cs-137 (pCi/g)

Summary of Fit

RSquare	0.5378
RSquare Adj	0.471771
Root Mean Square Error	797.7468
Mean of Response	2248.699
Observations (or Sum Wgts)	9

Analysis of Variance

Source	DF	Sum of Squares	Mean Square	F Ratio
Model	1	5183450.1	5183450	8.1450
Error	7	4454799.9	636400	Prob > F
C. Total	8	9638249.9		0.0245

Parameter Estimates

Term	Estimate	Std Error	t Ratio	Prob>|t|
Intercept	829.93131	563.7781	1.47	0.1845
Cs-137 (pCi/g)	3.8976e-6	1.366e-6	2.85	0.0245

Bivariate Fit of Sn-126 (pCi/g) By Cs-137 (pCi/g)

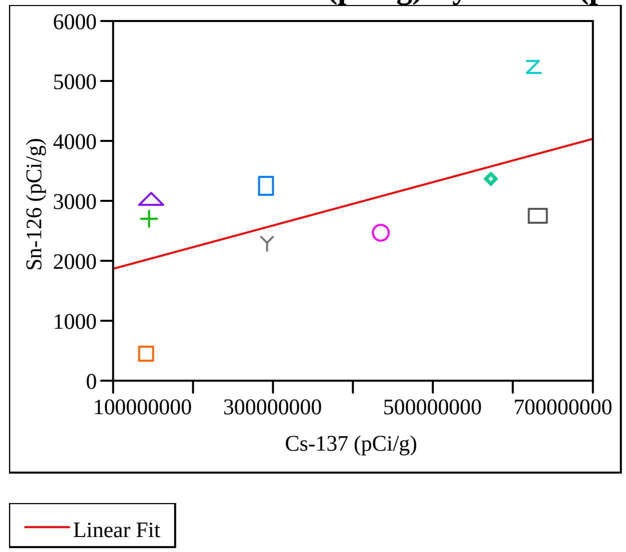

Linear Fit

Sn-126 (pCi/g) = 1512.8127 + 3.5934e-6 Cs-137 (pCi/g)

Summary of Fit

RSquare	0.353878
RSquare Adj	0.261575
Root Mean Square Error	1072.009
Mean of Response	2820.846
Observations (or Sum Wgts)	9

Analysis of Variance

Source	DF	Sum of Squares	Mean Square	F Ratio
Model	1	4405894	4405894	3.8339
Error	7	8044420	1149203	Prob > F
C. Total	8	12450314		0.0911

Parameter Estimates

Term	Estimate	Std Error	t Ratio	Prob>|t|
Intercept	1512.8127	757.6027	2.00	0.0860
Cs-137 (pCi/g)	3.5934e-6	1.835e-6	1.96	0.0911

Bivariate Fit of Tc-99 (ICP-MS) (pCi/g) By Cs-137 (pCi/g)

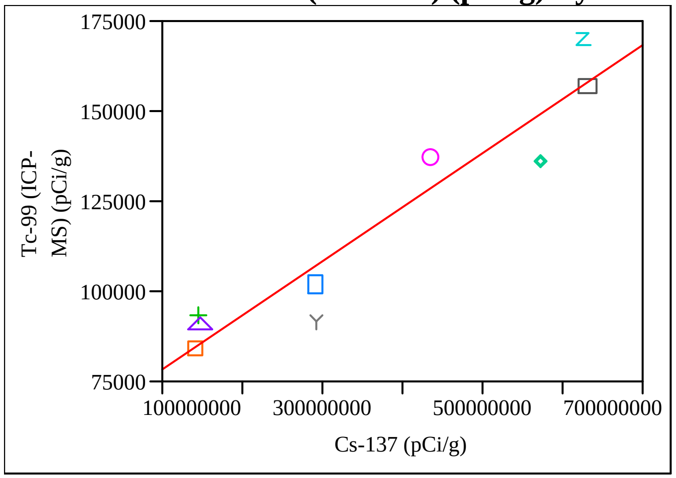

Linear Fit

Linear Fit

Tc-99 (ICP-MS) (pCi/g) = 63327.338 + 0.0001497 Cs-137 (pCi/g)

Summary of Fit

RSquare	0.90621
RSquare Adj	0.892811
Root Mean Square Error	10636.26
Mean of Response	117837.2
Observations (or Sum Wgts)	9

Analysis of Variance

Source	DF	Sum of Squares	Mean Square	F Ratio
Model	1	7651495191	7.6515e+9	67.6345
Error	7	791910109	113130016	Prob > F
C. Total	8	8443405300		<.0001

Parameter Estimates

Term	Estimate	Std Error	t Ratio	Prob>|t|
Intercept	63327.338	7516.784	8.42	<.0001
Cs-137 (pCi/g)	0.0001497	1.821e-5	8.22	<.0001

Bivariate Fit of H2O Fraction By Cs-137 (pCi/g)

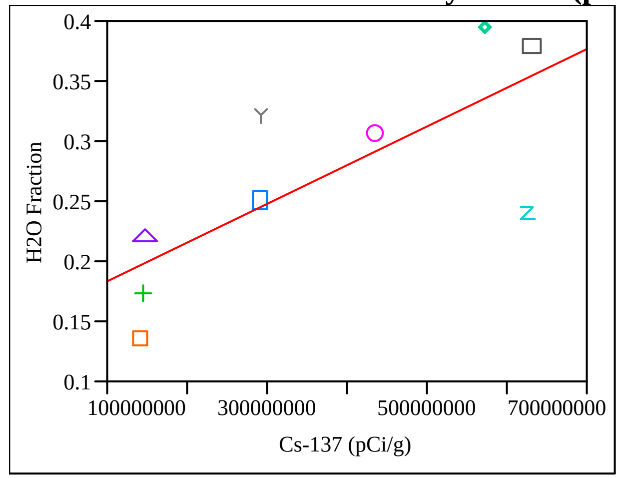

Linear Fit

Linear Fit

H2O Fraction = 0.1516497 + 3.22e-10 Cs-137 (pCi/g)

Summary of Fit

RSquare	0.563434
RSquare Adj	0.501067
Root Mean Square Error	0.062583
Mean of Response	0.26887
Observations (or Sum Wgts)	9

Analysis of Variance

Source	DF	Sum of Squares	Mean Square	F Ratio
Model	1	0.03538375	0.035384	9.0342
Error	7	0.02741647	0.003917	Prob > F
C. Total	8	0.06280022		0.0198

Parameter Estimates

Term	Estimate	Std Error	t Ratio	Prob>|t|
Intercept	0.1516497	0.044228	3.43	0.0110
Cs-137 (pCi/g)	3.22e-10	1.07e-10	3.01	0.0198

Bivariate Fit of Mass-133 (Cs) ICP-MS (wt%) By Cs-rem beta (pCi/g)

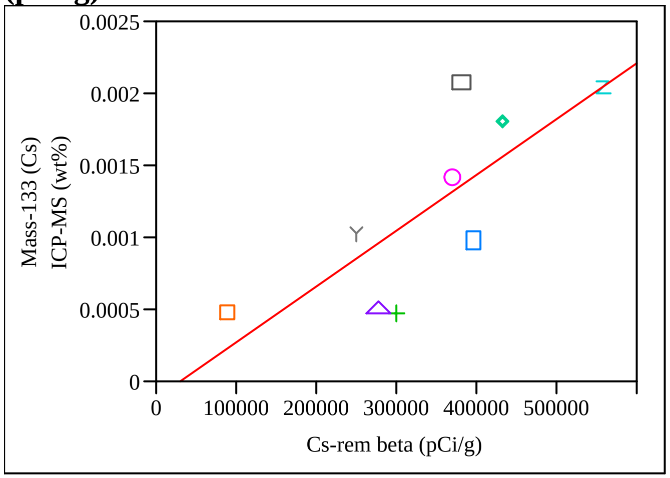

Linear Fit

Linear Fit

Mass-133 (Cs) ICP-MS (wt%) = -0.000114 + 3.8728e-9 Cs-rem beta (pCi/g)

Summary of Fit

RSquare	0.593431
RSquare Adj	0.535349
Root Mean Square Error	0.000452
Mean of Response	0.001195
Observations (or Sum Wgts)	9

Analysis of Variance

Source	DF	Sum of Squares	Mean Square	F Ratio
Model	1	2.09139e-6	2.0914e-6	10.2172
Error	7	1.43284e-6	2.0469e-7	Prob > F
C. Total	8	3.52423e-6		0.0151

Parameter Estimates

Term	Estimate	Std Error	t Ratio	Prob>|t|
Intercept	-0.000114	0.000436	-0.26	0.8017
Cs-rem beta (pCi/g)	3.8728e-9	1.212e-9	3.20	0.0151

Bivariate Fit of Mass-135 (Cs,Ba) ICP-MS (wt%) By Cs-rem beta (pCi/g)

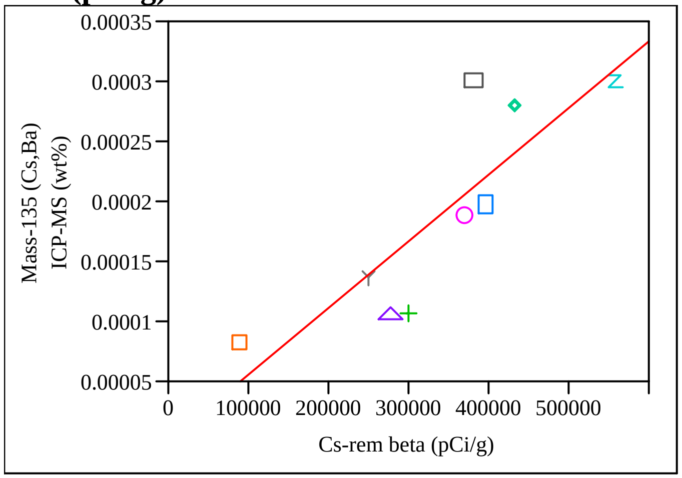

Linear Fit

Linear Fit

Mass-135 (Cs,Ba) ICP-MS (wt%) = -4.33e-7 + 5.574e-10 Cs-rem beta (pCi/g)

Summary of Fit

RSquare	0.708758
RSquare Adj	0.667152
Root Mean Square Error	5.043e-5
Mean of Response	0.000188
Observations (or Sum Wgts)	9

Analysis of Variance

Source	DF	Sum of Squares	Mean Square	F Ratio
Model	1	4.33271e-8	4.3327e-8	17.0350
Error	7	1.78039e-8	2.5434e-9	Prob > F
C. Total	8	6.1131e-8		0.0044

Parameter Estimates

Term	Estimate	Std Error	t Ratio	Prob>|t|
Intercept	-4.33e-7	4.865e-5	-0.01	0.9931
Cs-rem beta (pCi/g)	5.574e-10	1.35e-10	4.13	0.0044

Bivariate Fit of Mass-137 (Cs,Ba) ICP-MS (wt%) By Cs-rem beta (pCi/g)

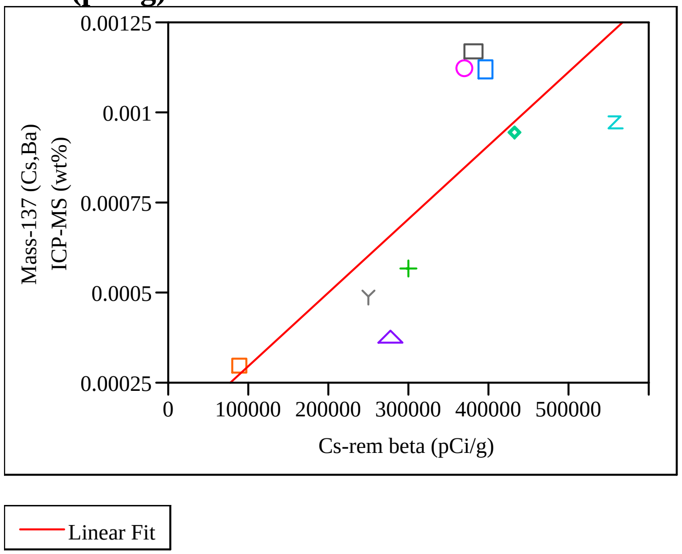

Linear Fit

Mass-137 (Cs,Ba) ICP-MS (wt%) = 9.4156e-5 + 2.0338e-9 Cs-rem beta (pCi/g)

Summary of Fit

RSquare	0.59448
RSquare Adj	0.536549
Root Mean Square Error	0.000237
Mean of Response	0.000782
Observations (or Sum Wgts)	9

Analysis of Variance

Source	DF	Sum of Squares	Mean Square	F Ratio
Model	1	5.76754e-7	5.7675e-7	10.2618
Error	7	3.93428e-7	5.6204e-8	Prob > F
C. Total	8	9.70182e-7		0.0150

Parameter Estimates

Term	Estimate	Std Error	t Ratio	Prob>|t|
Intercept	9.4156e-5	0.000229	0.41	0.6928
Cs-rem beta (pCi/g)	2.0338e-9	6.35e-10	3.20	0.0150

Bivariate Fit of NO2 wt % By Cs-rem beta (pCi/g)

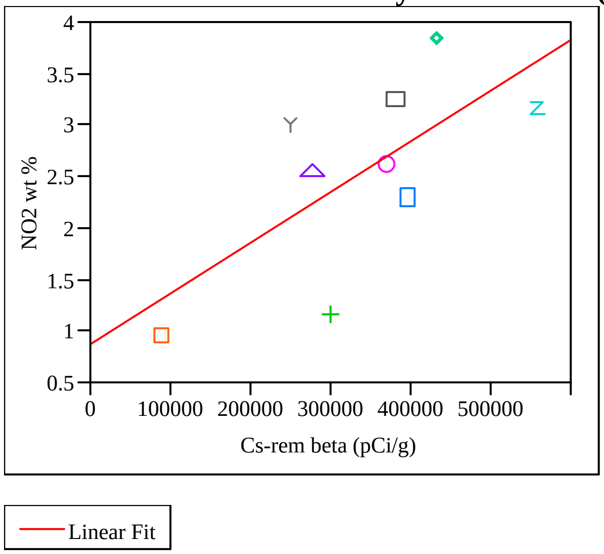

Linear Fit

NO2 wt % = 0.8655964 + 4.9434e-6 Cs-rem beta (pCi/g)

Summary of Fit

RSquare	0.468804
RSquare Adj	0.392919
Root Mean Square Error	0.742672
Mean of Response	2.536412
Observations (or Sum Wgts)	9

Analysis of Variance

Source	DF	Sum of Squares	Mean Square	F Ratio
Model	1	3.4074411	3.40744	6.1778
Error	7	3.8609328	0.55156	Prob > F
C. Total	8	7.2683739		0.0419

Parameter Estimates

Term	Estimate	Std Error	t Ratio	Prob>|t|
Intercept	0.8655964	0.716355	1.21	0.2661
Cs-rem beta (pCi/g)	4.9434e-6	1.989e-6	2.49	0.0419

Bivariate Fit of NO3 wt % By Cs-rem beta (pCi/g)

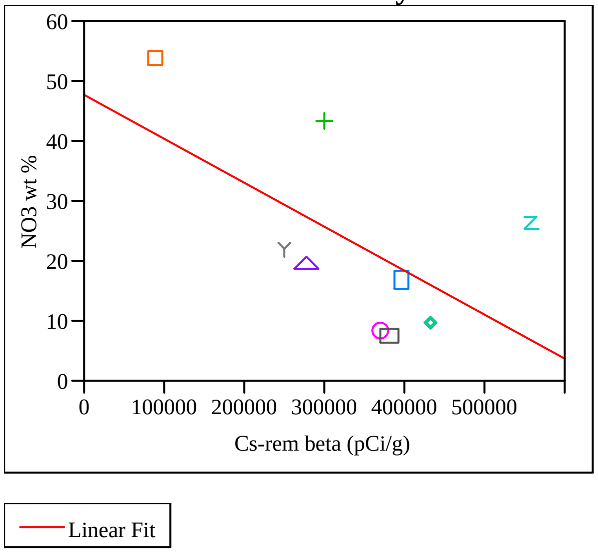

Linear Fit

NO3 wt % = 47.629836 - 7.3075e-5 Cs-rem beta (pCi/g)

Summary of Fit

RSquare	0.363486
RSquare Adj	0.272556
Root Mean Square Error	13.64793
Mean of Response	22.93134
Observations (or Sum Wgts)	9

Analysis of Variance

Source	DF	Sum of Squares	Mean Square	F Ratio
Model	1	744.5819	744.582	3.9974
Error	7	1303.8625	186.266	Prob > F
C. Total	8	2048.4444		0.0857

Parameter Estimates

Term	Estimate	Std Error	t Ratio	Prob>|t|
Intercept	47.629836	13.16431	3.62	0.0085
Cs-rem beta (pCi/g)	-0.000073	3.655e-5	-2.00	0.0857

Bivariate Fit of OH wt % By Cs-rem beta (pCi/g)

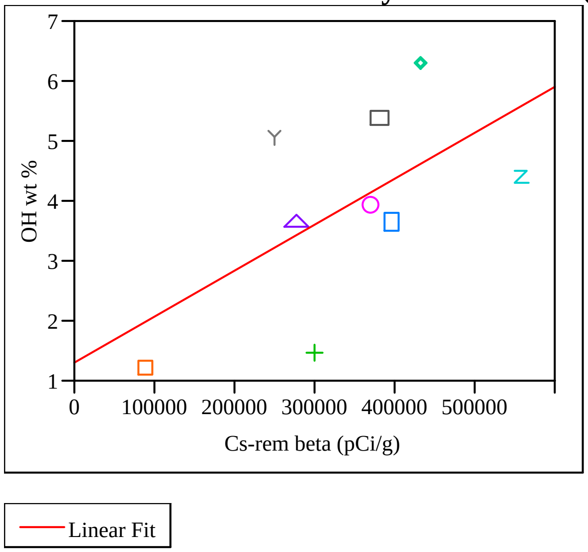

Linear Fit

OH wt % = 1.3000834 + 7.6498e-6 Cs-rem beta (pCi/g)

Summary of Fit

RSquare	0.356889
RSquare Adj	0.265016
Root Mean Square Error	1.449314
Mean of Response	3.885613
Observations (or Sum Wgts)	9

Analysis of Variance

Source	DF	Sum of Squares	Mean Square	F Ratio
Model	1	8.159631	8.15963	3.8846
Error	7	14.703583	2.10051	Prob > F
C. Total	8	22.863214		0.0894

Parameter Estimates

Term	Estimate	Std Error	t Ratio	Prob>|t|
Intercept	1.3000834	1.397956	0.93	0.3833
Cs-rem beta (pCi/g)	7.6498e-6	3.881e-6	1.97	0.0894

Bivariate Fit of P ICP-ES (wt%) By Cs-rem beta (pCi/g)

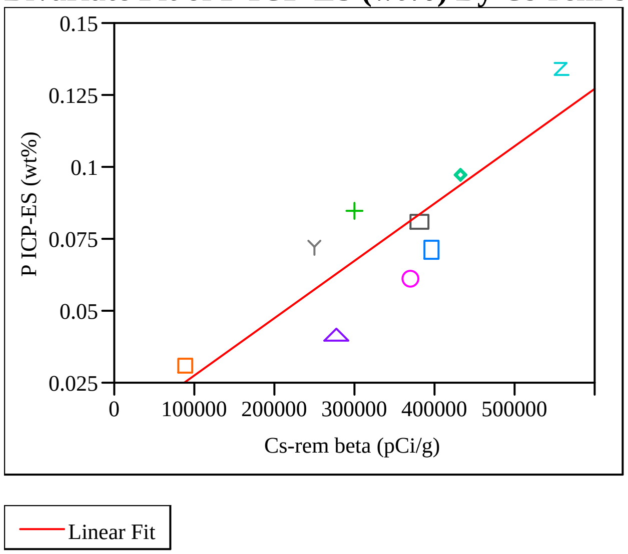

Linear Fit

P ICP-ES (wt%) = 0.0073727 + 1.9907e-7 Cs-rem beta (pCi/g)

Summary of Fit

RSquare	0.736266
RSquare Adj	0.69859
Root Mean Square Error	0.016815
Mean of Response	0.074656
Observations (or Sum Wgts)	9

Analysis of Variance

Source	DF	Sum of Squares	Mean Square	F Ratio
Model	1	0.00552560	0.005526	19.5419
Error	7	0.00197929	0.000283	Prob > F
C. Total	8	0.00750490		0.0031

Parameter Estimates

Term	Estimate	Std Error	t Ratio	Prob>|t|
Intercept	0.0073727	0.016219	0.45	0.6632
Cs-rem beta (pCi/g)	1.9907e-7	4.503e-8	4.42	0.0031

Bivariate Fit of Sb-126 (pCi/g) By Cs-rem beta (pCi/g)

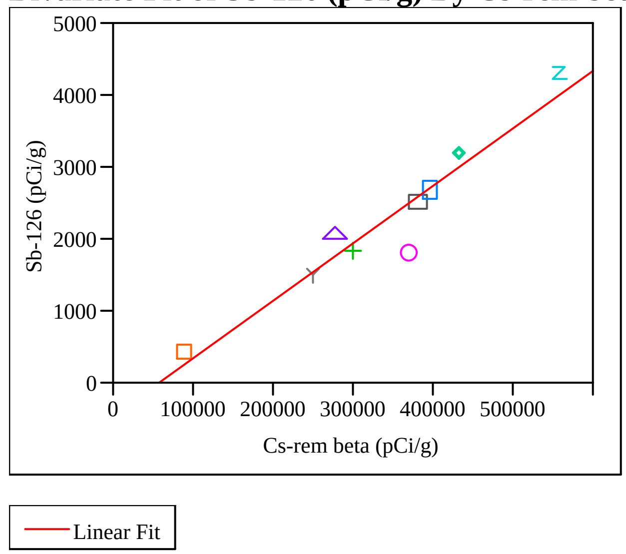

Linear Fit

Sb-126 (pCi/g) = -451.4607 + 0.0079889 Cs-rem beta (pCi/g)

Summary of Fit

RSquare	0.92332
RSquare Adj	0.912365
Root Mean Square Error	324.9315
Mean of Response	2248.699
Observations (or Sum Wgts)	9

Analysis of Variance

Source	DF	Sum of Squares	Mean Square	F Ratio
Model	1	8899186.6	8899187	84.2882
Error	7	739063.4	105580	Prob > F
C. Total	8	9638249.9		<.0001

Parameter Estimates

Term	Estimate	Std Error	t Ratio	Prob>|t|
Intercept	-451.4607	313.4172	-1.44	0.1929
Cs-rem beta (pCi/g)	0.0079889	0.00087	9.18	<.0001

Bivariate Fit of Sn-126 (pCi/g) By Cs-rem beta (pCi/g)

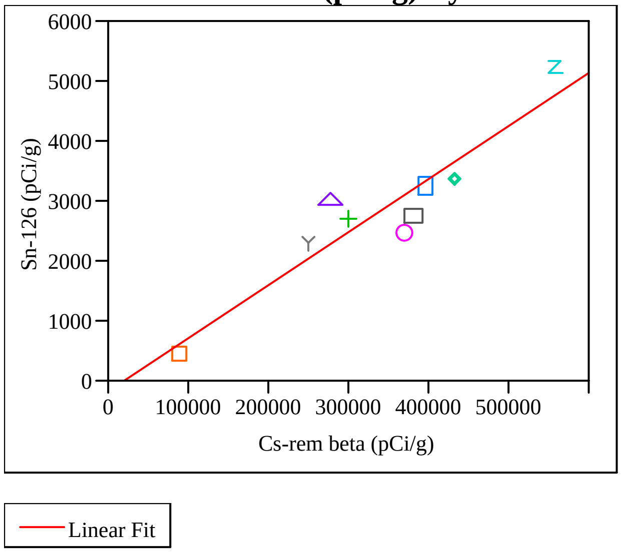

Linear Fit

Sn-126 (pCi/g) = -169.4163 + 0.0088472 Cs-rem beta (pCi/g)

Summary of Fit

RSquare	0.876617
RSquare Adj	0.85899
Root Mean Square Error	468.4567
Mean of Response	2820.846
Observations (or Sum Wgts)	9

Analysis of Variance

Source	DF	Sum of Squares	Mean Square	F Ratio
Model	1	10914153	10914153	49.7337
Error	7	1536161	219451.64	Prob > F
C. Total	8	12450314		0.0002

Parameter Estimates

Term	Estimate	Std Error	t Ratio	Prob>|t|
Intercept	-169.4163	451.8565	-0.37	0.7188
Cs-rem beta (pCi/g)	0.0088472	0.001255	7.05	0.0002

Bivariate Fit of Tc-99 (ICP-MS) (pCi/g) By Cs-rem beta (pCi/g)

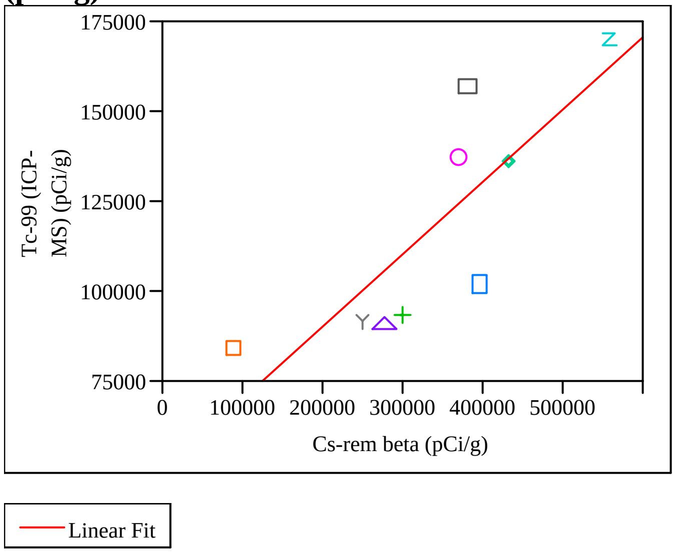

Linear Fit

Tc-99 (ICP-MS) (pCi/g) = 49824.125 + 0.2012292 Cs-rem beta (pCi/g)

Summary of Fit

RSquare	0.668711
RSquare Adj	0.621384
Root Mean Square Error	19990.03
Mean of Response	117837.2
Observations (or Sum Wgts)	9

Analysis of Variance

Source	DF	Sum of Squares	Mean Square	F Ratio
Model	1	5646196961	5.6462e+9	14.1296
Error	7	2797208339	399601191	Prob > F
C. Total	8	8443405300		0.0071

Parameter Estimates

Term	Estimate	Std Error	t Ratio	Prob>|t|
Intercept	49824.125	19281.66	2.58	0.0363
Cs-rem beta (pCi/g)	0.2012292	0.053534	3.76	0.0071

Bivariate Fit of Pu-239/240 (pCi/g) By F wt %

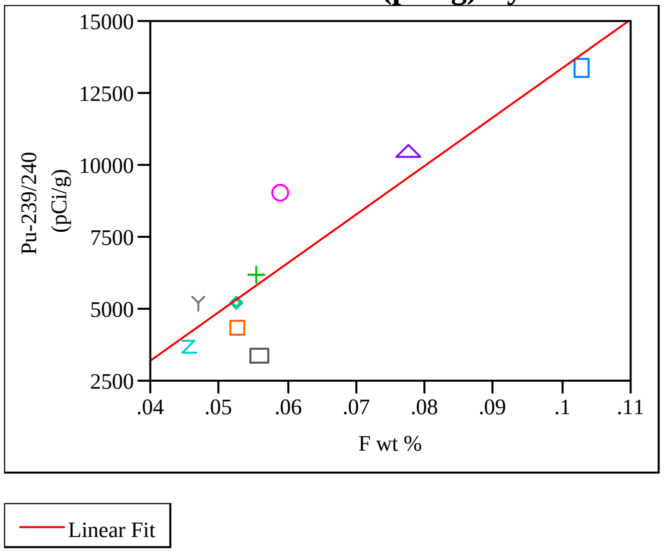

Linear Fit

Pu-239/240 (pCi/g) = -3547.408 + 169154.58 F wt %

Summary of Fit

RSquare	0.823372
RSquare Adj	0.79814
Root Mean Square Error	1532.795
Mean of Response	6742.492
Observations (or Sum Wgts)	9

Analysis of Variance

Source	DF	Sum of Squares	Mean Square	F Ratio
Model	1	76666181	76666181	32.6314
Error	7	16446219	2349459.8	Prob > F
C. Total	8	93112400		0.0007

Parameter Estimates

Term	Estimate	Std Error	t Ratio	Prob>|t|
Intercept	-3547.408	1872.389	-1.89	0.1000
F wt %	169154.58	29611.87	5.71	0.0007

Bivariate Fit of Mn ICP-ES (wt%) By Fe ICP-ES (wt%)

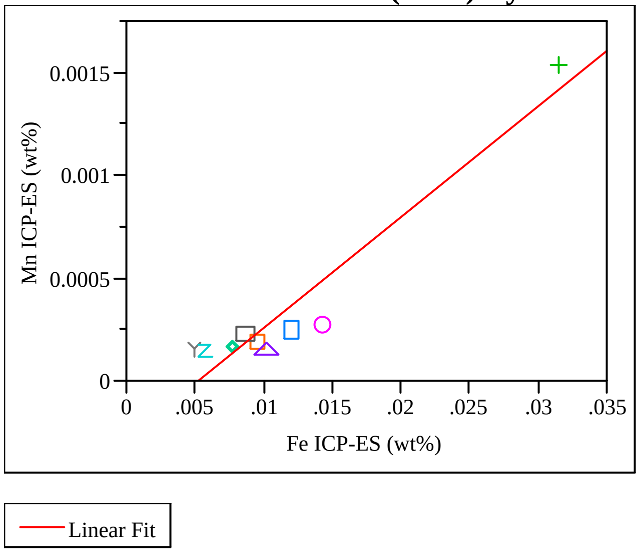

Linear Fit

Mn ICP-ES (wt%) = -0.00028 + 0.053781 Fe ICP-ES (wt%)

Summary of Fit

RSquare	0.909965
RSquare Adj	0.897102
Root Mean Square Error	0.000144
Mean of Response	0.000342
Observations (or Sum Wgts)	9

Analysis of Variance

Source	DF	Sum of Squares	Mean Square	F Ratio
Model	1	1.4704e-6	1.4704e-6	70.7472
Error	7	1.45487e-7	2.0784e-8	Prob > F
C. Total	8	1.61589e-6		<.0001

Parameter Estimates

Term	Estimate	Std Error	t Ratio	Prob>|t|
Intercept	-0.00028	8.817e-5	-3.17	0.0157
Fe ICP-ES (wt%)	0.053781	0.006394	8.41	<.0001

Bivariate Fit of NO2 wt % By Fe ICP-ES (wt%)

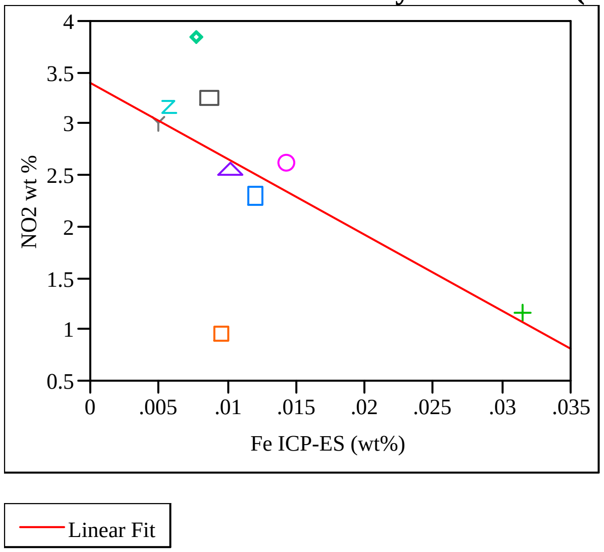

Linear Fit
NO2 wt % = 3.3921327 - 74.017202 Fe ICP-ES (wt%)

Summary of Fit

RSquare	0.383182
RSquare Adj	0.295065
Root Mean Square Error	0.800291
Mean of Response	2.536412
Observations (or Sum Wgts)	9

Analysis of Variance

Source	DF	Sum of Squares	Mean Square	F Ratio
Model	1	2.7851118	2.78511	4.3486
Error	7	4.4832621	0.64047	Prob > F
C. Total	8	7.2683739		0.0755

Parameter Estimates

Term	Estimate	Std Error	t Ratio	Prob>|t|
Intercept	3.3921327	0.489442	6.93	0.0002
Fe ICP-ES (wt%)	-74.0172	35.49436	-2.09	0.0755

Bivariate Fit of OH wt % By Fe ICP-ES (wt%)

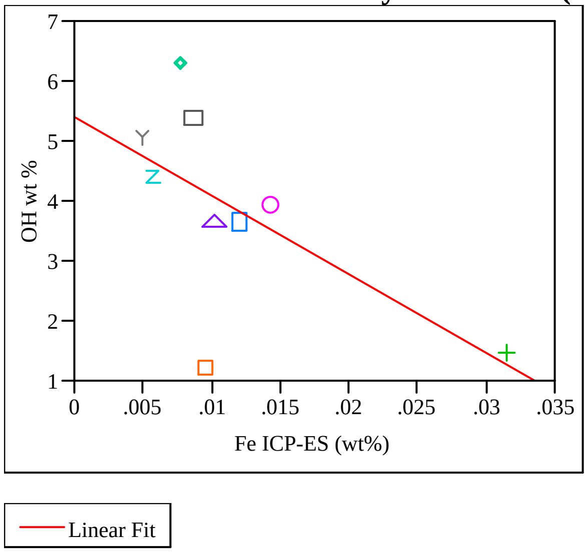

Linear Fit
OH wt % = 5.4054214 - 131.45867 Fe ICP-ES (wt%)

Summary of Fit

RSquare	0.384254
RSquare Adj	0.29629
Root Mean Square Error	1.418144
Mean of Response	3.885613
Observations (or Sum Wgts)	9

Analysis of Variance

Source	DF	Sum of Squares	Mean Square	F Ratio
Model	1	8.785284	8.78528	4.3683
Error	7	14.077930	2.01113	Prob > F
C. Total	8	22.863214		0.0750

Parameter Estimates

Term	Estimate	Std Error	t Ratio	Prob>|t|
Intercept	5.4054214	0.867309	6.23	0.0004
Fe ICP-ES (wt%)	-131.4587	62.89726	-2.09	0.0750

Bivariate Fit of Zn ICP-ES (wt%) By Fe ICP-ES (wt%)

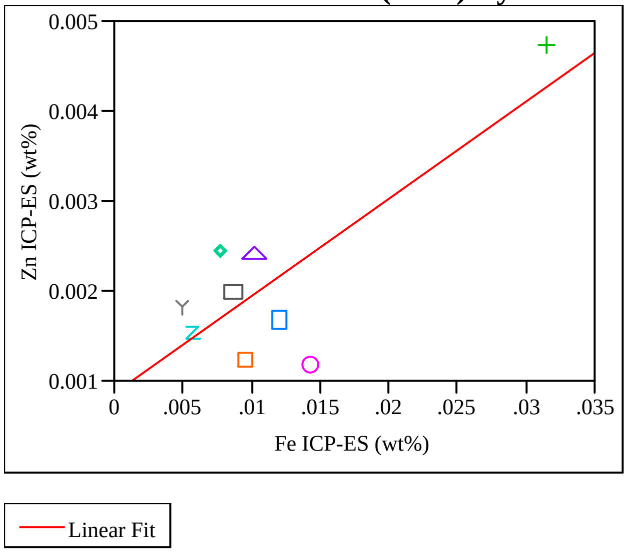

Linear Fit

Zn ICP-ES (wt%) = 0.0008518 + 0.1083477 Fe ICP-ES (wt%)

Summary of Fit

RSquare	0.638885
RSquare Adj	0.587297
Root Mean Square Error	0.000694
Mean of Response	0.002104
Observations (or Sum Wgts)	9

Analysis of Variance

Source	DF	Sum of Squares	Mean Square	F Ratio
Model	1	5.96784e-6	5.9678e-6	12.3844
Error	7	3.37319e-6	4.8188e-7	Prob > F
C. Total	8	9.34102e-6		0.0097

Parameter Estimates

Term	Estimate	Std Error	t Ratio	Prob>|t|
Intercept	0.0008518	0.000425	2.01	0.0848
Fe ICP-ES (wt%)	0.1083477	0.030788	3.52	0.0097

Bivariate Fit of NO2 wt % By Li ICP-ES (wt%)

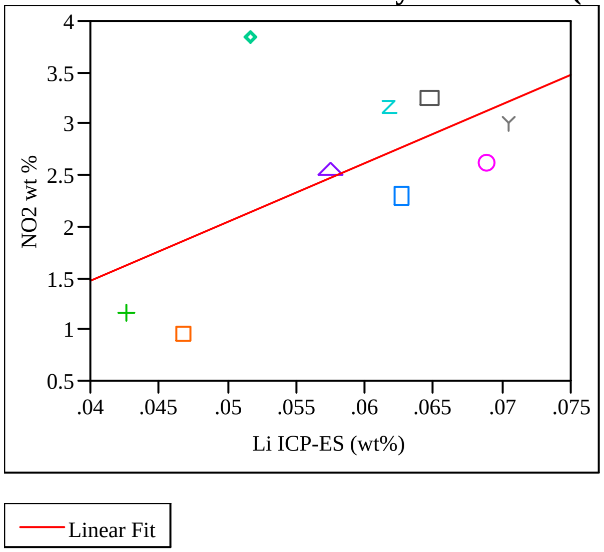

Linear Fit

NO2 wt % = -0.808975 + 57.191528 Li ICP-ES (wt%)

Summary of Fit

RSquare	0.340725
RSquare Adj	0.246542
Root Mean Square Error	0.827376
Mean of Response	2.536412
Observations (or Sum Wgts)	9

Analysis of Variance

Source	DF	Sum of Squares	Mean Square	F Ratio
Model	1	2.4765144	2.47651	3.6177
Error	7	4.7918595	0.68455	Prob > F
C. Total	8	7.2683739		0.0989

Parameter Estimates

Term	Estimate	Std Error	t Ratio	Prob>|t|
Intercept	-0.808975	1.780342	-0.45	0.6633
Li ICP-ES (wt%)	57.191528	30.06867	1.90	0.0989

Bivariate Fit of NO3 wt % By Li ICP-ES (wt%)

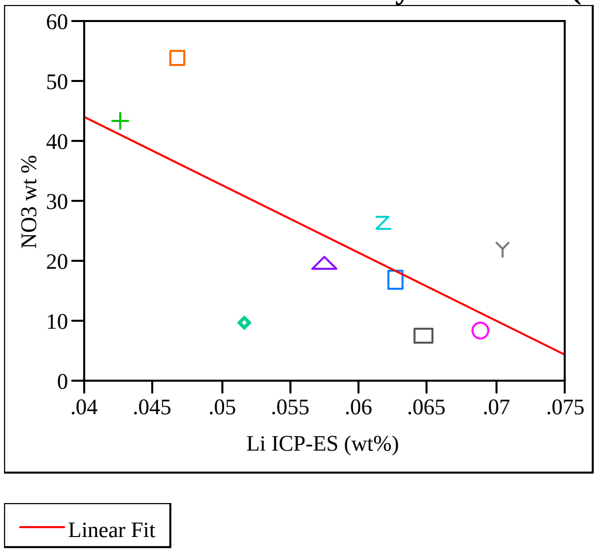

Linear Fit

NO3 wt % = 89.232016 - 1133.4525 Li ICP-ES (wt%)

Summary of Fit

RSquare	0.474854
RSquare Adj	0.399833
Root Mean Square Error	12.39662
Mean of Response	22.93134
Observations (or Sum Wgts)	9

Analysis of Variance

Source	DF	Sum of Squares	Mean Square	F Ratio
Model	1	972.7116	972.712	6.3296
Error	7	1075.7327	153.676	Prob > F
C. Total	8	2048.4444		0.0401

Parameter Estimates

Term	Estimate	Std Error	t Ratio	Prob>|t|
Intercept	89.232016	26.67494	3.35	0.0123
Li ICP-ES (wt%)	-1133.452	450.5204	-2.52	0.0401

Bivariate Fit of OH wt % By Li ICP-ES (wt%)

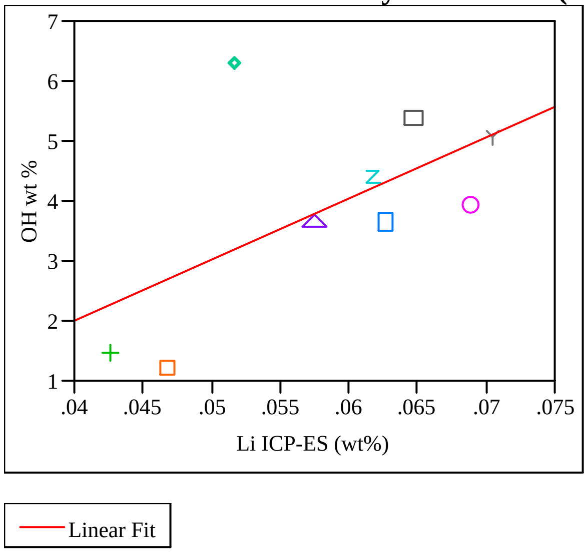

Linear Fit

OH wt % = -2.124211 + 102.74179 Li ICP-ES (wt%)

Summary of Fit

RSquare	0.34957
RSquare Adj	0.256652
Root Mean Square Error	1.457538
Mean of Response	3.885613
Observations (or Sum Wgts)	9

Analysis of Variance

Source	DF	Sum of Squares	Mean Square	F Ratio
Model	1	7.992299	7.99230	3.7621
Error	7	14.870915	2.12442	Prob > F
C. Total	8	22.863214		0.0936

Parameter Estimates

Term	Estimate	Std Error	t Ratio	Prob>|t|
Intercept	-2.124211	3.136318	-0.68	0.5200
Li ICP-ES (wt%)	102.74179	52.97014	1.94	0.0936

Bivariate Fit of S ICP-ES (wt%) By Li ICP-ES (wt%)

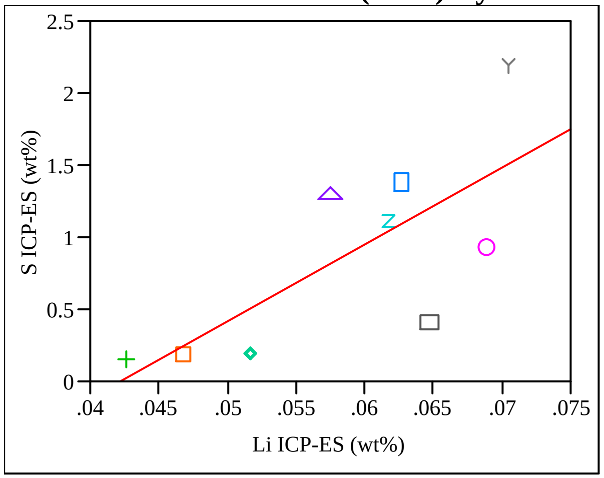

Linear Fit

Linear Fit

S ICP-ES (wt%) = -2.235113 + 53.055411 Li ICP-ES (wt%)

Summary of Fit

RSquare	0.550101
RSquare Adj	0.48583
Root Mean Square Error	0.499006
Mean of Response	0.868333
Observations (or Sum Wgts)	9

Analysis of Variance

Source	DF	Sum of Squares	Mean Square	F Ratio
Model	1	2.1312619	2.13126	8.5591
Error	7	1.7430466	0.24901	Prob > F
C. Total	8	3.8743085		0.0222

Parameter Estimates

Term	Estimate	Std Error	t Ratio	Prob>|t|
Intercept	-2.235113	1.073756	-2.08	0.0759
Li ICP-ES (wt%)	53.055411	18.13497	2.93	0.0222

Bivariate Fit of SO4 wt % By Li ICP-ES (wt%)

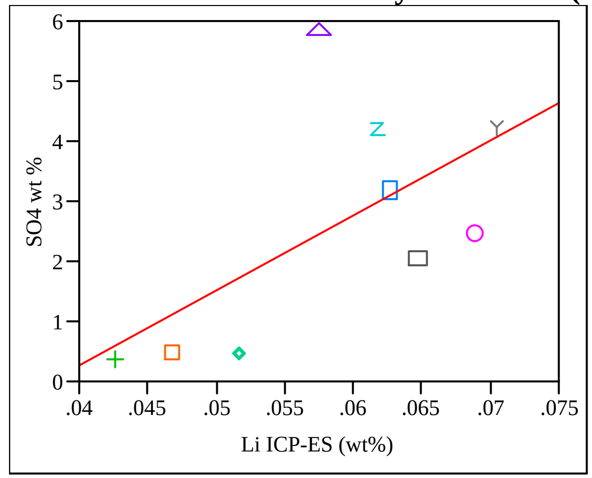

Linear Fit

Linear Fit

SO4 wt % = -4.693608 + 124.20811 Li ICP-ES (wt%)

Summary of Fit

RSquare	0.384631
RSquare Adj	0.296721
Root Mean Square Error	1.633938
Mean of Response	2.571877
Observations (or Sum Wgts)	9

Analysis of Variance

Source	DF	Sum of Squares	Mean Square	F Ratio
Model	1	11.680929	11.6809	4.3753
Error	7	18.688272	2.6698	Prob > F
C. Total	8	30.369202		0.0748

Parameter Estimates

Term	Estimate	Std Error	t Ratio	Prob>|t|
Intercept	-4.693608	3.515895	-1.33	0.2237
Li ICP-ES (wt%)	124.20811	59.38091	2.09	0.0748

Bivariate Fit of Zn ICP-ES (wt%) By Li ICP-ES (wt%)

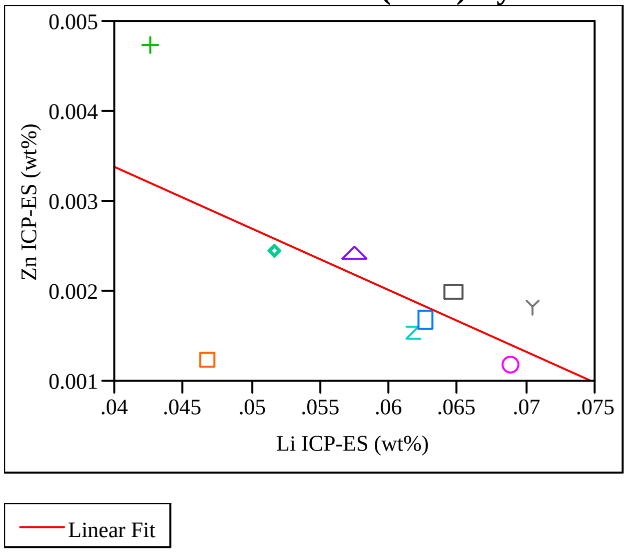

Linear Fit

Zn ICP-ES (wt%) = 0.0060973 - 0.06826 Li ICP-ES (wt%)

Summary of Fit

RSquare	0.377673
RSquare Adj	0.288769
Root Mean Square Error	0.000911
Mean of Response	0.002104
Observations (or Sum Wgts)	9

Analysis of Variance

Source	DF	Sum of Squares	Mean Square	F Ratio
Model	1	3.52785e-6	3.5278e-6	4.2481
Error	7	5.81317e-6	8.3045e-7	Prob > F
C. Total	8	9.34102e-6		0.0782

Parameter Estimates

Term	Estimate	Std Error	t Ratio	Prob>|t|
Intercept	0.0060973	0.001961	3.11	0.0171
Li ICP-ES (wt%)	-0.06826	0.033118	-2.06	0.0782

Bivariate Fit of Mass-135 (Cs,Ba) ICP-MS (wt%) By Mass-133 (Cs) ICP-MS (wt%)

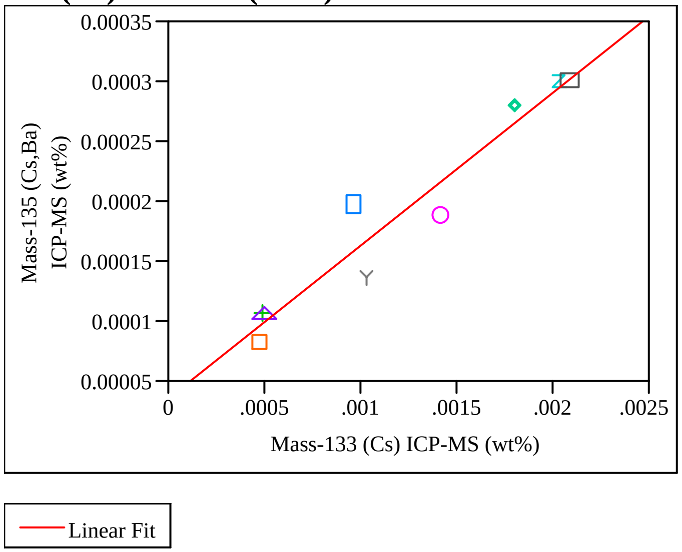

Linear Fit

Mass-135 (Cs,Ba) ICP-MS (wt%) = 3.5332e-5 + 0.1277172 Mass-133 (Cs) ICP-MS (wt%)

Summary of Fit

RSquare	0.940376
RSquare Adj	0.931858
Root Mean Square Error	2.282e-5
Mean of Response	0.000188
Observations (or Sum Wgts)	9

Analysis of Variance

Source	DF	Sum of Squares	Mean Square	F Ratio
Model	1	5.74861e-8	5.7486e-8	110.4014
Error	7	3.64491e-9	5.207e-10	Prob > F
C. Total	8	6.1131e-8		<.0001

Parameter Estimates

Term	Estimate	Std Error	t Ratio	Prob>|t|
Intercept	3.5332e-5	1.64e-5	2.15	0.0681
Mass-133 (Cs) ICP-MS (wt%)	0.1277172	0.012155	10.51	<.0001

Bivariate Fit of Mass-137 (Cs,Ba) ICP-MS (wt%) By Mass-133 (Cs) ICP-MS (wt%)

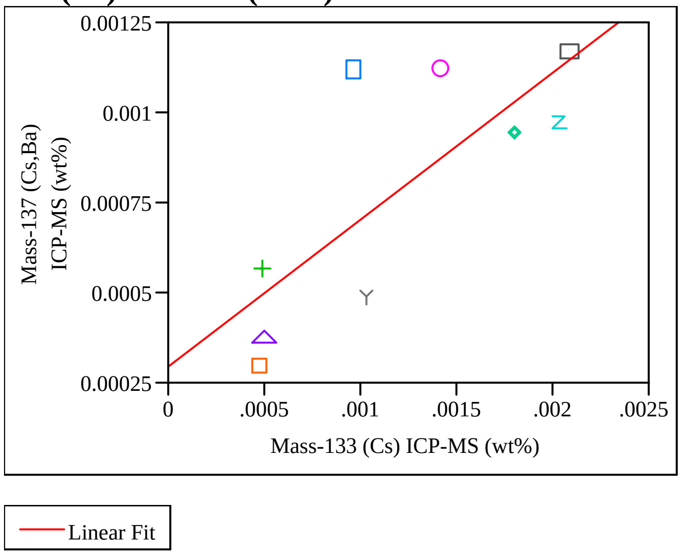

Linear Fit

Mass-137 (Cs,Ba) ICP-MS (wt%) = 0.0002943 + 0.407699 Mass-133 (Cs) ICP-MS (wt%)

Summary of Fit

RSquare	0.603796
RSquare Adj	0.547195
Root Mean Square Error	0.000234
Mean of Response	0.000782
Observations (or Sum Wgts)	9

Analysis of Variance

Source	DF	Sum of Squares	Mean Square	F Ratio
Model	1	5.85792e-7	5.8579e-7	10.6677
Error	7	3.8439e-7	5.4913e-8	Prob > F
C. Total	8	9.70182e-7		0.0137

Parameter Estimates

Term	Estimate	Std Error	t Ratio	Prob>|t|
Intercept	0.0002943	0.000168	1.75	0.1240
Mass-133 (Cs) ICP-MS (wt%)	0.407699	0.124826	3.27	0.0137

Bivariate Fit of Na ICP-ES (wt%) By Mass-133 (Cs) ICP-MS (wt%)

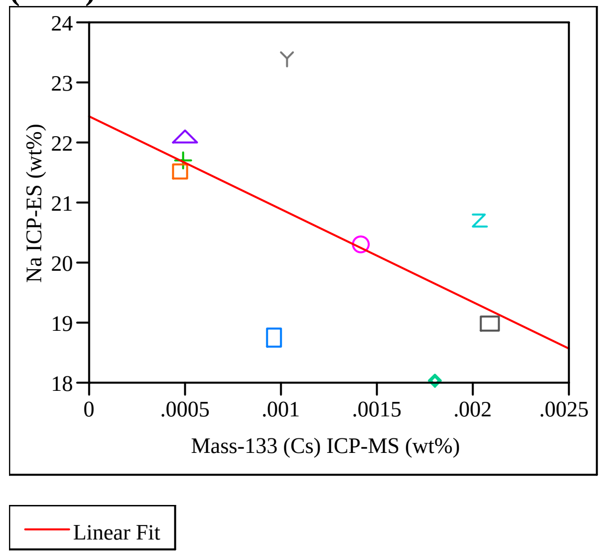

Linear Fit

Na ICP-ES (wt%) = 22.446676 - 1549.7974 Mass-133 (Cs) ICP-MS (wt%)

Summary of Fit

RSquare	0.339988
RSquare Adj	0.2457
Root Mean Square Error	1.532154
Mean of Response	20.59444
Observations (or Sum Wgts)	9

Analysis of Variance

Source	DF	Sum of Squares	Mean Square	F Ratio
Model	1	8.464746	8.46475	3.6059
Error	7	16.432477	2.34750	Prob > F
C. Total	8	24.897222		0.0994

Parameter Estimates

Term	Estimate	Std Error	t Ratio	Prob>|t|
Intercept	22.446676	1.101033	20.39	<.0001
Mass-133 (Cs) ICP-MS (wt%)	-1549.797	816.1509	-1.90	0.0994

Bivariate Fit of NO2 wt % By Mass-133 (Cs) ICP-MS (wt%)

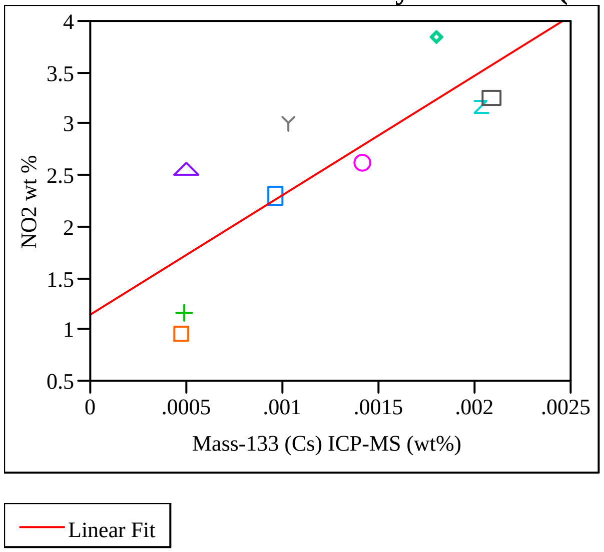

Linear Fit

NO2 wt % = 1.1507778 + 1159.3861 Mass-133 (Cs) ICP-MS (wt%)

Summary of Fit

RSquare	0.651753
RSquare Adj	0.602003
Root Mean Square Error	0.601331
Mean of Response	2.536412
Observations (or Sum Wgts)	9

Analysis of Variance

Source	DF	Sum of Squares	Mean Square	F Ratio
Model	1	4.7371838	4.73718	13.1007
Error	7	2.5311902	0.36160	Prob > F
C. Total	8	7.2683739		0.0085

Parameter Estimates

Term	Estimate	Std Error	t Ratio	Prob>|t|
Intercept	1.1507778	0.432127	2.66	0.0323
Mass-133 (Cs) ICP-MS (wt%)	1159.3861	320.318	3.62	0.0085

Bivariate Fit of NO3 wt % By Mass-133 (Cs) ICP-MS (wt%)

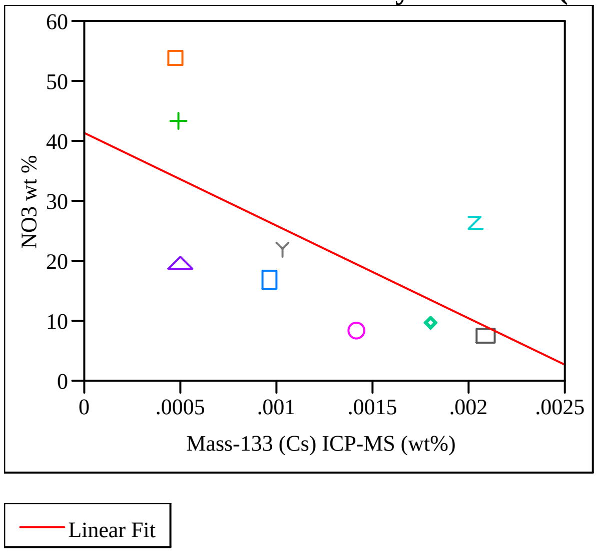

Linear Fit

NO3 wt % = 41.47392 - 15514.926 Mass-133 (Cs) ICP-MS (wt%)

Summary of Fit

RSquare	0.414133
RSquare Adj	0.330437
Root Mean Square Error	13.09371
Mean of Response	22.93134
Observations (or Sum Wgts)	9

Analysis of Variance

Source	DF	Sum of Squares	Mean Square	F Ratio
Model	1	848.3274	848.327	4.9481
Error	7	1200.1169	171.445	Prob > F
C. Total	8	2048.4444		0.0615

Parameter Estimates

Term	Estimate	Std Error	t Ratio	Prob>|t|
Intercept	41.47392	9.409371	4.41	0.0031
Mass-133 (Cs) ICP-MS (wt%)	-15514.93	6974.783	-2.22	0.0615

Bivariate Fit of OH wt % By Mass-133 (Cs) ICP-MS (wt%)

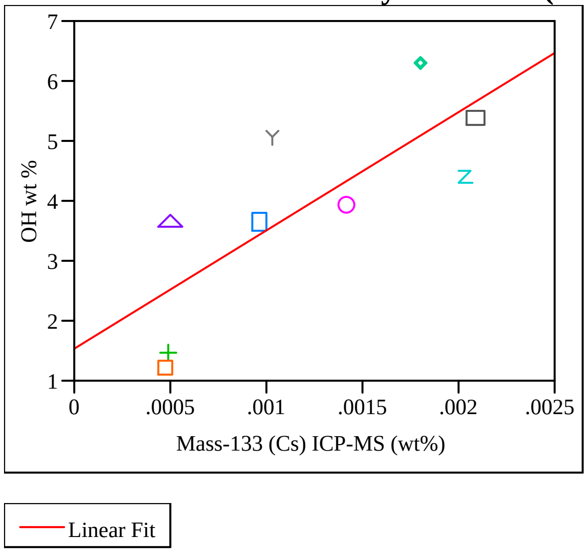

Linear Fit

OH wt % = 1.5273778 + 1973.1801 Mass-133 (Cs) ICP-MS (wt%)

Summary of Fit

RSquare	0.600151
RSquare Adj	0.543029
Root Mean Square Error	1.142794
Mean of Response	3.885613
Observations (or Sum Wgts)	9

Analysis of Variance

Source	DF	Sum of Squares	Mean Square	F Ratio
Model	1	13.721372	13.7214	10.5066
Error	7	9.141842	1.3060	Prob > F
C. Total	8	22.863214		0.0142

Parameter Estimates

Term	Estimate	Std Error	t Ratio	Prob>|t|
Intercept	1.5273778	0.821232	1.86	0.1052
Mass-133 (Cs) ICP-MS (wt%)	1973.1801	608.7456	3.24	0.0142

Bivariate Fit of P ICP-ES (wt%) By Mass-133 (Cs) ICP-MS (wt%)

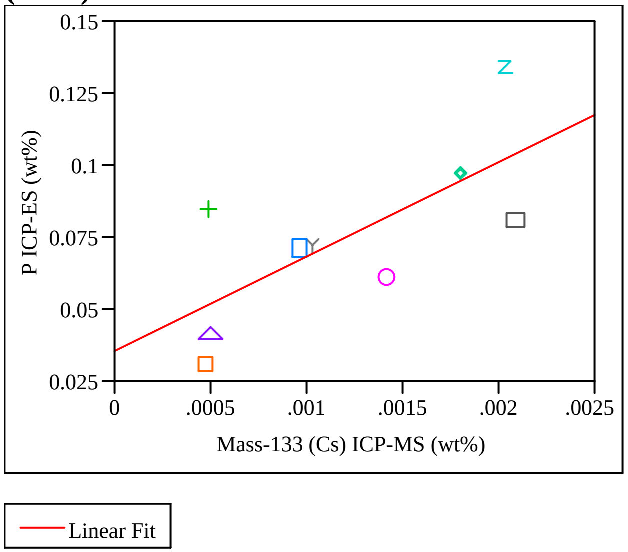

Linear Fit

P ICP-ES (wt%) = 0.0352519 + 32.969817 Mass-133 (Cs) ICP-MS (wt%)

Summary of Fit

RSquare	0.510449
RSquare Adj	0.440513
Root Mean Square Error	0.02291
Mean of Response	0.074656
Observations (or Sum Wgts)	9

Analysis of Variance

Source	DF	Sum of Squares	Mean Square	F Ratio
Model	1	0.00383087	0.003831	7.2988
Error	7	0.00367403	0.000525	Prob > F
C. Total	8	0.00750490		0.0306

Parameter Estimates

Term	Estimate	Std Error	t Ratio	Prob>|t|
Intercept	0.0352519	0.016463	2.14	0.0695
Mass-133 (Cs) ICP-MS (wt%)	32.969817	12.20366	2.70	0.0306

Bivariate Fit of Sb-126 (pCi/g) By Mass-133 (Cs) ICP-MS (wt%)

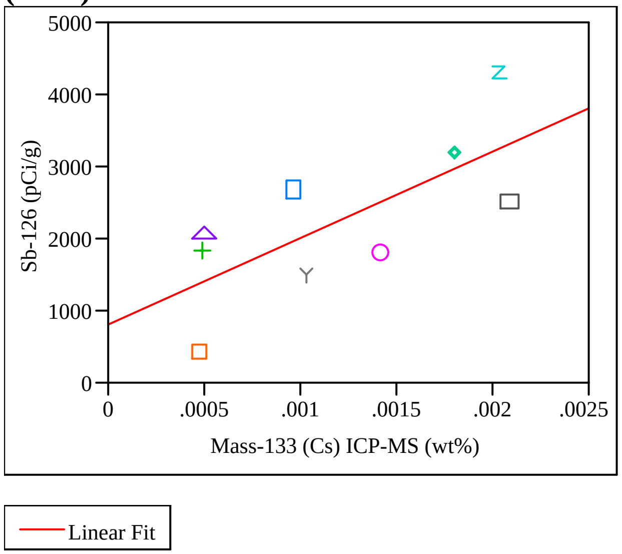

Linear Fit

Sb-126 (pCi/g) = 818.75772 + 1196458.7 Mass-133 (Cs) ICP-MS (wt%)

Summary of Fit

RSquare	0.523433
RSquare Adj	0.455352
Root Mean Square Error	810.0502
Mean of Response	2248.699
Observations (or Sum Wgts)	9

Analysis of Variance

Source	DF	Sum of Squares	Mean Square	F Ratio
Model	1	5044980.7	5044981	7.6884
Error	7	4593269.2	656181	Prob > F
C. Total	8	9638249.9		0.0276

Parameter Estimates

Term	Estimate	Std Error	t Ratio	Prob>|t|
Intercept	818.75772	582.1163	1.41	0.2024
Mass-133 (Cs) ICP-MS (wt%)	1196458.7	431499.1	2.77	0.0276

Bivariate Fit of Sn-126 (pCi/g) By Mass-133 (Cs) ICP-MS (wt%)

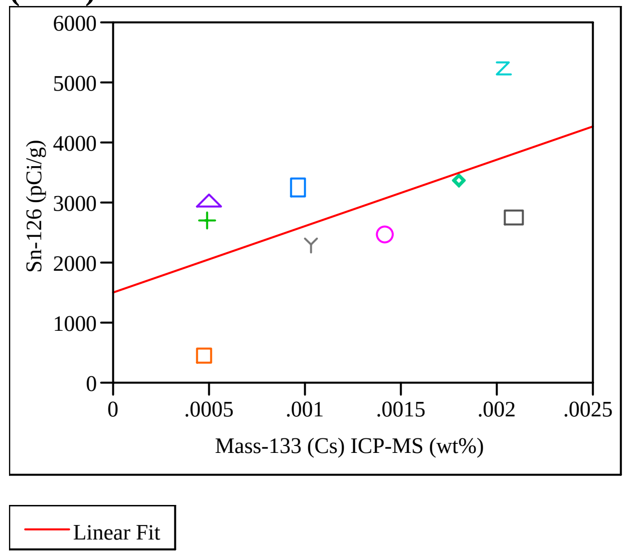

Linear Fit

Sn-126 (pCi/g) = 1493.5721 + 1110555.1 Mass-133 (Cs) ICP-MS (wt%)

Summary of Fit

RSquare	0.349111
RSquare Adj	0.256127
Root Mean Square Error	1075.956
Mean of Response	2820.846
Observations (or Sum Wgts)	9

Analysis of Variance

Source	DF	Sum of Squares	Mean Square	F Ratio
Model	1	4346546	4346546	3.7545
Error	7	8103768	1157681	Prob > F
C. Total	8	12450314		0.0939

Parameter Estimates

Term	Estimate	Std Error	t Ratio	Prob>|t|
Intercept	1493.5721	773.2008	1.93	0.0947
Mass-133 (Cs) ICP-MS (wt%)	1110555.1	573142.3	1.94	0.0939

Bivariate Fit of Mass-137 (Cs,Ba) ICP-MS (wt%) By Mass-135 (Cs,Ba) ICP-MS (wt%)

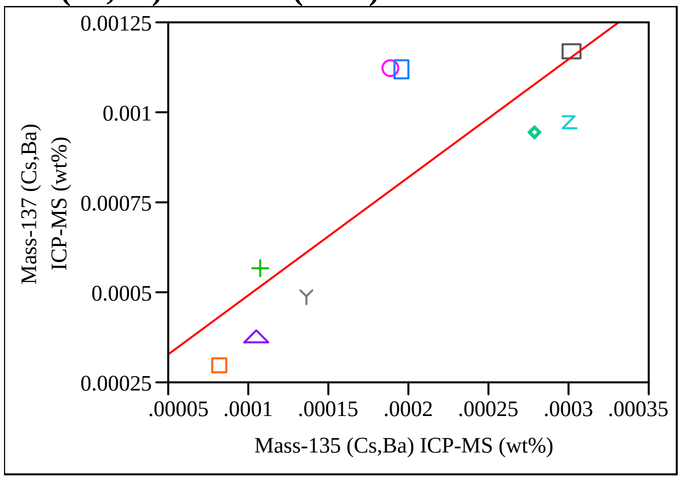

Linear Fit

Linear Fit

Mass-137 (Cs,Ba) ICP-MS (wt%) = 0.0001666 + 3.2713443 Mass-135 (Cs,Ba) ICP-MS (wt%)

Summary of Fit

RSquare	0.674312
RSquare Adj	0.627785
Root Mean Square Error	0.000212
Mean of Response	0.000782
Observations (or Sum Wgts)	9

Analysis of Variance

Source	DF	Sum of Squares	Mean Square	F Ratio
Model	1	6.54205e-7	6.5421e-7	14.4930
Error	7	3.15977e-7	4.514e-8	Prob > F
C. Total	8	9.70182e-7		0.0067

Parameter Estimates

Term	Estimate	Std Error	t Ratio	Prob>|t|
Intercept	0.0001666	0.000176	0.94	0.3762
Mass-135 (Cs,Ba) ICP-MS (wt%)	3.2713443	0.859306	3.81	0.0067

Bivariate Fit of Na ICP-ES (wt%) By Mass-135 (Cs,Ba) ICP-MS (wt%)

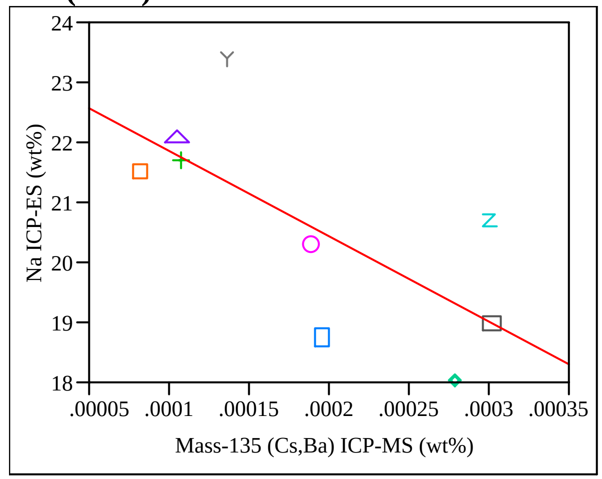

Linear Fit

Linear Fit

Na ICP-ES (wt%) = 23.273721 - 14253.535 Mass-135 (Cs,Ba) ICP-MS (wt%)

Summary of Fit

RSquare	0.498834
RSquare Adj	0.427239
Root Mean Square Error	1.335111
Mean of Response	20.59444
Observations (or Sum Wgts)	9

Analysis of Variance

Source	DF	Sum of Squares	Mean Square	F Ratio
Model	1	12.419576	12.4196	6.9674
Error	7	12.477646	1.7825	Prob > F
C. Total	8	24.897222		0.0334

Parameter Estimates

Term	Estimate	Std Error	t Ratio	Prob>|t|
Intercept	23.273721	1.108312	21.00	<.0001
Mass-135 (Cs,Ba) ICP-MS (wt%)	-14253.53	5399.91	-2.64	0.0334

Bivariate Fit of NO2 wt % By Mass-135 (Cs,Ba) ICP-MS (wt%)

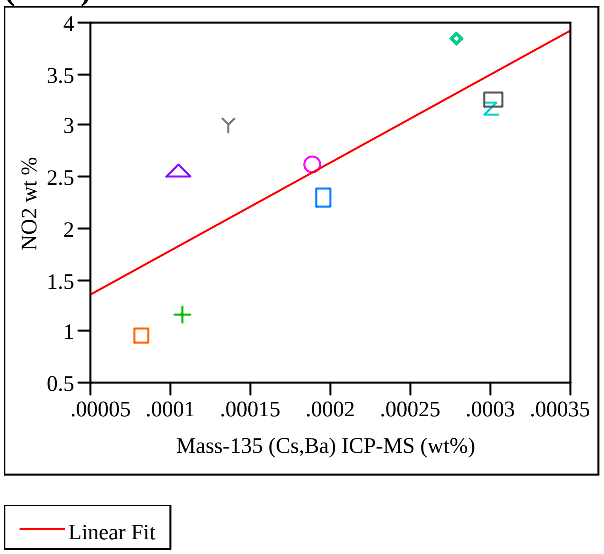

Linear Fit

NO2 wt % = 0.9283987 + 8554.4998 Mass-135 (Cs,Ba) ICP-MS (wt%)

Summary of Fit

RSquare	0.615479
RSquare Adj	0.560548
Root Mean Square Error	0.631872
Mean of Response	2.536412
Observations (or Sum Wgts)	9

Analysis of Variance

Source	DF	Sum of Squares	Mean Square	F Ratio
Model	1	4.4735350	4.47354	11.2045
Error	7	2.7948389	0.39926	Prob > F
C. Total	8	7.2683739		0.0123

Parameter Estimates

Term	Estimate	Std Error	t Ratio	Prob>|t|
Intercept	0.9283987	0.524535	1.77	0.1200
Mass-135 (Cs,Ba) ICP-MS (wt%)	8554.4998	2555.633	3.35	0.0123

Bivariate Fit of NO3 wt % By Mass-135 (Cs,Ba) ICP-MS (wt%)

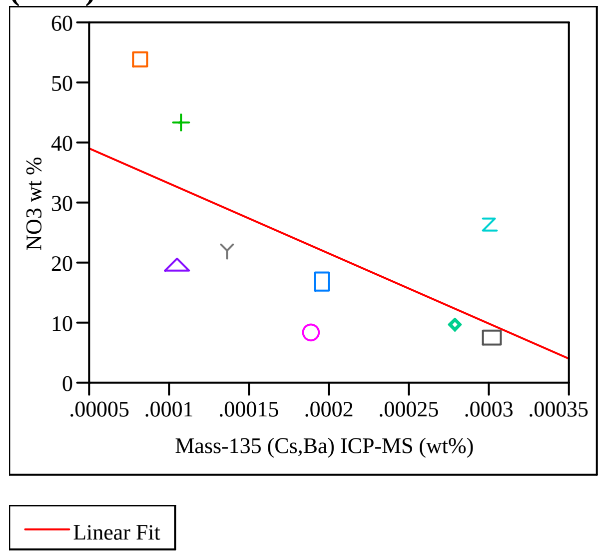

Linear Fit

NO3 wt % = 45.047979 - 117658.74 Mass-135 (Cs,Ba) ICP-MS (wt%)

Summary of Fit

RSquare	0.413129
RSquare Adj	0.32929
Root Mean Square Error	13.10492
Mean of Response	22.93134
Observations (or Sum Wgts)	9

Analysis of Variance

Source	DF	Sum of Squares	Mean Square	F Ratio
Model	1	846.2720	846.272	4.9277
Error	7	1202.1724	171.739	Prob > F
C. Total	8	2048.4444		0.0619

Parameter Estimates

Term	Estimate	Std Error	t Ratio	Prob>|t|
Intercept	45.047979	10.87875	4.14	0.0043
Mass-135 (Cs,Ba) ICP-MS (wt%)	-117658.7	53003.38	-2.22	0.0619

Bivariate Fit of OH wt % By Mass-135 (Cs,Ba) ICP-MS (wt%)

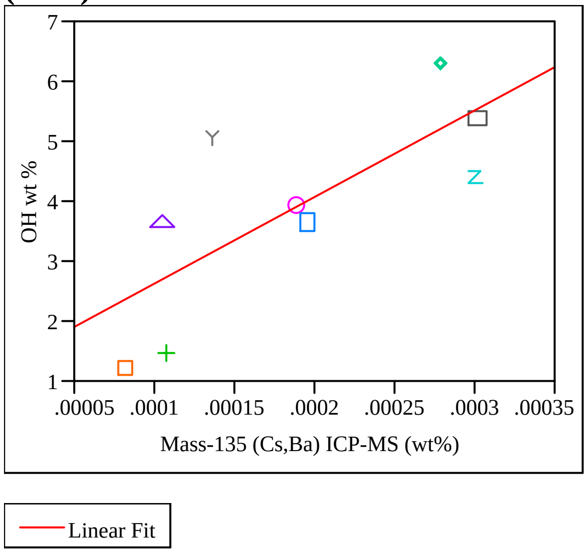

Linear Fit
OH wt % = 1.1642004 + 14477.697 Mass-135 (Cs,Ba) ICP-MS (wt%)

Summary of Fit

RSquare	0.560432
RSquare Adj	0.497637
Root Mean Square Error	1.198209
Mean of Response	3.885613
Observations (or Sum Wgts)	9

Analysis of Variance

Source	DF	Sum of Squares	Mean Square	F Ratio
Model	1	12.813288	12.8133	8.9247
Error	7	10.049926	1.4357	Prob > F
C. Total	8	22.863214		0.0203

Parameter Estimates

Term	Estimate	Std Error	t Ratio	Prob>|t|
Intercept	1.1642004	0.994666	1.17	0.2801
Mass-135 (Cs,Ba) ICP-MS (wt%)	14477.697	4846.203	2.99	0.0203

Bivariate Fit of Sb-126 (pCi/g) By Mass-135 (Cs,Ba) ICP-MS (wt%)

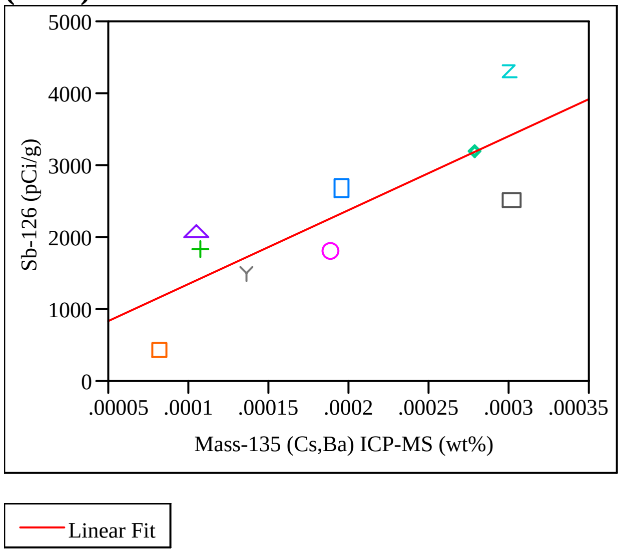

Linear Fit
Sb-126 (pCi/g) = 310.60354 + 10310511 Mass-135 (Cs,Ba) ICP-MS (wt%)

Summary of Fit

RSquare	0.674254
RSquare Adj	0.627719
Root Mean Square Error	669.714
Mean of Response	2248.699
Observations (or Sum Wgts)	9

Analysis of Variance

Source	DF	Sum of Squares	Mean Square	F Ratio
Model	1	6498632.5	6498632	14.4892
Error	7	3139617.4	448517	Prob > F
C. Total	8	9638249.9		0.0067

Parameter Estimates

Term	Estimate	Std Error	t Ratio	Prob>|t|
Intercept	310.60354	555.9479	0.56	0.5938
Mass-135 (Cs,Ba) ICP-MS (wt%)	10310511	2708685	3.81	0.0067

Bivariate Fit of Sn-126 (pCi/g) By Mass-135 (Cs,Ba) ICP-MS (wt%)

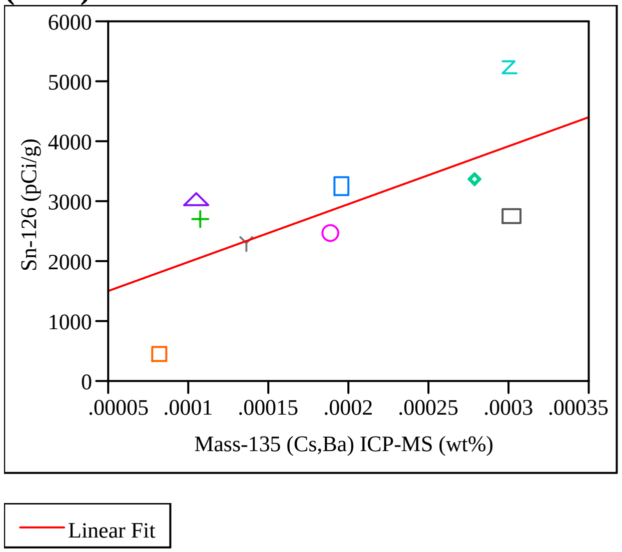

Linear Fit

Sn-126 (pCi/g) = 1004.2495 + 9664147.1 Mass-135 (Cs,Ba) ICP-MS (wt%)

Summary of Fit

RSquare	0.458573
RSquare Adj	0.381226
Root Mean Square Error	981.3211
Mean of Response	2820.846
Observations (or Sum Wgts)	9

Analysis of Variance

Source	DF	Sum of Squares	Mean Square	F Ratio
Model	1	5709376	5709376	5.9288
Error	7	6740938	962991	Prob > F
C. Total	8	12450314		0.0451

Parameter Estimates

Term	Estimate	Std Error	t Ratio	Prob>|t|
Intercept	1004.2495	814.6216	1.23	0.2575
Mass-135 (Cs,Ba) ICP-MS (wt%)	9664147.1	3968993	2.43	0.0451

Bivariate Fit of Tc-99 (ICP-MS) (pCi/g) By Mass-135 (Cs,Ba) ICP-MS (wt%)

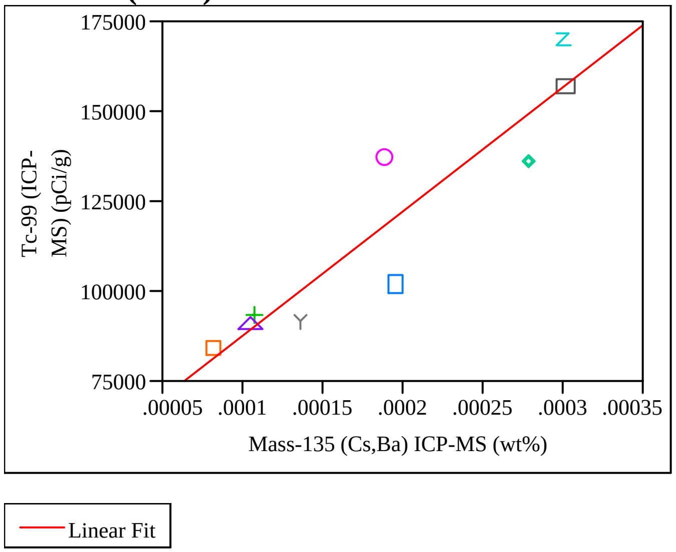

Linear Fit

Tc-99 (ICP-MS) (pCi/g) = 53043.789 + 344695629 Mass-135 (Cs,Ba) ICP-MS (wt%)

Summary of Fit

RSquare	0.860232
RSquare Adj	0.840265
Root Mean Square Error	12984.16
Mean of Response	117837.2
Observations (or Sum Wgts)	9

Analysis of Variance

Source	DF	Sum of Squares	Mean Square	F Ratio
Model	1	7263286093	7.2633e+9	43.0829
Error	7	1180119207	168588458	Prob > F
C. Total	8	8443405300		0.0003

Parameter Estimates

Term	Estimate	Std Error	t Ratio	Prob>|t|
Intercept	53043.789	10778.51	4.92	0.0017
Mass-135 (Cs,Ba) ICP-MS (wt%)	344695629	52514970	6.56	0.0003

Bivariate Fit of Ti ICP-ES (wt%) By Mass-135 (Cs,Ba) ICP-MS (wt%)

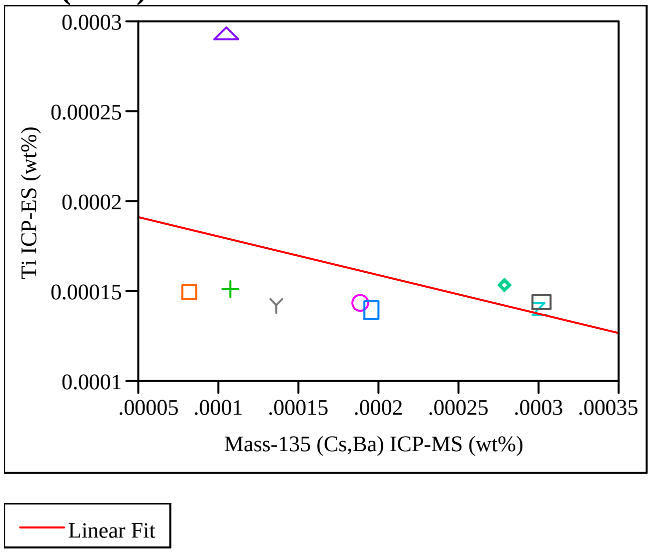

Linear Fit

Ti ICP-ES (wt%) = 0.0002016 - 0.213695 Mass-135 (Cs,Ba) ICP-MS (wt%)

Summary of Fit

RSquare	0.142929
RSquare Adj	0.02049
Root Mean Square Error	0.000049
Mean of Response	0.000161
Observations (or Sum Wgts)	9

Analysis of Variance

Source	DF	Sum of Squares	Mean Square	F Ratio
Model	1	2.79158e-9	2.7916e-9	1.1674
Error	7	1.67396e-8	2.3914e-9	Prob > F
C. Total	8	1.95312e-8		0.3158

Parameter Estimates

Term	Estimate	Std Error	t Ratio	Prob>|t|
Intercept	0.0002016	4.059e-5	4.97	0.0016
Mass-135 (Cs,Ba) ICP-MS (wt%)	-0.213695	0.197785	-1.08	0.3158

Bivariate Fit of H2O Fraction By Mass-135 (Cs,Ba) ICP-MS (wt%)

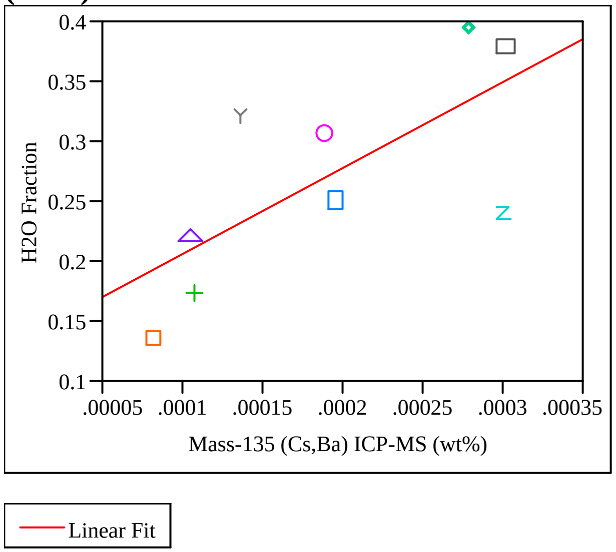

Linear Fit

H2O Fraction = 0.1337817 + 718.66018 Mass-135 (Cs,Ba) ICP-MS (wt%)

Summary of Fit

RSquare	0.502745
RSquare Adj	0.431708
Root Mean Square Error	0.066792
Mean of Response	0.26887
Observations (or Sum Wgts)	9

Analysis of Variance

Source	DF	Sum of Squares	Mean Square	F Ratio
Model	1	0.03157248	0.031572	7.0773
Error	7	0.03122774	0.004461	Prob > F
C. Total	8	0.06280022		0.0325

Parameter Estimates

Term	Estimate	Std Error	t Ratio	Prob>|t|
Intercept	0.1337817	0.055445	2.41	0.0466
Mass-135 (Cs,Ba) ICP-MS (wt%)	718.66018	270.141	2.66	0.0325

Bivariate Fit of Na ICP-ES (wt%) By Mass-137 (Cs,Ba) ICP-MS (wt%)

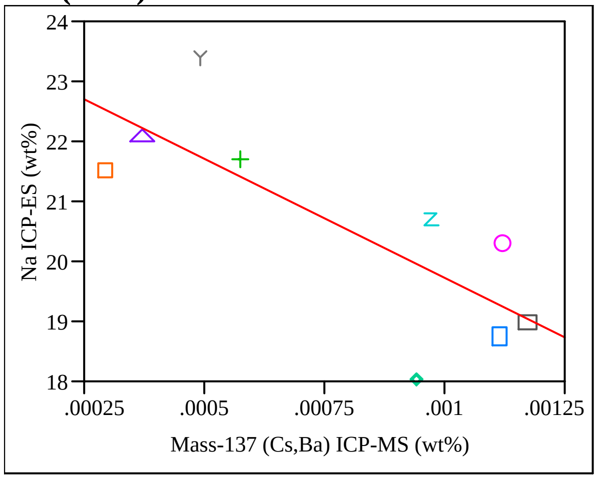

Linear Fit

Linear Fit

Na ICP-ES (wt%) = 23.684528 - 3953.7606 Mass-137 (Cs,Ba) ICP-MS (wt%)

Summary of Fit

RSquare	0.609148
RSquare Adj	0.553312
Root Mean Square Error	1.179051
Mean of Response	20.59444
Observations (or Sum Wgts)	9

Analysis of Variance

Source	DF	Sum of Squares	Mean Square	F Ratio
Model	1	15.166101	15.1661	10.9096
Error	7	9.731122	1.3902	Prob > F
C. Total	8	24.897222		0.0131

Parameter Estimates

Term	Estimate	Std Error	t Ratio	Prob>|t|
Intercept	23.684528	1.014747	23.34	<.0001
Mass-137 (Cs,Ba) ICP-MS (wt%)	-3953.761	1197.032	-3.30	0.0131

Bivariate Fit of NO3 wt % By Mass-137 (Cs,Ba) ICP-MS (wt%)

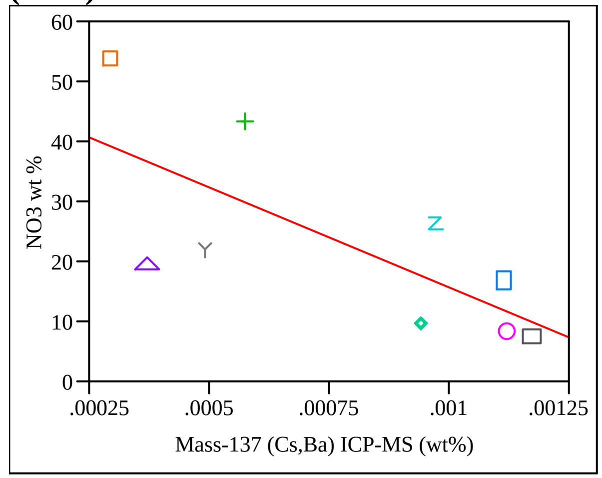

Linear Fit

Linear Fit

NO3 wt % = 48.778629 - 33071.593 Mass-137 (Cs,Ba) ICP-MS (wt%)

Summary of Fit

RSquare	0.518011
RSquare Adj	0.449156
Root Mean Square Error	11.87631
Mean of Response	22.93134
Observations (or Sum Wgts)	9

Analysis of Variance

Source	DF	Sum of Squares	Mean Square	F Ratio
Model	1	1061.1174	1061.12	7.5232
Error	7	987.3270	141.05	Prob > F
C. Total	8	2048.4444		0.0288

Parameter Estimates

Term	Estimate	Std Error	t Ratio	Prob>|t|
Intercept	48.778629	10.22131	4.77	0.0020
Mass-137 (Cs,Ba) ICP-MS (wt%)	-33071.59	12057.43	-2.74	0.0288

Bivariate Fit of Sb-126 (pCi/g) By Mass-137 (Cs,Ba) ICP-MS (wt%)

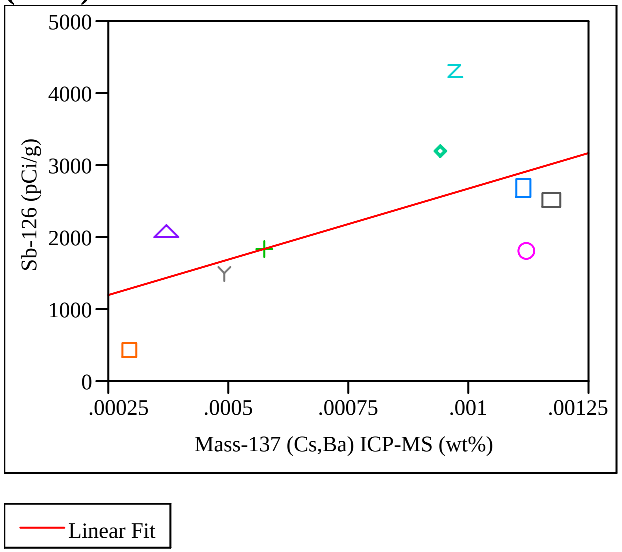

Linear Fit

Sb-126 (pCi/g) = 715.9852 + 1961106.3 Mass-137 (Cs,Ba) ICP-MS (wt%)

Summary of Fit

RSquare	0.38713
RSquare Adj	0.299578
Root Mean Square Error	918.6162
Mean of Response	2248.699
Observations (or Sum Wgts)	9

Analysis of Variance

Source	DF	Sum of Squares	Mean Square	F Ratio
Model	1	3731259.5	3731260	4.4217
Error	7	5906990.4	843856	Prob > F
C. Total	8	9638249.9		0.0736

Parameter Estimates

Term	Estimate	Std Error	t Ratio	Prob>|t|
Intercept	715.9852	790.6045	0.91	0.3952
Mass-137 (Cs,Ba) ICP-MS (wt%)	1961106.3	932626	2.10	0.0736

Bivariate Fit of Tc-99 (ICP-MS) (pCi/g) By Mass-137 (Cs,Ba) ICP-MS (wt%)

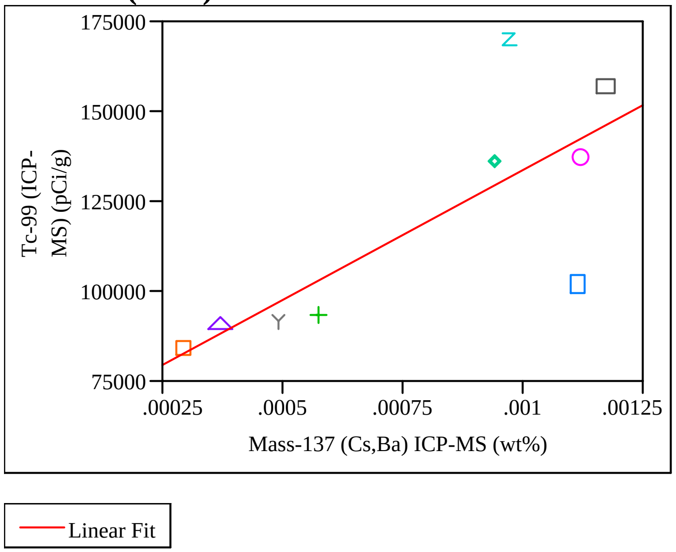

Linear Fit

Tc-99 (ICP-MS) (pCi/g) = 61694.597 + 71834406 Mass-137 (Cs,Ba) ICP-MS (wt%)

Summary of Fit

RSquare	0.592926
RSquare Adj	0.534773
Root Mean Square Error	22158.81
Mean of Response	117837.2
Observations (or Sum Wgts)	9

Analysis of Variance

Source	DF	Sum of Squares	Mean Square	F Ratio
Model	1	5006315427	5.0063e+9	10.1959
Error	7	3437089873	491012839	Prob > F
C. Total	8	8443405300		0.0152

Parameter Estimates

Term	Estimate	Std Error	t Ratio	Prob>|t|
Intercept	61694.597	19070.92	3.24	0.0144
Mass-137 (Cs,Ba) ICP-MS (wt%)	71834406	22496752	3.19	0.0152

Bivariate Fit of H2O Fraction By Mass-137 (Cs,Ba) ICP-MS (wt%)

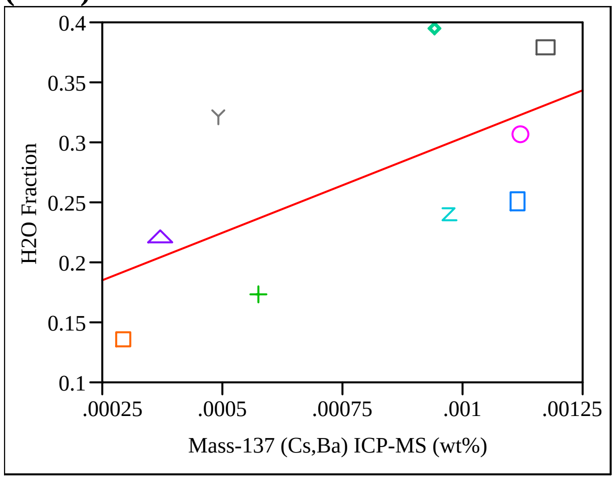

Linear Fit

Linear Fit

H2O Fraction = 0.1449891 + 158.5059 Mass-137 (Cs,Ba) ICP-MS (wt%)

Summary of Fit

RSquare	0.388135
RSquare Adj	0.300726
Root Mean Square Error	0.07409
Mean of Response	0.26887
Observations (or Sum Wgts)	9

Analysis of Variance

Source	DF	Sum of Squares	Mean Square	F Ratio
Model	1	0.02437497	0.024375	4.4404
Error	7	0.03842525	0.005489	Prob > F
C. Total	8	0.06280022		0.0731

Parameter Estimates

Term	Estimate	Std Error	t Ratio	Prob>|t|
Intercept	0.1449891	0.063765	2.27	0.0572
Mass-137 (Cs,Ba) ICP-MS (wt%)	158.5059	75.2199	2.11	0.0731

Bivariate Fit of Pu-239/240 (pCi/g) By Mass-238 (U) ICP-MS (wt%)

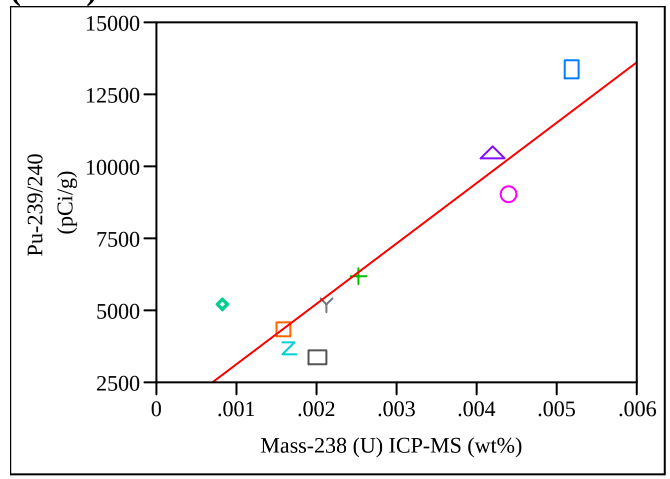

Linear Fit

Linear Fit

Pu-239/240 (pCi/g) = 1053.0863 + 2096056 Mass-238 (U) ICP-MS (wt%)

Summary of Fit

RSquare	0.851174
RSquare Adj	0.829913
Root Mean Square Error	1407.001
Mean of Response	6742.492
Observations (or Sum Wgts)	9

Analysis of Variance

Source	DF	Sum of Squares	Mean Square	F Ratio
Model	1	79254845	79254845	40.0348
Error	7	13857555	1979650.7	Prob > F
C. Total	8	93112400		0.0004

Parameter Estimates

Term	Estimate	Std Error	t Ratio	Prob>|t|
Intercept	1053.0863	1014.146	1.04	0.3336
Mass-238 (U) ICP-MS (wt%)	2096056	331271.6	6.33	0.0004

Bivariate Fit of NO3 wt % By NO2 wt %

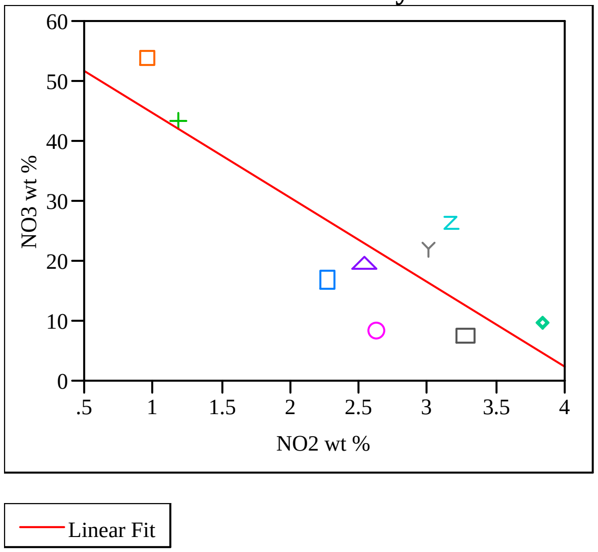

Linear Fit

NO3 wt % = 58.693363 - 14.099455 NO2 wt %

Summary of Fit

RSquare	0.705371
RSquare Adj	0.663281
Root Mean Square Error	9.285401
Mean of Response	22.93134
Observations (or Sum Wgts)	9

Analysis of Variance

Source	DF	Sum of Squares	Mean Square	F Ratio
Model	1	1444.9136	1444.91	16.7587
Error	7	603.5307	86.22	Prob > F
C. Total	8	2048.4444		0.0046

Parameter Estimates

Term	Estimate	Std Error	t Ratio	Prob>|t|
Intercept	58.693363	9.267888	6.33	0.0004
NO2 wt %	-14.09945	3.44415	-4.09	0.0046

Bivariate Fit of OH wt % By NO2 wt %

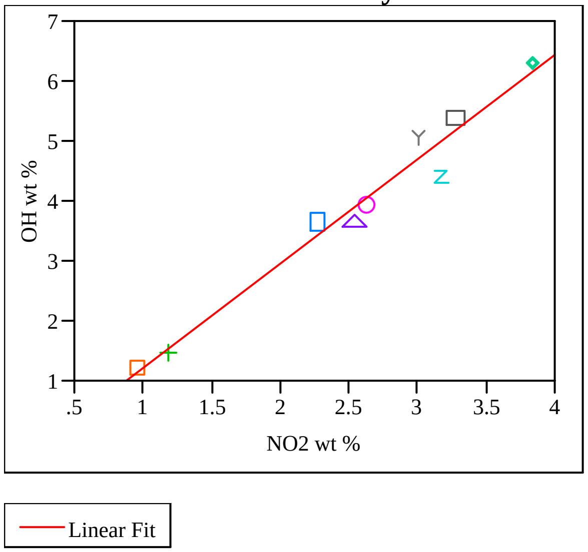

Linear Fit

OH wt % = -0.545197 + 1.7468812 NO2 wt %

Summary of Fit

RSquare	0.970123
RSquare Adj	0.965855
Root Mean Square Error	0.312385
Mean of Response	3.885613
Observations (or Sum Wgts)	9

Analysis of Variance

Source	DF	Sum of Squares	Mean Square	F Ratio
Model	1	22.180125	22.1801	227.2924
Error	7	0.683089	0.0976	Prob > F
C. Total	8	22.863214		<.0001

Parameter Estimates

Term	Estimate	Std Error	t Ratio	Prob>|t|
Intercept	-0.545197	0.311795	-1.75	0.1239
NO2 wt %	1.7468812	0.11587	15.08	<.0001

Bivariate Fit of Sb-126 (pCi/g) By NO2 wt %

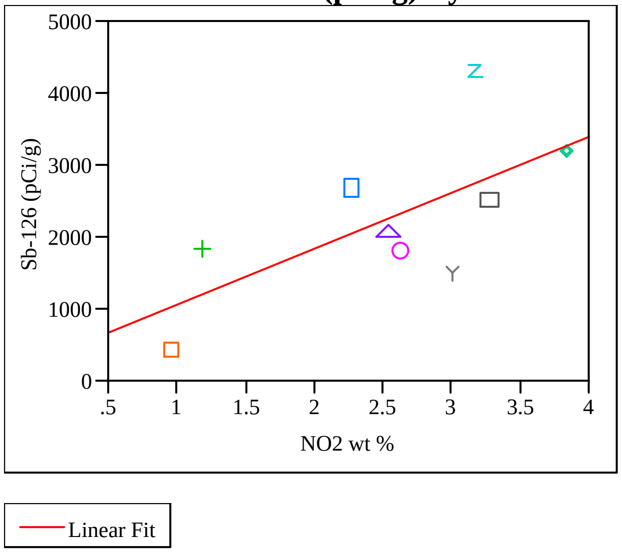

Linear Fit

Sb-126 (pCi/g) = 275.02694 + 778.13543 NO2 wt %

Summary of Fit

RSquare	0.456614
RSquare Adj	0.378988
Root Mean Square Error	864.9763
Mean of Response	2248.699
Observations (or Sum Wgts)	9

Analysis of Variance

Source	DF	Sum of Squares	Mean Square	F Ratio
Model	1	4400962.2	4400962	5.8822
Error	7	5237287.7	748184	Prob > F
C. Total	8	9638249.9		0.0457

Parameter Estimates

Term	Estimate	Std Error	t Ratio	Prob>|t|
Intercept	275.02694	863.3448	0.32	0.7594
NO2 wt %	778.13543	320.8378	2.43	0.0457

Bivariate Fit of Sn-126 (pCi/g) By NO2 wt %

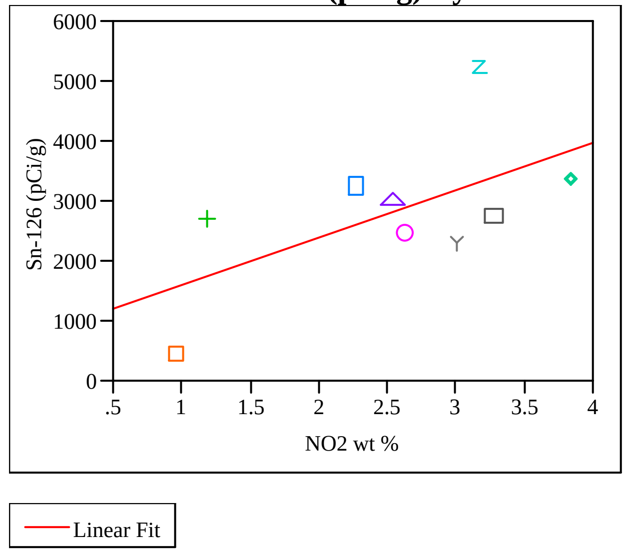

Linear Fit

Sn-126 (pCi/g) = 807.46993 + 793.7891 NO2 wt %

Summary of Fit

RSquare	0.367847
RSquare Adj	0.277539
Root Mean Square Error	1060.357
Mean of Response	2820.846
Observations (or Sum Wgts)	9

Analysis of Variance

Source	DF	Sum of Squares	Mean Square	F Ratio
Model	1	4579811	4579811	4.0733
Error	7	7870504	1124358	Prob > F
C. Total	8	12450314		0.0833

Parameter Estimates

Term	Estimate	Std Error	t Ratio	Prob>|t|
Intercept	807.46993	1058.357	0.76	0.4704
NO2 wt %	793.7891	393.3087	2.02	0.0833

Bivariate Fit of Tc-99 (ICP-MS) (pCi/g) By NO2 wt %

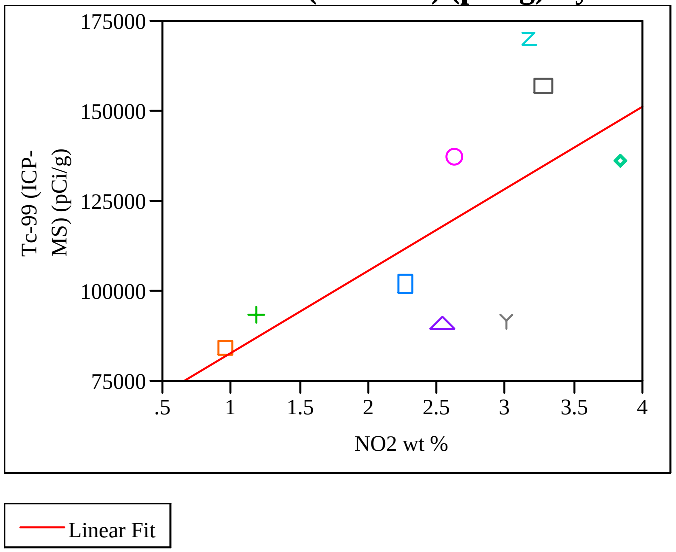

Linear Fit

Tc-99 (ICP-MS) (pCi/g) = 59992.39 + 22805.756 NO2 wt %

Summary of Fit

RSquare	0.447722
RSquare Adj	0.368825
Root Mean Square Error	25810.04
Mean of Response	117837.2
Observations (or Sum Wgts)	9

Analysis of Variance

Source	DF	Sum of Squares	Mean Square	F Ratio
Model	1	3780299642	3.7803e+9	5.6748
Error	7	4663105658	666157951	Prob > F
C. Total	8	8443405300		0.0487

Parameter Estimates

Term	Estimate	Std Error	t Ratio	Prob>|t|
Intercept	59992.39	25761.35	2.33	0.0527
NO2 wt %	22805.756	9573.483	2.38	0.0487

Bivariate Fit of H2O Fraction By NO2 wt %

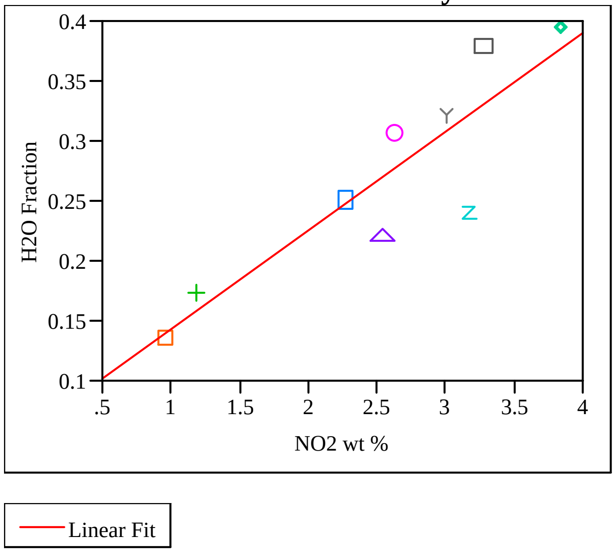

Linear Fit

H2O Fraction = 0.0596928 + 0.0824698 NO2 wt %

Summary of Fit

RSquare	0.787166
RSquare Adj	0.756761
Root Mean Square Error	0.043697
Mean of Response	0.26887
Observations (or Sum Wgts)	9

Analysis of Variance

Source	DF	Sum of Squares	Mean Square	F Ratio
Model	1	0.04943420	0.049434	25.8895
Error	7	0.01336602	0.001909	Prob > F
C. Total	8	0.06280022		0.0014

Parameter Estimates

Term	Estimate	Std Error	t Ratio	Prob>|t|
Intercept	0.0596928	0.043615	1.37	0.2134
NO2 wt %	0.0824698	0.016208	5.09	0.0014

Bivariate Fit of OH wt % By NO3 wt %

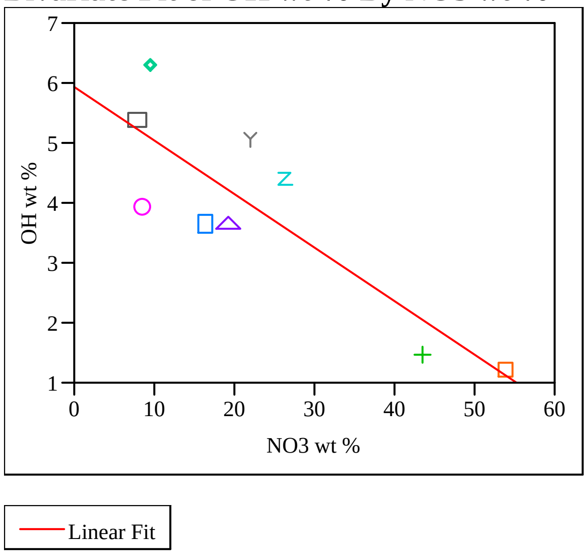

Linear Fit

OH wt % = 5.9346344 - 0.0893546 NO3 wt %

Summary of Fit

RSquare	0.715354
RSquare Adj	0.67469
Root Mean Square Error	0.964211
Mean of Response	3.885613
Observations (or Sum Wgts)	9

Analysis of Variance

Source	DF	Sum of Squares	Mean Square	F Ratio
Model	1	16.355289	16.3553	17.5919
Error	7	6.507925	0.9297	Prob > F
C. Total	8	22.863214		0.0041

Parameter Estimates

Term	Estimate	Std Error	t Ratio	Prob>|t|
Intercept	5.9346344	0.584774	10.15	<.0001
NO3 wt %	-0.089355	0.021304	-4.19	0.0041

Bivariate Fit of H2O Fraction By NO3 wt %

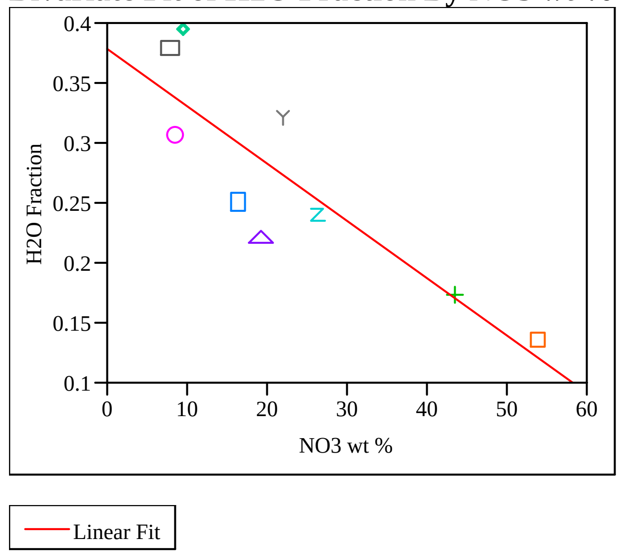

Linear Fit

H2O Fraction = 0.3783847 - 0.0047758 NO3 wt %

Summary of Fit

RSquare	0.743956
RSquare Adj	0.707379
Root Mean Square Error	0.047928
Mean of Response	0.26887
Observations (or Sum Wgts)	9

Analysis of Variance

Source	DF	Sum of Squares	Mean Square	F Ratio
Model	1	0.04672062	0.046721	20.3391
Error	7	0.01607960	0.002297	Prob > F
C. Total	8	0.06280022		0.0028

Parameter Estimates

Term	Estimate	Std Error	t Ratio	Prob>|t|
Intercept	0.3783847	0.029067	13.02	<.0001
NO3 wt %	-0.004776	0.001059	-4.51	0.0028

Bivariate Fit of Tc-99 (ICP-MS) (pCi/g) By OH wt %

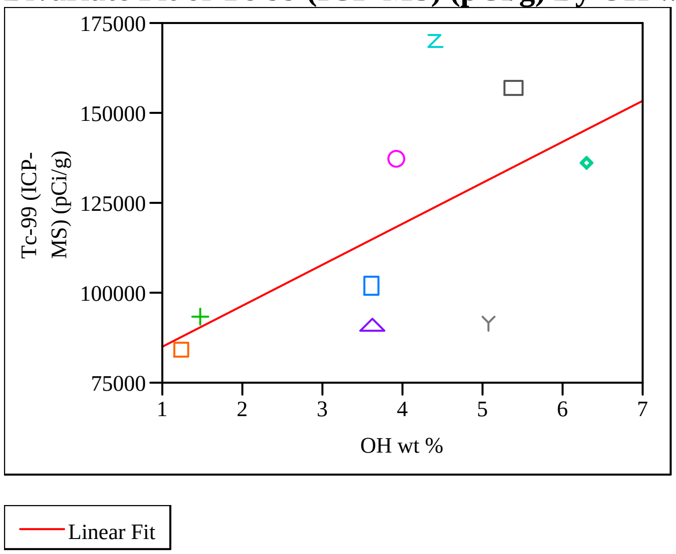

Linear Fit

Tc-99 (ICP-MS) (pCi/g) = 73557.152 + 11395.891 OH wt %

Summary of Fit

RSquare	0.351655
RSquare Adj	0.259034
Root Mean Square Error	27964.88
Mean of Response	117837.2
Observations (or Sum Wgts)	9

Analysis of Variance

Source	DF	Sum of Squares	Mean Square	F Ratio
Model	1	2969161858	2.9692e+9	3.7967
Error	7	5474243442	782034777	Prob > F
C. Total	8	8443405300		0.0924

Parameter Estimates

Term	Estimate	Std Error	t Ratio	Prob>|t|
Intercept	73557.152	24562.54	2.99	0.0201
OH wt %	11395.891	5848.499	1.95	0.0924

Bivariate Fit of H2O Fraction By OH wt %

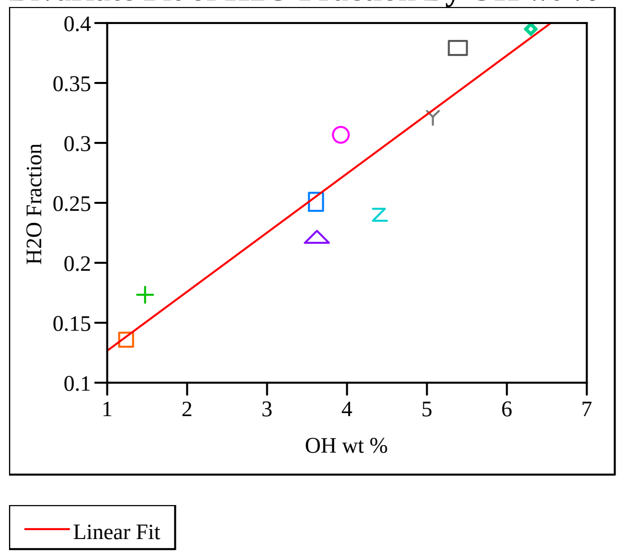

Linear Fit

H2O Fraction = 0.0780749 + 0.049103 OH wt %

Summary of Fit

RSquare	0.877794
RSquare Adj	0.860336
Root Mean Square Error	0.033111
Mean of Response	0.26887
Observations (or Sum Wgts)	9

Analysis of Variance

Source	DF	Sum of Squares	Mean Square	F Ratio
Model	1	0.05512566	0.055126	50.2804
Error	7	0.00767456	0.001096	Prob > F
C. Total	8	0.06280022		0.0002

Parameter Estimates

Term	Estimate	Std Error	t Ratio	Prob>|t|
Intercept	0.0780749	0.029083	2.68	0.0313
OH wt %	0.049103	0.006925	7.09	0.0002

Bivariate Fit of Cr ICP-ES (wt%) By P ICP-ES (wt%)

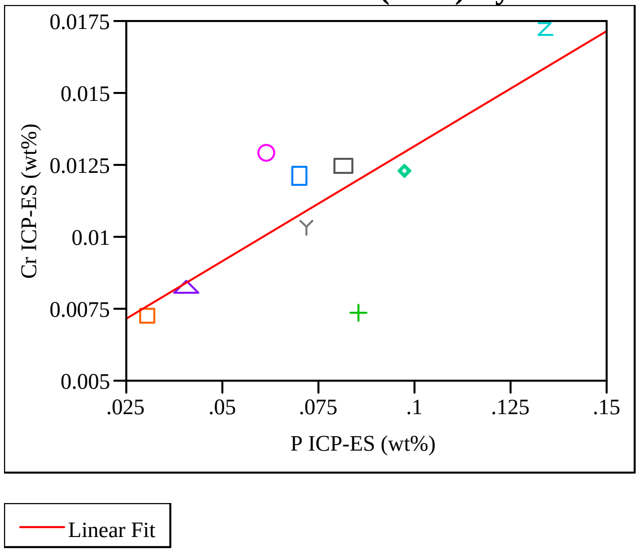

Linear Fit

Cr ICP-ES (wt%) = 0.0051265 + 0.0801187 P ICP-ES (wt%)

Summary of Fit

RSquare	0.582516
RSquare Adj	0.522875
Root Mean Square Error	0.002221
Mean of Response	0.011108
Observations (or Sum Wgts)	9

Analysis of Variance

Source	DF	Sum of Squares	Mean Square	F Ratio
Model	1	0.00004817	0.000048	9.7671
Error	7	0.00003453	4.932e-6	Prob > F
C. Total	8	0.00008270		0.0167

Parameter Estimates

Term	Estimate	Std Error	t Ratio	Prob>|t|
Intercept	0.0051265	0.002052	2.50	0.0411
P ICP-ES (wt%)	0.0801187	0.025636	3.13	0.0167

Bivariate Fit of Cs-137 (pCi/g) By P ICP-ES (wt%)

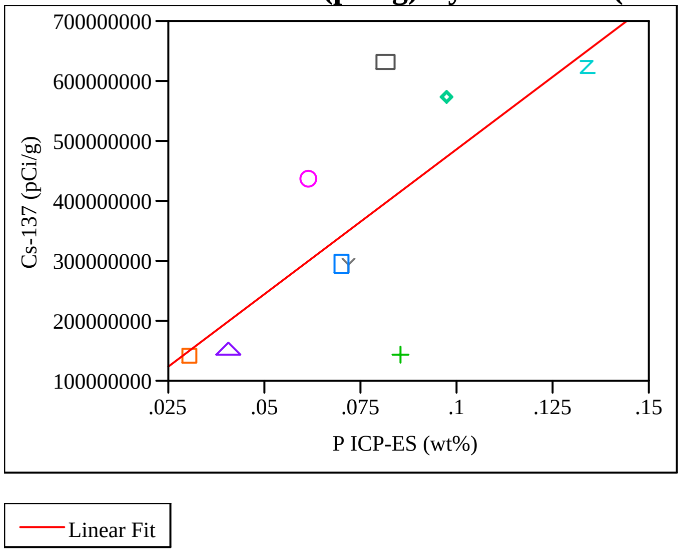

Linear Fit

Cs-137 (pCi/g) = 3569686.9 + 4.8281e+9 P ICP-ES (wt%)

Summary of Fit

RSquare	0.512701
RSquare Adj	0.443087
Root Mean Square Error	1.541e+8
Mean of Response	3.64e+8
Observations (or Sum Wgts)	9

Analysis of Variance

Source	DF	Sum of Squares	Mean Square	F Ratio
Model	1	1.7494e+17	1.749e+17	7.3649
Error	7	1.6628e+17	2.375e+16	Prob > F
C. Total	8	3.4122e+17		0.0300

Parameter Estimates

Term	Estimate	Std Error	t Ratio	Prob>|t|
Intercept	3569686.9	1.424e+8	0.03	0.9807
P ICP-ES (wt%)	4.8281e+9	1.779e+9	2.71	0.0300

Bivariate Fit of Cs-rem beta (pCi/g) By P ICP-ES (wt%)

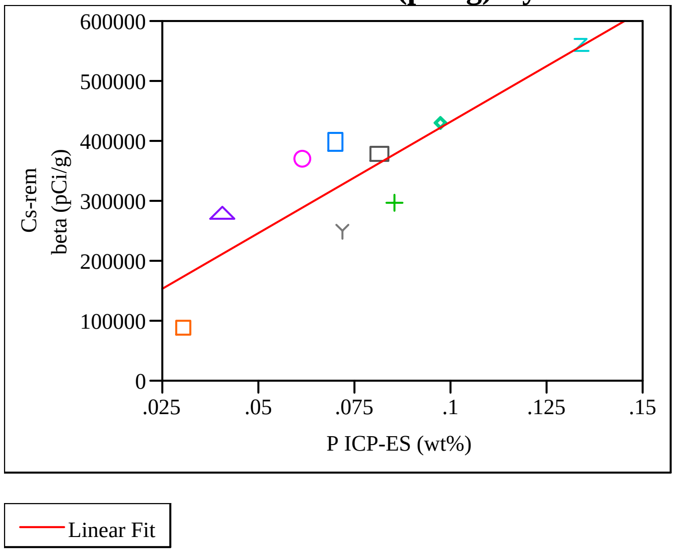

Linear Fit

Cs-rem beta (pCi/g) = 61870.276 + 3698555.5 P ICP-ES (wt%)

Summary of Fit

RSquare	0.736266
RSquare Adj	0.69859
Root Mean Square Error	72480.43
Mean of Response	337988
Observations (or Sum Wgts)	9

Analysis of Variance

Source	DF	Sum of Squares	Mean Square	F Ratio
Model	1	1.0266e+11	1.027e+11	19.5419
Error	7	3.6774e+10	5.2534e+9	Prob > F
C. Total	8	1.3944e+11		0.0031

Parameter Estimates

Term	Estimate	Std Error	t Ratio	Prob>|t|
Intercept	61870.276	66971.02	0.92	0.3863
P ICP-ES (wt%)	3698555.5	836658.8	4.42	0.0031

Bivariate Fit of Mass-133 (Cs) ICP-MS (wt%) By P ICP-ES (wt%)

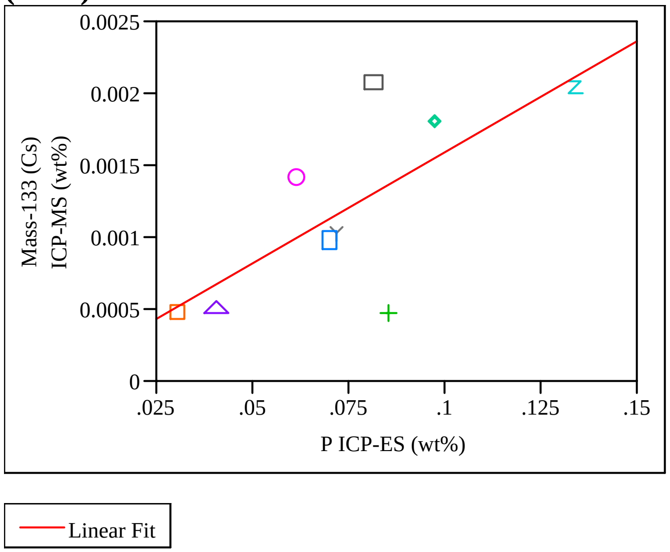

Linear Fit

Mass-133 (Cs) ICP-MS (wt%) = 0.0000393 + 0.0154823 P ICP-ES (wt%)

Summary of Fit

RSquare	0.510449
RSquare Adj	0.440513
Root Mean Square Error	0.000496
Mean of Response	0.001195
Observations (or Sum Wgts)	9

Analysis of Variance

Source	DF	Sum of Squares	Mean Square	F Ratio
Model	1	1.79894e-6	1.7989e-6	7.2988
Error	7	1.72529e-6	2.4647e-7	Prob > F
C. Total	8	3.52423e-6		0.0306

Parameter Estimates

Term	Estimate	Std Error	t Ratio	Prob>|t|
Intercept	0.0000393	0.000459	0.09	0.9341
P ICP-ES (wt%)	0.0154823	0.005731	2.70	0.0306

Bivariate Fit of Mass-135 (Cs,Ba) ICP-MS (wt%) By P ICP-ES (wt%)

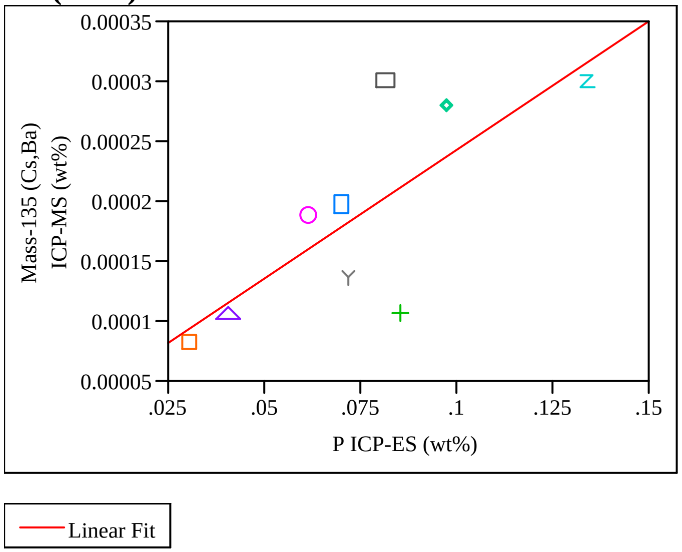

Linear Fit

Mass-135 (Cs,Ba) ICP-MS (wt%) = 2.6962e-5 + 0.0021567 P ICP-ES (wt%)

Summary of Fit

RSquare	0.571045
RSquare Adj	0.509766
Root Mean Square Error	6.121e-5
Mean of Response	0.000188
Observations (or Sum Wgts)	9

Analysis of Variance

Source	DF	Sum of Squares	Mean Square	F Ratio
Model	1	3.49086e-8	3.4909e-8	9.3187
Error	7	2.62225e-8	3.7461e-9	Prob > F
C. Total	8	6.1131e-8		0.0185

Parameter Estimates

Term	Estimate	Std Error	t Ratio	Prob>|t|
Intercept	2.6962e-5	5.655e-5	0.48	0.6481
P ICP-ES (wt%)	0.0021567	0.000707	3.05	0.0185

Bivariate Fit of Sb-126 (pCi/g) By P ICP-ES (wt%)

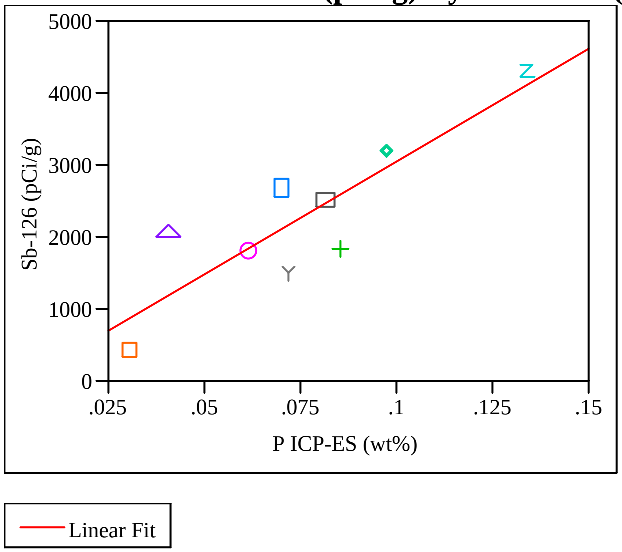

Linear Fit

Sb-126 (pCi/g) = -78.91012 + 31177.972 P ICP-ES (wt%)

Summary of Fit

RSquare	0.756907
RSquare Adj	0.722179
Root Mean Square Error	578.5444
Mean of Response	2248.699
Observations (or Sum Wgts)	9

Analysis of Variance

Source	DF	Sum of Squares	Mean Square	F Ratio
Model	1	7295254.9	7295255	21.7955
Error	7	2342995.0	334714	Prob > F
C. Total	8	9638249.9		0.0023

Parameter Estimates

Term	Estimate	Std Error	t Ratio	Prob>|t|
Intercept	-78.91012	534.5678	-0.15	0.8868
P ICP-ES (wt%)	31177.972	6678.275	4.67	0.0023

Bivariate Fit of Sn-126 (pCi/g) By P ICP-ES (wt%)

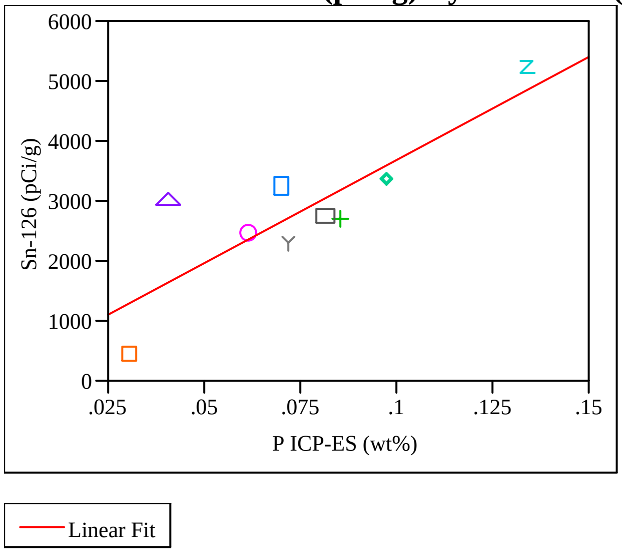

Linear Fit

Sn-126 (pCi/g) = 251.89156 + 34410.758 P ICP-ES (wt%)

Summary of Fit

RSquare	0.713761
RSquare Adj	0.67287
Root Mean Square Error	713.5188
Mean of Response	2820.846
Observations (or Sum Wgts)	9

Analysis of Variance

Source	DF	Sum of Squares	Mean Square	F Ratio
Model	1	8886551	8886551	17.4551
Error	7	3563763	509109	Prob > F
C. Total	8	12450314		0.0041

Parameter Estimates

Term	Estimate	Std Error	t Ratio	Prob>|t|
Intercept	251.89156	659.2825	0.38	0.7137
P ICP-ES (wt%)	34410.758	8236.316	4.18	0.0041

Bivariate Fit of Tc-99 (ICP-MS) (pCi/g) By P ICP-ES (wt%)

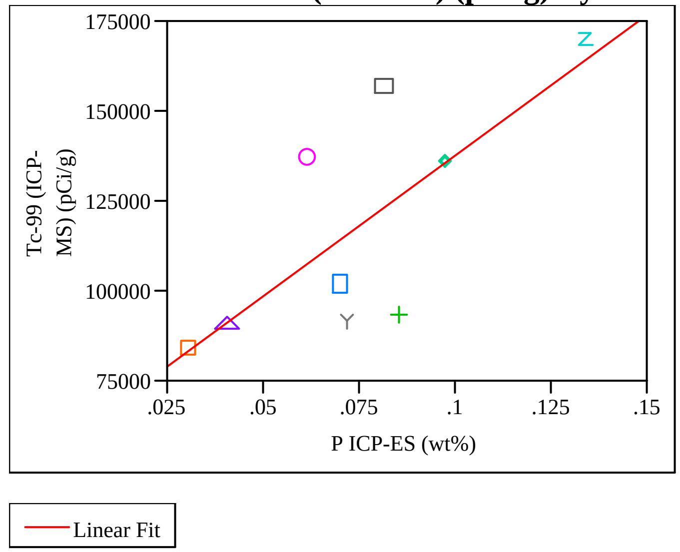

Linear Fit

Tc-99 (ICP-MS) (pCi/g) = 59639.834 + 779544.7 P ICP-ES (wt%)

Summary of Fit

RSquare	0.540143
RSquare Adj	0.47445
Root Mean Square Error	23551.63
Mean of Response	117837.2
Observations (or Sum Wgts)	9

Analysis of Variance

Source	DF	Sum of Squares	Mean Square	F Ratio
Model	1	4560650489	4.5607e+9	8.2221
Error	7	3882754811	554679259	Prob > F
C. Total	8	8443405300		0.0241

Parameter Estimates

Term	Estimate	Std Error	t Ratio	Prob>|t|
Intercept	59639.834	21761.41	2.74	0.0289
P ICP-ES (wt%)	779544.7	271862.1	2.87	0.0241

Bivariate Fit of Tc-99 (ICP-MS) (pCi/g) By Mass-133 (Cs) ICP-MS (wt%)

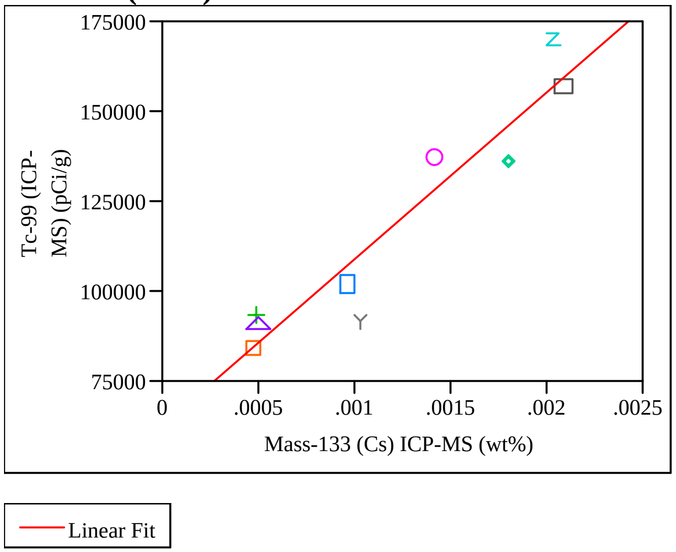

Linear Fit

Tc-99 (ICP-MS) (pCi/g) = 62334.321 + 46440290 Mass-133 (Cs) ICP-MS (wt%)

Summary of Fit

RSquare	0.900194
RSquare Adj	0.885936
Root Mean Square Error	10972.04
Mean of Response	117837.2
Observations (or Sum Wgts)	9

Analysis of Variance

Source	DF	Sum of Squares	Mean Square	F Ratio
Model	1	7600705911	7.6007e+9	63.1363
Error	7	842699389	120385627	Prob > F
C. Total	8	8443405300		<.0001

Parameter Estimates

Term	Estimate	Std Error	t Ratio	Prob>|t|
Intercept	62334.321	7884.7	7.91	<.0001
Mass-133 (Cs) ICP-MS (wt%)	46440290	5844607	7.95	<.0001

Bivariate Fit of H2O Fraction By Mass-133 (Cs) ICP-MS (wt%)

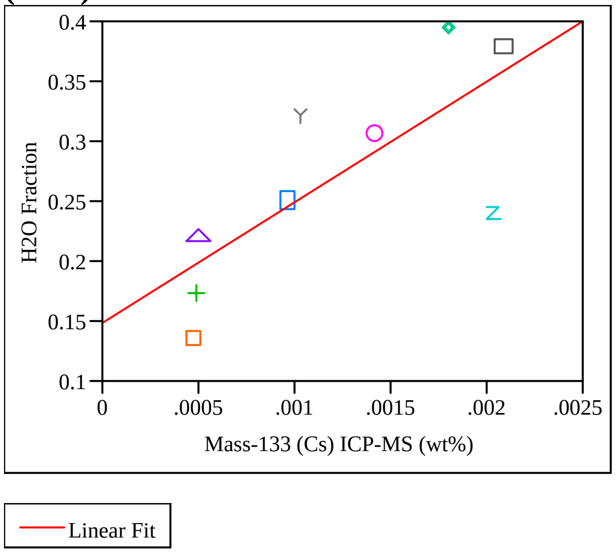

Linear Fit

H2O Fraction = 0.1485572 + 100.6682 Mass-133 (Cs) ICP-MS (wt%)

Summary of Fit

RSquare	0.568706
RSquare Adj	0.507092
Root Mean Square Error	0.062204
Mean of Response	0.26887
Observations (or Sum Wgts)	9

Analysis of Variance

Source	DF	Sum of Squares	Mean Square	F Ratio
Model	1	0.03571484	0.035715	9.2302
Error	7	0.02708538	0.003869	Prob > F
C. Total	8	0.06280022		0.0189

Parameter Estimates

Term	Estimate	Std Error	t Ratio	Prob>|t|
Intercept	0.1485572	0.044701	3.32	0.0127
Mass-133 (Cs) ICP-MS (wt%)	100.6682	33.13496	3.04	0.0189

Bivariate Fit of SO4 wt % By S ICP-ES (wt%)

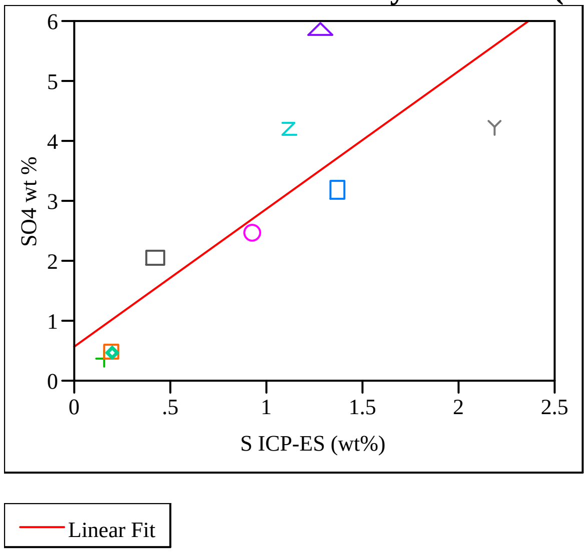

Linear Fit

SO4 wt % = 0.5797276 + 2.2942221 S ICP-ES (wt%)

Summary of Fit

RSquare	0.671478
RSquare Adj	0.624546
Root Mean Square Error	1.193851
Mean of Response	2.571877
Observations (or Sum Wgts)	9

Analysis of Variance

Source	DF	Sum of Squares	Mean Square	F Ratio
Model	1	20.392248	20.3922	14.3075
Error	7	9.976954	1.4253	Prob > F
C. Total	8	30.369202		0.0069

Parameter Estimates

Term	Estimate	Std Error	t Ratio	Prob>|t|
Intercept	0.5797276	0.660111	0.88	0.4090
S ICP-ES (wt%)	2.2942221	0.606531	3.78	0.0069

Bivariate Fit of Sn-126 (pCi/g) By Sb-126 (pCi/g)

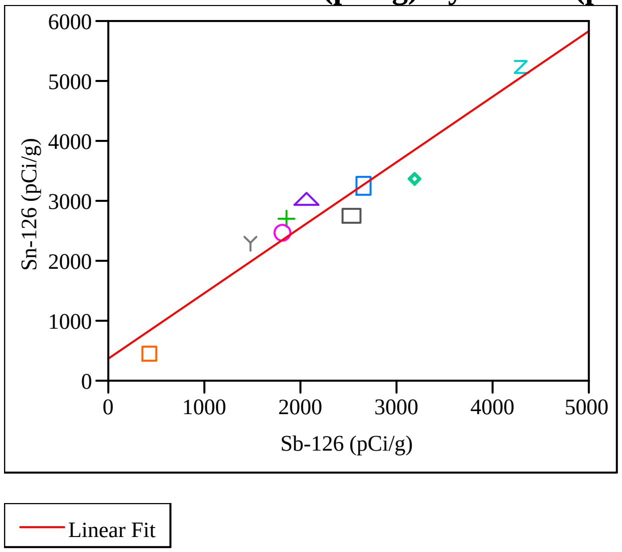

Linear Fit

Sn-126 (pCi/g) = 361.60267 + 1.0936295 Sb-126 (pCi/g)

Summary of Fit

RSquare	0.925888
RSquare Adj	0.9153
Root Mean Square Error	363.0667
Mean of Response	2820.846
Observations (or Sum Wgts)	9

Analysis of Variance

Source	DF	Sum of Squares	Mean Square	F Ratio
Model	1	11527592	11527592	87.4512
Error	7	922722	131817.46	Prob > F
C. Total	8	12450314		<.0001

Parameter Estimates

Term	Estimate	Std Error	t Ratio	Prob>|t|
Intercept	361.60267	289.4885	1.25	0.2518
Sb-126 (pCi/g)	1.0936295	0.116947	9.35	<.0001

Bivariate Fit of Tc-99 (ICP-MS) (pCi/g) By Sb-126 (pCi/g)

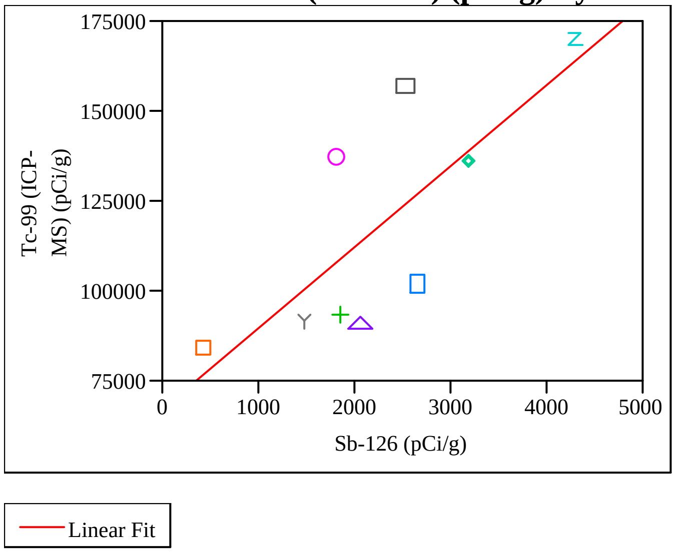

Linear Fit

Tc-99 (ICP-MS) (pCi/g) = 67150.069 + 22.54064 Sb-126 (pCi/g)

Summary of Fit

RSquare	0.57998
RSquare Adj	0.519977
Root Mean Square Error	22508.41
Mean of Response	117837.2
Observations (or Sum Wgts)	9

Analysis of Variance

Source	DF	Sum of Squares	Mean Square	F Ratio
Model	1	4897006156	4.897e+9	9.6659
Error	7	3546399144	506628449	Prob > F
C. Total	8	8443405300		0.0171

Parameter Estimates

Term	Estimate	Std Error	t Ratio	Prob>|t|
Intercept	67150.069	17946.91	3.74	0.0072
Sb-126 (pCi/g)	22.54064	7.250128	3.11	0.0171

Bivariate Fit of Tc-99 (ICP-MS) (pCi/g) By Sn-126 (pCi/g)

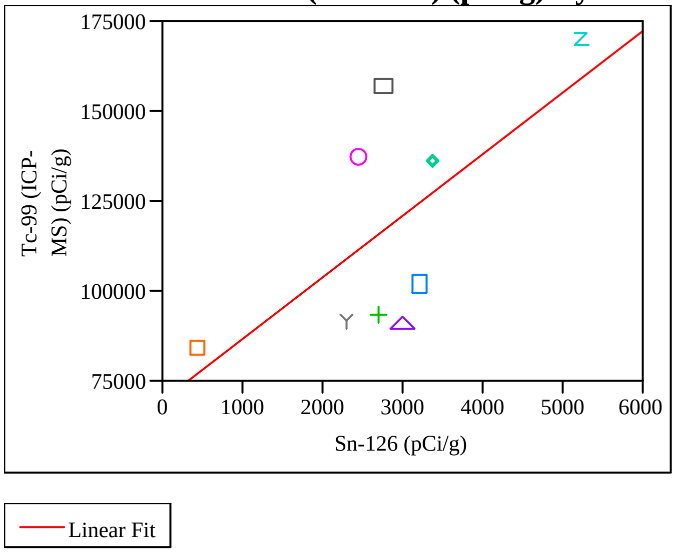

Linear Fit

Tc-99 (ICP-MS) (pCi/g) = 69439.438 + 17.157172 Sn-126 (pCi/g)

Summary of Fit

RSquare	0.434064
RSquare Adj	0.353216
Root Mean Square Error	26127.23
Mean of Response	117837.2
Observations (or Sum Wgts)	9

Analysis of Variance

Source	DF	Sum of Squares	Mean Square	F Ratio
Model	1	3664981060	3.665e+9	5.3689
Error	7	4778424240	682632034	Prob > F
C. Total	8	8443405300		0.0536

Parameter Estimates

Term	Estimate	Std Error	t Ratio	Prob>|t|
Intercept	69439.438	22630.24	3.07	0.0181
Sn-126 (pCi/g)	17.157172	7.404627	2.32	0.0536